ISBN: 978-3-95450-249-3 ISSN: 2673-5350 doi: 10.18429/JACoW-IBIC2024-TUAC2

OVERVIEW OF THE FCC-ee BEAM INSTRUMENTATION R&D

A. Boccardi, D. Butti, M. Gasior, E. Howling[1], R. Kieffer, T. Lefevre, S. Mazzoni*,
B. Salvachua, A. Schloegelhofer, C. Zamantzas, CERN, Geneva, Switzerland
B. Paroli, M. A. C. Potenza, M. Siano, Università degli Studi di Milano, Milan, Italy
U. Iriso, A. Nosych, L. Torino, ALBA-CELLS, Cerdanyola del Vallès, Spain
M. Reissig, E. Bründermann, B. Haerer, G. Niehues, R. Ruprecht,
A.-S. Müller, Karlsruhe Institute of Technology, Karlsruhe, Germany
[1]also at University of Oxford, Oxford, UK

Abstract

We present an overview of the FCC-ee beam instrumentation needs and the corresponding main challenges. We will review the different R&D activities being currently pursued, including beam position and loss monitoring, transverse and longitudinal monitoring systems as well as polarimetry and luminosity monitoring.

INTRODUCTION

The Future Circular Collider (FCC) is a study of novel research infrastructure composed of an electron-positron collider (FCC-ee) [1] followed by a hadron one (FCC-hh) [2] hosted in the same underground facility, following the successful strategy adopted for the LEP-LHC construction. The FCC study was motivated by the 2013 recommendations of the European Strategy for Particle Physics [3] to undertake design studies for accelerator projects with emphasis on proton-proton and electron-positron high-energy frontier machines to stay at the forefront of particle physics.

Following the Conceptual Design Report (CDR) in 2019, CERN is presently finalising a 5-years feasibility study for geological, technical, environmental and administrative aspects of the FCC complex that shall provide a consolidated cost estimate. These and other aspects of the study (physics case, detector concepts, funding model etc.) shall be part of a Feasibility Study Report (FSR) to be published in March 2025.

In this contribution we will present an overview of the Beam Instrumentation (BI) systems that are currently being studied as part of the FSR. The study focuses at present on the FCC-ee machine which overall design maturity is more advanced than the second-stage FCC-hh. We will present a summary of requirements and related measurement techniques and methods, as well as relevant R&D activities.

THE FCC-ee COLLIDER

FCC-ee consists of a 90.7 km collider ring that can host 4 detectors for electron-positron collision experiments. The collider is design to be operated at all times in collision mode with top-up injection from a booster ring hosted inside the main ring tunnel, in turn fed by a 20 GeV electron and positron injection complex. The FCC-ee is meant to study the electro-weak sector with beam energies ranging from 45 to 182 GeV (see Table 1). The beam current is determined by the requirement to keep the power dissipated by Synchrotron Radiation (SR) at 50 MW.

FCC-ee represents a formidable challenge for BI due to unprecedented operating conditions. The size of the machine, radiation levels and heat load during operation, several-keV-level critical wavelength of SR make it a harsh environment to guarantee stringent BI requirements as well as maintainability. We will here review the development status of the main BI systems for FCC-ee main ring.

Table 1: Some FCC-ee Parameters Relevant to BI Systems

Parameter	Z	WW	H	$t\bar{t}$
beam energy [GeV]	45.6	80	120	182.5
beam current [mA]	1270	137	26.7	4.9
# bunches	11200	1780	440	60
bunch intensity [10^{11}]	2.14	1.45	1.15	1.55
RMS bunch length [mm]	5.6	3.5	3.4	1.8
bunch spacing [ns]	25	25	25	25

BEAM POSITION MEASUREMENT

The FCC-ee requires approximately 10'000 BPMs throughout the accelerator complex. The collider arc BPMs are required to have submicron orbit resolution, turn by turn resolution in the order of microns, and an accuracy of 20 µm. The requirements for the BPMs around the interaction regions are even more challenging, with 1 µm IP BPM accuracy requested. The BPMs also need to be reliable, radiation tolerant and have a small impedance.

Initial estimates of impedance budget for the BPMs used a design scaled from DAΦNE, and estimated a total loss factor of 40.1 V C^{-1} [1]. More recent simulations of a simple 8 mm radius button in CST, as shown in Fig. 1, have demonstrated that the arc BPM contribution to the wakeloss could be an order of magnitude lower. These simulations also suggest that the signal amplitude would be sufficient from an 8 mm pickup. Further simulations are ongoing to optimise the design and take into account the winglets of the FCC-ee beam pipe.

Measurements of pickup response to an electron beam were recently taken using the eBPMs already installed at the AWAKE accelerator at CERN. These were bench-marked

* stefano.mazzoni@cern.ch

ISBN: 978-3-95450-249-3 ISSN: 2673-5350 doi: 10.18429/JACoW-IBIC2024-TUBI1

COMMISSIONING OF THE BEAM DIAGNOSTIC SYSTEM FOR NanoTerasu: A NEW 3 GeV LIGHT SOURCE IN JAPAN

K. Ueshima*, T. Asaka, Y. Hosaka, K. Kan, N. Nishimori, S. Obara, QST, Sendai, Miyagi, Japan
T. Aoki, K. Haga, Y. Iba, A. Ihara, K. Ito, T. Iwashita, M. Kadowaki, R. Kanahama, H. Kobayashi, K. Moriya, H. Nishihara, H. Oikawa, R. Yoshioka, R. Saida, K. Sakuraba, K. Takahashi, S. Takahashi, T. Tanaka, T. Tsuchiyama, NAT Corporation, Naka, Ibaraki, Japan
T. Abe, H. Dewa, T. Fujita, A. Kiyomichi, M. Masaki, S. Takano, JASRI, Sayo, Hyogo, Japan
H. Maesaka, RIKEN SPring-8 Center, Sayo, Hyogo, Japan

Abstract

NanoTerasu is a 4th generation 3 GeV light source newly constructed in Sendai, Japan. The storage ring circumference is 349 m and the natural emittance is 1.1 nm rad, which is realized by a double-double-bend lattice. The commissioning of the storage ring started in June 2023. The beam diagnostic system for NanoTerasu mainly consists of button BPMs to monitor both single-pass and COD beam orbit, a DCCT to monitor the stored current and an X-ray pinhole camera to measure the beam size. To suppress collective instabilities, a transverse bunch-by-bunch feedback (BBF) system is also in use. The BBF system can also measure the betatron tune. Using the BBF system, the stored beam current reached more than 100 mA with designed emittance in August 2023. The commissioning of the beam diagnostic system were performed smoothly. In addition, the first user operation at NanoTerasu was started on schedule with high reliability and high performance. The stored beam current was set to 160 mA with top-up beam injection. The operation availability was 99.5 % for first 1560 hours user operation period.

INTRODUCTION

The NanoTerasu is a compact 4th generation 3 GeV light source newly constructed in Sendai, Japan [1, 2]. The NanoTerasu construction was started in 2019. At the first phase, 10 beamlines were constructed. In total, 28 beamlines can be constructed. The accelerator system of NanoTerasu consists of full energy injector Linac and storage ring (SR) as shown in Fig. 1. The Linac system consists of 40 MeV pre-injector system and C-band accelerator system. The length of the Linac is only 110 m due to the high acceleration gradient of C-band accelerator. The 3 GeV C-band full-energy injector Linac enables the extension to the soft X-ray (SX) free electron laser in the future.

The SR circumference is 349 m and the natural emittance is 1.14 nm rad, which is realized by a 4 bend lattice as shown in Fig. 2. Four B-Q combined bending magnets, 10 quadrupole magnets and 10 sextupole magnets were installed in one unit cell. The SR consists of 16 cells in total. The new type of TM020 mode RF cavity with higher-order-mode dampers was developed [3]. In the beam injection point at SR, the in-vacuum off-axis beam injection system

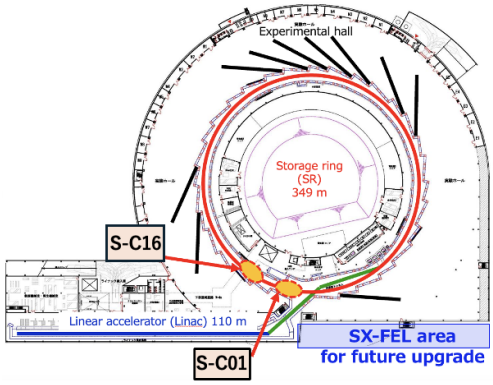

Figure 1: The layout of NanoTerasu accelerator system.

was installed for the stable top-up beam injection [4]. The beam diagnostic systems were installed in the two short straight sections (S-C01 and S-C16) [5]. Bunch-by-bunch feed back system (BBF) and BPM for bunch current monitor were installed in S-C01. Two DCCT sensor cores and a 3-pole wiggler (3PW) were installed in S-C16. The beam commissioning was started in April 2023 [6, 7].

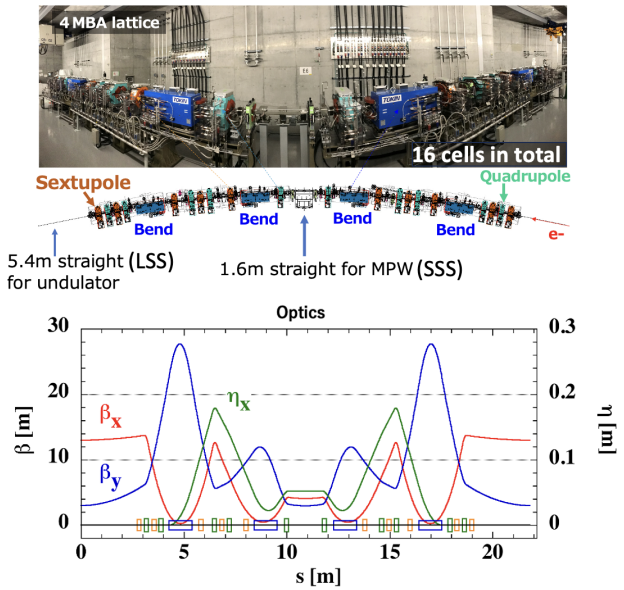

Figure 2: The magnets layout (top) and Lattice functions (bottom) in the one unit cell.

* ueshima.kouta@qst.go.jp

ISBN: 978-3-95450-249-3 ISSN: 2673-5350 doi: 10.18429/JACoW-IBIC2024-TUBI2

DESIGN OF HEPS BEAM DIAGNOSTICS*

Yanfeng Sui[1,†], Jun He, Dechong Zhu, Lingda Yu, Yaoyao Du, Taoguang Xu, Ying Zhao, Qiang Ye, Zhi Liu, Huizhou Ma, Xiaoyu Liu, Lin Wang, Wan Zhang, Shujun Wei, Fangqi Huang, Yanhua Lu, Fang Liu, Junhui Yue, Jianshe Cao[1]
Institute of High Energy Physics, Chinese Academy of Sciences, Beijing, China
[1]also at University of Chinese Academy of Sciences, Beijing, China

Abstract

High Energy Photon Source (HEPS) is a fourth-generation light source with a natural emittance of 34.82 pm, aiming to produce high-brilliance photon beams. The ultra-low emittance poses challenges for beam instrumentation, requiring high-resolution beam position and size measurements in the sub-micrometer range. The high current and multi-bunch operation necessitate a bunch-by-bunch feedback system to address beam instabilities. This paper will provide an overview of the beam instrumentation at HEPS.

INTRODUCTION

HEPS is the first fourth-generation synchrotron light source in China, located in Beijing. The HEPS project aims to establish a high-performance high-energy synchrotron light source with a beam energy of 6 GeV, and beam current of 200 mA, offering a radiation brightness potential of up to 1×10^{22} [photons$\cdot s^{-1} \cdot mm^{-2} \cdot mrad^{-2} \cdot (0.1\%\ bw)^{-1}$] in the typical hard X-ray regime [1]. The facility includes a 500 MeV S-band linac, a ramping booster spanning 0.5-6 GeV, transport lines, and a 6 GeV storage ring equipped with state-of-the-art beam instrumentation and diagnostics systems. The HEPS storage ring comprises 48 7BA cells grouped into 24 super-periods, with a circumference of 1360.4 m. The key beam parameters for the storage ring are detailed in Table 1.

Table 1: HEPS Storage Ring Parameters [2]

Parameters	Value
Energy	6.0 GeV
Circumference	1360.4 m
Main RF frequency	166.6 MHz
Harmonic cavity frequency	499.8 MHz
Harmonic number of main RF	756
Natural emittance	34.82 pm
Bunch Length	5.02 mm
Working point(x/y)	114.14/ 106.23
Bunch length (zero current)	5.02 / 29.70 (HC)
Damping time (x/y/z)	10.2 / 18.9 / 16.4 ms
Beam current	200 mA
Synchrotron frequency	$\sim 1.1 \times 10^{-3}$

In order to fully utilize the advantages of HEPS, such as high energy, high brightness, and small beam sizes, it is crucial that the photon beams remain extremely stable in both position and angle, with deviations ideally not exceeding 10% of the beam sizes and divergence. In the low beta section, where the beam size is approximately 3 μm in the vertical direction, users expect the orbit change to stay within 10% of the beam size itself (0.3 μm). To meet this requirement, the resolution of the beam position monitor should be better than 0.1 μm. Additionally, we require additional instrumentation to meet the requirements. The beam instrumentation to be installed at HEPS is detailed in Table 2.

Table 2: Beam Instrumentation in HEPS

Beam instrumentations	Linac	LB	BST	BR	RB	SR
BPM	8	8	80	11	13	578+24
ICT	7	2	-	2	2	-
NPCT	-	-	2	-	-	2
Bunch Current Monitor	-	-	1	-	-	1
OTR/YAG	7	2	-	2	2	-
Synchrotron Light Monitor	-	-	2	-	-	2
Tune measurement	-	-	1	-	-	1
Beam loss monitor	-	-	4	-	-	500
B&B feedback system	-	-	3	-	-	3
Streak camera	-	-	-	-	-	1
Bunch cleaning system	-	-	-	-	-	1
Energy analyse station	2					
Emittance	2					

INJECTION DIAGNOSTICS

The HEPS injector comprises a linear accelerator (Linac), a low-energy transport line (LB), two high-energy transport lines (RB & BR), and a booster (BST). Beam diagnostics within the injector are essential for monitoring the beam status and enhancing injection efficiency.

Linac

The linac beam instrumentation includes 6 integrating current transformers (ICT) for monitoring the total bunch train charge. During routine operations, the beam trajectory

* Work supported by NSFC No.12475167.
† syf@ihep.ac.cn

ISBN: 978-3-95450-249-3 ISSN: 2673-5350 doi: 10.18429/JACoW-IBIC2024-TUBC3

BEAM DIAGNOSTICS FOR CSNS-II LINAC COMMISSIONING AND OPERATION*

J. Peng[1,2†], Y. L. Han[1,2], Z. P. Li[1,2], Y. Li[1,2], Y. Yuan[1,2], X. Y. Feng[1,2], M. Y. Huang[1,2], H. C. Liu[1,2], S. Wang[1,2], S. N. Fu[1,2]

[1]Institute of High Energy Physics, Chinese Academy of Sciences, Beijing, China
[2]Spallation Neutron Source Science Center, Dongguan, China

Abstract

The China Spallation Neutron Source (CSNS) facility began operation in 2018. By 2020, its accelerator achieved the design power of 100 kW and currently operates at a power of 160 kW. This year, the power upgrade project (CSNS-II) has been launched to meet the growing scientific demands. Our goal is to enhance the accelerator power to 500 kW primarily by increasing the beam current. A comprehensive suite of beam diagnostics has been developed to support commissioning and operation of the accelerator at higher intensities. In this paper, we first review the commissioning and operational status of the existing linac, and then outline the new requirements for the linac upgrade.

INTRODUCTION

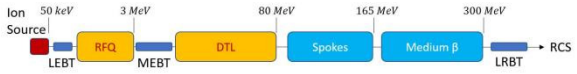

Figure 1: Overview of the CSNS-II linac layout.

Table 1: Upgraded Parameters of the CSNS Accelerator

Parameter	Units	CSNS	CSNS-II
Average power	kW	100	500
Beam energy	GeV	1.6	1.6
Peak linac current	mA	15	40
Pulse length	μs	500	650
Pulse repetition frequency	Hz	25	25+25[1]

[1] The 25 Hz beam pules are injected downward into the RCS, while the other 25 Hz pules are directed upward to the experimental stations.

The CSNS accelerator comprises an 80 MeV linac serving as the injector and a 1.6 GeV rapid cycling synchrotron (RCS) [1-2]. The linac includes a 50 keV H- ion source, a 3 MeV RFQ, an 80 MeV DTL, and several beam transport lines. In 2024, the CSNS power upgrade project was launched. The beam power of the accelerator will be increased to 500 kW by raising the beam peak current from 15 mA to 40 mA, as shown in Table 1. To mitigate the space charge effect [3], the linac energy will be upgraded from 80 MeV to 300 MeV by adding a superconducting linac after the DTL. As shown in Fig. 1, the superconducting linac consists of two sections: a 324 MHz spoke section and a 648 MHz elliptical section. With the increase in both current and energy of the linac, the beam transport lines have been completely redesigned, and the diagnostics installed in these lines have also been adjusted accordingly. This paper reviews the beam commissioning status and provides a summary of the changes in diagnostics.

DIAGNOSTICS LAYOUT

LEBT

The Low Energy Beam Transport (LEBT) is equipped with two BCMs to measure the beam current and calculate beam transmission. Additionally, it contains a double-slit emittance monitor designed to measure the transverse phase space distribution of the beam.

MEBT

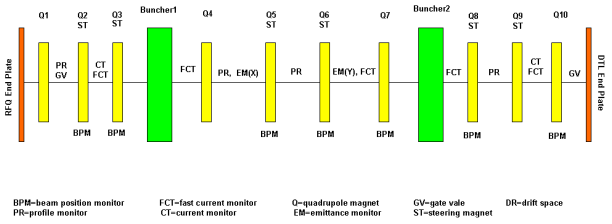

Figure 2: MEBT layout for the CSNS linac.

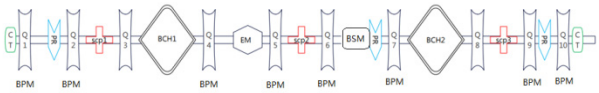

Figure 3: New MEBT scheme for the CSNS-II linac.

The Medium Energy Beam Transport (MEBT) of the CSNS is shown in Fig. 2, and it has been redesigned for the CSNS-II linac, shown in Fig. 3. Comparing to the old MEBT layout the numbers of magnets and bunchers remained unchanged in the new MEBT scheme, so the lengths of two MEBTs are nearly the same. To explore characteristics of high-intensity beam, more diagnostics have been incorporated into the new MEBT scheme. Wire scanners and double-slit emittance monitor have proven useful for determining the phase space of the beam output from the RFQ. The emittance monitor can directly plot the phase space distribution of beam in the middle of the MEBT, as shown in Fig. 4. The Wire scanners can be used to monitor the beam envelope along the MEBT, as shown in Fig. 5. Figure 6 depicts the simulated beam distribution at the location of the emittance monitor by fitting with the measured beam profile. Compared to the results by emit-

* Work supported by 2023YFA1606802, DG24313511
† pengjun@ihep.ac.cn

ISBN: 978-3-95450-249-3 ISSN: 2673-5350 doi: 10.18429/JACoW-IBIC2024-TUBC4

BEAM SIZE MEASUREMENT WITH GRATINGS AT BEPCII*

Wan Zhang†, Dechong Zhu[1], Yanfeng Sui[1], Junhui Yue[1], Jianshe Cao[1], Jun He[1], Institute of High Energy Physics, Chinese Academy of Sciences, Beijing 100049, China
[1]also at University of Chinese Academy of Sciences, Beijing 100049, China

Abstract

The vertical beam size measurement was carried out at BEPCII using a phase grating and an absorption grating based on the Talbot effect. Due to the partial coherence of the source, coherence length can be calculated by measuring the visibility decay of interferograms recorded at different distances behind gratings. The vertical beam size of 68.19±2 μm was obtained based on the relationship between coherence length and source size. A comparison of the vertical emittance derived from grating Talbot method and synchrotron radiation visible light interferometer method was presented to evaluate the method. The vertical emittances from two methods are 1.41 nm·rad and 1.40 nm·rad, respectively. The 0.1% difference indicates the grating Talbot method for beam size measurement is reliable. This technique has great potential in small beam size measurement in the fourth-generation synchrotron radiation light source, considering its small diffraction limitation and simple experimental setups.

INTRODUCTION

The requirements of synchrotron radiation facilities about high coherence, high brightness and small beam sizes have been proposed in some x-ray beamlines for applications such as x-ray phase contrast imaging, coherent x-ray diffraction imaging and x-ray holography [1-3]. The beam size measurement is essential for beam adjustment and beam dynamics study.

Synchrotron light can afford to measure beam sizes in synchrotron radiation facility [4, 5]. Thanks to its short wavelength, x-ray can greatly improve the imaging resolution to meet small beam size measurements. The x-ray pinhole imaging, as a common method, has been applied at Diamond Light Source (DLS), European Synchrotron Radiation Facility (ESRF) and so on [6-8]. It is characterized by real-time and high measurement accuracy. However, it doesn't work for extremely small beam size due to low resolution caused by diffraction limitation and imaging. X-ray Fresnel zone plates (FZP) imaging and KB mirror focusing imaging show advantages in micron-scale beam size measurement. However, they suffer from high processing difficulties [9, 10]. In recent years, some new measurement systems have been established for beam size measurement. [11, 12].

For the case of synchrotron radiation sources with high coherence, it is feasible to derive light source size by spatial coherence. One of the Talbot effect applications is focused on spatial coherence measurements of x-ray in synchrotron radiation sources. The spatial coherence of x-ray emitted from a bending magnet has been measured using the Talbot effect of a π/2 phase checkerboard grating and a π/2 phase circular grating respectively at Advanced Photon Source (APS) [13, 14]. However, the above articles are of no interest to beam size measurement. Given the relationship between spatial coherence and source size, the grating Talbot method can afford to measure beam size owing to its little diffraction limitation. Most importantly, the experimental setup is simple, which only needs gratings, a displacement platform, and an x-ray camera without changing any components in the beamline front end.

At BEPCII, we measured the vertical beam size at 3W1 beamline employing the grating Talbot effect. A partially coherent quasi-monochromatic x-ray has been employed in this experiment. The vertical beam size is calculated successfully from the self-image interference fringes of a grating interferometer. Then the vertical emittance of the storage ring is calculated by the vertical beam size and β function. The vertical emittance from a bending magnet is derived using visible light interference method. An extremely small difference between the two vertical emittances is presented, which illustrates that the grating Talbot effect method is of great potential to measure beam size.

THEORY BACKGROUND

In 1836, Talbot found that a monochromatic parallel beam transmitting through a grating vertically will generate a series of grating images at certain distances behind the grating, which is called Talbot effect [15]. There is a specific relationship between the visibility of the Talbot image and the complex coherence function of the light source [16, 17].

The interference intensity of two beams from an extended source at any point can be written as

$$\begin{aligned} \mathrm{I} &= \langle [E(p_1)+E(p_2)]\,[E^*(p_1)+E^*(p_2)] \rangle \\ &= I_1 + I_2 + 2Re\{J_{12}\} \end{aligned} \quad (1)$$

where E(p_1) and E(p_2) are electric fields formed by two points on an extended source, and J_{12} is the mutual intensity function of the two light beams from the two points [18].

The normalized mutual intensity function j_{12}, called the complex coherence function, is expressed as

$$j_{12} = \frac{J_{12}}{\sqrt{J_{11}J_{22}}} = \frac{J_{12}}{\sqrt{I_1 I_2}} \quad (2)$$

Combining Eq. (1) and Eq. (2)

$$\mathrm{I} = I_1 + I_2 + 2\sqrt{I_1 I_2}|j_{12}|\cos(\varphi_{j_{12}}) \quad (3)$$

where φ_{j12}=Arg(j_{12}). The third term of Eq. (3) expresses the interference effect. $|j_{12}|$ takes the value 1 corresponding to the complete coherence of the two beams and takes the value 0 corresponding to the complete incoherence. In the case of partial coherence, it takes value between 0 and 1.

* Work supported by The Youth Innovation Promotion Association CAS (award No. Y202005).
† email address: zhangwan@ihep.ac.cn

ISBN: 978-3-95450-249-3 ISSN: 2673-5350 doi: 10.18429/JACoW-IBIC2024-TUCI1

BUNCH-RESOLVED 3D BEAM POSITION MEASUREMENT SYSTEM AND ITS APPLICATION IN FELiChEM*

X. Yang, Y. M. Deng, Z. Y. Zhao, H. R. Zhang, Y. F. Xu, Y. B. Leng†
NSRL, University of Science and Technology of China, Hefei 230029, P. R. China

Abstract

A new infrared free-electron laser FEL facility named FELiChEM has been built at University of Science and Technology of China in Hefei. It is a user facility dedicated for energy chemistry research and can deliver the infrared laser in the spectral range of 2.5-200 μm to five research stations. FELiChEM consists of mid-infrared MIR and far-infrared FIR free-electron laser oscillators driven by a 60 MeV linac. The time structure of the electron beam can be easily tuned with the macro bunch width of less than 10 μs macro bunch repetition rate of 1-10 Hz and optional micro bunch repetition rate within 238, 119, 59.5 and 29.75 MHz. A 3D bunch-by-bunch position measurement system was developed to monitor not just the average position of the macro bunch but also every individual bunch position in the train. With this toolkit, a significant beam loading effect can be easily observed downstream of the linear accelerator structure, and a strong dispersion effect is observable downstream of the optical oscillator. This diagnostic tool proves to be very useful for analyzing the status of the machine and implementing corresponding optimization measures. This paper will give a brief introduce of the machine, the hardware and software structure of the 3D position measurement system, and its application in machine commissioning and operation.

INTRODUCTION

FELiChEM is an experimental facility at the University of Science and Technology of China. Its core device is two free electron laser oscillators generating middle-infrared and far-infrared laser and covering the spectral range of 2.5-200 μm [1]. It is a dedicated infrared light source aiming at energy chemistry research [2]. In FEL, Electron beam should have a good quality for achieving enough gain to overcome single-pass loss. Cavity must strictly match the beam repetitive frequency to ensure the multi-pass gain. Good balance between output coupling and cavity loss to optimize the saturation output power. Waveguide modes should match the radiation wavelength to avoid the "spectrum gap". Optical axis must strictly match beam axis to maintain interaction between FEL and beam along undulator. The internal distribution of Multi bunches affects the laser quality.

The present beam instrumentation system measure charge using ICT, FCT and scope. This method can only get the average bunch train. The profile using YAG/OTR and normal CCD is not good enough for FEL performance improvement. The position measurement using button BPM and Libera Single Pass can only obtain the macro pulse transverse position. With the repetition rate of the micro pulse is 59.5 MHz or 119 MHz, the information inside the beam cannot be accessed. The difference of parameters inside the beam, including transverse position, angle, energy, etc., will lead to the reduction of radiation. Along with the upgrading of the device, we built a bunch-resolved 3D beam position measurement system and use it to perform a comprehensive diagnosis of the device. This paper introduces the principle and setup of the measuring system. The corresponding diagnostic results are presented.

3D BPM SYSTEM SETUP

HOTCAP is a high-speed oscilloscope-based three-dimension bunch charge and position measurement system. It can extract the charge and 3D position information from the oscilloscope results [3]. HOTCAP has made a lot of achievements in the diagnosis of beam parameters of storage ring [4]. It has high resolution and can further extract various optical parameters [5]. The core of the algorithm is to reconstruct the response function using the sampled signal. Then the amplitude and phase information of the sampled signal is obtained by correlation coefficient-based method. The 3D bpm system setup and algorithm structure of HOTCAP is shown in Fig. 1.

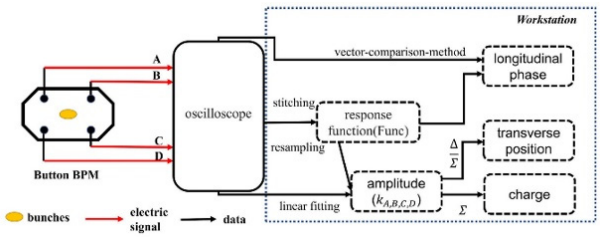

Figure 1: HOTCAP.

In the storage ring, same bunch passes through the bpm periodically. The different signals used to build the response function are all generated by the same bunch. In the FEL, all bunch pass through and produces signal only once. When the all bunches have the same charge, 3D position, and beam length, they can also be thought of as different signals produced by the same bunch. Therefore, we can port HOTCAP to FEL as the core of the measurement system.

should be indented approximately 0.33 cm (0.13 in). The last line of a paragraph should not be printed by itself at the beginning of a column nor should the first line of a paragraph be printed by itself at the end of a column.

In actual operation, bunch may be different. The difference of charge and the transverse position will cause the amplitude of the signal to differ. As shown in Fig. 2, the

† e-mail address: lengyb@ustc.edu.cn

ISBN: 978-3-95450-249-3 ISSN: 2673-5350 doi: 10.18429/JACoW-IBIC2024-TUCC2

LOW FREQUENCY POSITION MONITORING AT THE TRIUMF CYCLOTRON INJECTION LINE*

V. A. Verzilov†, TRIUMF, Vancouver, Canada

Abstract

A new 1 mA ion source and a new section of the injection beamline are presently under construction at TRIUMF for the 500 MeV H- cyclotron. A 300 keV ion beam is pulse modulated at the exit of the ion source with a duty cycle varying in the range 0.1% - 99%. The pulse repetition frequency is around 1 kHz and this is the only time varying beam structure available for a substantial fraction of the injection line, till the beam is bunched with an RF-frequency of 23 MHz, before being injected into the cyclotron. A set of new diagnostics was developed to support operation of the injection line including the beam position monitoring system operating in the kHz regime. The beam position measurements are based on capacitive pickups and high-impedance electronics to extend the sensitivity towards low frequencies. Details of the system and test measurements will be presented.

INTRODUCTION

The TRIUMF laboratory hosts and operates several accelerators to support its broad scientific portfolio. Still, the 50-years old 500 MeV H- cyclotron [1] remains the main workhorse and delivers proton beams for nuclear and material sciences, isotope production and other applications. In anticipation that the cyclotron operation continues yet for several decades, a program started some time ago to replace aging systems, applying improvements and adding new functionalities whenever possible.

As a part of the effort, the vertical section of a 34 m long injection beamline, used to transport the 300 keV H⁻ beam from the ion source to the cyclotron, was upgraded and commissioned in 2011 [2], and, since then, it operates very reliably. The horizontal section of the injection beamline, still being the original installation, continued to require significant amount of routine maintenance and to present a high risk of downtime due to ageing equipment (optics, diagnostics, vacuum, etc.). The construction of a completely new horizontal injection beam line [3] is currently ongoing in the framework of the TRIUMF 5-year program. Simultaneously, the second ion source will be added to the injection system for redundancy purposes. Installation and commissioning of new components is scheduled for the Spring of 2025.

Main parameters of the TRIUMF cyclotron injection system are given in Table 1. A DC beam produced by the ion sources is chopped in the form of pulses of a variable frequency and duty cycle. This is the only time varying beam structure available for a substantial fraction of the injection line, till the beam is bunched with an RF-frequency of 23.06 MHz.

A new set of beam diagnostics was developed to support different operation modes of the injection line. It includes Faraday cups, wire scanner profile monitors, various slits, AC current transformers and beam position monitors capable of operating with a kHz pulsed beam.

Table 1: Main Parameters of the Injection System

Parameter	Value	Unit
Beam species	H-	
Beam energy	300	keV
Beam current	< 1	mA
Pulse frequency	375 - 1 126	Hz
Pulse duty cycle	0.1 - 99	%
Bunching frequency	23.06	MHz

CONCEPT

Non-intercepting techniques for beam position monitoring are well proven at MHz frequencies and above. They are substantially less common for kHz pulsed beams. This is explained by the fact that the coupling between the AC component of the beam current and non-intercepting pickups is generally more efficient at higher frequencies and vanishes for true DC beams. Several options were evaluated at the conceptual level to be exploited with a chopped DC beam, e.g. inductance and wall-current based techniques, before the decision was taken in favour of capacitive type pickups. It is a well-known result, that the so-called transfer impedance of a capacitive pickup has a high pass response with the cut-off frequency determined by the pickup capacitance C_{PU} and the input impedance R_L of a circuit connected to the pickup output (see, e.g. [4]).

$$|Z_t| \propto \frac{\omega/\omega_c}{\sqrt{1+\left(\omega^2/\omega_c{}^2\right)}}$$

where the cut-off frequency

$$\omega_c = (R_L C_{PU})^{-1}$$

Thus, the response of the capacitive pickup can be extended towards lower frequencies provided it is loaded with a sufficiently high impedance circuit.

In the time domain, the response of such a circuit to a sharp step in the beam current is

$$V(t) = V_0 e^{-\omega_c t}$$

* Funded under a contribution agreement with National Research Council Canada

† verzilov@triumf.ca

ISBN: 978-3-95450-249-3 ISSN: 2673-5350 doi: 10.18429/JACoW-IBIC2024-TUDC2

THE STUDY OF HIGH-FREQUENCY PICK-UPS FOR ELECTRON BEAM POSITION MEASUREMENTS IN THE AWAKE COMMON BEAMLINE

C. Pakuza*, M. Krupa, T. Lefèvre, S. Mazzoni, E. Poimenidou,
E. Senes, N. Z. van Gils[1], M. Wendt, CERN, Genève, Switzerland
P.N. Burrows, B. Spear, W. Zhang
John Adams Institute, University of Oxford, Oxford, United Kingdom
S. Liu, Fermi National Accelerator Laboratory, Illinois, USA
V. Verzilov, TRIUMF, Vancouver, Canada
[1]also at UMCG-PARTREC, University of Groningen, Groningen, Netherlands

Abstract

The common beamline of the AWAKE experiment at CERN involves the co-propagation of two particle beams: protons with 48 nC bunch charge and 250 ps bunch length, and electrons with up to 600 pC bunch charge and approximately 4 ps bunch length. The existing operational beam position monitors at AWAKE cannot measure the electron bunches whilst the more-intense proton bunches are present, due to their low operating frequency. In order to try to address this challenge, two different types of high-frequency pick-ups were studied, a conical-shaped button pick-up and a Cherenkov diffraction radiation-based pick-up designed to operate at around 30 GHz. Both devices were installed at AWAKE and were connected to two identical read-out systems designed by TRIUMF. This contribution presents and discusses the results obtained from beam-based measurements during the current experimental year.

INTRODUCTION

The AWAKE experiment uses proton bunches from the Super Proton Synchrotron (SPS) at 400 GeV beam energy to resonantly drive wakefields in 10 m-long plasma through a process called seeded self-modulation (SSM) [1]. SSM divides the several cm-long proton bunch into a train of mm-scale micro-bunches. If electrons are injected at the correct phase with respect to the proton bunch, they can be accelerated. During AWAKE Run 1 (2016-2018), the SSM of proton bunches, seeded by the relativistic ionization front (RIF) of a short laser pulse, was demonstrated [2], along with the acceleration of externally injected electrons [1]. The goal of Run 2, which began in 2021, is to accelerate electrons to high energies (~ 0.5-1 GV/m), while controlling the beam quality and to demonstrate the scalability [3].

For more precise control of the electron beam before the entrance into the plasma, knowledge of the electron beam position in the presence of the more-intense proton bunches is required. However, the current stripline beam position monitors (BPMs) designed by TRIUMF [4] operate at 404 MHz which is in a region where the frequency spectrum is dominated by the proton bunch signal. Hence, in order to measure the electrons in the presence of protons, a higher operating frequency is required which should lie within the electron spectrum and well outside the proton spectrum.

Two different types of BPMs operating at a relatively high frequency have been investigated, both numerically and experimentally, to try to address this challenge. These include a conical-shaped button pick-up, based on a design by DESY [5], which will be referred to as the high-frequency BPM (HF BPM), and the Cherenkov diffraction radiation (ChDR) pick-up which will be referred to as the ChDR BPM designed by JAI and CERN [6, 7]. The former comprises four symmetrically arranged cone-shaped electrodes with tapered transitions from the beampipe to the connectors which reduce resonances within the pick-up. The latter is based on the generation of ChDR from the polarisation currents generated on the surface a dielectric material as the beam passes in close proximity to the material. For the design of the ChDR BPM for AWAKE, 6 mm-diameter, 86 mm-long alumina rods angled at 71° with respect to the long axis of the beampipe were chosen as the pick-up design, based on a series of simulations and geometrical constraints [8].

Both pick-ups were connected to two separate, but basically identical read-out systems designed by TRIUMF, for an operation at approximately 30 GHz, which should be in a region of the frequency spectrum where the electron signal dominates, assuming perfect longitudinal Gaussian bunches. The set-up and first results from beam-based measurements will be presented and discussed.

NUMERICAL SIMULATIONS

The mechanical designs of the pick-ups are described in [5] and [6]. Simplified numerical models were created in CST Studio Suite to compare the expected signals from the two pick-ups for an electron bunch charge of 200 pC and the measured corresponding bunch length of 3.4 ps at AWAKE [9]. By processing the peak voltage of the output signal of two opposite BPM electrodes, $U_R(x)$ and $U_L(x) = U_R(-x)$ vs. the beam position x, the relative peak signal difference between the two pick-ups can be observed in Fig. 1. Assuming perfect symmetry, the difference-over-sum of the peak voltage signals $\Delta U/\Sigma U$ provides the expected position sensitivity S of the system from numerical

* collette.pakuza@cern.ch

ISBN: 978-3-95450-249-3 ISSN: 2673-5350 doi: 10.18429/JACoW-IBIC2024-TUP05

DEVELOPMENT OF MULTI-CHANNEL TIME-DIVISION MULTIPLEXING RF SIGNAL CONDITIONING FRONT-END FOR CAfe2 BPM SYSTEM

Pengfei Deng†,1, Jinying Ma, Zheng Gao, Zhenglong Zhu, Guirong Huang, Zhen Ma[1], Yuan He, Feng Qiu*, Institute of Modern Physics, Chinese Academy of Sciences, Lanzhou, China
[1]also at Northwest Normal University, Lanzhou, China

Abstract

The construction of the China Accelerator Facility for Superheavy Elements (CAFe2) is advancing, building upon the foundation of the Chinese ADS Front-end Demo Linac (CAFe). However, the existing BPM read-out electronics from CAFe are insufficient to accommodate the increased number of BPM probes required for CAFe2 and cannot meet the measurement demands for low-intensity heavy ion beams. To address these issues, a high-speed RF switch array was developed, featuring multi-channel multiplexing, tunable gain and filtering, and web-based parameter configuration. This device functions as a front-end for RF signal conditioning, offering microsecond-level channel switching capabilities, and is capable of receiving, filtering, and amplifying multiple beam signals. When integrated with the existing RF front-end and digital signal processing platform, the new BPM read-out electronics system can support simultaneous measurement of 32 signals from 8 BPM probes. Test results indicate that the high-speed RF switch array achieves channel isolation exceeding 60 dB, with phase differences between channels less than 6° and amplitude discrepancies under 4%. These results demonstrate excellent amplitude-phase consistency and channel isolation performance, fully meeting the BPM measurement requirements of CAFe2.

INTRODUCTION

CAFe2 is designed to provide an advanced experimental platform for the synthesis of superheavy elements [1]. To ensure the provision of highly stable, low-energy spread beams, precise beam trajectory measurements are required, necessitating a sufficient number of BPM systems. According to the design, the Medium Energy Beam Line and Cryogenic Modules (CM1–CM4) of CAFe2 are equipped with 24 BPM probes along the beamline, with a required beam current of 10pμA. However, expanding the system using the existing approach would result in high costs and complex structures, and cumulative device errors could lead to inconsistencies in the input-output response curves of each channel, ultimately degrading the overall BPM system performance [2]. Moreover, the existing system can only measure beam currents down to 10 mA, which is inadequate for low-intensity beams.

* Work supported by the project of Large Research Infrastructures "China initiative Accelerator-Driven System" (No. 2017-000052-75-01-000590), "Studies of intelligent LLRF control algorithms for superconducting RF cavities" (No. E129851YR0), and the National Natural Science Foundation of China (No.12205344).
† dengpengfei@impcas.ac.cn

Therefore, an upgrade to the existing CAFe BPM read-out electronics is needed. This paper proposes a high-speed RF switch array as a front-end for RF signal conditioning. This solution increases the number of accessible signal channels without altering the existing hardware structure, enabling the CAFe2 BPM system to achieve multi-channel time-division multiplexing measurements of low-intensity heavy ion beams across varying beam currents.

DESIGN SCHEME FOR HIGH-SPEED RF SWITCH ARRAY

The high-speed RF switch array consists of four modules: high-speed switching, tunable filtering, tunable gain, and logic control, as shown in Fig. 1. RF IN 1 to RF IN 8 correspond to 8 selectable switch paths, each with 4 inputs (*X, Y, X', Y'*), supporting 32 signals from 8 BPM probes. The tunable filter selects different center frequencies, and the gain module adjusts levels. The logic control module manages signal interfaces, triggering switch control (FPGA SW CTL) for switching, filtering, and gain adjustment. Web-based configuration allows remote management and real-time parameter updates during measurements.

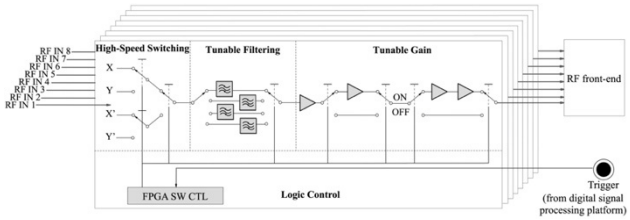

Figure 1: Schematic diagram of the high-speed RF switch array.

High-speed Switching Module

The high-speed switching module consists of three cascaded dual-channel SPDT switches (HMC199AMS8, Analog Devices, Inc.). The outputs of the first two switches connect to the inputs of the third, forming a four-channel selectable switch path. The module contains eight such paths, each independently controllable, and supports two operation modes. In fixed-channel mode, each switch remains on a specific path, functioning as a fixed 8-channel system. In automatic switching mode, the cycle for switching among four signals is configurable on a microsecond scale, with the logic control module managing switch states. This enables high-speed switching among four signals on a single channel, allowing multiple beam signals to be processed by one module, achieving multi-channel time-division multiplexing across the entire RF switch array.

ISBN: 978-3-95450-249-3 ISSN: 2673-5350 doi: 10.18429/JACoW-IBIC2024-TUP07

STRIPLINE DESIGN FOR TUNE MEASUREMENT IN THE ILSF STORAGE RING*

S. Mohammadi.A†, N. Khosravi, A. Danaeifard, Z. Rezaei
Institute for Research in Fundamental Sciences (IPM),
Iranian Light Source Facility (ILSF), Tehran, Iran

Abstract

The Iranian Light Source Facility Storage Ring is under design with a 528 m circumference and will store the electron bunches with 3 GeV energy to produce high-flux radiation that ranges from infrared to hard X-rays. The Stripline is planned to be installed in the ILSF storage ring for beam tune measurement and transverse feedback system (TFS). This stripline can be used for exciting the beam in tune measurement system and damping the transverse instabilities in TFS. In this paper, the design of the striplines for the ILSF storage ring is investigated. Each stripline is matched with 50Ω and has 4 strips (electrodes) that are placed at 45 degrees to the beam axis, the best geometry is achieved and optimized by CST Microwave Studio simulation.

INTRODUCTION

The Iranian Light Source Facility (ILSF) Storage Ring is under design with a 528 m circumference, 176 harmonic number, 100 MHz frequency, and ($a = 26$ mm) vacuum chamber diameter. It will store the electron bunches with 3 GeV energy to produce high-flux radiation that ranges from infrared to hard X-rays. The stripline is planned to be installed in the ILSF storage ring for beam tune measurement and transfer feed-back system.

Each stripline consists of four strips (electrodes), eight coaxial feed-throughs, and water colling connectors. This system is matched to the 50 Ω impedance of the coaxial feed-through cables. The mechanical design of the stripline depends to geometric parameters such as electrode thickness (t), opening angles (φ_s) and the distance between the electrode and chamber (housing) (G) ultimately aiming for a high geometry factors.

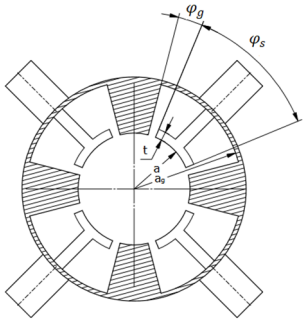

Figure 1: Overview of the ILSF stripline. The cross section of the nominal section.

† Email address samira.mohammadi@ipm.ir.

The kicker stripline plays a crucial role in manipulating the trajectory of the electron bunches by applying precise electromagnetic pulses. This ensures the stability and accuracy of the electron beam, which is essential for producing consistent and high-quality radiation. Additionally, the striplines are involved in tune measurement and beam position determination, contributing to the overall performance of the storage ring. In this paper geometric factors of several design with different geometric parameters are calculated to choose the best design. The wakefield impedance and loss factor of the optimal geometry are then determined using CST Microwave Studio.

DESIGN

Design of the Stripline Geometry

In this design 4 electrodes are placed in the 45,135,225, and 315 degrees at a distance equal to the radius of the storage ring vacuum chamber (a) (Fig. 1). The choice of these angles for the electrodes is to protect them from synchrotron radiation emitted from an upstream dipole magnet [1].

The electrode lengths are given by [2]:

$$l = \frac{c}{4f} = \frac{\lambda}{4} = 75 \text{ cm} \quad (1)$$

Where (c) is the speed of light, (f) is acceleration frequency and (λ) is the wave length. In this length, the first maximum voltage is will be obtained.

The design of the stripline depends to geometric parameters such as electrode thickness ($t = 2$ mm), opening angles (φ_s) and the distance between the electrode and chamber ($G = \varphi_g - a$).

Several designs with varying geometric parameters, were created. Their geometric factors were calculated using the geometry factor formula for comparison [1,3]:

$$g_\perp = \frac{8}{\varphi_g \pi} \sin\left(\frac{\varphi_g}{2}\right) \sin\left(\frac{\varphi_s + \varphi_g}{2}\right) \quad (2)$$

And the impedance is calculated by using CST Microwave Studio's Frequency domain solver (H and E are boundary conditions in ¼ models) by placing a port in the middle of the designs for 4 modes: vertical and horizontal dipole, quadrupole, and sum mode (Figs. 2, 3, 4, and 5). The shunt impedance is given by the following formula [4-6]:

$$Z_{ch} = \sqrt{Z_{sum} \times Z_{quad}} = \sqrt{Z_{V-dipole} \times Z_{H-dipole}} \quad (3)$$

ISBN: 978-3-95450-249-3 ISSN: 2673-5350 doi: 10.18429/JACoW-IBIC2024-TUP08

DESIGN OF BUTTON BEAM POSITION MONITOR FOR THE ILSF BOOSTER

S. M. Alamouti†, N. Khosravi, A. Danaeifard, Z. Rezaei
Iranian Light Source Facility (ILSF),
Institute for Research in Fundamental Sciences (IPM), Tehran, Iran

Abstract

The Iranian Light Source Facility Booster is under design with a 504 m circumference and will accelerate the electron bunches from 150 MeV to 3 GeV. The 50 button-type beam position monitors (BPMs) are considered the non-destructive tools to measure the beam position in the ILSF booster. In this paper, the design of the BPM for the ILSF booster is studied. The BPM blocks have 4 buttons (electrodes) that are placed at 45 degrees to the beam axis. to choose the best geometry, The BPMs with different button diameters and gaps are simulated by the CST Microwave Studio and BpmLab.

INTRODUCTION

The button beam position monitors are non-destructive and are the main beam diagnostics tools used to define and measure the beam position in all synchrotrons. For the ILSF booster, fifty BPMs have been considered to monitor and determine the beam position. Each BPM blocks consist of four identical buttons (electrodes), positioned at 45 degrees relative to the beam axis inside the vacuum chamber. These four electrodes are isolated using ceramic material, specifically alumina, which also prevents vacuum leakage. This system is designed to match the 50 Ω impedance of the coaxial feed-through cables.

As the beam passes through the vacuum chamber, an image charge is induced on the electrodes. By measuring the induced voltage (U) on every electrode, one can obtain the beam position in the horizontal and vertical plane via the following formulas [1]:

$$x = \frac{1}{S_x}\frac{U_{right}-U_{left}}{U_{right}+U_{left}} = \frac{1}{S_x}\frac{\Delta U_x}{\sum U_x} \quad (1)$$

$$y = \frac{1}{S_y}\frac{U_{up}-U_{down}}{U_{up}+U_{down}} = \frac{1}{S_y}\frac{\Delta U_y}{\sum U_y}.$$

In this paper the BPMs with different electrode diameters and thicknesses, upper gaps and gap between the electrodes and housing (gap side) are simulated by the CST Microwave Studio and BpmLab to compare and choose the best design.

DESIGN

In this design, four electrodes are placed at 45, 135, 225, and 315 degrees in the housing that has the same diameter as the booster vacuum chamber (diameter=33 mm) (see Figs. 1 and 2).

At first, four different button diameters were considered for the electrodes [1]. The BPMlab software with delta over sum approach was used to calculate the position detection and BPM sensitivity (see Figs. 3 and 4) [2].

The button capacitance is given by:

$$C_b = \frac{2\pi\varepsilon_0 t}{\ln(\frac{d+g}{d})} \quad (2)$$

where d is electrode diameter, t is button thickness and g is the upper gap.

The monitor constant given by:

$$k_{x,y}(mm) = \frac{1}{S_{x,y}(0,0)} \quad (3)$$

where $S_{x,y}(0,0)$ is the proportional constant when the beam is in the center of the chamber (see Table 2).

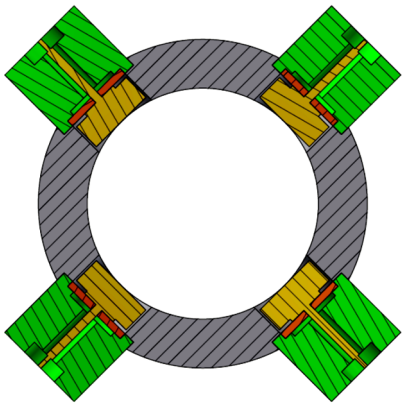

Figure 1: Overview of four button installed in the booster.

Table 1: Design of Button BPM for the ILSF Booster with Different Button Diameter

Geometry	Design			
	A	B	C	D
Button diameter(mm)	5	7	10	13
Button thickness (mm)	4	4	4	4
side gap (mm)	0.3	0.3	0.3	0.3
upper gap (mm)	0.5	0.5	0.5	0.5
button capacitance (pF)	1.963	2.707	3.823	4.934

† samira.mohammadi@ipm.ir

ISBN: 978-3-95450-249-3 ISSN: 2673-5350 doi: 10.18429/JACoW-IBIC2024-TUP09

PROTOTYPE OF BPM ELECTRONICS FOR FEL-HMF*

Wei Peng†, Shichuang Ding, Anhui University, Hefei, China

Abstract

This paper presents a prototype of BPM electronics for experimental installation of free electron laser and high magnetic field (FEL-HMF). FEL-HMF integrates mid-long Infrared free electron laser, high magnetic field and cryogenic, which is a critical apparatus for new advanced materials especially for low power-consume electronic materials. The BPM electronics consists of two ADC chips and one FPGA SoC. The ADC has two channels, and sampling rate is 240 Msps. The FPGA SoC implements high speed digital signal and data process. The logic part of FPGA SoC is running signal process. The processor part of FPGA SoC runs Linux operating system and EPICS-based user application program. This BPM electrons has been tested and analyzed in lab. Its X and Y position is ~1.4 μm (RMS).

INTRODUCTION

The experimental facility of free electron laser and high magnetic field (FEL-HMF) is been building by Anhui University in Hefei, China. It is the first large-scale scientific facility constructed by Anhui university and is a unique integration of free-electron laser, high magnetic field, and low-temperature environment. This cutting-edge technology is a vital tool for studying the energy level structure of materials, dynamical processes, and other scientific issues. The facility is primarily concerned with the investigation of quantum materials, with a particular emphasis on low-power electronic materials. However, it also serves as a crucial experimental platform for a diverse range of multi-disciplinary frontiers, including energy materials, bio-materials, medicine, and health materials.

To facilitate the advancement of multidisciplinary research on low-power electronic materials, the facility is equipped with five experimental stations. These stations can be enhanced or expanded in accordance with emerging research needs.

The Ultrafast Infrared Spectroscopy Experimental Station: is a research facility dedicated to the study of ultrafast phenomena. The objective is to achieve ultrahigh time resolution at low temperatures and in high magnetic field environments, and to explore the dynamics of ultrafast time resolution in materials.

The Scanning Probe Microscopy Station: combination of a mid-infrared laser, a low-temperature environment, and a scanning probe within a high magnetic field allows for the investigation of light-matter interactions at the nanoscale level, as well as the correlation between these interactions and the electronic density of states of materials.

The Magneto-Optical Experimental Station is a research facility dedicated to the study of magneto-optical phenomena. The system is designed for broad spectroscopic and optical polarisation measurements in magnetic fields. It integrates broad-energy and high-resolution spectroscopic characterisation, and is capable of resolving band relations and interactions of excited states in quantum materials.

The Multi-field Control Experimental Station has been established with the objective of achieving optical and electrical characterisation of electronic materials under in-situ multi-field control. Furthermore, the station is intended to facilitate multi-dimensional probing and control of quantum materials and devices.

The Integrated Characterization Station is a platform that enables the comprehensive analysis of materials and structures. The combination of integrated spectroscopy and near-field optical microscopy allows for the comprehensive analysis of light-matter interactions in materials, from macroscopic to microscopic scales.

The experimental facility of free electron laser and high magnetic field will provide the aforementioned experimental stations with radiation at long wavelengths of 2.5-200 micrometres and energies of 10-100 millijoules. The electron beam parameters of the electron linear accelerator are as shown in the Table 1.

Table 1: Margin Specifications

Parameter	Values
Wavelength (μm)	2.5-200
Frequency (THz)	120-1.5
Macro Pulse Average Power (@119MHz) (W)	0.6
Micro pulse power (MW)	5
Micro pulse energy (mJ)	10-100
Micro pulse width (ps)	<10
Bandwidths $\Delta\lambda/\lambda$(%)	0.5-2
Macro pulse repletion rate (Hz)	2-10
Micro pulse repletion rate (MHz)	119, 59.5, 29.75

The electron linear accelerator comprises a pulsed thermionic cathode grid-controlled electron gun (operating at repetition frequencies of 119, 59.5 and 29.75 MHz), a pre-buncher operating at a frequency of 476 MHz, a travelling-wave buncher operating at 2856 MHz ($2\pi/3$ mode), two travelling-wave linear accelerators operating at 2856 MHz ($2\pi/3$ mode) with lengths of approximately 2 m, and beam transport lines. Figure 1 shows layout of FEL-HMF.

The electron gun is controlled by a high-voltage pulse generator, and the repetition frequency of the electron beam is adjustable to 119, 59.5, and 29.75 MHz. The pulse structure is illustrated in Fig. 2. The electron beam is pre-polymerised by the pre-buncher and subsequently enters the buncher, where it is compressed to a length of

* Work supported by the Department of Education Anhui Province.

† 24013@ahu.edu.cn

ISBN: 978-3-95450-249-3 ISSN: 2673-5350 doi: 10.18429/JACoW-IBIC2024-TUP10

A HIGH-PRECISION LOW-LATENCY DBPM PROCESSOR FOR HALF*

J. J. Qin, Y. Tang, K. X. Hou, Z. Y. Li, L. Zhao†
State Key Laboratory of Particle Detection and Electronics, University of Science and Technology of China, Hefei, China
Department of Modern Physics, University of Science and technology of China, Hefei, China

Abstract

Hefei Advanced Light Facility (HALF) is a fourth-generation vacuum ultraviolet and X-ray diffraction limit synchrotron radiation (DLSR) light source under construction. It is expected to have an ultra-low emittance and an extremely small beam size, which requires high-precision orbit detection and fast feedback control. The processor is the key component of the digital beam position monitor (DBPM) and control system, which is required to provide a submicrometer resolution in beam position measurement with a processing latency of lower than 90 μs. This paper presents the design and testing of a high-precision low-latency DBPM processor. In order to reduce the latency and ensure the high position resolution, a specific higher sampling frequency is chosen to reduce the quantization noise platform of the analog to digital convertor and an optimized low-order filter is adopted. Specialized efforts are devoted to the low jitter sampling clock generation and low noise analog circuit design. Furthermore, a dual-pilot tone structure was employed to compensate the gain variations across the four channels of the beam monitor sensor. The laboratory test results show that the DBPM has a position resolution of better than 400 nm for turn-by-turn acquisition, better than 90 nm for fast acquisition at 20 kHz rate, and better than 20 nm for slow acquisition at 10 Hz rate, with a total latency of less than 80 μs.

INTRODUCTION

The fourth-generation synchronous radiation source has a higher brightness and smaller beam size compared to the previous light sources which means a higher stability of fast orbit feedback control is needed. Typically, a fast orbit feedback system consists of beam position monitors (BPMs), distributed controllers and correction magnets [1]. The stability of the beam orbit is critically dependent on obtaining high-resolution beam position data and minimizing feedback latency [2-3].

BPMs are non-invasive sensors installed along the cavities of synchrotron light sources to measure the lateral position of the beam. Their general structure is depicted in Fig. 1. Within the cavity, four probes interact electromagnetically with the passing particle beam to capture positional information. The electrical signals collected by these probes undergo analog manipulation, are subsequently digitized, and the beam position is then determined through digital signal processing.

* Work supported by the Fund of National Synchrotron Radiation Laboratory at University of Science and Technology of China (KY2360000005) and the Youth Innovation Promotion Association, CAS.
† zlei@ustc.edu.cn

The Hefei Advanced Light Facility (HALF) is a fourth-generation light source under construction using a diffraction-limited storage ring. Its radiation spectrum is mainly located in the vacuum ultraviolet and soft x-ray regions [4]. The main expected parameters of HALF storage ring are given in Table 1.

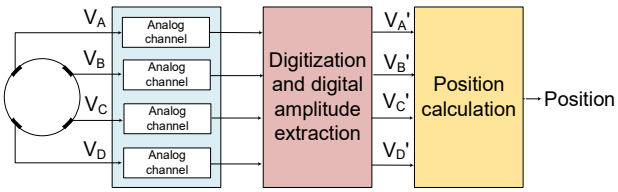

Figure 1: The general structure of beam position monitor.

Table 1: Expected Parameters of HALF Storage Ring

Parameter	Value
Circumference	480 m
Energy	2.2 GeV
RF frequency	499.8 MHz
Harmonic number	800
Current	>100 mA
Natural beam emittance	85.1 pm·rad
Horizontal beam size	>5 μm
Vertical beam size	>2 μm

To achieve ultra-low emittance and an ultra-small beam size, a high-resolution, low-latency beam position monitor is essential. In order to meet the beam orbit stability requirements of HALF, the beam position monitor system must achieve a position resolution of less than 200 nm in Fast Acquisition (FA) mode at a sampling rate of approximately 20 kS/s, providing precise position information for correction calculations. Additionally, the processing latency must be less than 90 μs to ensure that the feedback system maintains sufficient closed-loop bandwidth to suppress high-frequency interference.

This paper presents the design of a HALF Digital Beam Position Monitor (DBPM) prototype electronics. To achieve the desired high position resolution and low latency, we analyze the key factors influencing position resolution and system latency within the beam position monitor system. The design incorporates a pilot tone compensation structure, low-noise analog manipulation, and a low-jitter sampling clock to enhance resolution. Furthermore, a higher sampling frequency combined with a low-order digital low-pass filter is employed to minimize latency.

ISBN: 978-3-95450-249-3 ISSN: 2673-5350 doi: 10.18429/JACoW-IBIC2024-TUP11

BEAM POSITION MONITORS FOR THE HEPS

J. He*,[1], Y. F. Sui[1,2], Y. Y. Du[1], C. Y. Liang[1,2], H. Z. Ma[1], Y. Zhao[1], W. Zhang[1], T. G. Xu[1], J. H. Yue[1], J. S. Cao[1,2]

[1]Institute of High Energy Physics, Chinese Academy of Sciences, Beijing, China
[2]University of Chinese Academy of Sciences, Beijing, China

Abstract

At the High Energy Photon Source (HEPS), a high orbital stability of typically 10 % of the beam size and angular divergence must be achieved, which implies that the beam orbit must be stabilized to the sub-micrometer level. A button and stripline beam position monitor (BPM) were designed and fabricated. 3700 feedthroughs and 720 BPMs have been made and tested. The feedthroughs are sorted by the capacitance which was measured by the TDR. The position accuracy of the button and fiducial were measured by Coordinate Measuring Machine which shown an accuracy of dozens of μm. The characteristic impedances of the stripline were designed to be 50 Ω and confirmed by TDR measurements. Measurement results in the commissioning stage and a stretched wire calibration procedure show that the quality of the HEPS BPMs is pretty good.

INTRODUCTION

The High Energy Photon Source is the fourth-generation synchrotron light source being built by the Institute of High Energy Physics in Huairou, a suburb of Beijing [1-3]. It has extremely low emittance and extremely high beam orbit stability requirements. The beam position detector is one of the most important beam measurement systems, with a large number and wide distribution range, playing a crucial role in adjusting the beam of the accelerator and measuring multiple beam parameters.

Including spare parts, we have manufactured over 900 sets of BPM blocks, consuming over 200 pin-type and 3500 button-type feedthroughs [4-6]. We classified button type wall penetrators based on capacitance values and mechanical dimensions, and paired the measured values with BPM cavities one by one, see Table 1.

Table 1. Major Physical Parameters of the HEPS [1, 4]

	Parameter	Symbol	Value
Storage Ring	Energy (GeV)	E_0	6
	Circumference (m)	C	1360.4
	Current (mA)	I	200
	Bunch number (Normal/High charge mode)	N	680/63
	Bunch length without/with harmonic cavities (mm)	σ_z	3.0/30
	Harmonic number	H_f/H_h	756/2268
	RF frequency (MHz)	f_{RF}	166.6/499.8
LINAC	Accelerating frequency (MHz)	f_{linac}	2998.8
	Bunch charge of macro-bunch (nC)	Q_{linac}	2.5
Booster	Accelerating frequency (MHz)	$f_{booster}$	499.8
	Bunch charge / accumulation (nC)	$Q_{booster}$	2/15

* hejun@ihep.ac.cn

BUTTON CHARACTERIZATION

Button capacitance has been measured by TDR method and the results are shown in Fig. 1. The average value of 3500 button capacitance is 2.399 pF and the standard deviation is 0.053 pF. The capacitance is derivable from the risetime of the button measured by TDR which [7]. The hardware details can be found in reference [8].

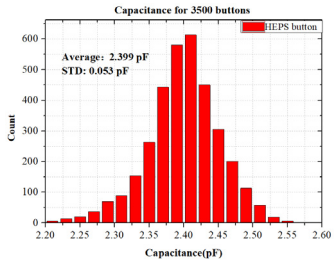

Figure 1: The distribution of 3500 buttons capacitance used in the HEPS.

Figure 2 shows the button position deviation measured by Coordinate Measuring Machine (CMM). The dynamics and physical aperture of the storage ring are smaller than the other locations, so the position accuracy for storage ring buttons are stricter too. The distance from the button to the center of the BPM pipe were measured then subtracted by the nominal value, which is 11 mm, the statistics histogram of 1500 buttons shown that the deviation average value is 40 μm and the standard deviation value is 22 μm. The corresponding values for the Booster ring buttons are 50 μm and 31 μm. Most of the button is sunken rather than protruding. The button position accuracy is determined by the precision of the machining process of the BPM block and the feedthroughs, the welding procedure.

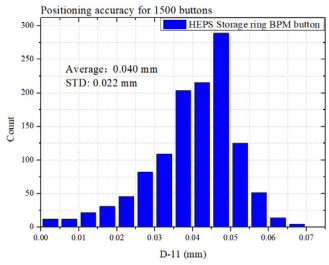

Figure 2: The position accuracy of 1500 buttons measured by CMM.

The nominal value of the distance between the welding point and the button is 20 mm as shown in [6]. Two batches button were measured and the results are shown in Fig. 3. There are two batches feedthrough provided by the same vendor, which the average and standard deviation are 20.103 and 0.027 mm for batch 1 which the amount is 200.

ISBN: 978-3-95450-249-3 ISSN: 2673-5350 doi: 10.18429/JACoW-IBIC2024-TUP12

OPTIMIZATION OF THE KICKER/BPM DESIGN WITH TAPERED STRIPLINES *

S. Bilanishvili†, M. Zobov, Accelerator Division, Laboratori Nazionali di Frascati, Frascati, Italy

Abstract

The injection kicker design exploiting striplines and linear taper connections of the striplines to the feedthroughs was proposed and has been successfully used in the DAΦNE electron-positron collider. Such a design has helped to reduce the device beam coupling impedance, to improve the uniformity of the deflecting electromagnetic fields and to provide better matching with the feedthroughs. In this paper we propose using nonlinear taper connections in order to decrease further the beam coupling impedance. We have performed numerical simulations and analytical studies of several nonlinear tapers demonstrating that the coupling impedance can be substantially reduced while keeping or even improving the transfer (signal) impedance of the stripline kickers (or BPM). The effect of the nonlinear tapering is particularly important for short stripline devices when the taper length is limited due to lack of available space and/or when the striplines are moved closer to the beam in order to increase the device shunt (signal) impedance.

INTRODUCTION

Stripline kickers are commonly used for injection in the storage rings and in the transverse feedback systems. The beam coupling impedances of the kickers, normally due to non smooth transitions from feedthroughs to striplines, show large contributions to the total impedance budget. In the high energy, low emittance light sources, the necessity of the short pulse bottom width and strong deflection field requires the kicker to have a short length and a small gap between the electrodes, respectively.

Besides, in the future machines a drastic reduction of the stored beam perturbation during the injection is mandatory to improve their performance. This is particularly important for the top-up operation in the modern synchrotron light sources. So the use of several advanced injection schemes has been proposed and elaborated in order to solve these problems and to overcome the limitations, one can see for example the review papers [1, 2]. These are swap-out injection, injection with a nonlinear magnet kicker, longitudinal on-axis injection, and a shared oscillation scheme using a fast kicker etc. For most of such schemes, kickers with short pulses with a pulse length comparable to the bunch spacing are required. Stripline kickers are a natural choice to satisfy this requirement. The beam coupling impedance of the striplines depends on the characteristic impedance of a transmission line formed by the strips and the vacuum chamber pipe Z_c, the strip length l and its radius r as well as on the strip coverage factor g, [3]

$$Z_{\parallel}(\omega) = Z_c \left(\frac{g}{2\pi}\right)^2 \left(\sin^2\frac{\omega l}{c} + j\sin\frac{\omega l}{c}\cos\frac{\omega l}{c}\right) \quad (1)$$

$$Z_{\perp}(\omega) = \frac{c}{r^2}\left(\frac{4}{g}\right)^2 \left(\sin^2\frac{g}{2}\right)\left[\frac{Z_{\parallel}}{\omega}\right]. \quad (2)$$

However, these formulas are obtained in the approximation that all RF power induced by the impedance is dissipated in the external loadings. One has to take into account the other very important impedance contribution arising due to the beam-excited electromagnetic fields which do not couple to the loadings. For example, the parasitic HOMs can be trapped in the kicker structure. In addition, the abrupt transitions between the striplines and feedthroughs can be yet another large impedance source. As a possible solution for impedance reduction, the tapered stripline kickers, designed and successfully used for beam injection in DAΦNE [4], can be considered. The same design with the linear tapers has been proposed also for use in the ILC damping rings [5] and is considered for application in DIAMOND-II [6] and APS-U [7].

In this paper we investigate if an application of nonlinear tapers connecting the striplines to the feedthroughs can help decreasing further the beam coupling impedance. Indeed, in the past it was demonstrated that a considerable impedance reduction can be achieved by using the nonlinear tapering for azimuthally symmetric structures [8–10]. Similarly we study if the nonlinear tapers can be useful also for the striplines. However, differently from the azimuthally symmetric case, the striplines have a finite width that has to vary along the tapers in such a way to keep the stripline characteristic impedance constant. This is necessary in order to avoid multiple reflections and to match the striplines and the external feedthroughs.

Here we considered several typical nonlinear functions for the tapered part of the strips Figs.1 and 2.

$$h(z) = h_{min}(1 + (h_{max}/h_{min} - 1)z/L) \quad (3)$$

$$h(z) = h_{min}(h_{max}/h_{min})^{z/L} \quad (4)$$

$$h(z) = \frac{h_{min}}{(1 + ((h_{min}/h_{max})^{1/2} - 1)z/L)^2} \quad (5)$$

$$h(z) = \frac{h_{min}}{1 + ((h_{min}/h_{max}) - 1)z/L}, \quad (6)$$

with h(z) being the distance between strips and a beam along the beam path z.

* This project has received funding from the European Union's Horizon 2020 research and innovation programme under grant agreement [871072].

† shalva.bilanishvili@lnf.infn.it

ISBN: 978-3-95450-249-3 ISSN: 2673-5350 doi: 10.18429/JACoW-IBIC2024-TUP13

DESIGN OF BEAM POSITION MONITOR OF WUHAN PHOTON SOURCE

Haoyu Dong, Zhengqiu Luo, Zhengzheng Liu†
Huazhong University of Science and Technology, Wuhan, China
Geng Wei, HaoHu Li, Wuhan University, Wuhan, China

Abstract

Wuhan Photon Source (WHPS), as a fourth-generation synchronous light source, imposes stringent requirements on the resolution and longitudinal coupling impedance of the Beam Position Monitor (BPM). To address the need for beam current monitoring in its 1.5 GeV diffraction-limited storage ring, an optimized design scheme for button BPM is proposed. Additionally, the structure of the BPM feedthrough is enhanced, and a detailed investigation into the impact of various materials on the longitudinal coupling impedance of the BPM is conducted. These findings serve as a valuable reference for the future design of similar BPM systems.

INTRODUCTION

WHPS utilizes a double-ring design [1], receiving full energy injection from a linear accelerator (LINAC). This configuration comprises a 180-meter-long low-energy diffraction-limited synchrotron radiation source operating at 1.5 GeV and a 927-meter-long fourth-generation medium-energy diffraction-limited synchrotron radiation source operating at 4.0 GeV. The overall schematic of the facility is illustrated in Fig. 1 [2].

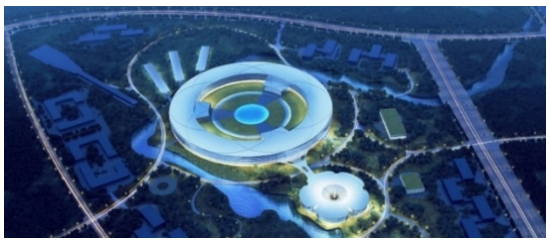

Figure 1: WHPS global schematic.

The fundamental design parameters of the WHPS are presented in Table 1 [3]. For the 1.5 GeV storage ring, as indicated in the Table 1, the beam bunch exhibits an RMS length of 5.4 mm, a beam current intensity of 500 mA, and operates at an RF frequency of 499.654 MHz, representing a short beam bunch characterized by a high repetition rate and substantial charge. Within the diffraction-limited storage ring light source, maintaining beam orbital stability at a sub-micrometer scale necessitates the provision of real-time and precise beam lateral position data by the beam position measurement system.

As the cornerstone of the beam position measurement system, the performance of the BPM significantly influences the overall measurement accuracy. In the realm of light sources founded on diffraction-limited storage rings, two primary types of BPM are employed for beam position monitoring: the stripline BPM, suitable for measuring short beam bunches with low charge, and the button BPM, more adept at measuring beam bunches with high charge and a rapid repetition rate. Consequently, the button BPM is better suited for determining the position of beams with high frequencies and currents within WHPS. Hence, this study aims to design a high-resolution button BPM tailored for the 1.5 GeV storage ring of WHPS. When the storage ring operates in SA mode, a position resolution of 0.2 μm is mandated. In FA mode, the required position resolution is 0.6 μm, while in TBT mode, a position resolution of 1 μm is necessary. These specifications serve as guidelines for the design of the electrode geometry.

Table 1: Major Physical Parameters of the WHPS

Parameter	Symbol	Value
Energy	E_{low}	1.5 GeV
Radio frequency	f_{RF}	499.654 MHz
Bunch length	$\sigma_{\mathrm{r\ ms.low}}$	5.4 mm
Current	$I_{avg.low}$	500 mA
Cyclotron frequency	$f_{acc.low}$	1665.5 kHz
Emittance	$\varepsilon_{\mathrm{low}}$	226.4 pm-rad

STORAGE RING BUTTON BPM DESIGN

The primary focus of the button BPM design lies in the feedthrough, with attention directed toward two key aspects: firstly, ensuring that the geometrical parameters of the button pickup electrode align with the position resolution requirements of the beam position measurement system across various operational modes of the storage ring; and secondly, optimizing the wakefield impedance. This optimization primarily involves the design of the structure and selection of materials for the coaxial section within the feedthrough.

BPM Electrode Design

The geometric parameters of the BPM pickup electrode, encompassing the button radius, button thickness, and button gap, play a pivotal role in determining the position measurement accuracy of the BPM system [4]. Drawing from the design expertise of BPMs utilized in prominent advanced light sources both domestically and internationally, as well as practical operational insights [5-7], the specific design choices for this study include a button radius of 3 mm, a button thickness of 2 mm, a button gap of 0.3 mm, and a position gain coefficient (k_i) of 11.5243 mm

† Corresponding author.
Email address：zzliu@hust.edu.cn.

ISBN: 978-3-95450-249-3 ISSN: 2673-5350 doi: 10.18429/JACoW-IBIC2024-TUP15

NEURAL NETWORK TECHNIQUE FOR IMPROVING ACCURACY, RELIABILITY AND ROBUSTNESS OF BEAM POSITION MONITOR SYSTEM

Fang-Qi Huang*[1], Tao-Guang Xu[1], Yan-Feng Sui†[1,2], Jun He[1]
[1]Institute of High Energy Physics, Chinese Academy of Sciences, Beijing, China
[2]University of Chinese Academy of Sciences, Beijing, China

Abstract

The beam position monitor (BPM) is a crucial instrumentation system for the commissioning and operation of the accelerator. Its accuracy and robustness are essential for ensuring the stability of the accelerator. Currently, the beam position is calculated by fitting a polynomial to the four voltage signals obtained from the BPM electrodes in BEPCII and HEPS. To improve the system's robustness, a formula is provided that expresses the relationship between the three voltage signals and the position. The average fitting error is 40 μm, but the error of the three-electrode calculation is not high. Therefore, we propose using neural networks for beam position calculation to improve the system's robustness while guaranteeing its accuracy. This will ensure that the beam position can be provided stably, even in the case of one single electrode error. In our experiments, we use BPM calibration data from HEPS. The trained neural network's performance on the test set meets the accuracy requirements, with an error of less than 15 μm in both four-electrode and three-electrode predictions, and an average value of fitting error is 1 μm. Furthermore, we validate the neural network's generalization ability by using data measured by BPM on HEPS.

INSTRUCTION

Beam Position Measurement (BPM) is a crucial instrumentation system in accelerators, serving as a vital reference for beam commissioning and operation, as well as a fundamental data source for physics research. In HEPS, there are over 700 BPMs used for beam orbit measurement and correction, beam current measurement, beam loss diagnosis and analysis, and other beam state monitoring[1]. The accuracy and robustness of the beam position measurement are essential for ensuring the stable operation of the accelerator. Currently, the beam position is calculated indirectly. Voltage signals measured from four electrodes on BPM, which are then calculated using a formula. The value corrected called beam position and reported to the database. Moreover, there is a set of three-electrode calculations to address the issue of single-electrode signal loss. The existing four-electrode polynomial fitting has an error of approximately 40 μm[2], but the three-electrode calculation does not meet the required level of accuracy. Therefore, we propose using neural networks for beam position calculation to enhance the robustness and ensure the accuracy. This approach will guarantee that the beam position can be provided reliably, even in the case of single-electrode error.

TRADITIONAL BEAM POSITION CALCULATION METHOD

The four electrodes of the BPM measure the voltage as the beam passes over the BPM. The normalized horizontal and vertical beam positions are calculated using Eq. (1)[2].

$$\begin{aligned} X_{\text{norm}} &= \frac{V_1 - V_2 - V_3 + V_4}{\sum_{i=1}^{4} V_i} \\ Y_{\text{norm}} &= \frac{V_1 + V_2 - V_3 - V_4}{\sum_{i=1}^{4} V_i} \end{aligned} \tag{1}$$

where Vi denotes the voltage measured by electrode i. The final beam positions X, Y are then obtained by polynomial fitting approximation as in Eq. (2).

$$\begin{aligned} X &= \sum_{i=0}^{n} \sum_{j=0}^{i} A_{i-j,j} X_{\text{norm}}^{i-j} Y_{\text{norm}}^{j} \\ Y &= \sum_{i=0}^{n} \sum_{j=0}^{i} B_{i-j,j} X_{\text{norm}}^{i-j} Y_{\text{norm}}^{j}, \end{aligned} \tag{2}$$

where n is the highest order of the polynomial fit. Based on the calibration data, the values of a, b were obtained by fitting. When n=6, the average value of the fitting error is 40 μm[2]. When one of the electrodes is out of order, the beam position can be obtained by using deviation[2], but the result is not satisfactory.

BP NEURAL NETWORK CALCULATION METHOD

The BP neural network is composed of neurons, including input, output, and activation functions. The structure of the neural network is divided into three layers: input, hidden, and output. The activation function allows for non-linear mapping of input data, and the number of layers in the hidden layer determines the complexity of the function that can be modeled. Theoretically, two layers of hidden layers are sufficient to fit any bounded continuous function[3]. When training the network, several factors must be considered, such as the neural network structure (including the choice of activation function, number of hidden layers, and number of neurons per layer), data processing (including the selection

* huangfq@ihep.ac.cn
† syf@ihep.ac.cn

ISBN: 978-3-95450-249-3 ISSN: 2673-5350 doi: 10.18429/JACoW-IBIC2024-TUP16

DEVELOPMENT STATUS OF THE BPM SYSTEM FOR THE SPring-8-II STORAGE RING

H. Maesaka*, [1], RIKEN SPring-8 Center, Sayo, Hyogo, Japan
H. Dewa, T. Fujita, M. Masaki, S. Suzuki, S. Takano[2], JASRI, Sayo, Hyogo, Japan
[1]also at JASRI, Sayo, Hyogo, Japan
[2]also at RIKEN SPring-8 Center, Sayo Hyogo, Japan

Abstract

We have developed a button-type BPM system for the fourth-generation light source, SPring-8-II, which is the low-emittance upgrade of SPring-8. In total, 340 BPMs will be fabricated and installed into SPring-8-II. The BPM prototype has been tested in present SPring-8 and almost the same BPM system was installed into the new 3 GeV light source, NanoTerasu. The design of the BPM head for SPring-8-II was recently modified, since the cross-section of the beam pipe was redesigned. BPM signals are transmitted to the readout electronics by radiation-resistant coaxial cables and processed by MicroTCA.4-based electronics. We evaluated the beam position sensitivity, impedance, thermal structure issues, position resolution, long-term stability, and electrical center displacement. The single-pass resolution was less than 100 μm std. for a 0.1 nC injected bunch and the COD resolution was less than 1 μm std. for a wide range of stored current. The long-term stability was within 5 μm for several weeks. The displacement of the electrical center is less than 150 μm std. These results are sufficient for the commissioning and operation of SPring-8-II.

INTRODUCTION

The construction of the fourth-generation light source, SPring-8-II [1–3], is being started, which is the low-emittance upgrade of the third-generation light source, SPring-8. The beam energy will be decreased from 8 GeV to 6 GeV and the lattice structure will be changed from double-bend achromat to five-bend achromat. As a result, the natural emittance will be improved from 2.4 nm rad to 100 pm rad or less and the X-ray brilliance around 10 keV will be increased by about 100 times.

To utilize brilliant X-rays effectively, the electron beam orbit should be monitored precisely and stably and the X-ray optical axis should be stabilized as much as possible. The stability of the beam orbit is required to be within 5 μm for one month. Furthermore, it is indicated that there is no stable closed orbit at the commissioning stage due to the strong quadrupole and sextupole magnets with finite alignment errors. Therefore, the single-pass beam trajectory must be precisely measured by the BPM system and the beam must be steered carefully until a stable closed orbit is found, so-called first-turn steering (FTS). Requirements for the FTS are a precise single-pass resolution of 100 μm std. for a 0.1 nC injected bunch and a small electric and mechanical center error within 200 μm.

We have developed a new button-type BPM system for SPring-8-II, which fulfills the above requirements. Almost the same BPM system was employed for a new 3 GeV light source, NanoTerasu [4–8], and it has been working stably in commissioning and user services. A part of the BPM readout electronics in SPring-8 was replaced with the new system [9] for the adaptive feedforward correction of fast helicity-switching beamlines [10] and the renewal of the old single-pass BPM system [11]. Based on these experiences, we are improving the BPM system design.

In this article, we describe an overview of the BPM system for SPring-8-II, the development status, and evaluated basic performances.

BPM SYSTEM

We employed a button-type BPM for SPring-8-II, which is common for many electron storage rings. In this section, we describe the BPM layout, the BPM head design, BPM support, signal cables, and readout electronics.

BPM Layout

The SPring-8-II storage ring has a total of 48 unit cells, consisting of 44 five-bend cells and 4 long-straight cells. Each five-bend cell has 7 BPMs and each long-straight cell has 8 BPMs, as shown in Fig. 1 together with the magnet arrangement. Thus, 340 BPMs in total will be fabricated and installed.

BPM Head

The cross-section of the beam pipe was originally designed as a squeezed octagonal shape [1, 12, 13] and this design was employed for NanoTerasu [4, 14]. The beam pipe has then been changed to a rhombus shape to reduce the resistive-wall impedance [15]. Since the original beam pipe made of stainless steel has a larger resistive-wall impedance than the new one, copper plating on the inner surface is necessary. However, the new beam pipe has a sufficiently small impedance even if it is made of stainless steel without copper plating.

Therefore, the design of the BPM head has also been modified to fit the new beam pipe, as shown in Fig. 2. The button electrode itself has not been changed from the original design [16]. The diameter of the electrode is 7 mm and that of the hole for the electrode is 8 mm. Therefore, the gap around the electrode is 0.5 mm. The distance from the

* maesaka@spring8.or.jp

ISBN: 978-3-95450-249-3 ISSN: 2673-5350 doi: 10.18429/JACoW-IBIC2024-TUP17

CAVITY BEAM POSITION MONITOR PULSE INJECTION SOURCE

M. S. McCallum*, A. Lyapin, M. Bosman
John Adams Institute at Royal Holloway, University of London, Egham, UK
A. Aryshev, K. Popov, N. Terunuma
The Graduate University for Advanced Studies (SOKENDAI) at
High Energy Accelerator Research Organisation (KEK), Tsukuba, Ibaraki, Japan

Abstract

The Cavity Beam Position Monitor (CBPM) system at Accelerator Test Facility 2 (ATF2, KEK, Japan) operates with attenuation at a reduced 250 nm (vs measured 20-30 nm) resolution to cope with CBPM to magnet misalignment. In addition, CBPMs need regular calibrations to maintain their performance. To address these limitations, a pulse injection system is under development. This system aims to compensate for static offsets by injecting an anti-phase replica of the average beam signal directly into the sensor cavities. The same signal can provide a calibration tone for the whole processing chain and eliminate lengthy beam-based calibrations. Proof of principle tests for such a system have been conducted in December 2023. In this paper, we report on the results of the first beam test, discuss the technical challenges and provide a preliminary hardware specification for future experiments.

INTRODUCTION

The Accelerator Test Facility (ATF) at KEK, Japan, is a dedicated research centre focused on the development and testing of advanced accelerator technologies, particularly for future linear colliders like the proposed International Linear Collider (ILC) [1] and Compact Linear Collider (CLIC) [2]. The primary objective of the ATF is to produce and refine electron beams with extremely low emittance, which is crucial for achieving high precision in particle collisions. To this end, the facility features a damping ring, where the electron beam undergoes a cooling and stabilization process, significantly reducing its emittance. Various sophisticated beam diagnostics tools are employed to measure and optimize beam properties, ensuring the beam's quality and stability.

An extension of the original ATF, the Accelerator Test Facility 2 (ATF2) serves as a critical testbed for the final focus system of the ILC. ATF2 is specifically designed to achieve an extremely small vertical beam size at the interaction point, which is essential for maximizing collision precision in future linear colliders. The facility extracts the electron beam from the ATF damping ring and employs it in experiments that not only validate the design concepts of the ILC's final focus system but also explore innovative methods for controlling and stabilizing the beam. The original goal of ATF2 was to achieve a beam size as small as 37 nm, with the best-reported achievement being a vertical beam size of 41 nm [3]. These advancements are vital for the success of global high-energy physics experiments, making ATF2 a cornerstone in the development of next-generation particle accelerators.

* mark.mccallum@rhul.ac.uk

MOTIVATION

To maintain the 250 nm position resolution at which ATF2 operates, the cavity BPM system is configured with a static beam offset of 250 µm. By injecting a burst of RF at the resonant frequency of the cavity BPM into one port and reading it out from the second port, it is possible to replicate the beam signal. If this replicated signal can be controlled in terms of phase, frequency, amplitude, and timing, it could be used to cancel out the cavity response to the beam signal via an anti-phase replication. This injected RF could effectively compensate for the static offset required to maintain position resolution. Additionally, such a signal could be employed to calibrate the cavity BPM system, either without the beam or in situ with the beam, potentially reducing the time required for beam-based calibration.

CAVITY BPM SYSTEM

One of the major diagnostic tools employed at ATF2 is the Cavity Beam Position Monitor (Cavity BPM) system [4,5] used to measure the position of the beam to within ±250 nm [5]. Cavity BPMs are an electromagnetic discontinuity within the beam line that is geometrically coupled to the dipole mode of the passing electron bunch. The dipole mode has been chosen as it is position-sensitive, as the amplitude of the outputting signal is proportional to the beam's position. The output signal of a CBPM is an exponentially decaying sine wave:

$$V(t) = q(Ax + Bx' + C\theta)e^{-\left(\frac{t}{\tau}+i\omega t\right)}, \quad (1)$$

where q is the bunch charge, A, B and C are sensitivities to beam displacement x, angle x' and bunch tilt θ, τ is the decay constant of the cavity mode and ω its angular frequency [6].

An example of Eq. 1 can be seen in Fig. 1. Here the blue line represents the fitted data and the orange line is the beam signal with the dc offset removed. This data was taken from the digitises at ATF2 with a sampling frequency of 103 MHz and a down-converted signal frequency of approximately 25 MHz.

ANALYSIS METHOD

The main analysis technique employed here is The Hilbert Transform. The transform is a convolution of the time do-

ISBN: 978-3-95450-249-3 ISSN: 2673-5350 doi: 10.18429/JACoW-IBIC2024-TUP18

DESIGN OF A STRIPLINE BPM FOR CSNS-II INJECTION UPGRADE*

B. Zhang, M. A. Rehman, R. Yang†, X. Li, S. Wang
Institute of High Energy Physics, Beijing, China
also at China Spallation Neutron Source, Dongguan, China

Abstract

The China Spallation Neutron Source (CSNS) accelerator complex is upgrading the injection area to improve the beam-loss control during beam injection and acceleration in the Rapid Cycling Synchrotron. The linac beam energy will be increased from 80 MeV to 300 MeV employing a new superconducting accelerating section, and the beam power at the spallation target will be 500 kW. To accomplish these requirements, a stripline-type beam position monitor(BPM) has been designed with a large aperture and 50 Ω stripline electrodes. This BPM has an inner diameter of 52 mm and is used to detect the beam with a current of 10-30 mA and a pulse width of 100-500 μs. Several geometrical and electrical parameters have been optimized with numerical simulation. This paper will describe the design and optimization of the stripline-type BPM in detail, and simulation results are discussed.

INTRODUCTION

The China Spallation Neutron Source (CSNS) complex is designed to provide a multidisciplinary platform for scientific research and applications by national institutions, universities, and industries [1]. The accelerator of CSNS consists of a low-energy linac, a Rapid Cycling Synchrotron (RCS) and two beam transport lines. For CSNS-II, the accelerator will be upgraded to 500 kW beam power with a beam energy of 1.6 GeV and a repetition rate of 25 Hz. This upgrade involves increasing the linac beam energy from 80 MeV to 300 MeV by using a new superconducting accelerating section [2]. This paper presents the optimization and design of a stripline-type beam position monitor (BPM) with large aperture and 50 Ω stripline electrodes through numerical simulation, while also including error analysis.

BEAM POSITION MONITOR (BPM)

The stripline BPM serves as a broadband coupler, with its pickups operating on the principle of image currents. For the off-centred beam in a beam pipe, the beam charge at the position ($x = r\cos\varphi, y = r\cos\varphi$) distributes wall charges in the beam pipe [3], as shown in Fig. 1.

By solving the equivalent 2-dimensional electrostatic image charge problem, the solution can be expressed as a series expansion in Eq. (1).

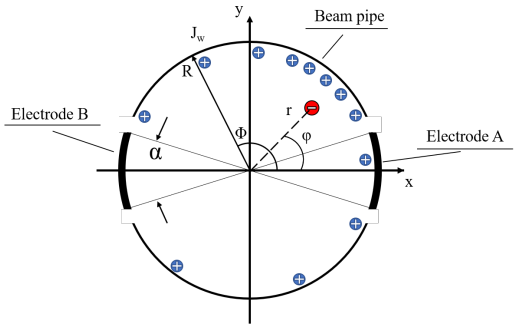

Figure 1: Cross section of BPM pick up model used for calculations.

$$J_w(R,\Phi,r,\varphi) = -\frac{I_{\text{beam}}}{2\pi R}\left[1+\sum_{n=1}^{\infty}\left(\frac{r}{R}\right)^n \cos n(\Phi-\varphi)\right] \quad (1)$$

Consequently the BPM electrode covering an arc α generates a wall current, as is shown in Eq. (2).

$$I_{\text{elec}} = R\int_{-\alpha/2}^{+\alpha/2} J_w(R,\Phi,r,\varphi)\mathrm{d}\Phi \quad (2)$$

Utilizing Eq. (2) and considering the identical BPM pickup electrode transfer impedance, the horizontal position characteristic with x/R being the normalized horizontal beam position can be deduced[3]:

$$\begin{aligned}\frac{\Delta}{\Sigma} = \frac{A-B}{A+B} &\simeq \frac{4\sin(\alpha/2)}{\alpha}\frac{x}{R} + \text{higher order terms} \\ &= \text{hor. position} \approx \frac{2}{R}x\end{aligned} \quad (3)$$

For the strip design of BPM, it is crucial to have impedance matching of vacuum feedthrough and stripline electrode to prevent the beam signal reflection. The impedance of the stripline can be calculated using the following equation[4]:

$$Z = \frac{Z_0}{4\pi}\ln\left\{1+4\left(\frac{h}{w_{eff}}\right)\left(8\left(\frac{h}{w_{eff}}\right)+\sqrt{64\left(\frac{h}{w_{eff}}\right)^2+\pi^2}\right)\right\} \quad (4)$$

where

$$w_{eff} = w + \left(\frac{t}{\pi}\right)\ln\left\{\frac{4e}{\sqrt{\left(\frac{t}{h}\right)^2+\left(\frac{t}{w\pi+1.1t\pi}\right)^2}}\right\} \quad (5)$$

Figure 2 shows the parameter. w is the width of the stripline determined by its angle due to the fixed inner electrode diameter. e is the natural constant (=2.718). h is the

* Work supported by National Natural Science Foundation of China (No. 12305166) and the Natural Science Foundation of Guangdong Province, China (No. 2024A1515010016)

† yangrenjun@ihep.ac.cn

ISBN: 978-3-95450-249-3 ISSN: 2673-5350 doi: 10.18429/JACoW-IBIC2024-TUP20

DEVELOPING A NEW BEAM POSITION MONITOR ELECTRONICS FOR HIPA, THE PSI HIGH INTENSITY PROTON ACCELERATOR

B. Keil†, P. Huber, Paul Scherrer Institute, Villigen, Switzerland

Abstract

The High Intensity Proton Accelerator (HIPA) at PSI presently has a radio frequency (RF) beam position monitor (BPM) system based on 20-year-old Xilinx Virtex-2 Pro System-on-Chips (SoC), with application-specific integrated circuits (ASICS) as direct digital downconverters (DDCs). For the planned upgrade of the electronics as well as for new HIPA projects, we started the development of a new HIPA BPM electronics, using a generic electronics platform called "DBPM3" that is already being used for SwissFEL and SLS 2.0 electron BPM systems. In this contribution, first test results of a DBPM3-based HIPA BPM electronics prototype are presented, including a comparison with the present electronics.

INTRODUCTION

The HIPA Accelerator Facility

In the HIPA facility, shown in Fig.1, a proton beam is accelerated in three stages. A Cockcroft-Walton pre-accelerator generates an 870 keV CW beam. Then a 1st cyclotron ("injector 2") accelerates this beam to 72 MeV, followed by a 2nd cyclotron ("ring cyclotron") with 590 MeV final beam energy. Up to 2.4 mA beam current result in a world leading CW beam power of up to 1.4 MW.

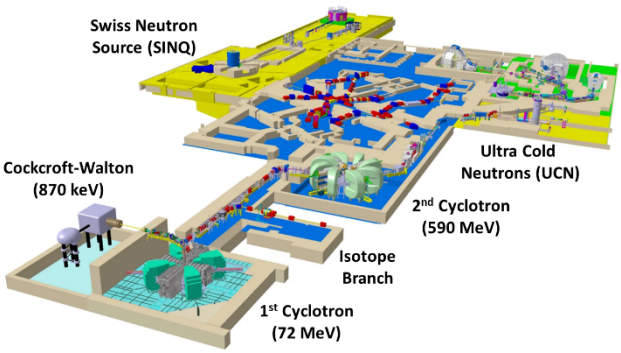

Figure 1: High Intensity Proton Accelerator (HIPA).

The 590 MeV beam passes two rotating targets, where a fraction of the protons is converted to muons and pions that are directed to several experimental beamlines. Most protons pass these targets, finally reaching the so-called SINQ (Swiss Spallation Neutron Source) target, where CW neutron beams for a larger number of beamlines are generated.

The 72 MeV proton beam can also be redirected to a side branch for production of radioactive isotopes, mainly for medical use. Part of the 590 MeV beam can be redirected with a fast kicker to another spallation target for the generation of ultracold neutrons ("UCN") for fundamental particle physics research. The UCN proton beam is usually pulsed with a low duty cycle, where the BPM system records data after an external trigger with multi-kHz data rates (presently 50 kSamples/s) and bandwidth (presently 22 kHz) for sub-millisecond time resolution.

Motivation

The present HIPA BPM electronics was developed at PSI about 20 years ago [1]. In the near future, additional BPMs are required, for new HIPA extension projects like IMPACT [2], as well as for improved monitoring of the HIPA beam especially downstream of the rotating targets. Due to the limited number of spares for our present electronics, we will equip these new BPM pickups with new electronics, based on the so-called DBPM3 platform. This generic BPM platform, developed at PSI, is already used at SwissFEL [3] and the Swiss Light Source [4].

In a 2nd step, we will replace all present HIPA BPM electronics with this DBPM3 based solution. This general upgrade is motivated primarily by maintenance reasons, due to the age and growing maintenance effort for the present system, the limited number of spares, and the growing number of obsolete electronics parts. Furthermore, the radiation-hard RF front-end (RFFE) electronics of the present system is installed in the accelerator bunker not too far from the beam pipe for historical reasons, with short coaxial cables from BPM pickup to RFFE, and long triaxial cables (partly re-used from the previous system) to the technical gallery where ADCs and digital back-end electronics are installed. For the DBPM3 upgrade, this historical topology (from times where HIPA had much lower beam current and radiation levels) will be changed, with new coaxial RF cables from pickups directly to the DBPM3 electronics (including RFFEs) in the technical gallery. This will avoid exposure of maintenance personnel during hardware replacements and repairs of activated RFFEs, in addition to speeding up replacements and reducing accelerator downtime and beam interruptions for accelerator bunker access.

BPM PICKUPS

The 72 MeV and 590 MeV cyclotrons in HIPA both use 50.63 MHz as working frequency for their main RF accelerating cavities, thus bunching the initial CW beam of the Cockcroft-Walton pre-accelerator at this frequency. The HIPA RF BPMs measure the position of this bunched beam with coils (having a single winding) rather than button electrodes as RF pickups in the beam pipe.

Measurement Frequency

As shown in Fig. 2, the HIPA BPM pickup coils have a broadband response, where the present HIPA RF BPM electronics uses the 2nd harmonic at 101.26 MHz for position measurement, instead of 50.63 MHz. This choice avoids systematic measurement errors that may be caused

† boris.keil@psi.ch

ISBN: 978-3-95450-249-3 ISSN: 2673-5350 doi: 10.18429/JACoW-IBIC2024-TUP21

ELECTRON BUNCH POSITION DETERMINATION USING A HIGH FREQUENCY BUTTON BEAM POSITION MONITOR IN THE AWAKE FACILITY

B. Spear*, P.N. Burrows, John Adams Institute, University of Oxford, Oxford, United Kingdom
C. Pakuza, M. Krupa, S. Mazzoni, T. Lefevre, M. Wendt, CERN, Geneva, Switzerland
S. Lui, TRIUMF, Vancouver, Canada

Abstract

The AWAKE facility uses novel proton beam-driven plasma wakefields to accelerate electron bunches over 10 m of Rubidium plasma. Precise monitoring of 2 diverse beam types necessitates an electron beam position monitor (BPM) working in a frequency regime of tens of GHz. A high frequency conical button-style BPM with a working regime of up to 40 GHz has been investigated as a way to discriminate the electromagnetic fields of 19 MeV, 4 ps electron bunches propagating spatially and temporally together with a 400 GeV, 170 ps proton bunch in the AWAKE common beamline. The sensitivity of the HF BPM to the electron beam position is determined under various beam conditions, with both electrons and protons, and integration with a TRIUMF front-end is discussed.

INTRODUCTION

In the Advanced Wakefield Experiment (AWAKE) at CERN, a 400 GeV, 48 nC proton bunch from the Super Proton Synchtrotron (SPS) is used to drive plasma wakefields in a 10m long rubidium vapor source. To ionize the rubidium vapor, a 100 femtosecond laser pulse delivering up to 500 mJ of energy is employed. Initially the proton bunches are 6 to 12 cm long, however, they undergo self-modulation in plasma, breaking into a series of microbunches that resonantly drive large wakefields. The self-modulation is seeded by the relativistic ionization front.

The proton beam, extracted from the SPS up to four times per minute, has a bunch population ranging between 1 and 3×10^{11} protons. Before entering the plasma, the beam is focused to a transverse size of 200 µm. When an electron beam is injected into the plasma at the correct position and phase relative to the proton microbunches, it can be accelerated through the wakefields generated in the plasma.

During the initial phase of AWAKE, known as Run 1 (2016-2018), the experiments successfully demonstrated the self-modulation process [1] and achieved electron acceleration from 18 MeV to 2 GeV [2], showcasing the potential of this novel acceleration technique. AWAKE Run 2 commenced in 2021, staged in four phases and due to operatate over a number of years. The goal of Run 2 is to accelerate electrons to high energies (gradient of 0.5 – 1 GV/m), while controlling the beam quality and to demonstrate the scalability of the acceleration [3].

* bethany.spear@physics.ox.ac.uk

Table 1: AWAKE Nominal Beam Parameters

Beam	proton	electron
Energy / MeV	4×10^5	19
Charge /nC	48	0.1-0.6
Bunch Length /ps	250	1-5

The beam structure in AWAKE is distinct to this experiment, as outlined in Table 1. The variation in bunch length and intensity results in a frequency spectrum dominated by different bunch types in various regimes, as illustrated in Fig. 1. The existing electron beam position monitors (eBPMs), operating at 404 MHz [4], register a significantly stronger signal from the proton beam compared to the electron beam, making it impossible to distinguish the electron position when both beams are present. At 1.88 GHz, the spectral power of the two beams is equal if one assumes Gaussian bunch profiles. To isolate and measure the electron signal effectively, a much higher operating frequency in the tens of GHz range is necessary.

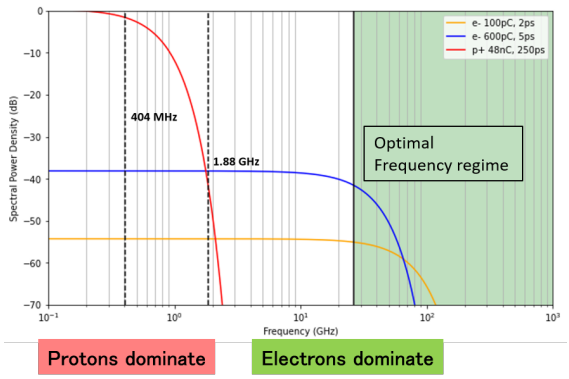

Figure 1: The Frequency spectra of the proton and electron bunches at AWAKE, assuming a Gaussian longitudinal bunch profile.

A HIGH FREQUENCY BUTTON BPM

The most widely used non-invasive beam position monitors are electrostatic, or capacitive pickups (PU). These pickups consist of 4 metallic electrodes placed symmetrically in the x and y planes of the beam pipe at the location where the beam position is to be measured. As the beam passes through the vacuum chamber, the horizontal and vertical displacement of the beam with regards to the centre of the beam pipe can be determined by the magnitude of the

ISBN: 978-3-95450-249-3 ISSN: 2673-5350 doi: 10.18429/JACoW-IBIC2024-TUP23

DEVELOPMENT OF AN AUTOMATIC CALIBRATION SYSTEM FOR BPM

L. L. Li†, P. L. He, H. M. Xie, J. Yin, R. X. Tian, F. F. Ni, Z. Du, Y. Zhang, J. X. Wu
Institute of Modern Physics, Chinese Academy of Sciences, Lanzhou, China

Abstract

Beam Position Monitor (BPM) is used to measure the horizontal and vertical positions of the beam in the vacuum pip of the accelerator facility. Before online installation, it usually needs to be calibration. High Intensity Heavy-ion Accelerator Facility (HIAF) and China initiative Accelerator Driven System (CiADS) will need a large number of BPM, so it is a great challenge for BPM calibration work. In order to complete this work efficiently and accurately, this research designs and develops an automatic BPM calibration system. This paper mainly described the control and processing programs in this system. The control software was designed by C language to realize automatic calibration functions based on EPICS. A high-order fitting algorithm programmed by Python used to solve the problem of smaller linear range of the capacitive BPM. It significantly improves the accuracy of position measurement after calibration.

INTRODUCTION

HIAF and CiADS will be a next-generation, internationally leading heavy-ion accelerator facility after being established. The precise measurement by the BPM is essential for the desired goal.

Beam position is a key parameter of the accelerator, and it is the judgment basis for beam experiments. In order to maintain the measurement accuracy, it is not only need to improve the technology level of detector design, processing and assembly and reasonable processing technology of signal acquisition, but also required to realize the accurate calibration of the detector [1].

The automatic BPM calibration system designed in this paper can complete the calibration work efficiently, and save lots of time for calibration user. It greatly simplifies the calibration mission of large amount of BPM.

HARDWARE ARCHITECTURE

The hardware architecture of the whole system is shown in Fig. 1. It consists of four major sections, including simulate beam current equipment, calibration platform and motion device, BPM signal processing electronics and industrial computer.

The automatic calibration system is usually performed using the metal wire stretch method. A straightened metal wire is passed through the BPM, and an RF signal is fed to the wire to simulate beam current. An RF signal generator feeds an RF signal by the SMA connector. The signal processing electronics connected the BPM detector via an RF coaxial line. It is used to process and analyse the output signal of the BPM, and acquire the position information of the metal wire relative to the measured BPM detector electrical center. After that it send these data to the industrial computer after calibration ending.

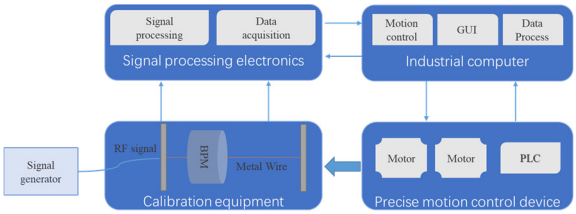

Figure 1: Hardware structure of calibration system.

Calibration Platform and Motion Device

The capacitive BPM is mounted on a two-degree-of-freedom motion platform, which is fixed on a test bench. The motion platform and test bench are shown in Fig 2. The motion platform is produced by Zolix Company in Beijing. Its repeat positioning accuracy is 1 μm, and the measurement precision is 0.1 mm. The motion range in both degrees of freedom is ±150 mm, which guarantees the precision and accuracy of the calibration result and the comprehensive scanning range.

The motion device is mainly combined by the product range of Beckhoff Automation Programmable Logic Controller (PLC) CX2020. It is a modern Industrial PCs (IPC) being produced since 2014 and running Microsoft Windows 7 Embedded operating systems. Equipped with powerful hardware. The CX2020 is capable of supervising and controlling multiple sections of a production process at the same time.

Figure 2: Motion platform and test bench.

BPM Signal Processing Electronics

The BPM system is one of the most important measurement systems for accelerator beam diagnostics and has a large amount of BPM detectors among the beam diagnostic equipment. A typical BPM system is a chain of an in-

† lli@impcas.ac.cn

ISBN: 978-3-95450-249-3 ISSN: 2673-5350 doi: 10.18429/JACoW-IBIC2024-TUP24

DEVELOPMENT OF DIGITAL BEAM POSITION MONITOR FOR HEPS*

Y. Y. Du†, Q. Ye, X. H. Tang, Z. Liu, S. J. Wei, J. He, T. G. Xu, J. H. Yue, Y. F. Sui, J. S. Cao
Key Laboratory of Particle Acceleration Physics and Technology, CAS, Beijing, China
Institute of High Energy Physics, CAS, Beijing, China

Abstract

High Energy Photon Source (HEPS) is a proposed new generation light source with a beam energy of 6 GeV, high brightness, and ultra-low beam emittance. An RF BPM electronic has been designed at IHEP as part of an R&D program to meet the requirements of both the injection system and storage ring. The RF BPM electronic architecture consists of an Analog Front-End (AFE) board and a Digital Front-End board (DFE) based on a custom platform. In this paper, we present the overall architecture of the RF BPM electronics system and the performance evaluation of the BPM processor, including position resolution and beam current dependence.

INTRODUCTION

High Energy Photon Source (HEPS) is a new 6 GeV synchrotron light source under construction in China. HEPS consists of a storage ring with a circumference of approximately 1360.4 m and energy of 6 GeV; a booster with a circumference of 454 m and energy range of 0.5 to 6 GeV; and a linear accelerator with a length of 49 m and energy of 0.5 GeV [1]. Figure 1 show the diagram of HEPS accelerator composition.

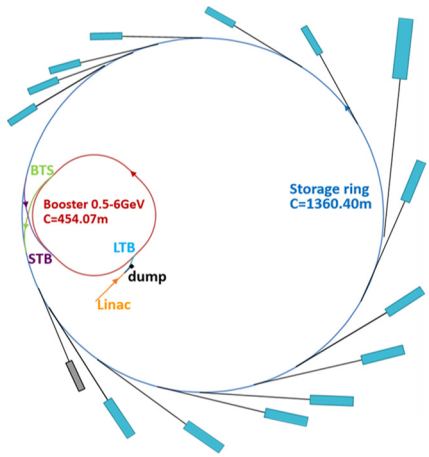

Figure 1: Layout of the HEPS accelerator.

With the HEPS storage ring to a multi-bend achromat lattice, about 700 digital Beam Position Monitors (DBPM) will be required, include LINAC BPM, booster BPM and storage ring BPM. The required numbers of DBPM are gathered in Table 1. And the HEPS beam sizes are below 10 microns in both horizontal and vertical planes, putting stringent requirements on the BPM electronics resolution, long-term stability, beam current dependency and instrument reproducibility.

* This work is supported by the National Natural Science Foundation of China (Grants No. 11805221)
† duyy@ihep.ac.cn

Table 1: HEPS BPM Number Requirements List

HEPS Accelerator	BPM Number
LINAC	8
LTB	8
BTS	12
STB	12
Booster	78
Storage Ring	578

SYSTEM ARCHITECTURE

The system architecture of the HEPS RF BPM electronics is shown in Figure 2. The hardware system is primarily divided into Analog front-end (AFE) electronics and digital Front-end (DFE) electronics, while the software system consists of signal processing algorithms, signal logic control, and EPICS driver design [2, 3].

The AFE electronics mainly consist of components such as RF conditioning modules for beam signal RF filtering, amplification, and attenuation, high-speed high-precision digital sampling modules, clock management and distribution modules, and pilot signal output modules.

The DFE electronics primarily utilizes the Xilinx ZYNQ FPGA as the core control unit to implement digital signal processing functions and signal control functions. The board can boot programs using a 32 Gbyte TF-Card and runs a custom Debian system embedded with an EPICS IOC on the ARM system within the FPGA chip. Data caching is performed using 2 Gbyte DDR3 Memory, and data transmission is carried out through a Gigabit Ethernet (GbE).

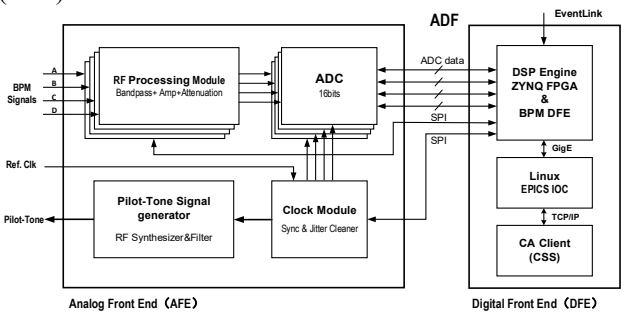

Figure 2: The diagram of HEPS BPM electronic.

Analog Front End (AFE)

The performance of the AFE electronics is a key factor in determining the quality of the entire digital BPM processor, affecting the measurement resolution, sensitivity, and long-term stability of the BPM processor. The beam signal spectrum at HEPS is broad, and the signal at 499.8 MHz is selected to represent the beam position information. In the RF front-end conditioning circuit of the digital BPM signal

ISBN: 978-3-95450-249-3 ISSN: 2673-5350 doi: 10.18429/JACoW-IBIC2024-TUP25

DEVELOPMENT OF STRIPLINE-TYPE BEAM POSITION MONITOR SYSTEM FOR CSNS-II*

M. A. Rehman†, R. Yang‡, Z. Xu, R. Liu, L. Fang, B. Zhang, W. Huang, S. Wang
Institute of High Energy Physics, Chinese Academy of Sciences (CAS), Beijing, China
also at China Neutron Spallation Source, Dongguan, China

Abstract

As part of the CSNS-II upgrade, the H⁻ LINAC beam energy will be increased from 80 MeV to 300 MeV using superconducting cavities. To accurately measure beam position, phase, and energy, the stripline-type Beam Position Monitors (BPM) are essential. The shorted-type stripline BPM was chosen for this upgrade due to its excellent S/N ratio and rigid structure. As space is limited in the LINAC's superconducting section, the BPMs must be embedded in the quadrupole magnet. Two prototypes, with inner diameters of 50 mm and 96 mm, were designed using numerical simulation codes and manufactured for beam testing. This paper will detail the simulation, design, and beam test results of the prototype BPM for CSNS-II.

INTRODUCTION

The China Spallation Neutron Source (CSNS) [1, 2] provides intense pulsed neutron beams for a wide range of scientific research and industrial applications. The CSNS accelerator complex comprises an 80 MeV Linac, a 1.6 GeV Rapid Cyclic Synchrotron (RCS), and a solid tungsten target station. The 80 MeV H⁻ beam from the Linac is injected into the RCS using a multi-turn charge exchange process. The RCS then increases the beam energy to 1.6 GeV, with a beam intensity of 1.56×10^{13}, delivering a beam power of 100 kW. The beam power has been raised to 160 kW with the incorporation of harmonic cavities [3].

The power of the beam will be increased to 500 kW for CSNS-II. As part of the CSNS-II upgrade, the beam energy in the Linac will be raised from 80 MeV to 300 MeV using superconducting cavities. To ensure precise measurement of beam position, phase, and energy in the new superconducting section of the Linac, a new stripline-type Beam Position Monitoring (BPM) system is crucial. The shorted-type stripline BPM has been selected for this upgrade because of its excellent signal-to-noise ratio and rigid structure. Due to limited space in the Linac's superconducting section, the BPMs must be embedded in the quadrupole magnets. Two prototypes, with inner diameters of 50 mm and 96 mm, were designed using numerical simulation codes and manufactured, one BPM of 96 mm diameter was also tested with the beam. The parameters of CSNS and CSNS-II are described in Table 1.

Table 1: CSNS and CSNS–II RCS Parameters

Parameters	CSNS	CSNS–II	Units
Beam Power	100	500	kW
Injection Energy	80	300	MeV
Bunch Frequency	324	324/648	MHz
Bunch length	20	8	ps
Ring Circumference	227.92	227.92	m
Extraction Energy	1.6	1.6	GeV
Repetition Rate	25	25	Hz
Number of Bunches	2	2	
RCS Beam Intensity	1.56×10^{13}	7.8×10^{13}	ppb

BEAM POSITION MONITOR

Two stripline BPMs will be placed into the quadrupole magnets after the normal conducting Drift Tube Linac (DTL). In the spoke cavity region, where beam energy will be increased from 80 MeV to 165 MeV, 10 BPMs will be placed in every other quadrupole magnet of the FODO lattice. The elliptical cavity region will boost the beam energy up to 300 MeV and contain 8 BPMs embedded in the quadrupole magnets. In the drift section (LRBT), after the elliptical cavity region, 10 BPM will be placed, and one BPM of small diameter will be placed at the injection point. Table 2 represents the BPM design parameters.

Table 2: Superconducting Section BPM Parameters

Parameters	Values
Position Accuracy	1% of R
Position Resolution	50 μm
Phase Accuracy	1°
Phase resolution	0.2°
Meas. Range	R/2

The shorted stripline-type BPM has been chosen for CSNS-II owing to its rigid structure and high S/N ratio. Due to the stringent space restriction in LINAC's superconducting section, BPMs must be embedded inside the quadrupole magnet. Therefore, the transverse and longitudinal size and shape of the BPMs are strictly restricted. In shorted-stripline BPM, four stripline electrodes with π/2 rotational symmetry are installed in the vacuum pipe, with their ends grounded to the vacuum duct.

The passage of a charged particle induced image current on a stripline is proportional to the distance between the electrode and the beam, beam intensity, the electrode's opening angle, and the stripline's length. If the character-

* Work supported by National Science Foundation for Young Scientists of China (12305166).

† rehman@ihep.ac.cn
‡ yangrenjun@ihep.ac.cn

ISBN: 978-3-95450-249-3 ISSN: 2673-5350 doi: 10.18429/JACoW-IBIC2024-TUP26

PRELIMINARY RESEARCH AND DEVELOPMENT OF BPM ELECTRONICS UPGRADE FOR THE RCS RING IN CSNS II*

R. Y. Qiu, R. J. Yang†, W. L. Huang, F. Li, Z. H. Xu, T. Yang, M. Y. Liu,
L. Zeng, W. W. Chen, H. B. Liu
Institute of High Energy Physics, Chinese Academy of Sciences, Beijing, China
Spallation Neutron Source Science Center, Dongguan, China

Abstract

The first phase of the China Spallation Neutron Source (CSNS) project aims to accelerate negative hydrogen ions to 80 MeV using a linear accelerator. Subsequently, these negative hydrogen ions are converted into protons after stripping, and then injected into a rapid cycling proton synchrotron. The proton beam is further accelerated to an energy of 1.6 GeV and guided through a beam transport line to a tungsten target, where spallation reactions generate neutrons. With the initiation of the Phase II project of the China Spallation Neutron Source (CSNS II), the target power is anticipated to increase significantly to 500 kW in the future. Upgrading the existing 32 sets of BPM electronics on the Rapid Cycling Synchrotron (RCS) ring is essential to accommodate the enhanced beam power and fulfill the new requirements of the beam measurement. This paper focuses on the novel design and validation of the BPM electronics, as well as the execution of tests during beam operation.

INTRODUCTION

The primary objective of the China Spallation Neutron Source (CSNS) project's first phase is to accelerate negative hydrogen ions to 80 MeV using a linear accelerator [1]. Subsequently, these negative hydrogen ions are converted into protons through stripping and then injected into a rapid cycling proton synchrotron [2]. The proton beam is further accelerated to 1.6 GeV and guided through a beam transport line to a tungsten target, where spallation reactions produce neutrons. With the initiation of the Phase II project of the China Spallation Neutron Source (CSNS II), the target power is anticipated to increase significantly to 500 kW in the future. Upgrading the existing 32 sets of BPM electronics on the Rapid Cycling Synchrotron (RCS) ring is necessary to accommodate the increased beam power and meet the new requirements of the beam tuning personnel.

ELECTRONICS SYSTEM DESIGN

System Architecture

In the Rapid Cycling Synchrotron (RCS) of the China Spallation Neutron Source (CSNS), there are four quadrants, each equipped with 8 BPM detectors. The dual-bunch revolution frequency ranges from 1 MHz to 2.44 MHz, with the bunch length compressed from 500 ns to 100 ns. Each bunch completes approximately 20,000 turns within an acceleration cycle of 20 ms. The signal dynamic range of the BPM is 10^4. The electronics system is divided into two parts. The Front-End Controller (FEC) readout boards handle digitizing the front-end signals, conducting real-time beam position calculations, and buffering raw ADC data and position data. The System-On-Chip (SOC) data aggregation boards manage reading data from 8 FECs, with a front-end data bandwidth of 80 Gbps. They

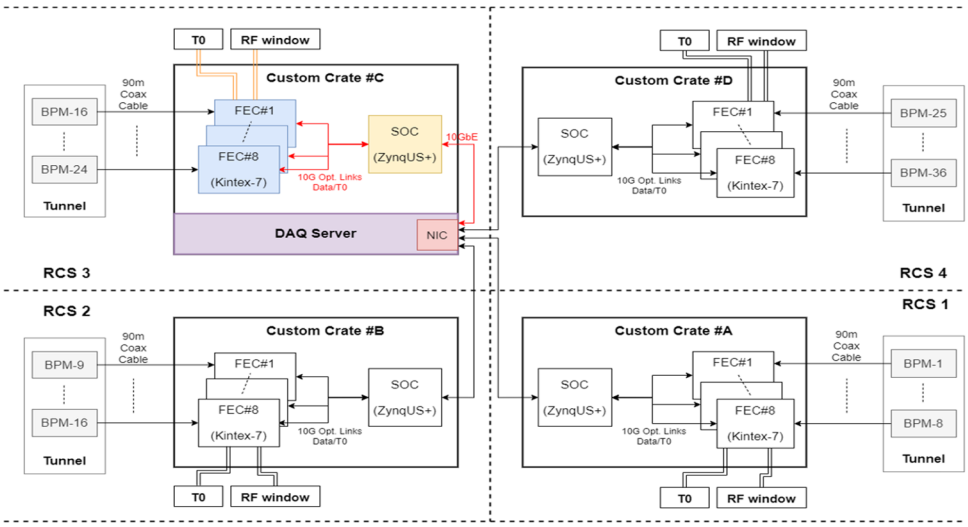

Figure 1: RCS-BPM system architecture diagram.

*Upported by the Open Fund of the China Spallation Neutron Source Songshan Lake Science City (Grants No. KFKT2022A01)
†email address: yangrenjun@ihep.ac.cn

ISBN: 978-3-95450-249-3 ISSN: 2673-5350 doi: 10.18429/JACoW-IBIC2024-TUP27

THE DEVELOPMENT OF NEW BPM SIGNAL PROCESSOR AT SSRF*

M. J. Zhang[1], Shanghai University, Shanghai, China
[1]also at Shanghai Institute of Applied Physics, CAS, Shanghai, China
L. W. Lai†, Y. M. Zhou, Y. B. Yan, Shanghai Advanced Research Institute, CAS, Shanghai, China
H. Jang[2], S. L. Wang[2], Nanchang University, Jiangxi, China
[2]also at Shanghai Advanced Research Institute, CAS, Shanghai, China

Abstract

A BPM signal processor has been developed for SSRF since 2009. It composed of Virtex5 FPGA, ARM board, and 4 125MSPS sampling rate ADCs. Since then, electronic technology has made significant progress. Such as Zynq UltraScale+ MPSoC FPGA contains both hard-core ARM and high-performance FPGA, and ADCs with a sampling rate of 1GSPS have been applied in mass production. A new BPM processor with Zynq UltraScale+ MPSoC FPGA and 1GSPS ADCs is under development at SSRF. Due to the application of new technologies, the processor performance will be significantly improved. The new processor can also meet the needs of ultra-low emittance measurement for the new generation of light sources. This paper will introduce the design of the processor and the relative tests.

INTRODUCTION

The Shanghai Synchrotron Radiation Facility (SSRF) is a high-performance electron storage ring with a circumference of 432 meters and an energy of 3.5 GeV. It operates with a harmonic number of 720, a cyclotron frequency of 693.964 kHz, and a radio frequency of 499.654 MHz. SSRF is recognized as one of the leading medium-energy light sources worldwide, delivering exceptional performance in its class [1].

SSRF early adoption is the third generation BPM processor Libera series launched by IT companies, it has high resolution, high reliability, a large number of users, convenient technical communication and many other ad vantages. In the construction and upgrading of a new generation of accelerators, SSRF has developed a new digital BPM signal processor with independent intellectual property rights, and its performance has reached the international advanced level. The digital BPM signal processor is based on the embedded sub-motherboard structure of FPGA+ARM, equipped with different front-end ADC sub boards to adapt to different applications, there are four channel signal input, the center frequency is 500 MHz, 16 bits ADC, its the maximum sampling rate is 125 MSPS and bandwidth is 650 MHz. The beam test results of the processor on the storage ring show that the resolution of TBT reaches 230 nm, the resolution of SA data reaches 78 nm, the resolution of 10-minute closing orbit is 57 nm, the temperature change of 80 hours is 1.2 degrees, and the horizontal and vertical slow drift is less than 0.4 microns. At present, it has been used in batch in SSRF, SXFEL, DCLS, Brazil light source linear accelerator, the number of about 200 units. Table 1 describes the main operational parameters of SSRF.

Table 1: Main Parameters of the SSRF

Parameter	Value
Perimeter	420 m
Beam energy	3.5 GeV
RF frequency	499.654 MHz
Harmonic number	720
current	240+0.5 mA
Emittance	3.9 nm/rad

Beam orbit stability is critical for the operation of synchrotron radiation sources, with drift being the primary factor affecting orbit stability. When beam position monitors (BPMs) measure beam position, slow drifts are introduced due to factors such as ambient temperature, humidity, pressure, and electromagnetic fields, which arise from channel inconsistencies. These drifts degrade the accuracy and resolution of the data, leading to inaccurate BPM feedback. Currently, two main approaches are employed for drift compensation: pilot tone and switching. Based on a survey of major scientific facilities worldwide, pilot tone compensation is used in Elettra 2.0 [2], Diamond-II, SLS, HEPS, and BEPC II, while switching is implemented in NSLS-II, Sir ius, HEPS, and IT Libera. SSRF has opted for the pilot tone compensation method due to its effectiveness in eliminating channel inconsistencies, and has developed a new generation of digital BPM signal processors to enhance performance.

NEW DIGITAL SIGNAL PROCESSORS

SSRF has upgraded the electronics for universal beam measurements, achieving a sampling rate of 117.28 MHz, and developed a new generation digital backboard based on the latest system-on-chip FPGA (Zynq UltraScale+ MPSoC) architecture. This new design incorporates 8 GB of PL DDR memory and offers more versatile external interfaces. The RF front-end board has also been upgraded with the addition of a pilot tone to enhance orbit stability. Currently, the hardware integration, FPGA, and software development have been completed, and corresponding pilot function tests and data analysis are underway in both the laboratory and accelerator facility. The primary design of the BPM electronics includes an RF analog front-end

* This work was support by the National Natural Science Foundation of China (Grant No. 12175293). Youth Innovation Promotion Association, CAS (Grant No. 2019290), Outstanding member of the Youth Innovation Promotion Association, CAS, SHINE R&D and project.
† Corresponding author: lailw@sari.ac.cn

ISBN: 978-3-95450-249-3 ISSN: 2673-5350 doi: 10.18429/JACoW-IBIC2024-TUP28

DESIGN OF BEAM POSITION MONITORING INTERLOCKING PROTECTION SYSTEM

R. X. Tian [1,3,†], J. X. Wu[1,2], Z. X. Li[1,3], K. W. Gu[1,2], J. J. Su[1,2], F. F. Ni[1], Y. Wei[1], H. M. Xie[1,2], L. L. Li[1], Y. Zhang[1,2], G. Y. Zhu[1,2]
[1]Institute of Modern Physics, Chinese Academy of Sciences, Lanzhou, China
[2]University of Chinese Academy of Sciences, Beijing, China
[3]Lanzhou University, Lanzhou, China

Abstract

The machine protection system guarantees the safe operation of the HIAF in different operating modes and prevents damage to the online equipment in the event of a failure. Beam current data such as beam current position and phase is an important basis for analyzing and diagnosing accelerator faults. In this paper, the beam position and phase interlock monitoring system were designed by the authors. The system is based on circular buffer and AXI4 protocol to realize the transmission and storing of interlock data and locking of interlock status. Laboratory tests show that the system could save the beam position, beam phase, SUM signals and amplitude of sensed signal with interlocking before and after 8 ms and latch the interlock status of 25 channels. The system was deployed at the CAFe-LINAC (LINear ACcelerator) in March 2024 and completed online measurements.

INTRODUCTION

The HIAF (High Intensity Heavy-ion Accelerator Facility) [1-4] is a new-generation heavy-ion accelerator research device with international leading level. It could provide the highest peak flow of low-energy heavy-ion beams in the world. In order to avoid radiation damage to on-line equipment in the event of a malfunction and to increase the availability of the entire installation. The Beam Position and Phase Interlock Protection System monitors physical quantities such as the horizontal position of the beam, the vertical position, the SUM signal (beam intensity), the beam intensity and the beam width of the pulsed beam. The system would send an interlocking signal to the MPS (Machine Protection System) [5-7] before a fault occurs or in the shortest possible time after a fault occurs. Simultaneously，the beam data would be saved in the local computer. The system provides a reference for beam commissioning, machine studies and beam structure analysis.

SYSTEM DESIGN

The beam position and phase interlocking protection system have two main functions: one is the locking of the state during interlocking; the other is the saving of data during interlocking. The monitored state quantities in the system are shown in Table 1. Whether the ADC (Analog-to-Digital Converter) sampling value is saturated or not directly affects the accuracy of the position calculation algorithm, so the ADC conversion value is likewise monitored in the system. The beam current strength that SUM signal, is too large to cause equipment damage [8-9]. For example, the intercept probe Faraday with high current strength in the continuous beam current is very easy to be destroyed [10].

This affects the normal operation of the beam current diagnostic system. The monitoring of the phase is the monitoring of the beam energy. The deposition of energy could lead to rapid melting of material, damage to equipment and vacuum disruption. A shift in the beam position could also cause a pipe breakdown with destruction of the vacuum in a short period of time. The drastic reduction in beam transfer efficiency means that beam losses are significant, resulting in costly repairs and disruption of scientific progress for co-workers.

Table 1: Monitored State Quantities

State Quantity	state	note
ADC raw value	saturation	4 channels
beam intensity	high	H1 & H2
beam intensity	low	H1 & H2
phase	high	H1 & H2
phase	low	H1 & H2
horizontal position	high	H1 & H2
horizontal position	low	H1 & H2
vertical position	high	H1 & H2
vertical position	low	H1 & H2
transmission efficiency	high	H1 & H2
transmission efficiency	low	H1 & H2

In the system, the interlocking status of the monitored state quantities is latched and transmitted to the ARM (Advanced RISC Machine) and then published to the user interface through the network. Figure 1 shows the block diagram of the entire system.

In addition to the locking of state quantities, the beam data before and after the occurrence of the interlock is also very important. The beam data could be analyzed to determine why failures occur and could also be used to predict failures. The authors used BRAM (Block Random Access Memory) as a buffer to store beam data in real time, including beam position, beam current intensity, beam phase and the sensed amplitude and phase of the four probes of the detector. The BRAM of the Zynq UltraScale+ MPSoC XCZU9EG is only 40.9 Mb, so the system could only store 8.192 ms of beam data at this stage.

†email: tianrx1028@impcas.ac.cn

ISBN: 978-3-95450-249-3 ISSN: 2673-5350 doi: 10.18429/JACoW-IBIC2024-TUP29

OFFLINE CALIBRATION AND ERROR CORRECTION OF THE STRIPLINE BPM FOR THE HALF INJECTOR*

Dongyu Wang, Jianye Wang, Chuhan Wang, An Wang, Mingdong Ma, Jinkai Lan, Ruizhe Wu, Xiaochao Ma, Ping Lu, Anxing Wang, Baogen Sun, Leilei Tang†
National Synchrotron Radiation Laboratory,
University of Science and Technology of China Hefei, China

Abstract

This study conducted offline calibration tests on the stripline Beam Position Monitor (BPM) designed for the Hefei Advanced Light Facility (HALF) injector. The Lambertson method was used to measure the offset between the electrical center and the mechanical center of the BPM, with results showing horizontal and vertical offsets of 0.1154 mm and 0.1661 mm, respectively. Additionally, the wire-scan method was employed to construct the BPM mapping, and polynomial fitting was applied to effectively reduce the BPM's nonlinearity and system errors. The experimental results provide essential data support for the optimization and practical application of the BPM in the HALF injector.

INTRODUCTION

With the continuous advancement of science and technology, fourth-generation synchrotron light sources based on diffraction-limited storage ring have become a global research focus due to their extensive applications in materials science, biology, chemistry, and other fields [1]. The high brightness and high coherence of synchrotron light sources place higher demands on the performance of storage ring. To achieve efficient beam injection and stable operation, the storage ring has high requirements for the injector. Hefei Advanced Light Facility (HALF) is a new fourth-generation synchrotron light source under construction, which injector mainly consists of two parts: a linear accelerator (LINAC) and a beam transport line. In HALF, the electron beam is accelerated by the LINAC, which energy is increased and ultimately reach 2.2 GeV. The high energy electron beam is injected into the storage ring through the beam transport line. The beam parameters of injector such as beam position, size, emittance, energy spread and so on must be measured and stringent controlled to excellent quality status to ensure the stable operation of the storage ring of HALF.

The stripline Beam Position Monitor (BPM) is a critical component in the injector, responsible for real-time monitoring of the beam position and intensity, thus enabling high-resolution beam measurement and feedback control. To ensure the accuracy and reliability of the stripline BPM in the HALF injector, this study conducted offline calibration using the Lambertson method and the wire-scan method. These calibration tests systematically assessed the performance of the stripline BPM and reduced system errors, providing data support for the optimization and practical application of the equipment.

* Supported by the National Science Foundation of China (11805204, 12075236) and the Hefei Advanced Light Facility Project.
† Corresponding author (email: tanglei@ustc.edu.cn).

CALIBRATION PRINCIPLES AND METHODS

In simulations, it is typically assumed that the beam, the vacuum chamber, and the BPM are in ideal conditions without any deviations. However, in practical applications, factors such as fabrication and installation accuracy can cause a discrepancy between the BPM's electrical center (the point where the signal amplitudes from the electrodes are symmetrically distributed) and its mechanical center. Additionally, mechanical structures may exhibit asymmetry, further contributing to measurement errors. To accurately measure the beam position within the vacuum chamber, it is essential to calibrate the BPM before installation to reduce system errors.

Lambertson Method

To evaluate the offset between the electrical center and the mechanical center of the BPM, the Lambertson method is commonly used [2]. This method assesses the electrical center's offset by measuring the S-parameter deviations at each port of the BPM under conditions without beam or simulated beam [3]. As an external verification method, the Lambertson approach mainly analyzes the asymmetry characteristics of the BPM, and its advantage lies in not requiring the system to be rigidly fixed on the test platform during measurement.

In the calibration process, each BPM electrode corresponds to a gain factor g. Differences among these gain factors are the primary reason for the misalignment between the BPM's electrical center and mechanical center. The Lambertson method utilizes the coupling relationships between ports to determine the gain factors g for each electrode and calculates the offset of the electrical center relative to the mechanical center accordingly. When the vacuum chamber is cylindrical and the BPM ports are distributed in the top, bottom, left, and right directions, the offset of the electrical center relative to the mechanical center can be calculated using Eq. (1).

$$x_{offset} = k_x \frac{g_B - g_D}{g_B + g_D}, y_{offset} = k_y \frac{g_A - g_C}{g_A + g_C}, \quad (1)$$

where x_{offset}, y_{offset} represent the offsets of the electrical center relative to the mechanical center in the horizontal and vertical directions, respectively. The terms $1/k_x$, $1/k_y$ denote the horizontal and vertical sensitivities of the BPM,

ISBN: 978-3-95450-249-3 ISSN: 2673-5350 doi: 10.18429/JACoW-IBIC2024-TUP30

DEVELOPMENT OF HIGH-PRECISION BEAM POSITION MONITOR FOR THE KOREAN 4GSR PROJECT

S.W. Jang†, D. Shin, S. Ahn, D. Kim, B. Shin, Pohang Accelerator Laboratory, Pohang, South Korea

Abstract

The Korean 4GSR project is currently under construction in Ochang, South Korea, with the aim of achieving first beam commissioning in 2027. Designed to achieve an emittance approximately 100 times smaller than that of third-generation synchrotron radiation storage rings, the project requires the development of several high-precision beam diagnostic devices. In particular, the beam position monitor is aimed at reducing longitudinal wake impedance to suppress heating and beam instability. This paper discusses the development of two types of 4GSR BPM pick-up antennas: one utilizing a SiO_2 glass insulator and another designed in a cone shape using Al_2O_3. We will also describe the performance of these designs through beam tests. Additionally, this paper provides an overview of the current development status of the BPM system for the 4GSR project.

DEVELOPMENT OF 4GSR BPM PICK-UP

Two types of beam position monitor (BPM) pickup antennas have been developed for the 4th generation storage ring (4GSR) project [1, 2]. The first type uses a SiO_2 glass insulator with a low dielectric constant, which shifts the frequency range of the longitudinal wake impedance generated by the BPM to higher frequencies. This helps reduce overall thermal loss in the BPM and allows for cleaner signal acquisition. The second type features a cone-shaped design using Al_2O_3, which, despite its higher dielectric constant of 9.9, has been optimized to perform at the same level as the SiO_2 BPM. These designs have been optimized through extensive 3D simulations to minimize ringing signals while achieving high beam position resolution [3]. The SiO_2 BPM consists of molybdenum pins and a SiO_2 glass insulator with a dielectric constant of 4, housed in ASTM-F15 material. In contrast, the Al_2O_3 BPM features titanium pins and a ceramic disc with a dielectric constant of 9.9, enclosed in an SUS316 stainless steel housing. Figure 1 shows that the developed two different type of 4GSR BPM sectional view for SiO_2 and Al_2O3 insulators.

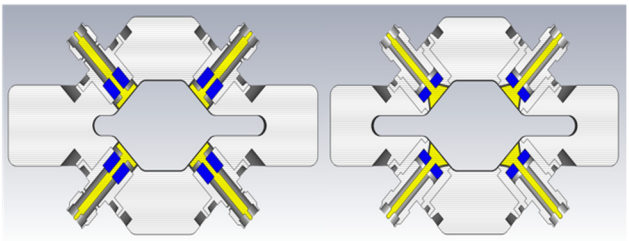

Figure 1: Development of 4GSR BPM pick-up antennas. SiO_2 glass BPM (left) & Al_2O_3 BPM (right).

† siwon@postech.ac.kr

TDR MEASUREMENT OF 4GSR BPM PICK-UP ATNENNA

Time Domain Reflectometry (TDR) is a powerful technique used to measure the impedance along the BPM structures. By sending a fast-rise time pulse along the transmission line and measuring the reflections, we can accurately determine the characteristic impedance and detect any discontinuities in the line.

The TDR measurement provides a direct way to calculate the capacitance of the BPM structures. The relationship between the impedance $Z(t)$ and the reflection coefficient $\Gamma(t)$ is given by Eq. 1:

$$\Gamma(t) = \frac{Z(t)-Z_0}{Z(t)+Z_0}, \quad (1)$$

where Z_0 is the characteristic impedance of the transmission line. Figure 2 shows the TDR simulation results of the two types of BPM pick-up antennas for 4GSR, as well as the actual TDR measurement results of the prototype BPM pick-up antenna samples.

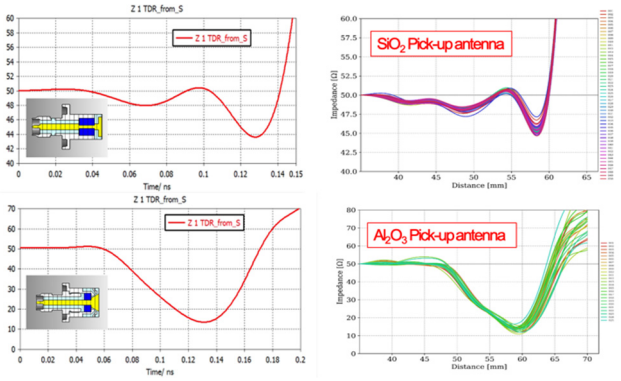

Figure 2: A proto-type of 4GSR BPM pick-up time domain reflection measurements results.

By using TDR data, the capacitance of the BPM pickup electrodes can be estimated through the analysis of the reflected signals. The time-domain reflectometry data provides the necessary information to calculate the capacitance C using the following relation: $C = \Delta t/Z_0$. Here, Δt refers to the time delay between the transmitted and reflected signals, and Z_0 represents the characteristic impedance of the transmission line.

Through TDR simulations, the expected capacitance for the SiO_2 BPM pick-up is approximately 1.5 pF, while the Al_2O_3 BPM pick-up is expected to have a capacitance of around 4 pF. The SiO_2 BPM pick-up showed good agreement between the simulation and measurement results, with a small standard deviation. However, as shown in Fig. 2, while the Al_2O_3 BPM pick-up meets the required impedance and capacitance specifications, the complex manufacturing process and challenges in high-precision

ISBN: 978-3-95450-249-3 ISSN: 2673-5350 doi: 10.18429/JACoW-IBIC2024-TUP31

FIRST EXPERIENCES WITH THE NEW PILOT-TONE-BASED eBPM SYSTEM IN ELETTRA STORAGE RING

G. Brajnik*, S. Bassanese, R. De Monte, G. Gaio, Elettra-Sincrotrone Trieste, Trieste, Italy

Abstract

This paper presents the first experiences acquired with the new eBPM system based on pilot tone compensation, developed for Elettra 2.0. After the successful delivery of seven complete systems, belonging to a pre-series production within the signed partnership with Instrumentation Technologies, we started their integration in the current machine, in order to gain experience and develop all the functionalities required for the future commissioning of the new accelerator, scheduled for 2026. To do so, an entire section of Elettra storage ring has been equipped with the new systems: eight Libera Electron units have been replaced by eight Pilot Tone Front End (PTFE) and four digital platforms (DAQ10SX). Tests were carried out during dedicated machine shifts, focusing on integration with the new global orbit feedback at different data rates (10 kHz, 100 kHz and turn-by-turn), with and without pilot tone compensation. Nevertheless, triggered acquisitions were made in order to test first turn capability of the system. Another unit has been attached to a pair of spare pick-ups (low-gap BPMs), to continue the development of new features and to provide different types of data (raw ADC data, turn-by-turn calculated positions, etc.) for machine physics studies, even during user-dedicated shifts.

INTRODUCTION

In previous papers we presented the global development of the new eBPM (electron beam position monitoring) system for Elettra 2.0, the low-emittance upgrade of the present lightsource based in Trieste, Italy, starting from the proof of concept regarding the pilot tone compensation [1], going through the integration of the first prototype in Elettra's global orbit feedback [2] and finally with the industrialization and series production of the complete system thanks to the partnership signed with Instrumentation Technologies [3, 4]. In this paper we present the first experiences with the new electronics installed in a cell of the current machine, and its operation with the new Global Orbit Feedback system.

SYSTEM INSTALLATION

Thanks to the modular design, we followed a modular design, the analog front end with pilot tone injection (PTFE) is separated from the digital unit (DAQ). The front ends have been installed in Elettra tunnel and connected to eight existing BPM pick-ups of section 6, as shown in Fig. 1. Every DAQ unit is capable to acquire signals from two BPMs. Moreover, for machine physics studies, another pair of front ends have been connected to two low-gap spare BPMs in section 7 (Fig. 2), not involved in orbit calculation and thus available anytime.

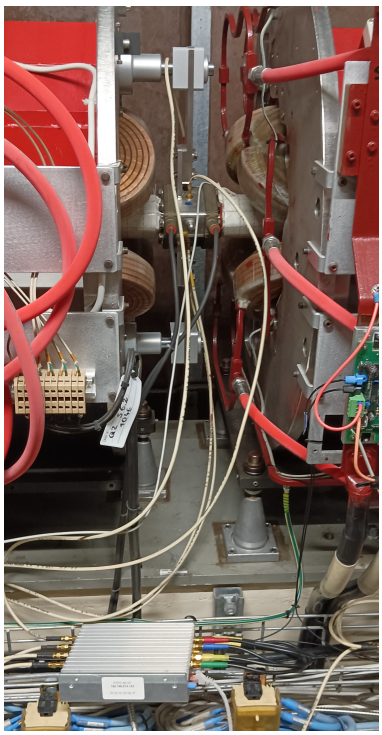

Figure 1: PTFEs in Elettra tunnel connected to BPM pick-ups.

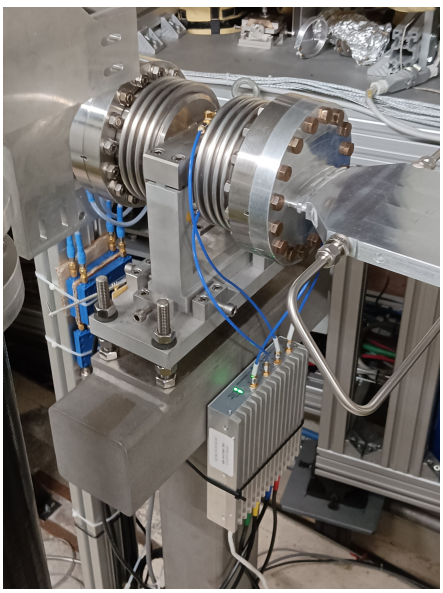

Figure 2: PTFE connected to low-gap BPMs.

* gabriele.brajnik@elettra.eu

ISBN: 978-3-95450-249-3 ISSN: 2673-5350 doi: 10.18429/JACoW-IBIC2024-TUP33

CHERENKOV DIFFRACTION RADIATION BEAM POSITION STUDIES AT DIAMOND LIGHT SOURCE

A. Clapp*,[1,2], P. Karataev[1], L. Bobb[2]
[1]Royal Holloway University of London, Egham, UK
[2]Diamond Light Source, Didcot, UK

Abstract

Beam position studies have been performed using a Cherenkov Diffraction Radiation (ChDR) based Beam Position Monitor (BPM) at Diamond Light Source (DLS). This work presents the characterisation of the BPM using the 3 GeV electron beam and comparing the effectiveness of this prototype to an existing Inductive Beam Position Monitor (IBPM) in use in the DLS Booster To Storage (BTS) transfer line. The functionality of the BPM is explored, utilising both wideband and narrowband ChDR emission with the application of filters to the ChDR detection system.

INTRODUCTION

Cherenkov Diffraction Radiation (ChDR) is emitted when a charged particle moves in the vicinity of a dielectric interface. The theory of ChDR has been developed in the form of the polarisation current approach shown in [1], which was used in the design process of the BPM system utilised in this paper. Due to the dependence of the properties of ChDR emission on beam parameters, ChDR can be exploited for diagnostics purposes, e.g. coherent ChDR as seen in [2] has been used for bunch length measurements [3] and beam position studies at the AWAKE experiment [4].

The ongoing experiment at Diamond Light Source began in 2018 [5] following successful incoherent experiments at CESRTA, Cornell University, USA [6]. This experiment used a single diamond target to produce incoherent ChDR, which was transported to a camera through the use of mirrors from the vacuum chamber window.

These previous experiments showed that the height of the target must be significantly larger than the effective electric field radius $\gamma\lambda$ where γ is the Lorentz factor and λ is the observation wavelength, otherwise significant suppression of the signal occurred. The new targets have been designed with a height of 32 mm, which for 500 nm emission is $11\gamma\lambda$, allowing for the target to be considered infinite and thus preventing signal suppression. The design of the new experiment is described in [7].

Figure 1 shows the structure of the BPM. It consists of two fused silica prisms positioned either side of the electron beam. As the beam passes through the aperture, it polarises atoms in both pick-ups, causing the emission of ChDR at the well-defined characteristic Cherenkov angle given by:

$$\theta_{Ch} = \arccos\left(\frac{1}{\beta n}\right) \quad (1)$$

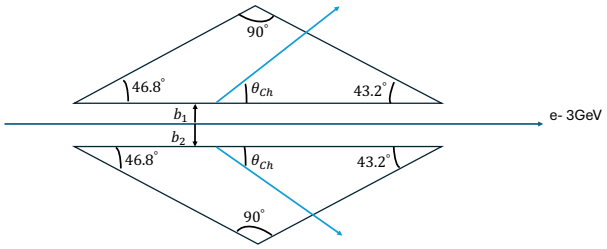

Figure 1: Outline of BPM structure.

where β is the velocity of the incident electron and n is the refractive index of the fused silica prism. These two prisms form a 1D Beam Position Monitor, that can measure beam position in the horizontal plane perpendicular to the path of the beam.

CHERENKOV DIFFRACTION RADIATION EMISSION WITH IMPACT PARAMETER

The intensity of ChDR decays exponentially as:

$$I = I_0 e^{\frac{-2\pi b}{\gamma\lambda}} \quad (2)$$

where I_0 is the intensity when the core of the beam is in contact with the target (i.e. for $b = 0$) and b is the impact parameter. Equation (2) shows that the signal decreases exponentially as the beam moves further away from the radiator. It also shows that the rate of decay is dependent on the wavelength of the emitted light. Signal is detected for impact parameters less than or comparable to $\gamma\lambda$, which for 500 nm is 3 mm.

To accurately determine the impact parameter of the beam with respect to the pick-up, data is acquired from an Inductive Beam Position Monitor [8]. The IBPM is positioned directly upstream from the ChDR BPM, and is used both to determine the beam position for impact parameter scans, and calibrate the ChDR BPM. Impact parameter data, such as in Fig. 2 is fitted using Eq. (2).

Figure 2 shows an impact parameter scan performed using a single target with no filtering. There is a very clear exponential dependence of the signal, with a fitted exponent placing the dominant emitted wavelength at 469 nm. This result confirms there is emission in the visible spectrum and close to 500 nm. The setup has been optimised for dominant emission of 500 nm to allow for ease of integration into existing fibre optic systems and to ensure the accessible range of impact parameters is in the millimetre scale. The full description of the design and optimisation is shown in [7].

* alec.clapp.2021@live.rhul.ac.uk

ISBN: 978-3-95450-249-3 ISSN: 2673-5350 doi: 10.18429/JACoW-IBIC2024-TUP35

CURRENT STATUS OF THE MANUFACTURING AND TESTING OF THE BPM ELECTRONICS FOR ELETTRA 2.0

A. Gabrscek, M. Cargnelutti, U. Dragonja, Instrumentation Technologies, Solkan, Slovenia
G. Brajnik, R. De Monte, Elettra-Sincrotrone Trieste, Trieste, Italy

Abstract

In this paper we are presenting the status of the partnership between Instrumentation Technologies and Elettra Sincrotrone Trieste for the realisation of 200 BPM electronics for ELETTRA 2.0. Last year, 200 Pilot Tone Front-End (PTFE) units were successfully developed and produced. During the present year, 100 Digital Acquisition platforms, each one used to digitize and process the signals from two BPM pickups, are in production after the successful pre-series tests.

Elettra Sincrotrone Trieste was more involved in concept design, prototype development, and firmware programming, while Instrumentation Technologies was focused on design for manufacturing, implemented rigorous testing procedures, and handled the production.

During the project, it was also necessary to overcome a period of material shortages, particularly for the chips used in the digital part.

Testing during the pre-series and series production phases ensured that each unit met the desired performance criteria necessary for stabilizing long-term measurement drifts in BPM systems. Additional units were produced to account for potential failures and performance variations, ensuring that all units delivered performed to specification.

INTRODUCION

Scheduled for operation in 2026, Elettra 2.0 is set to be a next-generation of storage ring-based light sources, designed for high precision analytical studies of matter at extremely fine spatial resolutions [1]. To meet the requirements for precise beam monitoring and orbit feedback, the machine will be equipped with 168 Beam Position Monitors (BPMs) and corresponding electronics.

Within the partnership project between Instrumentation Technologies and Elettra Sincrotrone Trieste, an innovative BPM readout system [2 - 4] has been developed, produced in small series [5] and is now in the phase of large series production. The following chapter introduces the BPM electronics architecture. Later, the test procedures that were defined for Factory Acceptance Test (FAT) and Site Acceptance Test (SAT) are presented. Finally, the results of the produced instruments are described.

ELETTRA BPM ELECTRONICS

Each of the Elettra BPM electronics consist of a Data Acquisition (DAQ) platform that is used to digitize and process the BPM signals coming from two Pilot-Tone Front Ends (PTFE) that are installed in the accelerator tunnel near the BPM sensor, as described in Fig. 1.

While the PTFE consists of a single electrical board to be tested after production, the DAQ platform consists of three different boards that are tested individually before the full system is assembled – see Fig. 2. The three boards are the main digital FPGA board, one input/output (IO) board and two FPGA Mezzanine Cards (FMC) ADC boards.

A first pre-series of 7 BPM electronics systems was already tested and delivered to the customer in 2023. Among the other parameters that were measured for each produced system, special attention was dedicated to the desired performance criteria: the expected standard deviation (RMS) on the calculated beam position should be less than 100 nm with a scale factor of 10 mm and a data rate of 10 kHz.

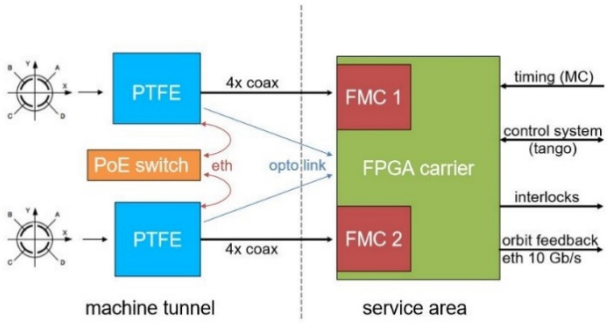

Figure 1: The Elettra 2.0 BPM electronics.

Figure 2: Assembled DAQ systems.

DEVELOPMENT OF THE TEST PROCEDURE

When a new product is developed or industrialized, before it can be mass produced, a test procedure needs to be defined. The test procedure defines the content of the tests that are performed at different stages of the production cycle: this Chapter explains how the test procedure is defined for the DAQ platform.

The first step is the execution of a system test on a limited amount of boards or devices, where their functionalities and performance is checked. The purpose is to make sure that every relevant aspect of the device can be checked or measured. After this, the manufacturing test and factory acceptance test are defined. As this project was in close

ISBN: 978-3-95450-249-3 ISSN: 2673-5350 doi: 10.18429/JACoW-IBIC2024-TUP37

ELECTRONIC TEST BENCH FOR THE VALIDATION OF MYRRHA BPM AC-QUISITION SYSTEMS*

Sidi Mohammed Ben Abdillah†, Fabrice Fournier, Université Paris-Saclay, CNRS/IN2P3, IJClab, Orsay, France

Abstract

MYRRHA (Multi-Purpose Hybrid Research Reactor for High-Tech Applications) aims to demonstrate the feasibility of high-level nuclear waste transmutation at industrial scale. MYRRHA Facility aims to accelerate 4 mA proton beam up to 600 MeV.

Beam Position monitors are key elements in many accelerators. for instance, once BPMs are installed along a linear accelerator or a storage ring, they remain inaccessible for any validation of updated or rejuvenated electronics. this paper addresses this issue with the realization of an electronic test bench simulating the outputs signals of BPM electrodes for a given beam energy, phase and position. the bench is realized for MYRRHA BPMs and it offers simulated beams with a position precision down to 50µm and phase precision down to 0.5° on a wide range.

GENERAL DESCRIPTION OF MYRRHA

MYRRHA is a high power proton accelerator with strongly enhanced reliability performances. The conceptual design is on-going for more than 15 years. The adopted LINAC scheme to fulfil the reliability goal is based on 2 distinct sections.

MYRRHA first phase (MINERVA) accelerates the beam up to a 100 MeV energy.

The HEBT line in MYRRHA phase 2 includes accelerator will deliver proton beam for various applications including fusion research and isotopes production.

MYRRHA beam properties are mentioned in Table 1.

Table 1: Beam Parameters & BPM Specifications

Parameter	Range
Energy E	1.5MeV-600 MeV
Current I	0.1 mA-4 mA
Duty cycle	2.10^{-4} to 0.125
F_{acc}	176.1 MHz
Beam pipe diameter	38, 56 80 mm

In nominal operation, beam position and transverse shape are measured with BPMs.

All BPMs will be aligned along MYRRHA sections. Their associated electronics will be installed in a dedicated room located several meters away from their locations.

Once the LINAC is in operation, access to these instruments is mostly denied. In case of BPM operation far from optimal or showing serious dysfunctions, it would be difficult to locate the source of the dysfunctions.

It would be of a great help to have a BPM "Simulator": an electronic card repeating religiously BPM operation.

BPM SIMULATOR CONSTRAINTS

BPM is equipped with 4 probes formed by a sealed 50Ohm feedthroughs attached to an electrode.

The beam induces electrical signal on each electrode.

MYRRHA BPM acquisition system processes the said signals by measuring the 1st and 2nd tone levels and using them to provide the following information:

- Beam position coordinates: they are measured with a sensitivity expressed in dB/mm. For MYRRHA project, this sensitivity at F_{acc} is expected to vary between 0.7 dB/mm and 1.63 dB/mm. BPM sensitivity at $2 \times F_{acc}$ could vary between 0.7 dB/mm and 2.5 dB/mm.
- The phase of the beam with respect to the main Radio Frequency reference signal. Beam velocity and energy are processed from this measurement.
- Beam Ellipticity figuring in the second order moment of the beam transverse distribution. Beam ellipticity corresponds to the difference between the squares of beam dispersions in both axes (X and Y). Beam ellipticity it is very useful for centered beams; it allows a partial comparison between beam shapes at different cells. For MYRRHA project, this sensitivity is expected to vary between 0.08 dB/mm² and 0.015 dB/mm² at both frequencies.

Based on different MYRRHA BPM prototypes [1, 2], Table 2 summarizes the tone levels expected the outputs of different BPMs along MYRRHA for beam location +/- 10 mm of BPM revolution axis.

Table 2: Output Level Range at MYRRHA Sections

Section	Range at F_{acc} (4 mA current)	Range at $2 \times F_{acc}$ (4 mA current)
RFQ exit	[-7; -23] dBm	
MEBT start	[-15; -29] dBm	[-14; -28] dBm
MEBT end	[-22; -35] dBm	[-19; -33] dBm
HEBT start	[-19; -26] dBm	[-18; -26] dBm

With a 100µA beam current, these levels are 32dB lower. BPM simulator should cope with these constraints.

BPM SIMULATOR DESIGN

There are different issues regarding the design:

- Deliver four synchronized output signals level in the range [-67 dBm to -7 dBm] at F_{acc} and $2 \times F_{acc}$.

* Work supported by SCK-CEN

† sidi-mohammed.ben-abdillah@ijclab.in2p3.fr

ISBN: 978-3-95450-249-3 ISSN: 2673-5350 doi: 10.18429/JACoW-IBIC2024-TUP38

DEVELOPMENT OF A BEAM POSITION MONITOR FOR MYRRHA HIGH ENERGY BEAMS

Sidi Mohammed Ben Abdillah*, Fabrice Fournier, Olivier Pochon
Université Paris-Saclay, CNRS/IN2P3, IJClab, Orsay, France
Alexander Bechtold, NTG Neue Technologien GmbH & Co KG, Gelnhausen, Germany

Abstract

MYRRHA (Multi-Purpose Hybrid Research Reactor for High-Tech Applications) aims to demonstrate the feasibility of high-level nuclear waste transmutation at industrial scale. The accurate tuning of LINAC is essential for the operation of MYRRHA and requires measurement of the beam transverse position and shape, the phase of the beam with respect to the radiofrequency voltage with the help of Beam Position Monitor (BPM) system. MYRRHA is divided in three phases, the first phase, called MINERVA, includes several sections allowing beam acceleration up to 100 MeV. the second phase includes a High Energy Beam Transport (HEBT) line connects to two users' facility. A BPM prototype was realized for the HEBT line. This paper addresses the design, realization, and calibration of this BPMs and its associated electronics. The characterization of the beam shape is performed by means of a test bench allowing a position mapping with a resolution of 0.02 mm.

GENERAL DESCRIPTION OF MYRRHA

MYRRHA is a high power proton accelerator with strongly enhanced reliability performances. The conceptual design is on-going for more than 15 years. The adopted LINAC scheme to fulfil the reliability goal is based on 2 distinct sections.

MYRRHA first phase (MINERVA) accelerates the beam up to a 100 MeV energy. The HEBT line in MYRRHA phase 2 includes accelerator will deliver proton beam for applications including fusion research and isotopes production.

HEBT line addresses topics that have been identified as priority ones to successfully pursue the research, design and development of the MYRRHA accelerator and prepare for its actual construction. Among the topics, beam characterization would deliver data of fundamental importance in all beam dynamics simulation tools.

Beam Position Monitor (BPM) is a non-destructive beam diagnostic system, it measures beam position, phase shift regarding the accelerating signal and also gives an indication on the beam transverse shape. IJClab is in charge of the realization of a BPM prototype in order to contribute to the characterization of the beam along the HEBT line, particularly at 100 MeV. This document details the steps of design, fabrication and qualification of this prototype.

GENERAL DESCRIPTION OF BPM

Capacitive BPM is used. Each BPM is equipped with 4 probes formed by a sealed 50 Ohm feedthroughs attached to an electrode. The probes (feedthrough + electrode) should be as identical as possible and they should be symmetrical regarding the center of the BPM.

BPM must meet a set of constraints (vacuum, magnetism, positioning, steaming, radiation hardness…).

The beam induces electrical signal on each electrode. The electronic module provides the following information by processing the electrical signals mentioned above:

- The horizontal and vertical position of the center of gravity of the beam.
- The phase of the beam with respect to the main Radio Frequency reference signal. Beam velocity and energy are processed from this measurement.
- Beam Ellipticity figuring in the second order moment of the beam transverse distribution.

Table 1 summarizes beam properties and BPM specifications for the HEBT line.

Table 1: Beam Parameters & BPM Specifications

Parameter	Range	Precision
Energy E	100 MeV-200 MeV	
Current I	0.1 mA - 4 mA	
Duty cycle	2.10^{-4} to 0.125	
Bunch length @100MeV	5°; 80 ps	
F_{acc}	176.1 MHz	
Beam pipe diameter	80 mm	
Measured Position on both axes	±5 mm	100 µm
Measured Phase	360 degrees	1 degree
Measured Ellipticity	±5 mm	Max (3.2 mm²;20%)

BPM DESIGN

Experience with MYRTE and MINERVA BPMs [1, 2] was of a great help. The relatively similar properties between the beams of MYRRHA and MYRTE led us naturally to match MINERVA BPM design to HEBT line.

* Work supported by SCK-CEN
† sidi-mohammed.ben-abdillah@ijclab.in2p3.fr

ISBN: 978-3-95450-249-3 ISSN: 2673-5350 doi: 10.18429/JACoW-IBIC2024-TUP40

PROGRESS OF LOW-β BPM CALIBRATION BASED ON HELICAL SLOW-WAVE STRUCTURE*

M.W. Wang†, Z.M. Wang, D. Wang, X. Zhuo
State Key Laboratory of Intense Pulsed Radiation Simulation and Effect,
Northwest Institute of Nuclear Technology, Xi'an, China

Abstract

Beam Position Monitors (BPMs) are essential in particle accelerators for the precise measurement of beam trajectories. Considering the inherent inaccuracies in manufacturing and assembly, rigorous offline calibration processes are essential to guarantee the precision of beam position measurements. The predominant calibration technique, specifically the wire test method, is tailored for relativistic beams and is inappropriate for low-β beams. This manuscript introduces an innovative approach employing a helical slow-wave structure to emulate the electromagnetic fields of low-energy beams, thus facilitating the calibration of BPMs for low-β scenarios. Employing a helix-based calibration platform, we conducted the calibration of the nonlinear response of BPMs at the Xi'an Proton Application Facility for a 7 MeV proton beam, with results aligning with the simulation. This advancement expands the precision and range of beam position measurements, substantially enhancing the operation and optimization of particle accelerators.

INTRODUCTION

Beam Position Monitors (BPMs) are essential for measuring the beam position and trajectory in linear accelerators [1]. Non-relativistic beams generate an electromagnetic field possessing a longitudinal component, resulting in distinct responses of BPMs to beams with diverse β values [2]. Utilizing the helical slow-wave structure effectively simulates the electromagnetic field produced by low-β beams, facilitating the calibration of BPMs [3]. To ensure precise calibration, the helix's bandwidth must at least match the spectrum range of a micropulse beam. The dispersion characteristics of the helix, including its phase velocity and the frequency-dependent impedance, are the primary determinants of its bandwidth.

OPTIMIZATION DESIGN

Drawing from the sheath-helix model, the literature [4] has formulated the dispersion equation for a helix structure encompassing a central conductor and proposed a rapid design method. To reduce the helix's phase velocity and impedance dependency on frequency, and to broaden the helix's bandwidth, it is essential to perform a dispersion analysis on the helix. From the equations $v = 1/\sqrt{C_0 L_0}$ and $Z_0 = \sqrt{L_0/C_0}$, it is evident that achieving low dispersion involves decreasing the frequency sensitivity of the helix's equivalent capacitance and inductance. Utilizing the dispersion equation, the equivalent capacitance and inductance of the helix are deduced below.

$$C_0 = 2\pi a\gamma\epsilon_0\left(\epsilon_r \cdot \frac{K_{0d}I_{1a}+K_{1a}I_{0d}}{K_{0a}I_{0d}-K_{0d}I_{0a}} - \frac{K_{0i}I_{1h}+K_{1h}I_{0i}}{K_{0h}I_{0i}-K_{0i}I_{0h}}\right)$$
$$L_0 = \frac{\beta_z^2\mu_0 cot^2\phi}{2\pi a\gamma^3}\frac{1}{\frac{K_{1b}I_{0a}+K_{0a}I_{1b}}{K_{1a}I_{1b}-K_{1b}I_{1a}} - \frac{K_{1d}I_{0a}+K_{0a}I_{1d}}{K_{1a}I_{1d}-K_{1d}I_{1a}}} \quad (1)$$

Assess the influence of geometric and electrical parameters on the helical line's equivalent capacitance and inductance utilizing the aforementioned formula, with the outcomes depicted in Fig. 1. Generally, the equivalent inductance decreases while the equivalent capacitance increases as the frequency increases, resulting in minimal changes to phase velocity and significantly reduced characteristic impedance with increasing frequency. Considering dispersion flatness, the frequency sensitivity of the equivalent capacitance and inductance is mitigated by a smaller helix radius coupled with a larger inner conductor radius, indicating that the closer the helix is to the inner conductor, the less pronounced the dispersion, as the coupling between the coils weakens with reduced spacing. Enhancing the helix pitch also mitigates inter-coil coupling, thereby diminishing dispersion. Increasing the dielectric constant of the insulating medium has a minor effect on the sensitivity of the capacitance to frequency but reduces the sensitivity of the inductance to frequency; in sum, augmenting the dielectric constant favors dispersion amelioration. However, an excessively high dielectric constant could lead to excessive equivalent capacitance, necessitating an increase in the separation between the helix and the inner conductor to preserve a characteristic impedance at 50 Ω. Hence, a heightened dielectric constant is at odds with minimal spacing, necessitating a trade-off. In terms of the impact on dispersion flatness, the separation between the helix and the inner conductor exerts the most significant influence, the helix pitch is the subsequent notable determinant, and the medium's dielectric constant has the least effect.

Given that the sheath-helix model posits an infinitely thin helical strip with its width equated to the pitch, it fails to account for the effects of the helix's width and thickness on its response; therefore, CST simulation is employed. Utilizing the periodic boundary conditions in the CST eigenmode solver, the relationship between phase velocity and frequency was obtained by calculating the mode frequency for different phase shifts. Furthermore, beginning

* Supported by National Natural Science Foundation of China (Grant No. 12105228).

† wmw13@foxmail.com

ISBN: 978-3-95450-249-3 ISSN: 2673-5350 doi: 10.18429/JACoW-IBIC2024-TUP41

TEST OF BPM CABLES VS TEMPERATURE AND HUMIDITY*

Chongyang Liang†,1, Jun He
Institute of High Energy Physics, Chinese Academy of Sciences, Beijing, China
[1]also at University of Chinese Academy of Sciences, Beijing, China

Abstract

Measuring the absolute position of the beam in the intensifier and storage ring of a high energy photon source (HEPS) requires measuring the offset between the electrical and mechanical centers of the beam position monitor (BPM). In the HEPS project, a four-electrode BPM is used, and the signals from each of the four electrodes of the BPM probe are led out by a cable. During the operation of the intensifier and storage ring, the influence of ambient temperature and humidity on the BPM cable and the difference between the four channels will directly lead to changes in the BPM measurement results. In this paper, vector network analyzer (VNA) is used to test the data of signal amplitude change of two BPM cables within ten hours when temperature and humidity change. The conclusion is that the influence of temperature on the signal is about 0.01 dB/℃, the influence of humidity on the signal is about 0.05 dB/10%, and the relative change between channels is about 5%.

INTRODUCTION

The High Energy Photon Source (HEPS), a fourth-generation high-performance synchrotron radiation source under construction in China, is designed with an electron energy of 6 GeV and boasts an ultra-low emittance of 34.2 pm·rad and a brightness reaching $5 \times 10^{22}\ \mathrm{s^{-1}mm^{-2}mrad^{-2}}$. Composed of a 500 MeV linear accelerator, a booster, a storage ring with a circumference of 1360.4 meters, a low-energy transport line, two high-energy transport lines, and a beam dump line, the schematic of the device is shown in Fig. 1 [1]. Upon completion, HEPS is expected to alleviate the tight supply and demand situation for experiments, providing a higher level platform for scientific research.

The beam position monitoring system is an essential component of particle accelerators, capable of directly measuring beam position information as well as indirectly calculating critical parameters such as working points, dispersion, and chromaticity. The various data obtained through the beam position monitoring system are employed to optimize the operational state of the device, ensuring the stable functioning of the accelerator.

Submicron-level stability requirements for the beam trajectory at the High Energy Photon Source (HEPS) necessitate a precise beam position measurement system along with a trajectory feedback system. The vertical dimension of the beam in the HEPS storage ring reaches a minimum size of approximately 1 μm, demanding a beam position monitor (BPM) resolution on the order of 0.1 μm and trajectory control accuracy around 0.3 μm [2]. To meet such stringent criteria, strict quality control of the BPMs used in HEPS is essential, and the performance of the cables under environmental influences must also be considered. This study has tested the signal amplitude of BPM cables for the high-energy synchrotron radiation source under varying temperature and humidity conditions using a vector network analyzer.

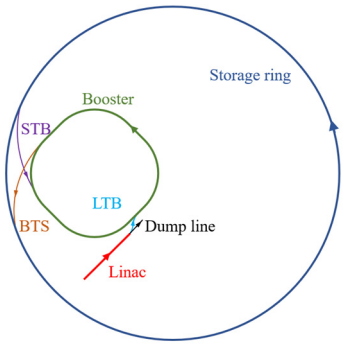

Figure 1: Schematic diagram of the HEPS.

BPM SYSTEM

A complete beam position measurement system is typically comprised of two main components: BPM probes and BPM signal processing electronics, often connected by coaxial cables, with the basic structural framework illustrated in Fig. 2. The BPM probes are designed to detect electromagnetic field signals produced as the beam passes, thereby acquiring information on the beam's position. Each BPM probe consists of a cavity with two or four symmetrically arranged electrodes, depicted in the left section of Fig. 2. The signals captured by the BPM probes are transmitted via coaxial cables to the BPM signal processing electronics, where they first undergo processing by the Analog Front End (AFE) circuitry to handle the analog signals. Subsequently, these signals are converted into digital signals by the Digital Front End (DFE), and after algorithmic processing, the final beam position information is obtained.

BPM probes consist of a cavity that mirrors the shape of the vacuum pipe and four symmetrically arranged electrodes. These electrodes capture electromagnetic field signals generated by the beam, which are then converted into electrical signals and transmitted through the output port to the connecting cable. BPM probes are typically situated near the quadrupole magnets of the accelerator. There are various types of BPMs, with button and stripline types being the most commonly utilized.

* Chongyang Liang. Work for accelerator beam measurement and control.
† liangcy@ihep.ac.cn

ISBN: 978-3-95450-249-3 ISSN: 2673-5350 doi: 10.18429/JACoW-IBIC2024-TUP43

BUNCH-BY-BUNCH BEAM POSITION MEASUREMENTS AT PETRA III

C. Alvarez*, G.Kube, H.-T. Duhme, J. Neugebauer, T. Marwedel
Deutsches Elektronen-Synchrotron DESY, Germany
D. Bisiach, I-Tech, Solkan, Slovenia

Abstract

The PETRA IV project is set to enhance the current PETRA III synchrotron into an ultra-low-emittance source. The reduced emittance will impose stringent requirements on machine stability and operation. In order to cope with these requirements, bunch-by-bunch information is required from some monitor systems. For precise monitoring of beam position and charge, the Libera Digit 500 instrument from Instrumentation Technologies is tested as a readout electronics for BPMs at the existing machine PETRA III. This system features four channels with a 500 MHz sampling rate, synchronized with the accelerator's RF, enabling observation of beam properties with a bunch-by-bunch resolution, thus facilitating a more comprehensive understanding of beam behavior. This contribution provides an overview of the latest beam measurements at the single bunch level, allowing observation of beam oscillations and injection dynamics.

INTRODUCTION

The 6 GeV synchrotron light source PETRA III [1] at DESY (Hamburg, Germany) has been in user operation since 2010. It features a circumference of 2304 m, its harmonic number is 3840, and it operates with RF frequency of 500 MHz. In the coming years, PETRA III is planned to be turned into an ultra-low-emittance fourth-generation source, PETRA IV. The small beam emittances result in significantly smaller beam sizes, about 7 µm horizontally and 3 µm vertically [2]. To meet these requirements, and get more information on beam oscillations over each turn, bunch-by-bunch information can be essential. For this reason, the Libera Digit500 was installed as the readout electronics for one of PETRA III's BPMs. The time-dependent signals to be analyzed are the $SUM = A+B+C+D$, $X = K_x \frac{(B+C)-(A+D)}{SUM}$ and $Y = K_y \frac{(A+B)-(C+D)}{SUM}$, by their Power Spectral Density (PSD(ω)):

$$\mathrm{PSD}(\omega) = \lim_{T\to\infty} \frac{1}{T}|u(\omega)|^2, \qquad (1)$$

where $u(\omega)$ is the Fourier transform of the data measured in the time domain; with $t = n \times t_{sample}$, t_{sample} is the ADC sampling time; and n is an index [0, N], with N the maximum number of samples.

Firstly, the instrument commissioning is conducted, and, the linearity of the RF front end, as well as that of the instruments' internal attenuators is tested.

Then, PETRA III's injection oscillations are studied. Two cases are examined; injecting single bunches in an empty accelerator, and injecting additional intensity to a previously 40 bunch filled machine. This enables to obtain the individual bunches' longitudinal and transverse oscillations resulting from the injection scheme; and any additional impacts on single bunches arising from the injection kickers.

Secondly, a study of the injection and excitation kickers is carried out, analyzing transverse oscillations on individual bunches for the cases of MBFB enabled and disabled. The horizontal and vertical tunes are obtained, along with the decay times, and coupling between the horizontal and vertical orbits for the different scenarios.

Lastly, the intensity dependent tune shift is investigated. For this study, an inhomogeneous 60 bunch filling pattern is implemented into the accelerator, and the vertical excitation kickers are used, with and without the MBFB system. This can help understand the tune dependency with the single bunch current.

READOUT ELECTRONICS: LIBERA DIGIT500

The Libera Digit500 digitizer, a commercial product from the company Instrumentation Technologies [3], is experimentally tested as the readout of a dedicated BPM. A schematic for the functioning of this instrument is shown in Fig. 1. It features four input channels (A,B,C,D), that are connected to the four BPM pickups, and sampled with a 500 MHz sampling rate, and enabling to perform bunch-resolved measurements. Each channel is adjusted in amplitude with a 31 dB software-controlled variable attenuator, and later sampled by an Analog-to-Digital converter (ADC). Sampling is controlled by an external reference signal (Ref), synchronized to the accelerator's Radio Frequency (f_{ADC}) through a Phase Lock Loop (PLL).The data acquisition is triggered by a Trigger signal (T2), and data is stored into a 2 GB ADC buffer. External attenuators are added before the front-end to ensure the signal power coming from the BPM pick-ups stays within the instrument specifications, as well as to test the front-end linearity.

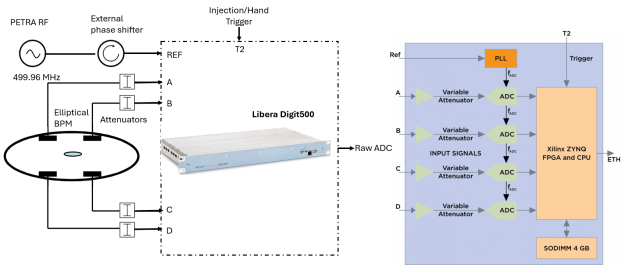

Figure 1: Experimental setup for the bunch-by-bunch measurements, and Libera Digit 500 Dataflow, Image from Instrumentation Technologies [3].

* carolina.alvarez.de.santiago@gmail.com

ISBN: 978-3-95450-249-3 ISSN: 2673-5350 doi: 10.18429/JACoW-IBIC2024-TUP44

SOLEIL II BPM : DESIGN, SIMULATIONS AND BUTTON PROTOTYPING

M. El Ajjouri*, F. Alves, Z. Fan, A. Gamelin, N. Hubert
Synchrotron SOLEIL, Gif sur Yvette, France

Abstract

SOLEIL II is the low emittance upgrade project for Synchrotron SOLEIL, targeting an emittance of ~80 pm.rad. The new lattice includes 180 Beam Position Monitors (BPM). Due to the different constraints on the magnet yokes, beam stay clear and synchrotron radiation, 3 different types of BPM will be installed on the storage ring with an inner diameter distributed between 16 and 24 mm. Electromagnetic and thermal simulations have been conducted to validate the designs. Manufacturing feedthroughs is a challenge due to the conical shape of the button and the small (200 µm) thickness of the gap with the BPM body. Prototypes of the button have been made. These prototypes will be tested in the current machine to validate the simulation results.

INTRODUCTION

SOLEIL is the French third generation light source routinely operated for external users since 2008 with a low electron horizontal emittance of 4 nm.rad at an energy of 2.75 GeV in high intensity (500 mA, 416 bunches) and temporal structure (8 bunches) modes. After 16 years of SOLEIL successful operation, a new storage ring lattice with a significantly higher photon beam brightness has been designed [1]. The financing of the SOLEIL II project has been approved in December 2023 and the construction phase will start in early 2025. The new storage ring commissioning phase including the 29 beamlines is planned for 2030. As much of the other diagnostic systems, the Beam Position Monitor (BPM) system will be completely renewed for SOLEIL II.

BPM MECHANICAL INTEGRATION

SOLEIL II baseline lattice includes 180 button type BPM distributed along the storage ring. All BPM are in the shadow of the synchrotron radiation with enlarged tapered section with respect to the vacuum chamber diameter. Depending on their location, BPM will have a different design (Fig. 1) :

- BPM16-6 (128 units) : achromat BPM with an inner diameter of 16 mm and button diameter of 6 mm.
- BPM20-7 (40 units) : Nominal straight section (SS), or nearby long SS adaptative section BPM with an inner diameter of 20 mm and button diameter of 7 mm.
- BPM24-7 (12 units) : Long SS BPM with an inner diameter of 24 mm and button diameter of 7 mm.

All BPM are the fixed point of the vacuum chamber with dedicated stands to mechanically bind them either to the girder (arcs) or to the ground (SS). To reduce the thermal expansion of the stand, Invar will be used in the straight sections, and steel with water cooling is foreseen for the arcs (to be confirmed by thermal and vibration studies). To minimize the mechanical constraints from the vacuum chamber almost all BPM are between two bellows (except the last BPM of the arcs with only one bellow due to limited space). Whereas the vacuum chamber is in copper chrome zirconium (CuCrZr) alloy, all BPM chambers will be in stainless steel, with a 10 µm Cu coating for impedance optimization. The BPM are independent pieces of the vacuum chamber with MO-Type vacuum Flange.

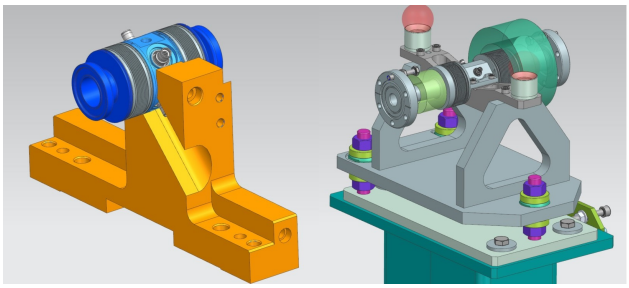

Figure 1: BPM16 for the arcs (left). Including bellows and flanges the BPM length is only 74.2 mm. BPM20 for the nominal straight sections with Invar stand (right). The block includes two bellows and a dedicated small thickness section to host a fast corrector.

BPM BUTTON DESIGN

In particle accelerators, one of the critical challenges is managing the power losses that occur as a result of the beam's interaction with the accelerator structure. As high-energy particle beams travel through the accelerator, they induce electromagnetic fields in the surrounding components, leading to energy dissipation primarily in the form of heat. Accurately calculating this power dissipation is vital for maintaining the efficiency and stability of the accelerator, as well as preventing potential damage to its components [2]. The total power loss by taking into account the beam's current spectrum and the real part of the longitudinal impedance at various harmonic frequencies. Understanding and minimizing this power dissipation is essential to optimize the efficiency and performance of the accelerator.

Button Shape

Detailed studies and simulations were carried out to determine the most appropriate button geometry for the beam position monitors [3]. These analyses considered the specific challenges posed by the design of modern accelerators, such as compact dimensions and the need to minimise energy loss. Two button geometries have been rigorously compared : conventional cylindrical and conical shapes.

* moussa.elajjouri@synchrotron-soleil.fr

ISBN: 978-3-95450-249-3 ISSN: 2673-5350 doi: 10.18429/JACoW-IBIC2024-TUP45

THE DESIGN AND ACCURATE CALIBRATION OF HIAF-RING BPM*

Peilin He†, Junxia Wu, Ze Du, Jia Yin, LiLi Li, Ruixia Tian, Zhixue Li, Hongming Xie, xiaodong Zhang, Yong Zhang, Institute of Modern Physics, Chinese Academy of Sciences, Lanzhou, China

Abstract

Beam Position Monitors (BPM) are the non-destructive monitors used most frequently at nearly all linacs, cyclotrons, and synchrotrons. The most basic function of BPM is to provide the accurate position of the centre of mass of the beam for closed orbit feedback and other demands. However, due to the error of actual processing, the k value and the actual electric center will be different with the ideal k value and electric center of BPM, which requires us to accurately measure the k value and offset value of each set of BPM offline.

There are 79 sets of BPMs in HIAF BRing, SRing & HFRS, with 10 specifications and plate radius ranging from 180 mm to 330 mm, but the shape and size of the front and back pipes connected to bpms are variety during actual installation. Based on theoretical analysis, the k value and offset value of the BPM which electrode plates are too close to the flange are greatly affected by the pipes connected to bpm at both ends, and the measurement error can even reach 9 mm. Therefore, this paper takes HIAF BRing and SRing BPM calibration as examples to explain how to accurately calibrate BPM.

INTRODUCTION

BPM types include capacitive BPM, linear-cut BPM, stripline BPM, and button BPM [1-3]. We will use different types of BPM according to different application scenarios. In the BPM design of HIAF BRing and SRing, combined with the beam profile size at the BPM probe installation position and the vacuum size at both ends, the inner diameter of our BPM plate was finally determined to be 180 mm~330 mm. However, due to the existence of the edge field effect, the k value and offset value of BPM are greatly affected by the shape and size of the pipes on both sides of the plate, and the ring BPM probe is generally only processed by the probe itself due to its huge size, unlike the straight line and other BPM which have its own pipes at both ends during processing, so the longitudinal length is only enough for the design of the plate part of the BPM, it is necessary to pay more attention on calibration, we need to add some short pipe which are consistent with the actual vacuum pipes during calibrating. There are 40 sets of HIAF BRing BPM probes, 4 specifications, 7 different operating conditions during calibration; There are 32 sets of HIAF SRing BPMs, 6 specifications, 29 different operating conditions during calibration, and several examples are used in this article to introduce this theory.

SIMULATION AND DESIGN OF BPM

Initial Simulation Analysis

The initial design version of the HIAF BRing & SRing BPM is shown in Fig. 1. And the main dimensions are: plate inner diameter 200 mm, plate length 178 mm, vacuum pipe inner diameter 274 m, middle individually gnd diameter 264 mm, overall longitudinal length 400 mm.

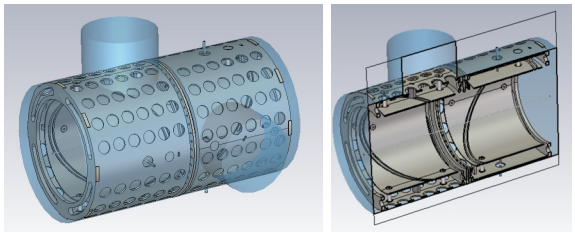

Figure 1: CST simulation model.

CST was used to model and simulate different structural details [4]. For example, whether it needs to add a separated ground structure between the plate and the vacuum tube, the simulation results are shown in Fig. 2. The results show that compared with the structure without the addition of ground, the use of adding separate ground structure and the non-perforated separate ground structure will introduce new resonance points, therefore, the removal of the separate ground structure in this structure. Meanwhile, the removal of the structure greatly simplifies the structure of the BPM itself, and is also more friendly to the vacuum, and brings great benefits to the processing and assembly of large-scale BPM equipment in the later stage. At the same time, the spacing between the plate and the isolation ring structure was simulated and calculated, as shown in Fig. 3. And the size with the highest sensitivity was selected according to the fitting structure of the position information and difference ratio and data.

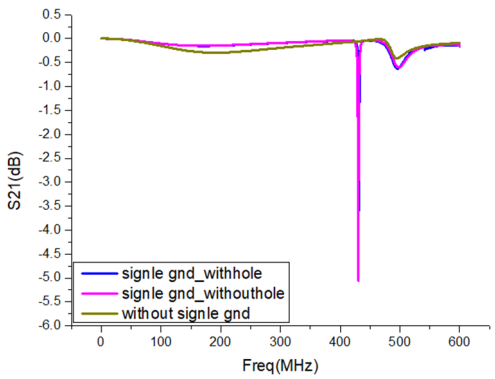

Figure 2: The effect of different individual structures on the resonance point.

ISBN: 978-3-95450-249-3 ISSN: 2673-5350 doi: 10.18429/JACoW-IBIC2024-TUP46

DESIGN AND DEPLOYMENT OF AN IN-VACUUM ELECTRO-OPTIC BPM AT THE CERN SPS

M.Z.C. Bosman*, S.M. Gibson, D.M. Harryman, A. Arteche
John Adams Institute at Royal Holloway, University of London, UK
T. Lefèvre, T.E. Levens, CERN, Geneva, Switzerland

Abstract

The Electro-Optic Beam Position Monitor employs electro-optically active Lithium Niobate crystals with fibre-coupled laser interferometry to measure the propagating electric field from passing proton bunches in the Super Proton Synchrotron to infer their position and intra-bunch instabilities. A feedback algorithm continually adjusts the laser wavelength, and thereby the phase offset, so the interferometric bias point is kept in the linear range. Tests to validate the EO-BPM were conducted with comparison to current technology. Results show that the EO-BPM can identify turn-by-turn oscillations and its optical centre is offset from the beam pipe centre.

INTRODUCTION

The High-Luminosity Large Hadron Collider (HL-LHC) project at CERN aims to significantly increase the luminosity of the LHC and allow for more data to be collected by the LHC experiments. Part of the luminosity increase will be achieved by installing crab cavities to induce a transverse displacement within the proton bunches in order to improve the overlap of the colliding bunches in the interaction point [1].

An Electro-Optic Beam Position Monitor (EO-BPM) is being developed as a high-bandwidth (at least 4 GHz) diagnostic tool for crabbing and intra-bunch instability detection at HL-LHC. The EO-BPM senses the propagating electric field, induced by the passing proton bunch, using electro-optic crystals [2].

Following previous tests of an in-air design in HiRadMat [3], an ultra-high vacuum compatible device has recently been installed in the Super Proton Synchrotron (SPS) as a proof of concept of the HL-LHC design.

WORKING PRINCIPLE

Background

Some electro-optically active crystals incur a change in refractive index that is linear with the electric field induced in the crystal. This is known as the Pockels effect [4].

Lithium niobate (LNB) is an electro-optical birefringent crystal [5]. This means that the refractive index of one of its three principal axes differs from the other two. Due to the Pockels effect, this difference between the two refractive indices can be further enhanced by applying an external electric field to the crystal. Using linearly polarised laser light, this change due to the external field can be measured using interferometry. In such a way the external field, which in our case resembles the bunch shape, can be inferred [2].

EO Button Design

To focus the beam's electric field inside the crystal, a 9 mm diameter, electrically floating, electrode is placed in contact with the LNB crystal (shown in Fig. 1) [6]. The electric field induced by the bunch is focused by this bottom electrode and projected into the LNB crystal and via the top electrode to a termination on top.

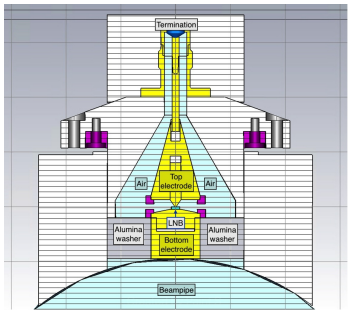

Figure 1: Transverse profile slice of 3D render EO-BPM, showing the beam pipe, floating electrode connected to LNB crystal and the top electrode.

Another method used to enhance the electric field in the crystal is the use of a waveguide. Narrowing the crystal to a 10 μm waveguide significantly concentrates the projected electric field from the bottom electrode. The fibre-coupled laser is attached to the narrowest part to maximise effectiveness [3].

A fibre-coupled laser is split and passes through two waveguides placed on opposite sides of the beam pipe. The outputs are then recombined to act as a Mach-Zehnder (MZ) interferometer (see Fig. 2) with two outputs in antiphase (C+, C-). The fibres are connected to the waveguide perpendicular to the profile in Fig. 1.

Output

The output of this interferometer is of the form

$$V = A + B\,cos(\phi_0 + \pi\frac{\Delta E_c}{E_\pi}), \tag{1}$$

and the normalised transfer function is

$$T_{inter} = \frac{1}{2} + \frac{1}{2}\,cos(\phi_0 + \pi\frac{\Delta E_c}{E_\pi}), \tag{2}$$

where ϕ_0 is defined as the phase offset, ΔE_c the difference in electric field in both waveguides, and E_π the electric field required for a phase advance of π.

* max.bosman@rhul.ac.uk

ISBN: 978-3-95450-249-3 ISSN: 2673-5350 doi: 10.18429/JACoW-IBIC2024-TUP51

MAXIMUM ENTROPY TOMOGRAPHY OF 4D TRANSVERSE PHASE SPACE DISTRIBUTIONS USING 2D MEASUREMENT RESULTS

L. W. Liu*, Z. J. Wang, J. C. Wong, Y. Du, T. Zhang, H. Y. Zhou, B. H. Ma
Institute of Modern Physics, Chinese Academy of Sciences, Lanzhou, China
also at University of Chinese Academy of Sciences, Beijing, China
also at Advanced Energy Science and Technology Guangdong Laboratory, Huizhou, China

Abstract

Obtaining the complete distribution of a beam in high-dimensional phase space is crucial for predicting and controlling beam evolution. Based on the theory of maximum entropy tomography, we developed an algorithm for reconstructing the four-dimensional (4D) transverse phase space distribution. Our algorithm can take any number of 2D linear projections as constraints and iteratively converges to the unique numerical solution, which is the maximum-entropy distribution satisfying the constraints. Having verified the algorithm with simulation experiments, we plan to use it to conduct 4D phase space tomography in the MEBT and HEBT of the heavy ion linac CAFe II.

INTRUDUCTION

Tomography is the process of reconstructing a high-dimensional distribution from multiple low-dimensional projections. In the case of finite constraints, there is generally no unique solution for the high-dimensional distribution. The maximum entropy theory can be used to find the solution with the maximum information entropy among all solutions satisfying the constraint conditions. A discussion of maximum entropy theory and information entropy can be found in reference [1]. The maximum entropy theory has been applied to the reconstruction of phase space distribution in reference [2]. The extension of maximum entropy tomography from two to four dimensions is discussed in reference [3]. In this paper, we extended two-dimensional to four-dimensional maximum entropy tomography to more general cases. We developed algorithms that are more applicable to general cases, allowing us to use more constraints when reconstructing the phase space distribution to obtain more reliable results. We designed an experiment to measure the four-dimensional transverse beam phase space distribution at the entrance and exit positions of the superconducting cavity. We employed parallel and vertical scanning schemes to obtain the required projections as constraints for the algorithm. Parallel scanning is the conventional slit-grid method to measure the information in the (x, x') plane and (y, y') plane [4]. Vertical scanning can measure the coupling information between the x and y directions, and this scanning method has been used in reference [3]. In the following sections of this paper, we will discuss the theoretical formulas for tomography from two-dimensional to four-dimensional, the combined parallel and vertical scanning method, and then we will present the results of our simulation experiments.

* liuliwen@impcas.ac.cn

MAXIMUM ENTROPY TOMOGRAPHY

As in reference [3], we express the information entropy of the four-dimensional function as Eq.(1). $\rho(x, x', y, y')$ is the four-dimensional distribution we want to solve.

$$H[\rho] = -\iiiint \rho(x, x', y, y') \ln \rho(x, x', y, y')\, dx\, dx'\, dy\, dy' \tag{1}$$

We denote the j-th of the total n two-dimensional projections as $g(u_j, u_j')$, which represents the two-dimensional projection of ρ in the four-dimensional space (u_j, u_j', v_j, v_j'). We use Eq. (2) to write the j-th constraint.

$$G_j = g(u_j, u_j') - \iint \rho(f_j(x, x', y, y'))\, dv_j\, dv_j' = 0 \tag{2}$$

Although we only discuss linear mappings in this paper, the mapping between (u_j, u_j', v_j, v_j') and (x, x', y, y') can actually be any invertible mapping. Therefore, we denote the mapping from (x, x', y, y') to (u_j, u_j', v_j, v_j') as $f_j(x, x', y, y')$. To solve for the solution that satisfies all the constraint conditions and maximizes Eq. (1), we write the function $K[\rho]$ that includes n Lagrange multipliers as follows, where n is the number of constraint conditions:

$$K[\rho] = H[\rho] + \sum_{j=1}^{n} \iint \lambda(u_j, u_j') G_j[\rho]\, du_j\, du_j' \tag{3}$$

The solution that satisfies the conditions should maximize Eq. (3). If we denote this solution as ρ^*, then when ρ takes the value ρ^*, the partial derivative of $K[\rho]$ with respect to ρ needs to be zero.

$$\left(\frac{\partial K[\rho]}{\partial \rho}\right)\Big|_{\rho=\rho^*} = -\iiiint \left(\ln \rho^* + 1 + \textstyle\sum_{j=1}^{n} \lambda(u_j, u_j')\right) dx\, dx'\, dy\, dy' \tag{4}$$

We can express ρ^* as a product of n two-dimensional functions originating from different planes, denoted as Eq. (5). C is a constant, and since we are only concerned with the probability distribution density of the distribution function, we can ignore the value of C.

$$\rho^* = C \cdot \exp\left(-\sum_{j=1}^{n} \lambda(u_j, u_j') - 1\right) = C \cdot \prod_{j=1}^{n} h(u_j, u_j') \tag{5}$$

In Eq. (5), $h(u_j, u_j')$ is a function defined on the same plane as the j-th constraint $g(u_j, u_j')$. We can use an iterative algorithm to solve for all $h(u_j, u_j')$. By combining Eq. (2) and

ISBN: 978-3-95450-249-3 ISSN: 2673-5350 doi: 10.18429/JACoW-IBIC2024-TUP54

ESTIMATION OF BEAM TRANSVERSE PARAMETERS THROUGH A MULTIMODE FIBER USING DEEP LEARNING

Q. Xu*, A. Hill, H. D. Zhang, C. P. Welsch
Cockcroft Institute and University of Liverpool, Warrington, UK
F. Roncarolo, G. Trad, CERN, Meyrin, Switzerland

Abstract

In response to CERN's need for alternative imaging solutions of scintillating screens due to the discontinuation of radiation-hardened VIDICON tubes, the single large-core multimode fiber has been identified as a potential medium to transmit image signals to a CMOS camera situated away from radiation-prone areas. However, significant challenges in image distortion at the fiber's output end complicate the reconstruction of the original beam distribution.

To address this, a novel machine learning-based approach was introduced that utilizes a deep convolutional encoder-regressor network. It first compresses the fiber image into a latent space. Subsequently, a fully connected regression network directly estimates the beam parameters, such as centroids and widths, from the encoder output without reconstructing the detailed image. This contribution will showcase an end-to-end system capable of estimating transverse beam parameters from the fiber output patterns and offering a safe, camera-preserving solution for beam imaging in high-radiation environments.

INTRODUCTION

At CERN, the monitoring of 2D transverse beam profiles was mostly done by rad-hard VIDICON cameras. With the cessation of this kind of camera on a global scale, the transfer to other imaging solutions is required. This has led to the exploration and adoption of CMOS cameras as a viable alternative. However one of the primary concerns using CMOS cameras is the radiation damage when operating close to the accelerator. A potential solution is to use optical fibers relaying the initial image signal so that the camera can be placed somewhere safe. Multimode fiber (MMF) has been studied as a direct imaging medium over the past decades. The large core diameter of MMF supports a high number of light propagation modes, which is proportional to the square of the fiber core radius according to the mode calculation formula [1], and this correlates with the amount of information it can encode and transmit. Since the mode is a distinct way light propagates in an MMF, finer resolution and higher bandwidth are provided for image transmission, potentially preserving most of the input information and therefore it is selected for this task.

The reconstruction challenge caused by MMF after transmission is largely due to mode coupling inside the fiber [2]. This phenomenon occurs when light energy is transferred between different propagation modes within the fiber due to changes in geometry and refractive index, making the transmission property of the fiber more dynamic. The methods to reconstruct the original image from the MMF output speckle pattern range from initial methods involving phase conjugation to wavefront shaping that uses spatial light modulators (SLM). These methods have certain limitations, such as the reconstructed image must appear at the proximal end of the fiber, which is the same side as the original light source, or requiring precise control of the image source [3], making them impractical for our scenario.

Statistical-based methods that use computers to model the optical system digitally are another popular means of MMF image reconstruction, such as a complex value transmission matrix (TM) that tries to approximate the mapping relationship between fiber input and output planes in terms of intensity and phase. However, TM is relatively susceptible to environmental perturbations and usually requires a complex equipment setup for precise measurement [4]. More recent approaches show that neural networks have very good generalization ability, capable of modeling both linear and non-linear effects within the fiber, and require only intensity measurements from relatively small datasets, making them one of the most suitable approaches for retrieving information from the distorted output.

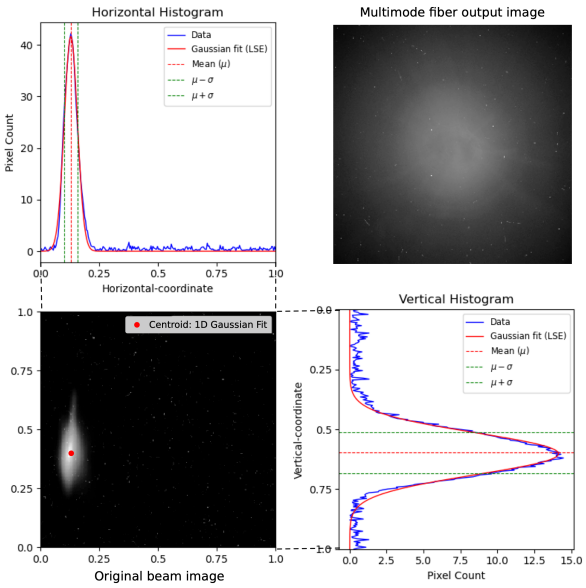

Figure 1: A representative example of transverse parameter calculation from a scintillating screen and the corresponding MMF output pattern.

* qiyuan.xu@liverpool.ac.uk

ISBN: 978-3-95450-249-3 ISSN: 2673-5350 doi: 10.18429/JACoW-IBIC2024-TUP55

DESIGN OF THE BPM BUTTON FOR ALBA II

L. Torino*, U. Iriso, O. Traver, ALBA CELLS, Cerdanyola del Vallés, Spain

Abstract

As many other light sources, ALBA is also going through an upgrade phase leading to ALBA II. In this context, new Beam Position Monitors (BPMs) have to be designed to fit the reduced vacuum chamber. The buttons and the block were designed to be as compact as possible minimizing the impedance to avoid overheat and maintaining a good signal level. Different shapes and materials were simulated and the best were selected to be produced as prototype. In this proceeding, we present the process and the simulations that lead to the ALBA II BPM button design.

INTRODUCTION

Beam Position Monitors (BPMs) are an essential part of the diagnostics of any particle accelerators. They measure the transverse position of the beam and and they provide the input for the Fast Orbit Feedback that guarantees the beam stability. This aspect is crucial in the arising fourth generation of light sources. Among these new machines, ALBA is also proposing an upgrade of the existing storage ring called ALBA II [1], and, in this framework, new BPMs buttons have to be designed to fit the new vacuum chamber.

The miniaturization of the vacuum chambers goes together with a miniaturization of the BPMs: the buttons are now very close to the beam and this demand for detailed study and simulation of the impedance and thermal response.

In this proceeding, we will outline the journey that brought us to the design of the new BPM buttons for ALBA II, starting from a theoretical approach and ending to CST simulation to optimize the material.

ALBA VS ALBA II

As a staring point for our consideration we take the Vacuum chamber and the BPM button designed for ALBA [2]. We know that with this buttons we are able to measure the beam with the required accuracy and precision.

Figure 1 shows a comparison in scale of ALBA and ALBA II vacuum chamber while the main characteristics of chambers and buttons are listed in Tab. 1 for both the machines. ALBA chamber is "flat", as in the majority of third generation light sources, while it will be round for ALBA II.

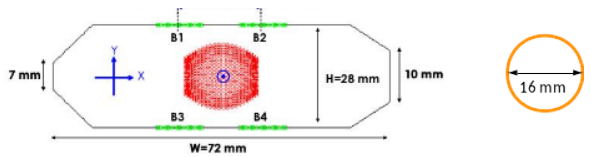

Figure 1: Comparison between ALBA and ALBA II vacuum chamber.

Table 1: Beam pipe and button characteristics for ALBA and ALBA II

	ALBA	ALBA II
Chamber radius a (mm)	14	8
BPM radius r_b (mm)	3.5	1-5
Gap g (µm)	300	100, 200, 300

Calculations and tests were performed for different radius and gaps for ALBA II BPMs button and the best combination have finally be selected.

THEORETICAL CONSIDERATION

To optimize BPM button performance, we aim to maximize transfer impedance, minimize coupling impedance, and avoid TE11 mode resonances. To do so we follow the approach presented in [3, 4].

Transfer impedance (Z_t) quantifies the button's ability to convert beam current into a measurable voltage. It is defined as:

$$Z_t = \frac{R}{1 + i\omega RC}\frac{r_b^2}{2ac} i\omega, \tag{1}$$

where R is the detector resistance, C is the equivalent capacitance between the button and the block, ω is the angular frequency, and c is the speed of light.

A higher Z_t improves signal-to-noise ratio.

Coupling impedance (Z_l) represents power dissipation caused by the button's interaction with the beam and is defined as:

$$Re(Z_l) = \frac{1}{c^2}\left(\frac{r_b^2}{2a}\right)^2 R\omega_c^2 \frac{\left(\frac{\omega}{\omega_c}\right)^2}{1 + \left(\frac{\omega}{\omega_c}\right)^2} \tag{2}$$

$$Im(Z_l) = \frac{1}{c^2}\left(\frac{r_b^2}{2a}\right)^2 R\omega_c^2 \frac{\left(\frac{\omega}{\omega_c}\right)}{1 + \left(\frac{\omega}{\omega_c}\right)^2}, \tag{3}$$

where ω_c is the cutoff frequency of the equivalent RC circuit.

Minimizing Z_l reduces heat load and potential instabilities.

The TE11 mode is a resonant frequency that can affect button performance. It can be parameterized as:

$$f_1 = \frac{c}{\pi(r_h + r_b)}, \tag{4}$$

where r_h is $r_b + g$. Shifting this frequency away from the beam spectrum is crucial.

Finally, achieving high intrinsic resolution is crucial for accurate beam position measurements. This involves optimizing the signal-to-noise ratio (SNR), which is calculated as:

$$SNR = \frac{P(\omega)}{P_{Th}}, \tag{5}$$

* ltorino@cells.es

ISBN: 978-3-95450-249-3 ISSN: 2673-5350 doi: 10.18429/JACoW-IBIC2024-TUP56

NEW INTERFEROMETRIC APERTURE MASKING TECHNIQUE FOR FULL TRANSVERSE BEAM CHARACTERIZATION USING SYNCHROTRON RADIATION

U. Iriso*, L. Torino, ALBA-CELLS Synchrotron, Cerdanyola del Valles, Spain
C. Carilli, National Radio Astronomy Observatory (NRAO), Socorro - NM, USA
B. Nikolic, University of Cambridge, Cambridge, UK
N. Thyagarajan, CSIRO, Bentley WA, Australia

Abstract

Emittance measurements using synchrotron radiation are usually performed using x-rays to avoid diffraction limits. Interferometric techniques using visible light are also used to measure either the horizontal or the vertical beam projection. Several measurements rotating the interferometry axis are needed to obtain a full beam reconstruction. In this report we present a new interferometric multi-aperture masking technique and data analysis, inspired by astronomical methods, that are able to provide a full 2-D transverse beam reconstruction in a single acquisition. Results of beam characterization obtained at ALBA synchrotron light source will also been shown.

INTRODUCTION

Two-dimensional (2D) transverse characterization of the particle beam is of fundamental importance in accelerators, as it provides a measurement of the beam emittance, one of the key figures of merit of an accelerators. The emittance describes the transverse distribution of particles, which is well described by a 2D Gaussian ellipse, parameterised by its major axis, minor axis, and tilt angle. In synchrotron light sources, beam size measurements are based on the Synchrotron Radiation (SR) emitted by the electron beam. The most commonly used methods to measure the beam size are the x-ray pinhole and the double-aperture interferometry [1].

The double-aperture interferometry was originally developed using visible light in [2], but it only provides a one dimensional measurement in the direction given by the baseline joining the aperture centers. Full 2D reconstruction can be obtained by rotating the aperture mask at different orientations [3], but at least 4 orientations are needed, meaning at least 4 inteferograms. A four-aperture square mask has been used to obtain the 2D source size with one single interferogram [4], but such mask suffers from decoherence due to redundant sampling in Fourier space and it is also affected by the non-uniform illumination of the SR [5].

These detrimental effects can be mitigated with a combination of techniques widely used in astronomy [6,7]. During the last year, we developed full 2D characterization of the ALBA electron beam using a single visible light interferograms with multi-aperture masks (from 3 to 7-holes) [8]. In these masks, the vector baseline between every pair of holes is unique, whence the term *Non-Redundant Aperture* (NRA). This report describes the technique, shows the results obtained by changing the beam coupling in the ALBA storage ring, and compares them with measurements using well-established techniques at ALBA: the rotating 2-aperture mask (which provides beamsize measurements at the same location), or calculations using the emittances obtained with LOCO [9] and the x-ray pinhole [10].

EXPERIMENTAL SETUP

Figure 1 shows the basic setup to perform Synchrotron Radiation Interferometry (SRI). At ALBA, the SR is emitted by a dipole and the visible part is brought to the BL34 beamline using a set of 7 mirrors: one of which is in-vacuum and it is used to select just the visible light, the other mirrors are in atmospheric pressure. Once the light arrives at the beamline, the SR hits the NRA mask, and the interferometric pattern is imaged through a focusing lens and a magnifier onto the CCD. We have used 2, 3, 5 and 7-hole aperture masks [8].

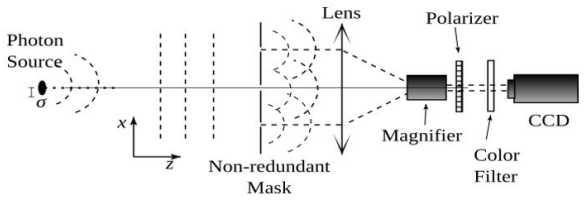

Figure 1: Experimental set-up. The mask is exchanged to perform either NRA or rotating double-aperture inteferometry.

Figure 2 shows the geometry of the 5-hole (left) and 7-hole mask (right), adapted from [11]. All holes are 3 mm diameter. The 3-hole mask is basically the same as the 5-hole, but only uses Ap-0, 1 and 2.

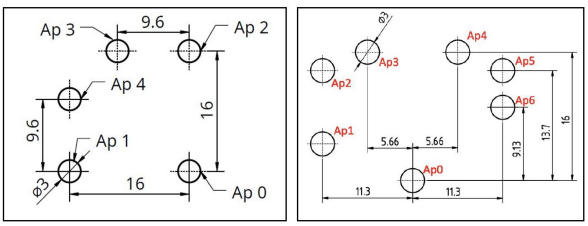

Figure 2: Sketch of the 5-hole NRA mask (left) and 7-hole mask (right). Distances are given in mm.

* uiriso@cells.es

ISBN: 978-3-95450-249-3 ISSN: 2673-5350 doi: 10.18429/JACoW-IBIC2024-TUP57

HETERODYNE NEAR-FIELD SPECKLE SIMULATIONS USING SRW AT THE ALBA FE21

U. Iriso*, J.M. Alvarez, A. Nosych, J. Núñez,
E. Solano, L. Torino, ALBA-CELLS, Cerdanyola del Vallès, Spain
B. Paroli, M. A. C. Potenza, M. Siano, Università degli Studi di Milano, Milan, Italy
D. Butti, S. Mazzoni, G. Trad, CERN, Geneva, Switzerland

Abstract

Several experiments were done to measure the transverse beam size at the NCD ALBA beamline using the Heterodyne Near Field Speckles (HNFS) technique. Inside the FCC collaboration, it was decided to move these experiments to the ALBA Front End 21, where currently an x-ray pinhole camera is working since 2021. The goal is that the two measurement techniques can work alternatively and measure the electron beamsize of the same source point, so that a direct comparison between both techniques can be done. This paper reports the SRW simulations performed in order to investigate the feasibility of the HNFS experiments at this new location. In particular, it focuses on the effect of the dipole radiation and the design of the high energy and high bandwidth monochromator required to perform HNFS experiments at this location.

INTRODUCTION

During standard operation, the transverse beam profile of the electron beam at ALBA Synchrotron is measured via the X-ray pinhole camera technique [1]. This direct imaging technique allows a fast rendering of the transverse profile but presents a limited beam-size resolution due to diffraction effects. Amongst other options, the X-ray Heterodyne Near Field Speckle technique (XHNFS) promises to solve this issue and also provides an effective measurement of the spatial coherence properties of the radiation beam.

The XHNFS method is based on the interference between the weak spherical wavefronts scattered by small obstacles (with size in the sub-μm range, in our case a water-based suspension of colloidal particles) and the intense transmitted X-ray beam. This interference is called ”speckle” pattern. From the Fourier analysis of the speckle pattern, we measure the coherence length, which ultimately allows to measure the source (electron) beam size. This method has been already tested at the NCD-Sweet ALBA Beamline [2], but also at other labs [3, 4].

This method is one of the candidates to measure the beam size at the Future Circular Collider (FCC) [5]. As part of the FCC collaboration between ALBA, CERN, and the University of Milano, and with the goal of properly calibrate this technique, it was decided to move these experiments to the ALBA Front End 21 (FE21), where an x-ray pinhole camera is working since 2021 [1]. The goal is that the two measurement techniques can work alternatively and measure the electron beam size of the same source point, so that a direct comparison between both techniques can be done.

The sketch of the FE21 is shown in Fig. 1, with components (already installed) for the x-ray pinhole and the required XHNFS components currently under design. The black elements show the fixed components, whereas the components in green need to be designed. Using remote control motors, either pinhole measurements or XHNFS measurements can be taken alternatively.

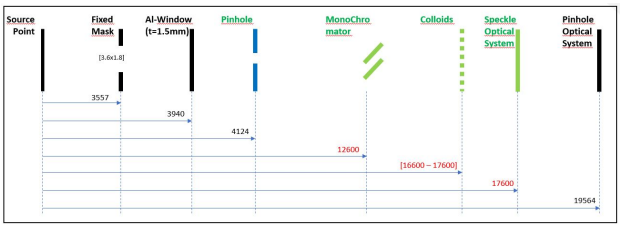

Figure 1: Sketch of FE21, with the elements of the x-ray pinhole and the components that need to be designed for the XHNFS (in green).

Note that FE21 is equipped with an Al-window with a thickiness of 1.5 mm, which filters out the soft x-rays for the pinhole camera. Although this radiation is enough to produce a good image using the pinhole technique, it might not be enough for the XHNFS experiments. Actually, Fig. 2 compares the flux produced by the In-Vacuum Undulator at the NCD beamline (red) with the flux produced by the bending dipole at FE21 (blue). The green trace shows the flux remaining after the Al-window in the FE21. Note that there is around 2-3 orders of magnitude difference. Therefore the design of the XHNFS experiments needs to optimize as much as possible the flux impinging on the detection system.

In order to increase the flux arriving at the sample, we look for a high bandwidth monochromator allowing more intensity to pass through the optical system and onto the detection screen. However, in this case, the effects of temporal coherence might start to be noticeable reducing the visibility of the interference fringes. Thus, the goal of this work is to find the appropriate monochromator bandwidth, providing a good trade-off between 1) the high flux at the detection system (to properly see the speckle interference pattern) and 2) the speckle pattern is not affected by the temporal coherence due to the large bandwidth. These effects have been simulated using the code Synchrotron Radiation Workshop - SRW [6].

* uiriso@cells.es

ISBN: 978-3-95450-249-3 ISSN: 2673-5350 doi: 10.18429/JACoW-IBIC2024-TUP58

STUDY OF X-RAY FRESNEL DIFFRACTOMETRY FOR SMALL BEAM SIZES AT DIAMOND LIGHT SOURCE

N. Vitoratou*, L. Bobb, Diamond Light Source, Didcot, UK

Abstract

The feasibility of X-ray Fresnel diffractometry in measuring small beam sizes beyond the resolution of X-ray pinhole cameras is studied in the case of Diamond Light Source. After the Diamond-II upgrade, beam sizes as small as 4 µm are anticipated and are not resolvable by the X-ray pinhole cameras, which are the workhorse for beam size, emittance, and energy spread measurements. X-ray Fresnel diffractometry employs a single aperture with an optimised width, producing a double lobe diffraction pattern. The visibility of this double lobe intensity distribution relates to the beam size and promises micron-scale beam size measurement. Numerical studies and simulations have been conducted to assess the feasibility of diffractometry for Diamond Light Source. The parameters for the experimental setup have been determined and preliminary experimental results are presented. Challenges and improvements for achieving this measurement for Diamond-II are discussed.

INTRODUCTION

The Diamond-II machine upgrade will increase brightness and coherence, and increase photon flux at higher energies. Two pinhole cameras will continue to serve as the main diagnostic for beam size monitoring and emittance calculation with a minimum resolvable beam size of 7.1 µm and 7.6 µm, respectively. For a squeezed beam following optics correction, the estimated vertical emittance is 1 pm rad, resulting in a beam size of 4 µm at the source points [1]. Since the expected beam sizes in Diamond-II will be smaller than the minimum resolvable beam size from the pinhole cameras, complementary high-resolution monitors are under investigation.

X-ray Fresnel diffractometry involves observing a double-lobed diffraction pattern produced by an aperture with width A. The correlation between the extent of the central dip in the diffraction pattern and the electron beam size is used to determine the electron beam size [2].

For a spherical wave with a flux distribution broader than the aperture width, the Point Spread Function (PSF) at the screen is given in one dimension by the Fresnel integral [2–4]:

$$I(y, y_e) \propto \left| \int_{-A/2}^{A/2} \sqrt{(I(y_s - y_e)} e^{\frac{ik}{2z}(y_s - y_e)^2} e^{\frac{-ik}{2R}(y - y_e)} dy_s \right|^2 \quad (1)$$

where $\sqrt{(I(y_s - y_e)}$ is the radiation intensity distribution in the aperture plane, $k = \frac{2\pi}{\lambda}$ where λ is the wavelength, y_e is the electron position at the source point, y_s and y are the coordinates on the aperture and the screen, R is the aperture-to-screen distance, and $z = RL/(R + L)$ where L is the source-to-aperture distance.

To achieve a double-lobed PSF, the aperture width should be optimised under specific conditions, including a monochromatic light source with wavelength λ, the source-to-aperture distance L, and the aperture-to-screen distance R following the relation [2]:

$$A \approx \sqrt{7\lambda \frac{L \times R}{L + R}} \quad (2)$$

NUMERICAL CALCULATIONS

The diffraction pattern for the case of Diamond was studied numerically prior to the experiment to determine the optimal experimental setup for the measurement. The spectral power distribution for the bending magnet, which is the source of the X-ray beam, is observed between 15 keV and 60 keV with peak power at approximately 25 keV as shown in Fig. 1.

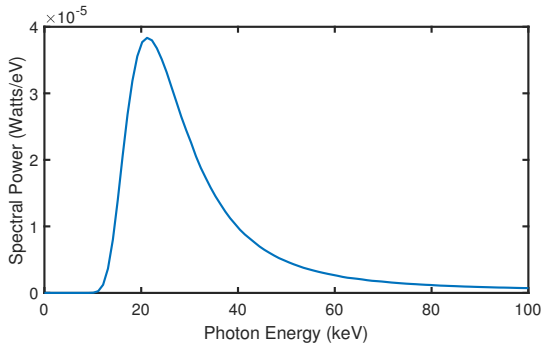

Figure 1: The spectral power distributions of the bending magnet source point for the case of Diamond after 1 mm aluminium and 10 m air calculated by XOP [5].

The calculations were conducted for energies ranging from 15 keV to 35 keV and the optimised aperture widths for this range are between 40 µm to 15 µm respectively, according to the relationship shown in Eq. (2).

To estimate the distribution at the image plane (i.e. at the scintillator, which is imaged with a magnification of 1 to the camera), the PSF assuming a constant flux intensity distribution of radiation at the aperture was calculated based on Eq. (1). This was then convoluted with Gaussian-distributed sources (taking into account the magnification from the source to the screen) and the PSF contribution from the screen, lens, and sensor. The resulting distribution at the image plane for a Gaussian distribution with 4 µm beam size for different energies and optimised apertures are shown in Fig. 2.

* niki.vitoratou@diamond.ac.uk

ISBN: 978-3-95450-249-3 ISSN: 2673-5350 doi: 10.18429/JACoW-IBIC2024-TUP59

DESIGN OF X-RAY IONIZATION BEAM PROFILE MONITOR FOR KOREA-4GSR

W. Song, M. Chung, Pohang University of Science and Technology, Pohang, Korea
S. Kim, H. Hyun, S. Hwang, S. Lee, M. Seo, J. Kim, Y. Park, J. Lim and G. Hahn*
Pohang Accelerator Laboratory, POSTECH, Pohang, Korea

Abstract

A photon beam generated by the Insertion Device (ID) of a synchrotron light source can be contaminated by radiation from upstream and downstream bending magnets, leading to position measurement errors in blade-type monitors. The operation of the Korea-4GSR, which has an extremely low emittance, is particularly sensitive to photon beam position variations, necessitating more accurate position measurements. To robustly measure the position and simultaneously obtain the profile of a photon beam in a non-destructive manner, we are developing an ionization profile monitor.

We designed a noble gas environment to ensure adequate signal strength and incorporated a defocusing electrode structure to fully utilize the relatively large active area of the readout. Since magnification in the defocusing field depends on the vertical position, we proposed a calibration method to correct the non-linearity, which we then verified through particle tracking simulation.

INTRODUCTION

The Ionization Profile Monitor (IPM) is used in many synchrotrons [1–5] to monitor the profile and position of the beam. As shown in Fig. 1, the beam ionizes the residual gas by the photoelectric effect, and the resultant ions or electrons are collected to measure the beam information. Diagnostics using ionization have the advantage of being non-destructive, as the beam is not blocked and only a small fraction of the beam participates in the reaction.

At the ID beamline of the synchrotron light source, the X-ray from the undulator as well as light from the upstream and downstream bending magnets arrive at the same time [6]. The center of this X-ray is measured using a blade-type Photon Beam Position Monitor (PBPM), which uses the edge information of the beam to determine the position to avoid heating. In this case, contamination can affect the position measurement and cause errors. IPM is free from this problem because it measures the entire intensity distribution without using a part of the beam so that it can overcome errors caused by contamination.

IPM with its many benefits has already been studied in PETRA-III [7], FLASH [8], etc, for X-ray beam position monitoring. Higher spatial resolution is required for precise measurement of position, especially profile, in low emittance storage rings such as Korea-4GSR. Therefore, this study shows the IPM design for resolution improvement and the calibration method for precise profile and position measurement.

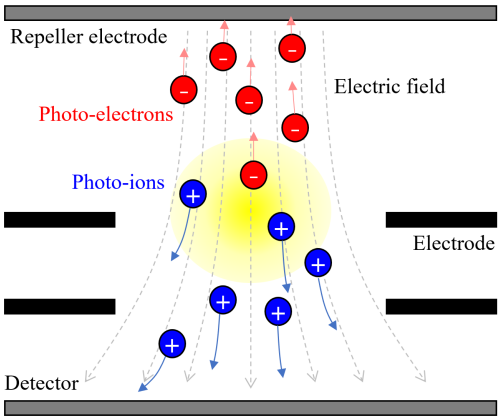

Figure 1: Schematic diagram of IPM.

IONIZATION PROFILE MONITOR DESIGN

The major components that determine the resolution of IPM are extraction field quality, transverse growth of photo-ion, readout device resolution, and data processing. Non-uniformity of the electric field induced by fabrication tolerance or errors in the applied voltage creates measurement errors. In addition, the thermal energy and space charge of the initial photo-ion have the effect of increasing the point spread function due to transverse spread during the drift of the ion. The optical readout using the MCP produces errors of more than 100 µm due to the channel pitch of the MCP, the chevron structure, the phosphor, and the camera resolution. In addition, errors in image processing also contribute to the resolution of the IPM.

Our IPM design intends to use a noble gas (Xenon) with a large ionization cross-section instead of a residual gas to increase the signal gain and the signal-to-noise ratio. Furthermore, the transmission ratio of ions was improved by removing the grid mesh for sustaining field uniformity. In this process, a shield plate was installed on the MCP to ensure the uniformity and isotropy of the extraction field, and the electrode and repeller structures were also optimized. The design of the extraction field is 1:1 mapping to increase the resolution by utilizing the active area of the MCP, which is relatively large compared to the beam. The measurement result changes depending on the initial ion generation position in the defocusing field, which causes profile and position measurement errors. The error was corrected by the magni-

* garam@postech.ac.kr

ISBN: 978-3-95450-249-3 ISSN: 2673-5350 doi: 10.18429/JACoW-IBIC2024-TUP63

A PROJECT FOR A COMPTON PHOTON SOURCE AT THE SKIF SYNCHROTRON FACILITY

Viacheslav V. Kaminskiy*,[1], Oleg I. Meshkov[1],
Budker Institute of Nuclear Physics, Siberian Branch Russian Academy of Sciences (BINP SB RAS), Novosibirsk, Russian Federation
[1]Novosibirsk State University (NSU), Novosibirsk, Russian Federation

Abstract

SKIF is a synchrotron radiation facility under construction in Novosibirsk, Russia. Its main storage ring has unique parameters, including an electron beam energy of 3 GeV, a beam current of up to 0.4 A, and a horizontal beam emittance of 75 pm · rad. These parameters make it suitable for creating a highly efficient high-energy photon source using Compton backscattering (inverse Compton scattering) of infrared, ultraviolet, and visible laser radiation. Using modern high-power lasers, it is possible to achieve Compton photons with energies hundreds-MeV range and rates up to 300 MHz. Additionally, higher Compton photon energies (up to 2.6 GeV) can be generated by reflecting synchrotron radiation towards the electron beam. A preferred method for photon monochromatization is tagging photons by their recoil electrons. The discussed Compton source can be used for photonuclear processes such as photofission and the production of π, η, Δ at nuclei, as well as for other applications such as nonlinear QED and calibration of electromagnetic detectors.

SKIF SYNCHROTRON RADIATION FACILITY

The Siberian Circular Photon Source SKIF [1] is a synchrotron radiation facility of "4+" generation currently under construction in Novosibirsk, Russian Federation. Its parameters (see Table 1) make it possible to create a high-quality source of Compton photons.

Table 1: Some Parameters of SKIF Synchrotron Facility

Energy	3.0 GeV
Perimeter	475.14 m
Electron beam current	400 mA
Horizontal emittance	75 pm · rad
Revolution frequency	629.63 kHz
Number of bunches	567
Time between bunches	2.8 ns (84 cm)

PROPERTIES OF COMPTON BACKSCATTERING

Compton backscattering is an interaction between a relativistic electron and a head-on, low-energy photon (see Fig. 1). The photon gains the maximum energy when it is scattered back ($\theta = 0$):

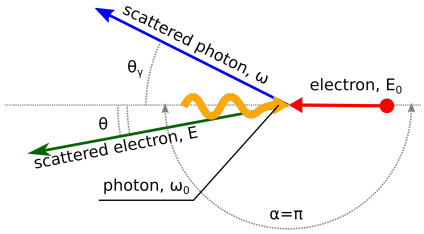

Figure 1: Scheme of Compton backscattering.

$$\omega_{\max} = \frac{E_0\kappa}{1+\kappa} \overset{\substack{\kappa\ll 1\\ \alpha=\pi}}{\approx} 4\gamma^2\omega_0, \quad \kappa = \frac{4\omega_0 E_0}{m^2}. \tag{1}$$

The scattered photon energy depends on the scattering angle (see notations in Fig. 1):

$$\omega(\theta) = \frac{\omega_{\max}}{1+(\theta/\theta_c)^2}, \quad \theta_c = \frac{m}{E_0}\sqrt{1+\kappa} \overset{\kappa\ll 1}{\approx} \frac{1}{\gamma}. \tag{2}$$

Electron recoil energy:

$$E = E_0 - \omega, \quad E_{\min} = E_0 - \omega_{\max} = \frac{E_0}{1+\kappa}. \tag{3}$$

The differential cross-section of Compton backscattering and the polarization of scattered photons are shown in Fig. 2.

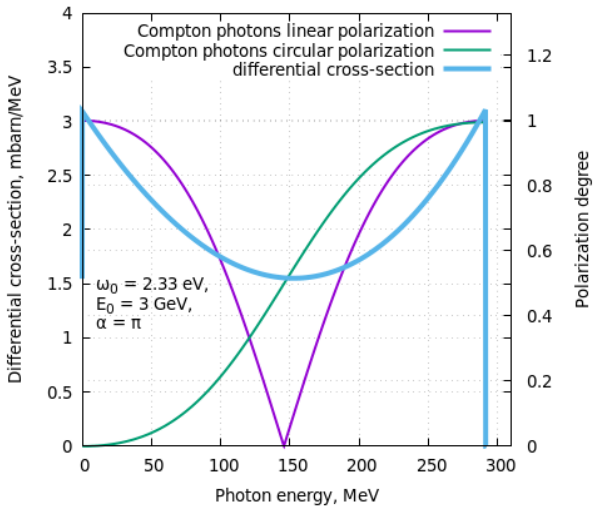

Figure 2: Differential cross-section and polarization degree of Compton backscattering.

* V.V.Kaminskiy@inp.nsk.su

ISBN: 978-3-95450-249-3 ISSN: 2673-5350 doi: 10.18429/JACoW-IBIC2024-TUP66

CERTIFICATION TESTING OF PROTOTYPE SUPERCONDUCTING QUARTER-WAVE AND HALF-WAVE RESONATORS FOR HIAF*

Z. H. Liang[1,2†], M. Xu[1‡], C. L. Li[1], Q. T. Huang[3], Y. He[1,3], S. X. Zhang[1], L. B. Liu[1], G. C. Liu[1,2], J. Y. Wang[1], H. Guo[1], P. R. Xiong[1], T. C. Jiang[1], S. C. Huang[1], P. A. Xiang[3], T. Tan[1], Y. Tao[1], Z. J. Wang[1,3], F. F. Wang[1], J. C. Yang[1,3]
[1]Institute of Modern Physics, Chinese Academy of Sciences, Lanzhou, China
[2]University of Chinese Academy of Sciences, Beijing, China
[3]Advanced Energy Science and Technology Guangdong Laboratory, Huizhou, China

Abstract

The 81.25 MHz quarter-wave resonator (QWR) and 162.5 MHz half-wave resonator (HWR) are selected as the main accelerating cavities for the superconducting ion linac of the **H**igh **I**ntensity heavy-ion **A**ccelerator **F**acility (HIAF) at the Institute of Modern Physics (IMP). Six QWR007 (βopt = 0.07) cavities and eight HWR015 (βopt = 0.15) cavities have been fabricated before the mass production to verify the design and production quality control. Two cavities of the both types have been random chosen to surface processing and vertical testing for performance validating before welding helium vessel. In this paper, the development of SRF cavity for HIAF will be addressed, which including the fabrication, surface processing and vertical testing results. The achieved gradients for both cavities have exceeded 60%~100% of requiring operation gradients. The Q0 of both types cavities have met the 2 K operation requirement too. These results inspired to push the cavity production for the HIAF project forward to the mass production stage.

INTRODUCTION

The HIAF is under construction by the Institute of Modern Physics, Chinese Academy of Sciences (IMP, CAS) for nuclear physics, high energy state physics, and atomic physics research. As shown in Fig. 1, this facility comprises five main components: a superconducting ECR ion source (SECR), a superconducting ion-Linac (iLinac), a fast cycle Booster Ring (BRing), a High energy FRagment Separator (HFRS) and a Spectrometer Ring (SRing). The heavy ions will be accelerated by iLinac up to the energy of 17 MeV/u. Then the BRing should be able to accumulate and accelerate beam up to 0.8 GeV/u for atomic and nuclear physic experiments [1-2].The iLinac included two types of superconducting cavities: QWR with optimal beta = 0.07 (QWR007) and HWR with optimal beta = 0.15 (HWR015). These cavities are hosted by 17 cryomodules. Six of which are QWR cryomodules with five cavities and five superconducting solenoids in each one; eleven HWR cryomodules with six cavities and six superconducting solenoids in each one. The cavities and solenoids will operate at 2 K. Six QWR007 cavities and eight HWR015 cavities have been fabricated by two vendors to validate the design before mass production [3-4]. Two of each type of cavity have been processed and assembled in the cleanroom for vertical testing. The detailed results will be presented in this paper.

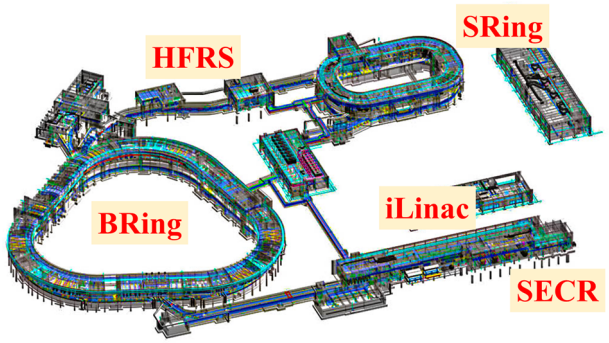

Figure 1: Layout of HIAF.

BACKGROUND AND OVERVIEW

Cavity Design

Basing on the successful experience of the China Accelerator Facility for superheavy Elements (CAFE) superconducting linac, we have developed HWR015. The HWR015 cavity shares a similar structure with the HWR cavity of the CAFE, but the shape of the donut drift tube in the high electric field region has been modified to lower the Epk/Eacc from 4.89 to 4.7. To manage the peak magnetc field, the top section of the inner conductor was enlarged into a tapered structure.

Otherwise, the QWR007 cavity is a new design that incorporates many features from the QWR of SPIRAL II. The inner conductor diameter in the straight section was optimized to 120 mm, ensuring the peak magnetic field remains below 50 mT. This section was also extended to potentially accommodate a mechanical damper, a decision to be made following the initial cryomodule tests. The distance between the outer conductor's bottom section and the beam tube was adjusted to provide adequate coupling for the coupler while staying clear of the peak electric field region. The nose structure of the beam tube section mirrors that of the HWR015 cavity, with a sloped angle added to correct dipole components and prevent beam steering. Both types of cavities are equipped with four rinsing ports—two on the top and two on the bottom—to

* Work supported by Large Research Infrastructures "High Intensity heavy-ion Accelerator Facility" (Grant No. 2017-000052-73-01-002107) and the CAS BR project "The Development of High Stability Cryomodule [E129812YR0]".
† Email: liangzehua@impcas.ac.cn
‡ Corresponding author, Email: xumx@impcas.ac.cn

ISBN: 978-3-95450-249-3 ISSN: 2673-5350 doi: 10.18429/JACoW-IBIC2024-TUP67

FIRST RESULTS OF INR RAS LINAC TIMING SYSTEM UPGRADE

A.I. Titov[1 †], S.A. Gavrilov[1],
D.E. Donets[2], I.N. Zhabin[2], D.S. Letkin[2], I.V. Shirikov[2], I.K. Spiridonova[2]
[1] Institute for Nuclear Research of the Russian Academy of Sciences, Moscow, Russia
[2] LLC DIALTEK, Dubna, Russia

Abstract

INR RAS linac was developed in late 1970s and build during 1980s. Its timing system is based on the fifty years old technologies and requires full upgrade due to system stability decrease, lack of spare parts, progressing hardware degradation and increase in RF jamming. Moreover, the timing system upgrade should be done without additional accelerator complex shutdowns. In this paper a project of a new timing system that fulfills all requirements is presented. Various features and production peculiarities of the new timing system hardware and software are described. Results of the implementation of new system first parts and its commissioning and plans for future upgrade are discussed.

INTRODUCTION

INR RAS Linac and Its Timing System

INR linac is a high-intensity proton and negatively charged hydrogen ions (or H- ions) linear accelerator. Whole accelerator complex is divided into six sectors, five sectors are for the linac itself and the sixth is for Research Complex that includes two spallation sources, a neutron spectrometer and a proton therapy complex. Diagram of INR linac with its experimental stations is presented in Fig. 1.

Timing system of INR linac is a part of an automatic control system (ACS) and is also divided into six sectors that have a sequential connection with each other by coaxial cables. The second sector is considered as a main one because it has a timing system kernel that produces all necessary timing series. Current timing system produces eleven timing series that are used by other accelerator systems. In one sector timing series are spread to ACS end-point devices that are connected with the other equipment. One end-point device can provide only two series from eleven. Also timing system architecture makes it a part of linac machine protection system (MPS). The internal structure of timing series that are used by ion sources depend on the alarm status of linac. That feature is used as an additional protection measure.

System Upgrade Motivation

INR linac was developed in late 1970s and build during 1980s. Most parts of the timing system are based on the technologies of that times. Since the commissioning, hardware of the timing system has never got any serious upgrades. Spare parts are not produced for more than thirty years. Moreover, during the last several years RF feeding system of the drift-tube linac part started to produce excessive jamming signals that perfectly transfer via timing system connection cables and disrupt the work of the timing system. All these factors eventually led to a decision that our timing system needs a full upgrade.

NEW TIMING SYSTEM

Main Requirements

Development of the new timing system started at September-October 2021th with colleagues from DIALTEK [1], who agreed to participate in the INR linac timing system upgrade. There were several most crucial requirements:

- full compatibility with an old system, so timing system can be partially old, partially new;
- saving of all features of the old system, so there would be no downgrade in the abilities of the system;
- ability to go back in case of upgrade failure;
- all connections between elements of the new timing system should be done only by fiber connections to prevent RF jamming;
- all timing series could be transferred to each channel.

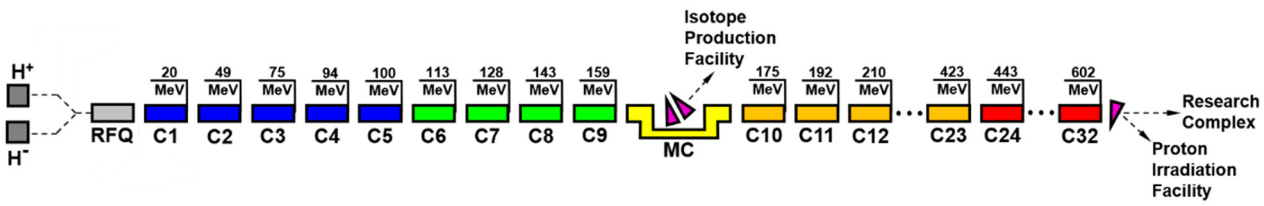

Figure 1: INR RAS linac diagram.

† alexander.i.titov@yandex.ru

ISBN: 978-3-95450-249-3 ISSN: 2673-5350 doi: 10.18429/JACoW-IBIC2024-TUP68

DIAGNOSTICS BEAMLINE FOR THE SUPERCONDUCTING RF PHOTOINJECTOR TEST STAND AT DESY*

S. Jaster-Merz†, D. Bazyl, W. Decking, K. Floettmann, M. Krasilnikov, D. Lipka, S. Mogk, A. Novokshonov, E. Vogel, Deutsches Elektronen-Synchrotron DESY, Germany

Abstract

For future continuous wave (CW) and high-duty-cycle operation of the European XFEL, research and development of the DESY L-band CW photoinjector is ongoing. The implementation of a superconducting radio frequency (SRF) gun operated at 1.3 GHz with a copper photocathode is the baseline option. The electron beam quality, in particular the slice emittance, produced by this injector is key for the successful operation of the free-electron laser. In order to study the beam quality and stability of operation, a dedicated test stand and diagnostics beamline is being developed at DESY. Here, we present an overview of the foreseen diagnostic components and methods at the SRF CW photoinjector test stand.

INTRODUCTION

A future upgrade of the European XFEL to continuous wave (CW) and high-duty-cycle (HDC) operation is being explored to enable high average brilliance and a flexible time structure of the produced photon pulses for the users [1–3]. Such an upgrade requires a CW photoinjector capable of delivering electron bunches with a high electron quality, i.e., a small normalized emittance at the level of 0.2 µm for 100 pC charge bunches. A photoinjector based on the DESY CW L-band SRF gun cavity is the preferred solution. This design allows for high field gradients, high peak currents, and small transverse emittances and thus enables the direct matching of the beam into a booster cavity [4, 5]. The DESY CW SRF gun cavity with an integrated Cu cathode has repeatedly demonstrated a peak electric field on axis of up to 55 MV m^{-1} in vertical tests [5]. In order to characterize the electron beam quality produced by these SRF gun cavities, a dedicated SRF photoinjector test stand (Ts4i) [6] is being built at DESY. This includes a diagnostics beamline allowing for measurements of the energy, charge, emittances, and other beam parameters. Here, we present an overview of this Ts4i diagnostics beamline with a main focus on the foreseen diagnostic components and methods.

SRF PHOTOINJECTOR TEST STAND - TS4I

The SRF photoinjector test stand is designed and optimized for the electron bunch parameters expected from the DESY CW L-band SRF gun cavity. Bunches with 100 pC charge, an energy of 4 MeV to 6 MeV, and normalized transverse emittances from 0.2 µm to 0.4 µm are expected. A full list of the beam parameters is provided in Table 1. The Ts4i beamline consists of a cryostat hosting the SRF gun cavity, a superconducting (SC) solenoid for emittance compensation [7, 8], and two dipole steerers. The SC solenoid was produced by the company Niowave and is an improved copy of the model developed at HZB [9]. A commercial Pharos laser (PH1-20-0200-10-N2-NS) is foreseen to be installed on the roof of the Ts4i bunker. The wavelength of the laser beam will be converted from infrared to ultraviolet and is coupled into the beamline downstream of the cryostat. The complete layout of the test stand is shown in Fig. 1. The diagnostics beamline starting downstream of the cryostat consists of a straight and a dispersive section. Its main purpose is to characterize the quality and stability of the produced electron bunches as well as study the level of the dark current. A small transverse emittance is key for the successful operation of free-electron lasers (FELs) which require a high electron brightness. Especially the value of the transverse slice emittance is of interest as the performance of the FEL depends on the transverse emittance within one cooperation length [10, 11]. The diagnostics beamline is therefore specifically designed to measure the slice emittance of the beam.

Table 1: Design Beam Parameters

Parameter	Unit	Value
Beam energy	MeV	4 – 6
Charge per bunch	pC	100
Normalized emittance	µm	0.2 – 0.4
Repetition rate of bunches	MHz	0.1 – 1
Average beam current	µA	10 – 100

The different elements of the diagnostics beamline foreseen to perform all the above-mentioned measurements are described in more detail in the following while a more detailed description of the slice emittance measurement setup is provided in the next section.

Screen Stations

Four screen stations (S1 - S4) will be installed in the Ts4i diagnostics beamline to measure the transverse profiles of the bunches. When inserted into the beam path, the bunch repetition rate will be reduced to 10 Hz in order to protect the hardware components. All stations are European XFEL-type screen stations [12] with a 200 µm thick Gadolinium Aluminum Gallium Garnet doped with cerium (GAGG:Ce) scintillating screen [13]. The setup uses a 1:2 optics with a 45° observation angle and a Scheimpflug optics to reduce

* This work is performed in the framework of R&D for future accelerator operation modes at the European XFEL and is financed by the European XFEL GmbH.

† sonja.jaster-merz@desy.de

ISBN: 978-3-95450-249-3 ISSN: 2673-5350 doi: 10.18429/JACoW-IBIC2024-TUP72

DEVELOPMENT OF THE BEAM DIAGNOSTIC SYSTEM OF THE HUST-PTF TRANSPORT LINES

Shaokun Zhou, Chengyong Liu, Yu Chen, Bin Qin, Qushan Chen†, Xu Liu, Dong Li, Aote Chen, Yicheng Liao, Ruiying Luo, Wei Wang, State Key Lab. of Advanced Electromagnetic Engineering & Technology, Huazhong University of Science & Technology Wuhan, China

Abstract

Huazhong University of Science and Technology is building a cyclotron-based Proton Therapy Facility (HUST-PTF). The facility mainly consists of a 240 MeV superconducting cyclotron, a beam transport line, a fixed treatment room and two rotational treatment rooms. HUST-PTF uses three kinds of detectors, Scintillation, Faraday cup and ionization chamber, for the beam parameter measurements. In terms of structure, the HUST PTF beam diagnostic system is built according to the standard distributed three-layer structure, which is divided into hardware device layer, data processing layer and GUI layer. Different protocols are used to communicate between the three layers, which can improve reliability and expand flexibly in each layer.

INTRODUCTION

Cancer is a serious disease. Traditional cancer treatment methods include surgical resection, radiation therapy, and chemotherapy, each with its limitations and side effects. Proton therapy, a more precise approach, uses high-energy proton beams to kill cancer cells while minimizing damage to healthy tissue. Huazhong University of Science and Technology is building a cyclotron-based Proton Therapy Facility, known as HUST-PTF, which consists of a 240-MeV superconducting cyclotron, beam transport lines, a fixed treatment room, two rotational treatment rooms, and many other support equipment [1]. At present, all equipment tests have been completed, and the next beam tuning work can be carried out. The beam diagnostic system of HUST-PTF, comprising scintillation detectors, Faraday cups, ionization chambers, and corresponding software programs [2], can display the position, size, and intensity of the beam in the beam transport line. These beam parameters will be an important reference in beam tuning process.

DETECTORS AND SOFTWARES OF THE DIAGNOSTIC SYSTEM

As a subsystem of the accelerator system, the HUST-PTF beam diagnosis system is mainly composed of hardware (beam detector) and software (control system) The hardware layout is shown in Fig. 1. The entire beam transport line contains 21 scintillators, 6 Faraday cups and 6 ionization chambers. These probes can be used to measure beam profile, position and intensity.

In terms of its overall architecture, the HUST-PTF beam diagnosis control system adopts the standard distributed system architecture, with the overall structure divided into three layers: the hardware equipment layer, the data processing layer, and the GUI layer. The hardware equipment primarily consists of beam detectors, pneumatic devices, and high-voltage modules, which can collect beam information and convert it into the corresponding analog signal. The data processing mainly encompasses the controller of the front-end detector, I/O modules, motion controllers, etc., which primarily achieve the digitization of beam parameters, transmit the collected beam parameters to the upper control system, and facilitate data exchange between the front-end detector and the user interface. In the GUI layer, the operator can control the motion of the detectors and the detection of beam parameters, as depicted in Fig. 2.

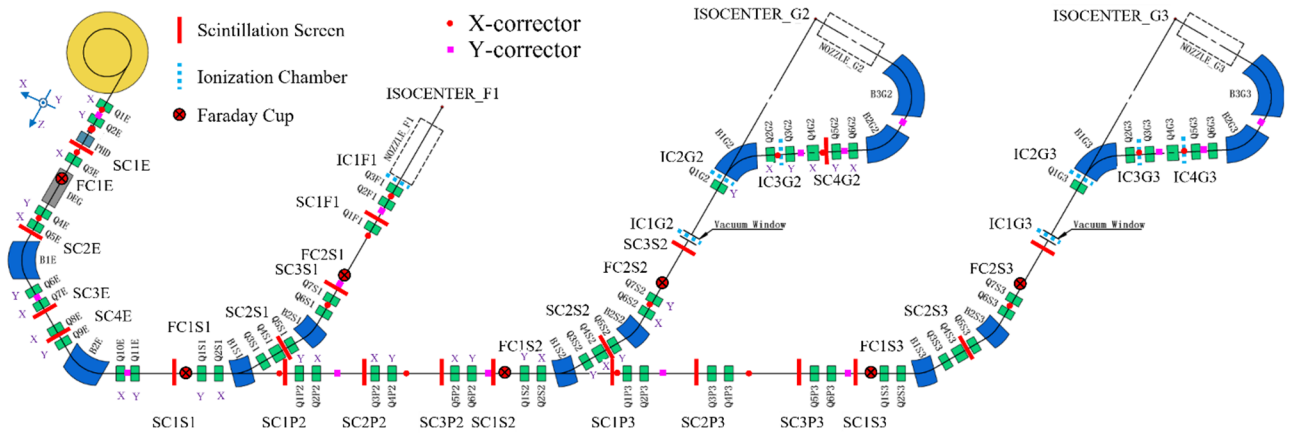

Figure 1: HUST-PTF beam transport line layout.

†chenqushan@hust.edu.cn

ISBN: 978-3-95450-249-3 ISSN: 2673-5350 doi: 10.18429/JACoW-IBIC2024-TUP73

FEATURES OF NON-DESTRUCTIVE BEAM INSTRUMENTATION AT THE INR RAS HIGH-INTENSITY HYDROGEN IONS LINAC*

S. A. Gavrilov†, I. I. Polonik, A. I. Titov
Institute for Nuclear Research of the Russian Academy of Sciences, Moscow, Russia

Abstract

The linac of INR RAS is a high-intensity accelerator of protons and H-minus ions, which is used for a complex of neutron sources, isotope production, proton irradiation and investigations in proton flash therapy. A non-destructive beam instrumentation plays a key role in the linac tuning. The general peculiarity of this multi-component system is that all detectors are home-made devices with a wide operation range and can be used at different ion linacs with a minimum adaptation to beam parameters. Beam current transformers for standard and in-air measurements, resonance and capacitive position and phase monitors, BIF-monitor for 1D and beam cross-section monitor for 2D non-destructive profile diagnostics. Different operation features and manufacturing peculiarities are presented in this paper. Results of implementation, operation and continuous upgrade are discussed. Also, typical scalable designs of some detectors are described.

INTRODUCTION

Multipurpose research complex (MRC) [1] of INR RAS, based on the linac, includes four beam outlets: three neutron facilities of neutron investigations laboratory (time-of-flight Radiation Experiment, pulse neutron source IN-06, lead neutron slowing-down spectrometer LNS-100) and research Complex of Proton Therapy, which is a part of medical physics laboratory. Also, there are isotope production and proton irradiation facilities at the linac (Fig. 1). So, depending on beam user requirements, the linac has to provide beam parameters in a wide range of values: beam energy 20÷305 MeV, pulse current 0.001÷10 mA, pulse repetition rate 1÷50 Hz, pulse duration 0.3÷150 μs.

Moreover, these parameters can be changed several times during a shift for different research groups, that needs not only reliable operation of the linac in different duty cycles, but also a beam instrumentation available for routine control in a wide range of parameters.

Last years the linac non-destructive diagnostic system has been supplemented and upgraded with new instrumentation, software and tuning procedures. In particular, the system of beam current transformers (BCT) was enhanced by several new detectors, including device for in-air measurements, a new beam-induced fluorescence (BIF) monitor was installed at H+ injection channel, an operation of Beam Cross Section Monitor (BCSM) based on ionization principles was improved by a new software. Meanwhile some types of detectors, such as phase monitors, neutron and γ-detectors continued to work confidently in routine operation without significant upgrade.

BEAM CURRENT TRANSFORMERS

There are about 40 BCTs (ACCT-type) at the accelerator complex. They are mainly based on ferrite rings installed in vacuum with different design and electronics. Standard BCTs with preamplifiers, based on AD810 op-amps, are used for routine range of beam parameters. Three sensitive BCTs with OPA827 and ADA4627 – for medical beams with pulse currents down to 10 μA. Four fast BCTs with low input impedance preamplifiers, based on AD844 – for short-pulses down to 0.3 μs for RADEX and LNS-100.

Current signals and calibration signals of all BCTs are transmitted in differential mode by twisted-pair cables, so interferences are minimized, and preamplifiers can be distant for hundreds of meters from a control room.

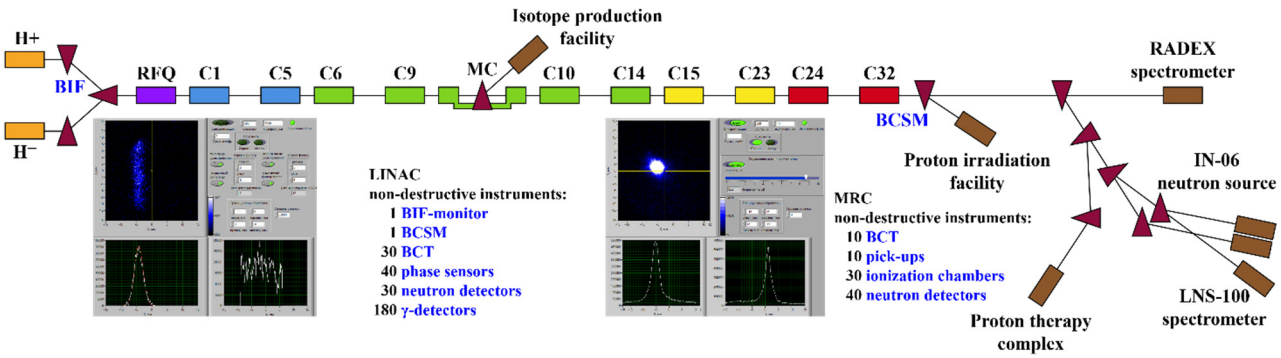

Figure 1: INR RAS accelerator complex layout.

* Work supported by the National Centre for Physics and Mathematics
† s.gavrilov@inr.ru NCFM 6 2325-113

ISBN: 978-3-95450-249-3 ISSN: 2673-5350 doi: 10.18429/JACoW-IBIC2024-WEAI2

REMOTE SENSING OF FAST BEAM SIGNALS USING ELECTRO-OPTICAL MODULATORS

A. Schlögelhofer*, T. Lefèvre, T.E. Levens, S. Mazzoni, CERN, Geneva, Switzerland

Abstract

Electrical measurements of fast signals, as generated in particle accelerators, encounter severe limitations due to the high-frequency losses in radio frequency transmission lines. This study describes measurements conducted with electro-optical modulators employing various radio-over-fibre techniques. Experimental data consist of different beam-generated signals, which underline the versatility of such a system. Signals from electromagnetic devices such as wall current monitors, as well as those captured from coherent transition radiation screens and coherent Cherenkov diffraction radiators, are presented. Furthermore, the potential deployment of such a remote sensing acquisition system in large-scale facilities is discussed.

INTRODUCTION

In many particle accelerators, particle acceleration is achieved through the use of radio frequency (RF) cavities. This method forces the particles to form a train of particle bunches, resembling the structure of the accelerating RF field. As particle energies increase, the bunches become compressed in the longitudinal direction, which in turn extends bunch-induced signals to higher frequencies. Acquiring these high-frequency signals poses several challenges. Long transmission lines cause significant attenuation of the high-frequency components of the RF signals. The need for short transmission lines implicates dedicated development of radiation-hardened electronics, as most often radiation levels in the accelerator hall are not negligible. In this work, we address these challenges by employing various radio-over-fibre techniques for the transmission of beam-generated signals. We utilise Mach-Zehnder electro-optical modulators (Exail NIR-MX800-LN-20) to modulate the intensity of the optical carrier with the beam-induced electrical signals. By encoding these signals onto an optical carrier, we achieve transmission bandwidths of several tens of GHz over distances of hundreds of meters, enabling real-time, high-bandwidth measurements which are resistant to electromagnetic interference.

ELECTRO-OPTICAL MODULATOR

A Mach-Zehnder-type electro-optical modulator is an interferometric device that operates based on the Pockels effect in electro-optical crystals. The Pockels effect refers to the linear change of the refractive index of a material when exposed to an external electric field. For Lithium Niobate ($LiNbO_3$) crystals, which are used in this work, the Pockels effect is described by [1]

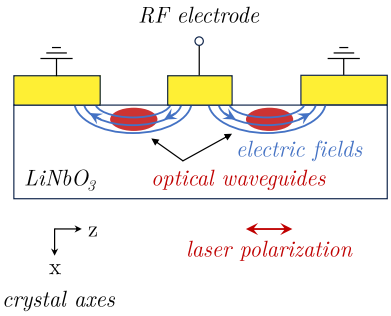

Figure 1: Schematic cross-section of an x-cut Mach-Zehnder type electro-optical modulator [2]. The RF input generates electric fields that alter the effective refractive index of the Lithium niobate ($LiNbO_3$) crystal, introducing a phase delay between the two interferometer arms (optical waveguides). The recombination of the light from both arms results in the modulation of the laser light intensity.

$$\Delta n_z = -\frac{1}{2} n_e^3 r_{33} E_z, \tag{1}$$

where Δn_z is the change of refractive index in z-direction, n_e is the extraordinary refractive index, r_{33} is an electro-optic coefficient of the electro-optic tensor of $LiNbO_3$, and E_z is the external field applied in z-direction. A schematic of the geometry used in x-cut Mach-Zehnder electro-optical modulators is shown in Fig. 1. The electric field lines overlap with the optical waveguides on either side, resulting in a symmetric design where the induced change in refractive index is positive in one arm and negative in the other.

After passing through the two modulator arms, the light is recombined, experiencing either constructive or destructive interference depending on the relative change in optical path length between the two interferometer arms. This phase modulation results in an intensity variation of the light at the output, which is why this type of electro-optical modulator is often referred to as an intensity modulator. The transfer function T of an ideal intensity modulator can be described as [2]

$$T(V) = \sin^2\left(\frac{\pi\,(V - V_0)}{2\,V_\pi}\right), \tag{2}$$

where V is the modulating voltage amplitude, V_0 is the bias voltage amplitude and V_π is the voltage required to transition from minimum to maximum transmission. The transfer function $T(V)$ is illustrated in Fig. 2 along with an electrical input signal and the corresponding optical output signal. Typically V_0 is a DC voltage chosen in such a way, that with $V = 0$ the optical transmission is at 50% of its total intensity. This is referred to as the quadrature point of the modulator (indicated by the yellow marker in Fig. 2). Any variation in $V = V_{RF}$ modulates the optical intensity relative

* andreas.schloegelhofer@cern.ch

ISBN: 978-3-95450-249-3 ISSN: 2673-5350 doi: 10.18429/JACoW-IBIC2024-WEBI2

DEVELOPMENT OF HIGH-RESOLUTION SINGLE-SHOT EMITTANCE DIAGNOSTICS

Ji-Gwang Hwang*, Gangneung-Wonju National University, Gangneung, Republic of Korea
Garam Hahn†, Pohang Accelerator Laboratory, Pohang, Republic of Korea

Abstract

A Pepper-pot diagnostics, which breaks the beam into several beamlets with well-defined holes and observes the spot size at a fixed distance that implies the angle of the beam, was proposed for measuring the beam distribution in the transverse phase-space and is widely used in the low energy beams, particularly for the hadrons. While technological advances have been made in several aspects, there are unsolved issues in terms of theoretical modelling for the emittance resolution, precise hole manufacturing, and noise removal without harming the signal. These effects strongly dilute the measured phase space distribution, resulting in the inaccurate gauge of the emittance as well as Twiss parameters. We developed to accurately and robustly retrieve particle distribution in horizontal and vertical phase spaces by single-shot emittance measurements.

INTRODUCTION

The pepper-pot emittance meter, which fundamentally consists of a metallic mask for manipulating the particle distribution in the $x - y$ space, a scintillation screen for imaging the charged particles, and an imaging system is widely used at low-energy beams [1, 2]. The basic principle of the pepper-pot emittance meter is to measure the beamlets on the scintillating screen located downstream of a well-defined mask which tailors charged particles transversely by appropriately distanced small holes arranged in the x, y-plane like the elements of lines and columns in a matrix [3]. Since the hole shapes the initial particle distribution, the spot size on the screen can be interpreted by the convolution of the hole shape and the angular component of the beam converted to the transverse direction by the distance from the mask to the screen. This enables the quantification of the angle and size of the beam simultaneously. It is evident that the design of the hole pattern has to be adapted to the expected emittances to avoid overlap of beamlets [4]. Taking this into account, the pattern of light spots will represent a four-dimensional hyperemittance [5, 6]. The schematic layout of the pepper-pot emittance meter is shown in Fig. 1. A hole diameter of a and a distance from mask to screen of L limit the measurement accuracy of the beam emittance.

Since the diameter directly determines the intensity of beamlets, regulating the measurement accuracy, in the early phase, the devices have relatively large holes to yield enough light output. Since then, Macro-Channel Plates (MCP) have been applied, which enables the reduction of the hole diameter to sub-mm. It also opens an opportunity to perform a single-shot measurement. However, due to the noisy feature of the MCP, it is limited in its capability to resolve emittances in the sub 0.1 mm·mrad regime [7]. In this paper, we presented theoretical resolution limits, precise mask fabrication methods, precise alignment with respect to the beam, and cluster noise removal algorithm to obtain the optimal resolution.

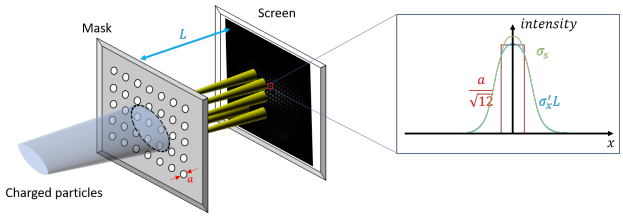

Figure 1: Schematic layout of the pepper-pot emittance meter with a hole diameter of a and a distance from mask to screen of L. These two parameters limit the measurement accuracy of the beam emittance.

MASK PRODUCTION

Since the hole tailors the shape of the beam in the real space $x - y$, while the particle propagates in the free space between the mask and the screen, it will draft with its angle. Therefore, the spot on the screen is determined by the angular distribution of the particles. The rms spot size on the screen σ_s with a hole diameter of a in a mask is given by

$$\sigma_s = \sqrt{\left(\frac{a}{\sqrt{12}}\right)^2 + (\sqrt{\varepsilon\gamma}L)^2}\,, \tag{1}$$

where L represents the distance between the mask and the screen, ε denotes the beam emittance and γ is the Twiss parameter. The factor $1/\sqrt{12}$ comes from considering the rms of the flattop distribution created by the slit projection.

Depending on the shape and size of the hole in the mask, the profile can be significantly distorted, resulting in incorrect emittance measurements as presented in Eq. (1). There are two methods available for precisely manufacturing hole arrays: laser-cutting (or drilling) and photolithography. For the laser cutting process, the diameter of the hole can be controlled by adjusting the spot size on the sample, but it can be different from the expected condition. For the lithography process, the radius of the holes can be manipulated by controlling immersion time in the solvent during the etching process, which makes all the holes equal in size, but with size inaccuracies. The measurement error of the emittance as a function of the manufacturing error Δa can be expressed as

* hwang@gwnu.ac.kr
† garam@postech.ac.kr

ISBN: 978-3-95450-249-3 ISSN: 2673-5350 doi: 10.18429/JACoW-IBIC2024-WEBC3

FIRST PROOF-OF-CONCEPT TRANSVERSE BEAM PROFILE MEASUREMENTS WITH GAS JET IN-VIVO DOSE PROFILER FOR MEDICAL ACCELERATORS

N. Kumar*,1,2, M. Patel[1, 2], W. Butcher[1,2], F. Thesni M. P.[1,2], C. P. Welsch[1,2]
[1]The Cockcroft Institute, Warrington, United Kingdom
[2]University of Liverpool, Liverpool, United Kingdom

Abstract

To ensure patient safety, treatment efficacy, and facility efficiency, a full online characterization of the charged particle beam is required for every ion beam therapy facility. Current dosimetry methods offer limited information or are invasive to the beam, asking for the development of in-vivo dosimetry solutions. The QUASAR Group, based at the Cockcroft Institute in the UK, has been developing non-invasive beam monitor for medical accelerators since 2015. Detailed transverse beam profile monitoring is the first step towards in-vivo dosimetry. The current monitor applies a supersonic beam gas curtain, interacting with a charged particle beam to then exploit the resulting impact ionization to record the transverse beam profile. A prototype monitor was tested at Dalton Cumbrian Facility's pelletron accelerator for proof-of-concept (POC) beam measurements in summer 2023. The measurements were carried out for different beam energies, sizes and intensities and with both, proton and carbon ion beams. This contribution presents the monitor design and functioning principle, results from the experimental campaign, and planned upgrades to achieve real-time, non-invasive dosimetry.

INTRODUCTION

As the demand for hadron beam therapy grows due to its unique Bragg peak characteristic, there is an increasing need for a fully online, non-invasive technique to characterize the charged particle beams. Real-time, accurate beam/dose monitoring is critical to ensure patient safety, optimize treatment effectiveness, and improve facility efficiency, as incorrect dose delivery can adversely affect healthy tissues. In hadron beam therapy, several dosimetry techniques are employed for characterizing the charged particle beams i.e. ionization chambers , Faraday cups, Radiochromic film, diodes, Thermo-luminescent dosimeter (TLDs), Calorimeter and more [1, 2]. However, most of these techniques either lack the ability to provide real-time online feedback or are invasive to the particle beams.

At the Cockcroft Institute, the QUASAR Group has been developing non-invasive beam monitor for medical accelerators such as LHCb VELO Detector [3] and Gas Jet monitor [4]. To achieve the goal of in-vivo dosimetry, the initial focus is on providing a detailed 2D transverse beam profile of the charged particle beam. A supersonic gas curtain-based transverse beam profile monitor was tested at Dalton Cumbrian Facility (DCF) in July 2023 to conduct first POC measurements with beam parameters similar to medical accelerators. The monitor was integrated into one of the beam-lines of the pelletron accelerator at Dalton Cumbrian Facility (DCF), where multiple measurements were conducted for various beam parameters for both proton and carbon ion beams. This contribution provides an overview of the monitor with the experimental results from the measurements, and planned upgrades to improve the performance of the monitor towards achieving the real-time, non-invasive dosimetry.

GAS JET DOSE PROFILER

Gas jet in-vivo dose profiler is a modified version of the supersonic gas curtain monitor originally developed for High Luminosity LHC (HL-LHC) at CERN [5]. While the monitor designed for HL-LHC utilizes beam-induced fluorescence to provide the 2D transverse beam profile, the version designed for medical accelerators detects the ions generated due to interaction between the supersonic gas jet curtain and the primary ionizing beam. These ions are detected using an Ionization Profile Monitor (IPM) unit. The combination of the supersonic gas curtain and IPM is referred as the Supersonic Gas Curtain based real-time Ionization Profile Monitor (SGC-IPM). SGC-IPM represents the inital step towards the in-vivo dosimetry. Figure 1 illustrates the schematic and 3D cross-sectional design view of the system.

The system is divided into three sections: gas curtain generation system, interaction chamber and the gas curtain dump section. Details on the gas curtain generation process can be found in our previous works [4, 5]. Key characteristics of the supersonic gas curtain- such as its density, width and thickness at the interaction point- depend on the configuration of the nozzle skimmer assembly, as well as the position and geometry of the skimmer III. The required gas density, width and thickness of the gas curtain can vary for different accelerators. For the first POC measurements, a 400 µm skimmer I, a 2 mm skimmer II and a rectangular 20 mm × 0.4 mm skimmer III configuration was considered to provide curtain without degrading the vacuum. Skimmer III was inclined at a 45-degree angle to form a curtain that intersects with the primary particle beam at a 45-degree.

The interaction chamber houses an IPM unit, depicted in green in Fig. 1. The ions generated from the interaction of the supersonic gas certain with the primary particle beam are collected by the IPM unit, which then coverts the ions distribution into an image to be captured by a standard

* narender.kumar@cockcroft.ac.uk

ISBN: 978-3-95450-249-3 ISSN: 2673-5350 doi: 10.18429/JACoW-IBIC2024-WEBC4

EVALUATING THE USE OF COMMON STATISTICAL DIVERGENCES TO QUANTIFY THE DIFFERENCES BETWEEN BEAM DISTRIBUTIONS IN HIGH-DIMENSIONAL PHASE SPACE

Y. Du*,[1,2,3], J. C. Wong†,[1,2,3], Z. J. Wang[1,2,3], T. Zhang[1,2,3], L. W. Liu[1,2,3], C. G. Su[1,2,3], L. Y. Gong[1,2], M. Yi[3], T. L. Wang[1,2,3], H. Y. Zhou[1,2,3], B. H. Ma[1,2,3], Y. M. Chu[1,2,3], T. Y. Li[1,2,3]
[1]Institute of Modern Physics, Chinese Academy of Sciences, Lanzhou, China
[2]University of Chinese Academy of Sciences, Beijing, China
[3]Advanced Energy Science and Technology Guangdong Laboratory, Huizhou, China

Abstract

Quantifying the difference between two beam distributions in high-dimensional phase space is crucial for interpreting experimental or simulation results. This study aims to analyze and compare several common statistical divergences that quantify the differences in high-dimensional distributions, and to determine which of them are suitable for beam physics applications. We tested these divergences with common kinds of initial distributions by computing how the difference values vary when the mismatch factor and emittance change, between the same and different kinds of distributions. These results, along with similar comparisons after extended beam transport, provided guidance on the use and choice of statistical divergences for beam phase space distributions.

INTRODUCTION

Accurately assessing the difference between two beam distributions in high-dimensional phase space is crucial for interpreting experimental or simulation results. For instance, when performing beam phase space tomography, we need to compare the differences between the true and reconstructed distributions to determine the reliability of the reconstruction algorithm and the correctness of the reconstructed results [1]. A common method is to use the mismatch factor [2], which measures based on the RMS phase ellipse boundaries, but it can incorrectly conclude that there is no difference between different kinds of distributions with the same RMS moments. Another method that can distinguish between distribution types is to compare the differences point by point, which is the method of statistical divergences. They give the total contribution of the differences at all points, commonly including: Kullback-Leibler divergence, Jensen-Shannon divergence, Total Variation distance, and Hellinger distance. These are collectively known as f-divergences [3–7], defined as follows:

$$D_f[\rho_1(\mathbf{x})||\rho_2(\mathbf{x})] = \int \rho_2(\mathbf{x}) f\left[\frac{\rho_1(\mathbf{x})}{\rho_2(\mathbf{x})}\right] \mathrm{d}^n\mathbf{x}, \qquad (1)$$

where $\rho_1(\mathbf{x})$ and $\rho_2(\mathbf{x})$ are the probability density functions of two distributions. $f(\cdot)$ is a convex function and satisfies $f(1) = 0$. Different $f(\cdot)$ correspond to different statistical divergences, as shown in Table 1.

Table 1: 4 Forms of f-Divergences; $t = \frac{\rho_1(\mathbf{x})}{\rho_2(\mathbf{x})}$, $\mathbf{x} \in \mathbb{R}^n$

Name	$f(t)$	$D_f[\rho_1(\mathbf{x})\|\|\rho_2(\mathbf{x})]$
Kullback-Leibler	$t \ln t$	$\int \rho_1(\mathbf{x}) \ln\left[\frac{\rho_1(\mathbf{x})}{\rho_2(\mathbf{x})}\right] \mathrm{d}^n\mathbf{x}$
Jensen-Shannon	$\frac{1}{2}\left[\ln\left(\frac{2}{t+1}\right)^{t+1} + t\ln t\right]$	$\frac{1}{2}\int\left\{\rho_2(\mathbf{x}) \ln\left[\frac{2\rho_2(\mathbf{x})}{\rho_1(\mathbf{x})+\rho_2(\mathbf{x})}\right] + \rho_1(\mathbf{x}) \ln\left[\frac{2\rho_1(\mathbf{x})}{\rho_1(\mathbf{x})+\rho_2(\mathbf{x})}\right]\right\} \mathrm{d}^n\mathbf{x}$
Total Variation	$\frac{1}{2}\lvert t-1\rvert$	$\frac{1}{2}\int \lvert\rho_1(\mathbf{x}) - \rho_2(\mathbf{x})\rvert \mathrm{d}^n\mathbf{x}$
Squared Hellinger	$(\sqrt{t}-1)^2$	$\int\left[\sqrt{\rho_1(\mathbf{x})} - \sqrt{\rho_2(\mathbf{x})}\right]^2 \mathrm{d}^n\mathbf{x}$

In this paper, we tested these divergences with Gaussian, Parabolic, and Waterbag distributions by computing how the difference values vary when the mismatch factor and emittance change, between the same and different kinds of distributions. The aim is to provide guidance on the use and selection of statistical divergences for beam phase space distributions through these results.

F-DIVERGENCES BETWEEN DIFFERENT KINDS OF DISTRIBUTIONS

Given two different kinds of beam distributions $\rho_1(\mathbf{x})$ and $\rho_2(\mathbf{x})$ with the same RMS moments, the divergence value between them can be directly calculated through mathematical integration. The values we obtained are shown in Table 2.

Synchronously altering the RMS moments of $\rho_1(\mathbf{x})$ and $\rho_2(\mathbf{x})$, and recalculating the f-divergences between them. We find the results to be consistent with those in Table 2. This indicates that the f-divergences between different types of distributions with the same RMS moments (regardless of the values) are fixed.

Table 2: The D_f of Different Kinds of Distributions With the Same RMS Moments

$\rho_1(\mathbf{x})$–$\rho_2(\mathbf{x})$	D_{KL}	D_{JS}	D_{TV}	D_{Hel}
Parabolic–Gaussian	0.1858	0.0548	0.2269	0.2629
Waterbag–Gaussian	0.4959	0.1341	0.3913	0.4077
Waterbag–Parabolic	0.2319	0.0714	0.2239	0.3090

* Email: duyu@impcas.ac.cn
† Corresponding author, Email: wong@impcas.ac.cn

ISBN: 978-3-95450-249-3 ISSN: 2673-5350 doi: 10.18429/JACoW-IBIC2024-WECI1

BUNCH BY BUNCH FEEDBACK SYSTEM REVIEW *

T. Nakamura†, High Energy Accelerator Research Organization (KEK), Tsukuba, Japan
for contributors and organizers of I.FAST Workshop 2024 on Bunch-by-Bunch Feedback Systems and Related Beam Dynamics, The Karlsruhe Institute of Technology, Germany

Abstract

Bunch-by-bunch feedback (BBF) is a system designed to control the betatron or synchrotron oscillation of each bunch independently. It not only serves as a tool to dampen these oscillations, primarily for the suppression of beam instabilities, but also to excite individual bunches independently and to record their position or timing on a bunch-by-bunch, turn-by-turn basis. This paper reviews the applications of BBF presented at the I.FAST Workshop 2024 on Bunch-by-Bunch Feedback Systems and Related Beam Dynamics.

INTRODUCTION

Bunch-by-bunch feedback system (BBF) is a system that controls horizontal/vertical betatron oscillations ("transverse") or synchrotron oscillation ("longitudinal") for each bunch individually, with the bunch separation down to a few nanoseconds. The BBF has a wide variety of applications, not only for the suppression of beam instabilities. We will review these various applications based on presentations at the I.FAST Workshop 2024 on Bunch-by-Bunch Feedback Systems and Related Beam Dynamics [1], held at The Karlsruhe Institute of Technology, Germany.

BUNCH-BY-BUNCH FEEDBACK

The block diagram of a typical BBF system [2] is shown in Fig. 1. In the figure, both transverse and longitudinal BBF are shown, however, horizontal/vertical/longitudinal BBF can be installed and operated independently.

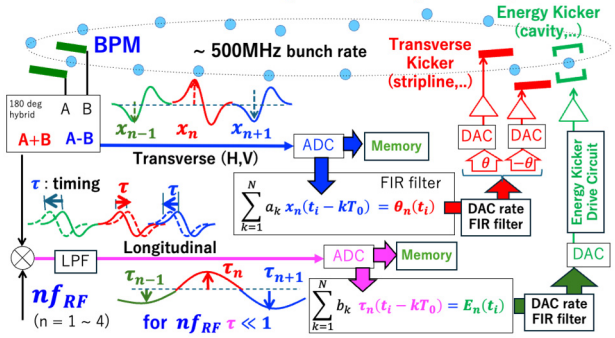

Figure 1: Block diagram of a typical BBF system. Both transverse and longitudinal BBFs are shown.

In a BBF, the two signals generated on the two electrodes of a beam position monitor (BPM) as an electron bunch passes between them are sent to a 180-degree hybrid, which produces their difference and sum signals. The difference signal has a voltage proportional to the transverse position and is used for a transverse BBF, while the sum signal contains bunch arrival timing information and is used for a longitudinal BBF. This timing information is converted to a voltage by mixing it with the carrier frequency, which is usually a multiple of the bunch rate or the acceleration RF frequency. These position and timing signals are sampled by an ADC and converted to digital data. This digital data is then sent to an FIR filter where the kick signal is calculated, and the resultant kick is sent to a DAC, which converts the digital kick data into an analog signal that drives a kicker system.

FIR FILTER

Each bunch has its own FIR filter, where the input is the turn-by-turn position history of the bunch, and the output is the kick signal required to damp betatron (transverse) or synchrotron (longitudinal) oscillations, as shown in Fig. 1.

An FIR filter has the form of

$$\theta_n(t) = \sum_{k=N_D}^{N_D+N_T-1} a_k \; x_n(t - kT_0)$$

where x_n and θ_n are the position and kick of n-th bunch, respectively, as illustrated in Fig. 2, T_0 is the revolution period of the bunch, and N_D is the number of turn (delay) required to prepare the kick at a kicker. The number of input data points, N_T, is called the "number of taps". The tune response of the FIR filter is given by:

$$G(\nu)e^{i\psi(\nu)} = \sum_{k=N_D}^{N_D-1+N_T} a_k \; e^{-ik\,2\pi\nu}$$

where $G(\nu)$ and $\psi(\nu)$ are real numbers representing the gain and the phase shift at tune ν, respectively, as s illustrated in Fig. 3.

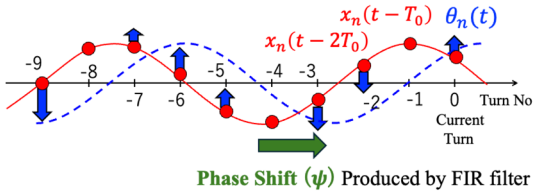

Figure 2: FIR filter for each bunch, converting the turn-by-turn position history into kick by producing phase shift.

For the transverse BBF, the phase shift is adjusted so that the relative phase between the position and kick oscillations at the kicker is -90 degrees, w achieving maximum feedback damping. If this relative phase is set to 0 degrees or -180 degrees with an FIR filter, the feedback acts as a defocusing or focusing quadrupole, respectively, introducing tune shift. Therefore, by controlling the phase shift with the FIR filter, the BBF can simultaneously produce damping/anti-damping and a tune shift of the betatron or

* Work supported by I.FAST (https://ifast-project.eu)
† nkmrpost.kek.jp

ISBN: 978-3-95450-249-3 ISSN: 2673-5350 doi: 10.18429/JACoW-IBIC2024-WECC2

MODELING OF THE SIRIUS FAST ORBIT FEEDBACK CONTROL LOOP

L. A. Pelike*, J. C. S. Carvalho, G. R. Cruz †, A. F. Giachero, A. C. S. Oliveira,
G. S. Ramirez, E. N. Rolim, F. H. de Sá, D. O. Tavares
Brazilian Synchrotron Light Laboratory (LNLS/CNPEM), Campinas, Brazil

Abstract

The SIRIUS Fast Orbit Feedback system was put into routine operation for users in 2022. New system identification experiments were conducted to develop an accurate black box MIMO model of the feedback loop. The high frequency response discrepancies among several fast corrector magnets are captured in this model and allow prediction of the closed loop behavior, which is especially important for designing high gain controllers. This paper describes the obtained model, its validity and enabled improvements on the feedback loop performance and robustness.

INTRODUCTION

SIRIUS is a 4$^{\text{th}}$ generation light source with a storage ring circumference of 518.4 m and 3 GeV electron beam. Its Fast Orbit Feedback system (FOFB) [1] was designed to provide orbit disturbance attenuation from 0.1 Hz to 1 kHz. The system currently employs 78 fast correctors magnets (156 coils) and 80 BPMs (160 beam position readings), and operates at an update rate of 48 kHz.

This paper describes the black box modeling of the feedback loop performed with system identification techniques. Open loop experiments were performed to obtain the complete multiple-input multiple-output (MIMO) system model and closed-loop experiments were conducted for model validation. The obtained model is used to study possible control loop optimization strategies.

PROPOSED MODEL

The proposed model is similar to the one presented in [2] and follows a basic feedback construction. Figure 1 shows the diagram representing its main components. The

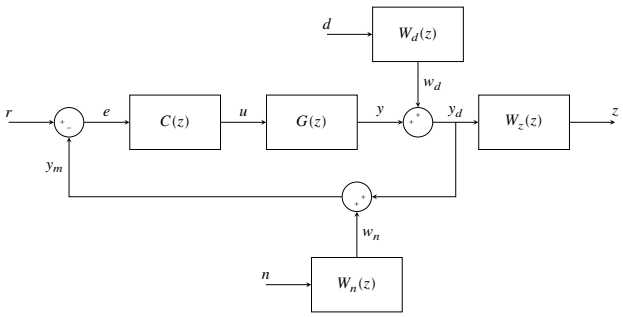

Figure 1: Proposed model with all available inputs and outputs shown.

MIMO transfer function $G(z)$, with n inputs (number of corrector coils) and m outputs (number of BPM readings), is obtained by extending the fitted ARX models and scaling them by the Orbit Response Matrix M. This extension is done by constructing an auxiliary actuators matrix $A(z)$ such that $\{A(z)\}_{ij} = \delta_{ij}A_i(z)$, where $A_i(z)$ represents the discrete transfer function for the i-th corrector obtained with system identification experiments to be described and δ_{ij} is the Kronecker delta. Indexing for the correctors and BPM readings is defined by plane, first the horizontal, then the vertical, and by correctors and BPMs location in the ring, starting from the injection point.

An addition to the basic FOFB model is the beam's longitudinal dynamics, in order to track orbit distortions prompted by oscillations in the beam energy. This inclusion is based on the work presented in [3], with the proposed transfer function

$$\frac{X(s)}{\Theta(s)} = \eta H(s),\ H(s) = \frac{\Omega^2}{\omega_{\text{rf}}\alpha_c}\frac{s}{s^2 + 2s\alpha_s + \Omega^2}$$

where $X(s)$ and $\Theta(s)$ are the Laplace transform of the beam position and RF phase respectively, Ω is the angular synchrotron frequency, ω_{rf} is the RF angular frequency and α_c is the momentum compaction factor, α_s is the damping rate of synchrotron oscillations and $\eta \in \mathbb{R}^n$ is the RF column in the augmented Orbit Response Matrix [1].

The plant $G(z)$ is then given by multiplying the extended Orbit Response Matrix with a matrix built by joining the matrix A with the transfer function $H(s)$ as the last element in the main diagonal. More explicitly,

$$G(z) = [M \mid \eta]\left[\begin{array}{ccc|c} A_1(z) & \cdots & 0 & 0 \\ \vdots & \ddots & \vdots & \vdots \\ 0 & \cdots & A_n(z) & 0 \\ \hline 0 & \cdots & 0 & H(z) \end{array}\right]$$

where $H(z)$ was obtained with a zero-order hold from the described $H(s)$ with added practical considerations (delay of 2 samples and units conversion).

In the results shown using our model, the longitudinal dynamics were not considered and null values were set at some location in the $G(z)$ matrix to this end. A future goal is to develop this interaction further and establish $H(s)$ for SIRIUS. The used plant $G(z)$ could then be expressed simply by $G(z) = MA$.

The controller $C(z)$ is given by

$$C(z) = F(z)\left(K_I\frac{T_s z}{z-1}\right)M^+$$

where $F(z)$ is an optional shaping filter stage, K_I is the controller's integral gain, T_s is the control loop's sampling time

* lucas.pelike@lnls.br
† guilherme.ricioli@lnls.br

ISBN: 978-3-95450-249-3 ISSN: 2673-5350 doi: 10.18429/JACoW-IBIC2024-WEP02

BUNCH-BY-BUNCH PROFILE MEASUREMENT DURING BEAM AVAILABLE TIME

Ruizhe Wu, Xiaochao Ma, Ping Lu, Leilei Tang, Jigang Wang, Baogen Sun*
University of Science and Technology of China (USTC), Hefei, Anhui, China

Abstract

This paper presents a bunch-by-bunch profile measurement system, which is capable of measuring the transverse positions and sizes of each bunch in the storage ring during the beam availability period of the Hefei Light Source II (HLS-II). By finely processing the collected data, the system can effectively recognize the dynamic characteristics of the beams and monitor the performance of the light source. Here, the paper elaborates on the system's design principles, optical layout and system configuration. It also introduces the program workflow of data processing, along with an analysis of the corresponding measurement errors.

BACKGROUND

In synchrotron radiation (SR) light sources, the measurement of the beam profile is not only the key to understanding beam dynamics, but also an important factor for accurately controlling the synchrotron light quality of the light source. The beam profile of the bunches is correlated in the following ways: 1) Brightness: This is a key factor in synchrotron radiation experiments, determining whether the experiment can achieve the required resolution and accuracy. Smaller beam profile means a higher beam density, resulting in higher brightness, which makes the experimental results more accurate. 2) Stability: A stable beam profile is a prerequisite for reliable operation of the accelerator performance. It is especially critical for long-term stability, which is directly related to the duration and reliability of the experiment. 3) Spectrum: Small beam profiles help to produce higher energy SR photons, which is very important for experimental research of different material properties, especially when a wide range of spectra is required. Hence timely and accurate monitoring and adjustment of the beam profile is important to improve the performance of synchrotron radiation sources. Now we have developed one oscilloscope-based online beam profile measurement system to obtain the transient beam profile information of bunches. Its successful implementation at HLS-II provides early research experience and technical reserves for the Hefei Advanced Light Facility (HALF), one 4th generation SR light source under construction.

LAYOUT OF THE SYSTEM

The layout of the bunch-by-bunch profile measurement system is shown in Fig. 1, where M1~M6 are total reflection mirrors; Len1~Len3 are combined convex lenses; MAPMT is the multi-anode photomultiplier R5900U-L16 [1], driven by a high-voltage power supply; D is an optical linear attenuator used to adjust the intensity of the SR light to ensure that the channels of MAPMT are operating in a linear range. Below the MAPMT is a horizontal translation stage, which is used to adjust the imaging position of the beam profile on the MAPMT imaging plane. Subsequently, MAPMT will convert the SR light into 8-channel electrical signals, which will be collected by the oscilloscope SDS6208L [2] and transmitted to the computer for processing. Finally, the computer outputs the transverse positions and transverse sizes of each bunch after data processing.

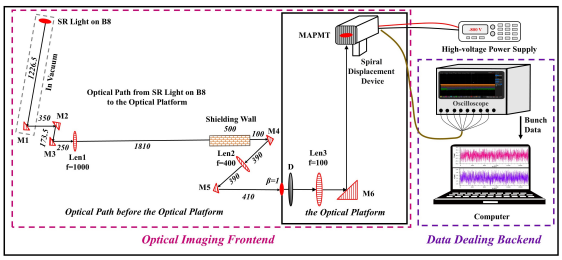

Figure 1: Layout of the profile measurement system.

It should be noted that the light path before the optical platform is a fixed configuration for leading SR light from Beamline 8 at HLS-II, which cannot be changed. And the fixed configuration only magnifies the SR beam size with ratio 1:1. For adjusting the beam size on the final focusing image plane, a combined convex lens Len3 and a total reflector M6 are added to the optical platform, as shown in Fig. 2. By changing the distance between Len2 and Len3 and the image distance between MAPMT and Len3, the beam size on the MAPMT image plane, the focusing image plane, is changed accordingly.

Figure 2: The optical path on the optical platform.

CONFIGURATION OF THE SYSTEM

Using 8 adjacent imaging elements of the R5900U-L16 MAPMT, these 8 imaging elements can cover an imaging area of 6mm. In order to concentrate 99.994 % of the energy of the beam within this area, the distance between Len2 and

* bgsun@ustc.edu.cn

ISBN: 978-3-95450-249-3 ISSN: 2673-5350 doi: 10.18429/JACoW-IBIC2024-WEP03

TWO-DIMENSIONAL RECONSTRUCTION BY THE MULTI-STRIP IONIZATION CHAMBER AT PREF

Tong Liu*[1], Liping Yao[1], Hang Ren[1], Zhixue Li[2], Tian Wang[2],Kewei Gu[2], Junxia Wu[2], Yongliang Yang[2], Guangyu Zhu[2], Xiaoxuan Qiu[2], Jiajian Ding[1], Lili Li, Long Jing[2], Lingxiao Hou[2]
Institute of Modern Physics, Chinese Academy of Sciences, Lanzhou, China
[1]also at Huizhou Ion Science Research Center, Huizhou, China
[2]also at University of Chinese Academy of Sciences, Beijing, China
Ning Li, Advanced Energy Science and Technology Guangdong Laboratory

Abstract

The 60 MeV Proton Radiation Effects Facility (PREF) spent nearly 1 month at the commissioning phase, during which the multi-strip ionization chamber (MIC) at the experimental terminal offered the core parameters, beam spot, scanning area, scanning uniformity, beam flux. However, the projection distribution provided by the MIC loses some information, such as the flux and the uniformity in a selected area less than the scanning area. This paper used a method of two-dimensional reconstruction to provide a 2D (two dimensional) uniformity of selected area. Revealing the trace of the pencil beam at a sampling rate of 10 ksps.

INTRODUCTION

Aiming for displacement damage effect experiments, the 60 MeV Proton Radiation Effects Facility (PREF) [1] was completed the commissioning phase at September, 2023 after a 5-year construction. To improving the radiation hardness of various materials, each experimental terminal equipped a MIC with large sensitive area to monitor the beam position, intensity, radiation field and uniformity. In general, MICs [2–4] or PICs (Pixel Ionization Chambers) [4–6] are applied at the slow extraction radiation terminals.

The homemade electronics with 128 ultralow noise analog front-ends (AFEs) and 16 eight-channel simultaneous sampling analog-to-digital converters (ADCs) [7] were developed for the MIC. The typical parameters of the electronics are listed in Table 1. With the electronics, the MICs worked successfully during the commissioning phase and the last expert acceptance examination.

Table 1: Typical Parameters of the Electronics

Parameter	Value
Channels	128×2
Current	25 pA - 1.8 µA
Sampling Rate	10 kHz
Nonlinearity	<0.12 %
ENOB at a gain of 50 kΩ	12 bits

Providing the 1D (one dimensional) projection information, the MIC lost the values of the 2D uniformity and flux. Developing a 2D reconstruction method, a 2D Gaussian fitting based on a 10 ksps data is built. In this contribution, the examination setup and conception is described. We report the 2D reconstruction and the trace of the pencil beam.

* Corresponding author: liutong@impcas.ac.cn

EXPERIMENTAL SETUP AND CONCEPTION

The MIC collected the 1D projection information, the calculated uniformity lost the 2D information after 1 spill. In this way, we couldn't directly provide the 2D uniformity and the flux in a selected area when the area is less than the radiation field. The frequency of the scanning magnet is from dozens to 200 Hz. When the scanning frequency is 150 Hz with a 150 mm × 150 mm radiation field. Apparently, each direction of the spot moves as follows:

$$\Delta x = \frac{f \cdot D_x}{SR} = 2.25\,\text{mm}, \Delta y = \frac{f \cdot D_y}{SR} = 2.25\,\text{mm}\,, \quad (1)$$

here, Δx and Δy are the distance changing within 100 µs. D_x and D_y are horizontal and vertical scanning dimension respectively. SR is the sampling rate of the MIC. The sigma of the beam spot projection is around 6 mm. So the error of each direction is shown as:

$$\epsilon_x = \frac{\Delta x}{6 \cdot \sigma_x} = 6.25\,\%, \epsilon_y = \frac{\Delta y}{6 \cdot \sigma_y} = 6.25\,\%\,, \quad (2)$$

ϵ_x and ϵ_y are the horizontal error and vertical error respectively. The full width of the spot is $6 \cdot \sigma_y$. Thus, the error caused by the moving is derived as :

$$\epsilon = \sqrt{\epsilon_x^2 + \epsilon_y^2} = 8.84\,\%\,, \quad (3)$$

ϵ is the 2D error. Equation (1) tells that the error will be lower if the scan dimension is lower than 150 mm or the scanning frequency is less than 150 Hz.

In this way, a radiation field of 120 mm × 120 mm and a scanning frequency of 110 Hz, 115 Hz with respect to horizontal and vertical were set in an experiment. The beam parameters are listed in Table 2. With the 10 ksps raw data, a minimal 2D Gaussian fitting of 100 µs is built. The sum and part of the sum of the fittings shows the 2D information of the whole 1.5 - second spill.

ISBN: 978-3-95450-249-3 ISSN: 2673-5350 doi: 10.18429/JACoW-IBIC2024-WEP04

AN X-RAY PINHOLE CAMERA FOR SESAME STORAGE RING

H. Al-Mohammad, A. Hasoneh, M. Shehab, O. Kailani, SESAME, Allan, Jordan

Abstract

An X-Ray pinhole camera beamline has been installed recently at SESAME storage ring as a very beneficial non-destructive tool, used to characterize the electron beam size and behaviour. The design of the beamline is kept as simple as possible with a modification on the copper absorber to provide a sufficient flux of X-ray proper for imaging. The beamline is under operation now and used for the measurement of beam size, emittance, coupling in the ring, and detection of beam instabilities. This paper describes the design details, simulations and measurement results obtained during the beamline commissioning.

INTRODUCTION

The SESAME Storage Ring (SR) is a 2.5 GeV 133.2 m circumference composed of 8 DBA cells with dispersion in all straight sections (8*4.4 m and 8*2.4 m). It offers a maximum capacity of 25 beamlines, phase 1 current up to 300 mA and Emittance 26 nm.rad [1]. The designed parameters of the storage ring are presented in Table 1.

The X-ray diagnostic beamline was installed and commissioned in the SESAME storage ring in the beginning of 2023. This beamline has been designed to measure the transverse beam profile and emittance and monitor beam stability during the beam decay.

Table 1: Storage Ring Main Parameters

Energy (GeV)	2.5
Circumference (m)	133.2
RF Frequency (MHz)	499.654
Betatron tunes Q_X / Q_Y	7.23 / 6.19
Horizontal emittance ε_x (nm.rad)	26
Momentum compaction factor	0.0083
Circulating Current(mA)	300
Energy loss per turn (keV)	603

PINHOLE CAMERA SETUP

The X-ray pinhole camera consists of a source, a pinhole, a screen, and a camera. At SESAME, the X-ray pinhole camera is installed in cell 16 of the storage ring (SR) to measure the beam size from the 6.5° port of the bending magnet (BM). The X-ray beam passes through a beam port absorber, which is a copper block designed to absorb the majority of the X-ray beam while allowing a portion of the high-energy X-rays to pass through to the pinhole assembly in air, and subsequently to the YAG screen and imaging system. The system layout is illustrated in Fig. 1. The pinhole assembly should be positioned as close to the source as possible to achieve greater magnification; in our setup, it is located 3.5 meters away. The pinhole is created using 1 mm thick tungsten bars separated by chemically etched shims, with four layers of shims (10, 25, 50, and 400μm) forming a grid [2]. To image the source, a fluorescent screen, which absorbs X-rays and fluoresces in the visible spectrum, is used. This screen is placed 5.3 meters away from the pinhole assembly, resulting in an image magnified by a factor of approximately 1.5. A CCD camera with a zoom lens is employed to capture and measure the size of the source.

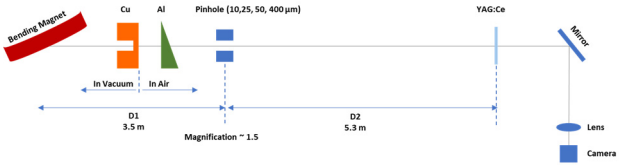

Figure 1: Layout of X-ray pinhole camera beamline.

X-Ray Beam Absorber

The X-ray beam absorber was originally designed to be made of copper, featuring a slot for a port leading to an aluminium window. However, due to financial constraints, an alternative approach was adopted. The solution involved repurposing a defective full copper mirror, previously used in the diagnostics beamline in the storage ring, designed to handle an X-ray beam of 400 mA at 2.5 GeV.

To repurpose the mirror as an absorber and beam extractor with minimal absorption in its thin layer that will extract part of the beam after polishing its surface, simulations and finite element analysis (FEA) were conducted. The primary challenge was drilling the mirror and offsetting the hole from the centre to avoid damaging the cooling channels, one of them is located at the centre. This offset was then compensated by precisely aligning the entire absorber (mirror) chamber.

The absorber is expected to receive a maximum normal peak power of 26.08 W/mm² from the dipole magnet at 300 mA. FEA results indicate that the maximum temperature will reach 84.8°C, with a maximum Von Mises stress of 146 MPa. A 3 mm circular slot was drilled from the inner face and a 6 mm slot from the outer face of the mirror, leaving a 0.5 mm thick layer of copper to allow the beam to pass through while maintaining vacuum integrity, as illustrated in Fig. 2. The 0.5 mm thickness was chosen to provide an adequate amount of flux while meeting mechanical requirements and ensuring the feasibility of in-house fabrication. As a consequence of using copper instead of aluminium the intensity of the final beam is significantly reduced, as illustrated in Fig. 3, and the electron beam at injection energy (800MeV) can't be seen or measured. The beam is started to be seen at ~ 2.4 GeV, and the photon intensity at 2.5 GeV keeps sufficient to see the beam over the decay time in the SR. The aluminium wedge was ultimately not used due to the reduced photon intensity. The copper absorber shifted the X-ray beam energy to be

ISBN: 978-3-95450-249-3 ISSN: 2673-5350 doi: 10.18429/JACoW-IBIC2024-WEP05

DIAGNOSTICS VISIBLE BEAMLINE AT SESAME STORAGE RING

H. Al-Mohammad, A. Hasoneh, M. Al-Najdawi, SESAME, Allan, Jordan

Abstract

Visible light range of Synchrotron radiation is a versatile diagnostics tool for accelerator studies and measurements. SESAME's storage ring has a dedicated diagnostics visible light beamline from 6.5-degree beam port of bending magnet source point. The beamline will host in future a time-correlated single photon counting unit to measure the bunch filling pattern, fast gated camera and a streak camera for longitudinal diagnostics. Recently, the beamline has been extended to be operational from outside the tunnel (dedicated hutch) to allow more flexible studies with direct source imaging and a double-slit interferometry for beam size measurement and study transverse instabilities. In this paper we give an overview of the design of the beamline, modifications and present first results.

INTRODUCTION

The SESAME Storage Ring (SR) is a 2.5 GeV, 133.2 m circumference composed of 8 DBA cells with dispersion in all straight sections (8*4.4 m and 8*2.4 m). It offers a maximum capacity of 25 beamlines, phase 1 current up to 300 mA and Emittance 26 nm.rad [1]. The designed parameters of the storage ring are presented in Table 1.

The visible diagnostics beamline (VDBL) was initially installed and commissioned in the SESAME Storage Ring (SR) during the accelerator's commissioning phase. At that time, it was located inside the tunnel, which posed significant challenges due to the limited space and difficulty in controlling the environment. However, this summer, the beamline was relocated outside the tunnel into a dedicated hutch. This move provides more flexibility for conducting studies, managing the optical system, and accommodating additional equipment in the future. The VDBL is designed to measure the transverse beam profile and monitor the emittance and stability throughout the beam decay.

BEAMLINE SETUP

From the outset, the design was intended to be simple and cost-effective. As a result, the system was compactly installed in cell 14 inside the tunnel, positioned vertically in front of the viewport. The measurement and monitoring of the transverse beam profile were conducted using direct beam imaging for both planes. However, due to the limited vertical resolution caused by diffraction from a crotch absorber in the vacuum chamber, the vertical beam size was measured using double slit interferometry [2].

The beamline accommodated both measurement methods by utilizing a motorized filter wheel, which housed the double slits and neutral density filters. Since the beamline was installed inside the tunnel, all calibration and optimization of the optical lenses and other components were performed in the lab before being transferred to the tunnel. This setup made calibration and fine focusing more challenging.

Table 1: Storage Ring Main Parameters

Energy (GeV)	2.5
Circumference (m)	133.2
RF Frequency (MHz)	499.654
Betatron tunes Q_X / Q_Y	7.23 / 6.19
Horizontal emittance ε_x (nm.rad)	26
Momentum compaction factor	0.0083
Circulating Current(mA)	300
Energy loss per turn (keV)	603

The New Setup

The new setup introduces some adjustments to the layout of the vacuum components inside the tunnel, making it more compact and modifying certain girders. The same in-vacuum mirror is used, with a design originally borrowed from the ANKA light source (now KARA), but with modified cooling circuit in order to handle our full future beam current of 400 mA. All FEA (Finite Element Analysis) have been conducted on the mirror, as shown in Fig. 1.

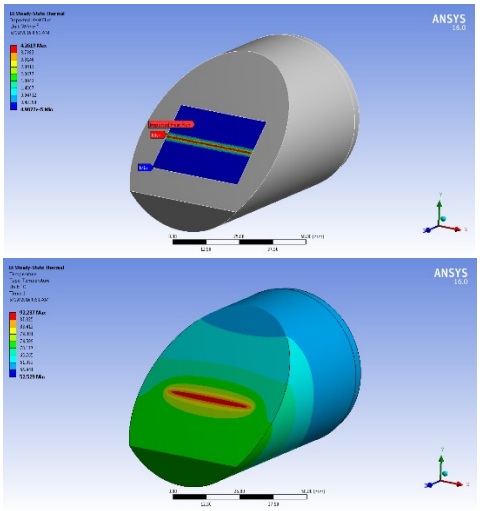

Figure 1: VDBL in-vacuum mirror FEA analyses, showing power at the mirror (up) and temperature distribution (down).

The mirror is a water-cooled OFHC (Oxygen-Free High Conductivity) copper block, brazed onto a CF63 stainless steel flange, and coated with aluminium optimized for the visible light range. This design achieves over 90% reflection efficiency at 500 nm, with quarter-wavelength flatness and surface roughness of less than 20 nm. The mirror is installed in a CF63 cube vacuum box, which is mounted on

ISBN: 978-3-95450-249-3 ISSN: 2673-5350 doi: 10.18429/JACoW-IBIC2024-WEP08

THE PROJECT OF KIRKPATRICK – BAEZ FOCUSING SYSTEM FOR BEAM DIAGNOSTICS ON THE SKIF

O. I. Meshkov†,1,2, V. L. Dorokhov[1], D. F. Reshetov[1], E. Glushkov[2,3], I. Malushev[2,3]
[1]Budker Institute of Nuclear Physics, Novosibirsk, Russia
[2]also at Novosibirsk State University, Novosibirsk, Russia
[3]Institute of Applied Physics, N. Novgorod, Russia

Abstract

The Siberian Ring Radiation Source (SKIF) is an upcoming 4th-generation SR source under construction in Novosibirsk, Russia. The designed beam emittance for SKIF is 75 pm-rad, which corresponds to a beam size of 6 micrometers at the observation point within the dipole magnet. The transverse beam dimensions are essential parameters for tuning and reliable operation of the facility. The SKIF diagnostic suite includes a double-slit interferometer operating in the ultraviolet region of the spectrum. This device's spatial resolution should be sufficient to measure the radial size of the beam to an accuracy of 10 percent. These diagnostics will be used during the commissioning of SKIF and afterwards. Although an additional source of information on beam dimensions and dynamics would be desirable for assurance, taking into account the record designed value of beam emittance. The application of X-ray optics and the Kirkpatrick-Baez focusing system seem to be the most suitable option. The paper discusses the project of this system, which will acquire X-rays from a SKIF dipole magnet.

INTRODUCTION

SKIF [1] is the 4-generation synchrotron light source designed by the Budker Institute of Nuclear Physics (BINP) with an energy of 3 GeV. It is expected to be completed in 2024 and put into operation in 2025.

The magnetic structure of the SKIF is based on the modified mTME cell and consists 16 superperiods. Figure 1 presents the beam transverse dimensions within a single superperiod. A superperiod comprises four "soft" magnetic dipoles with a field strength of 0.55 T and four of "hard" magnetic dipoles with a field of 2.2 T. The synchrotron radiation (SR) of the beam emitted from these dipoles can be used for the beam diagnostics, specifically for measuring beam dimension. This paper will focus solely on the application of the SR from the "soft" magnet. The critical energy in the SR spectrum emitted from this magnet is E_{cr} = 3 keV. Detailed information about the properties of the SR can be found in [2]. The choice between two magnets determines by the lower heat load on the first mirror surface of the KB system.

The well-known limitations of a spatial resolution are determined by the properties of SR [3]. These includes the diffraction limit: $\sigma_{df} \approx 0.25\sqrt[3]{\frac{\pi}{6}}\lambda^2\rho$, a visible segment of the beam trajectory: $\sigma_{arc} \approx \frac{1}{2}\sqrt[3]{\left(\frac{3}{4}\frac{\lambda}{\pi}\right)^2\rho}$; and a depth of field: $\sigma_{dp} \approx 2\sigma_{arc}$. A total restriction on the radial beam dimension is given by $\sigma_t^{rad} = \sqrt{\sigma_{df}^2 + \sigma_{arc}^2 + \sigma_{dp}^2}$. This limit for the vertical beam dimension is also given by $\sigma_t^{vert} = \sqrt{\sigma_{df}^2 + \sigma_{dp}^2}$, where λ - is the wavelength of the radiation, and ρ = 18.8 m is radius of curvature of the beam trajectory. These limitations make it impossible to measure transverse beam dimensions in the visible area of the SR using projection optics because $\sigma_t^{rad}, \sigma_t^{vert} \approx 70$ mkm if the light at wavelength λ = 550 nm from the "soft" magnet is applied for that.

It is possible to measure the transverse dimensions of a beam using double-slit interferometer [4] and this technique for the SKIF is discussed in [2, 5].

Nonetheless, the capacity to observe the beam transverse profile of the beam has some advantages when compared to acquiring an interferometric pattern. Thus, it becomes possible to investigate dynamics of a beam during injection and monitor a spectra of beam oscillations [6]. Because of that we aim to develop a method for diagnosing the transverse profile of a beam based on an optical projection system operating in the X-ray range, utilizing multilayer mirrors [7]. The shift to the soft X-ray region significantly reduces the limitations for $\sigma_t^{rad}, \sigma_t^{vert} \approx 2.5$ mkm if a radiation with an energy of E = 400 eV is employed.

The optical system should be capable of providing a magnification of about ×5 in order to enlarge the dimensions of the captured beam image to several tens of micrometers. This will allow for a reliable digitization of the beam image. There are two well-known optical systems which are used for similar purposes: the Kirkpatrick-Baez focusing system [8–10] and the Schwarzschild objective [11–13]. Their key characteristics under specific conditions of the SKIF are outlined below.

KIRKPATRICK – BAEZ FOCUSING SYSTEM

The Analyse of the Spatial Resolution of the KB Focusing System

The KB mirrors (Fig. 2) which we intend to use for beam imaging in the main storage ring of the SKIF are essentially analogous to a type of microscope described in [14, 15],

† O.I.Meshkov@inp.nsk.su

ISBN: 978-3-95450-249-3 ISSN: 2673-5350 doi: 10.18429/JACoW-IBIC2024-WEP10

OPTIMIZED DESIGN OF AN CONSECUTIVE DOUBLE-SLIT EMITTANCEMETER FOR THE C-BAND PHOTOCATHODE RF GUN*

W. Chen, S. Jiang, R. Liu, T. Yang, R. Yang†, X. Li, S. Wang
Institute of High Energy Physics, 100049 Beijing, China
also at China Spallation Neutron Source, Dongguan, China
X. Li, Deutsches Elektronen-Synchrotron, Zeuthen, Germany

Abstract

To enhance the performance of the next generation of X-ray free electron lasers (XFEL), it is essential to produce a high quality electron beam with a low emittance, for instance, below 0.2 mm-mrad for a 100 pC bunch charge. In order to demonstrate the fundamental techniques required for future FEL facilities, a C-band photoinjector test facility has been constructed aligning with the Southern Advanced Photon Source (SAPS) pre-research project. An emittancemeter based on the consecutive double-slit-scan concept has been proposed and designed for determining such small emittance. This paper presents the further optimization of the primary parameters of this emittancemeter employing numerical simulations in the presence of the measured motion accuracy and the expected observation resolution.

INTRODUCTION

Next-generation XFEL is rapidly moving towards providing more flexible photon pulse time patterns and higher average brightness. This has brought new requirements on the high-brightness electron source to deliver the electron beam with a low transverse normalized emittance (below 0.2 mm-mrad for a bunch charge of 100 pC). High-brightness photocathode electron gun plays a decisive role in the overall performance of XFEL. Among the brightest electron sources, the photoinjector equipped with a low-intrinsic-emittance photocathode has been widely used. For a photocathode radio-frequency gun (RF gun), the beam emittance usually reaches its minimum for an acceleration gradient of about 140-150 MV/m [1, 2]. However, the existing L-band and S-band photocathode RF gun could hardly reach such high acceleration gradient. The C-band photocathode RF gun features a maximum gradient of above 150 MV/m and can provide small-emittance beam for the future XFEL. Moreover, the C-band RF gun has a reasonable requirement on the mechanical processing accuracy (about 20 μm) that could be met with the state-of-art techniques.

The C-band photoinjector test facility at the Institute of High Energy Physics (IHEP/CAS) employs a 5.712 GHz 3.6-cell gun with the designed acceleration gradient above 150 MV/m [3]. To optimize the beam emittance, the beam tracking software Astra combined with Python's lume-astra and Geatpy libraries have been used. An evolutionary algorithm has optimized the minimum emittance at a distance of 1 m from the cathode surface as summarized in Table 1. The cathode material is copper, and the beam energy at the electron gun exit is 7-8 MeV. For a bunch charge of 100 pC, the 100 % and 95 % emittances are 0.18 and 0.11 mm-mrad, respectively. To quantify the beam quality at the gun exit, a diagnostic beamline has been designed. It consists of an emittancemeter (EM), an integral beam transformer (ICT), two screen monitors and a Faraday cup (FC), as shown in Fig. 1.

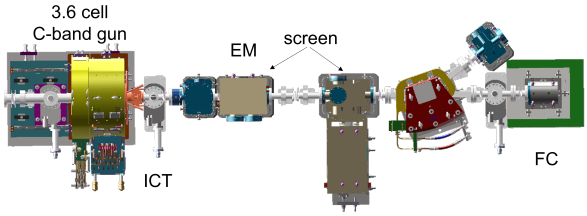

Figure 1: Layout of the C-band photocathode RF gun test facility.

Table 1: Optimum Simulated Photoinjector Parameters for Bunch Charge 100 pc

Parameter	Unit	Value
RF frequency	GHz	5.712
Accelerating gradient	MV/m	150
Repetition rate	Hz	1-100
Beam energy at the gun exit	MeV	7.3
Transverse emittance	mm-mrad	0.175
Bunch length	ps	5
Beam rms size	μm	42.5

METHODS

For the C-band photoinjector, beam emittance increases rapidly from 0.18 mm-mrad to about 0.8 mm-mrad as the beam drifts from a distance of 1 m to 1.8 m. The conventional quadrupole scan and multi-screen method could not be adapted. Alternatively, the multi-slit method or single-slit methods have been widely used at many photoinjector [4–7]. For instance, PITZ measured an emittance of 0.26 mm-mrad employing a 10 μm slit [8]. The both methods employ a tight slit to divide the beam into smaller beamlets and then visualize the beamlet downstream using a profile monitor. Thus, it allows the reconstruction of the phase space distribution and emittance with an acceptable impact from the space-charge effect. The multi-slit method has the merit of single-shot

* GUANGDONG BASIC AND APPLIED BASIC RESEARCH FOUNDATION (2022A1515140179).
† yangrenjun@ihep.ac.cn

ISBN: 978-3-95450-249-3 ISSN: 2673-5350 doi: 10.18429/JACoW-IBIC2024-WEP11

THE UPGRADE OF THE TARGET MULTIWIRE PROFILE MONITOR FOR THE CSNS-II PROJECT*

R. Y. Qiu, X. J. Nie, R. H. Liu, Z. H. Xu, F. Li, L. Zeng, W. L. Huang, M. Y. Liu, Q. R. Liu, W. W. Chen, R. J. Yang, T. G. Xu, T. Yang†, Institute of High Energy Physics, Chinese Academy of Sciences, Beijing, China and Spallation Neutron Source Science Center, Dongguan, China
A. X. Wang, National Synchrotron Radiation Laboratory, University of Science and Technology of China, Hefei, China
M. Meng, Laboratory for Ultrafast Transient Facility, Chongqing university, Chongqing, China

Abstract

The beam power is lifted up to 500 kW for the phase II of the China Spallation Neutron Source (CSNS-II) project, which is five times the power of CSNS-I. At the CSNS, the neutron beams are generated by the spallation reaction of 1.6-GeV protons striking on a tungsten target. The multi-wire profile monitor (MWPM) in front of the proton beam window is the only instrument for long-term monitoring of proton beam distribution when the protons are delivered to the spallation target. The wire interval of the target MWPM of CSNS-I is 7 mm, which is slightly sparse for beam profile measurements during the beam operation in recent years. To ensure the precisely monitoring and provide accurate signal for the Machine Protection System (MPS) when the beam is abnormal, an upgraded design was proposed and implemented. The design mainly employs the Printed Circuit Board (PCB) technique to route the signal originated from the tungsten wires. Four bias planes comprised of tungsten wires are added to mitigate the crosstalk effect brought about by stray electrons and enhance the secondary emission effect. The minimal wire interval of present design is 2 mm and the whole equipment is more compact compared with the previous one due to the PCB scheme. This paper will detail the design and manufacturing of the CSNS target MWPM.

INTRODUCTION

For long-term stability and safety considerations of the beam instrument, the MWPM is almost the only option to monitor the proton beam transverse profile in front of the proton beam window (PBW) in most spallation neutron source laboratories [1-4]. The proton beam profile at the PBW will trigger an MPS signal if the beam is abnormal (i.e., abnormal beam position and size), which is not only rather crucial for the machine safety, but it also holds significant meaning for the personnel safety since the high dose rate will occur if the beam deviates severely from the orbit center.

The present target MWPM at the CSNS [4] was operated in August 2017, since then, this instrument had played an important role for the accelerator stable operation. The signal wire of CSNS-I target MWPM is made of tungsten (ϕ100 μm), and the wire interval is 7 mm. To meet more precisely monitoring requirements, an upgrade scheme with a smaller wire interval is necessary for the CSNS-II project. We have developed a PCB-based profile monitor to achieve a wire interval of 2 mm, and we also add several bias planes to mitigate the crosstalk effect due to the stray electrons.

MAIN DESIGN CONSIDERATIONS

The main beam parameters of CSNS I & II are listed in Table 1 [4].

Table 1: Main Parameters of CSNS I & II

Parameters	CSNS-I	CSNS-II
Beam Power (kW)	100	500
Beam Energy (GeV)	1.6	1.6
Average Beam current (μA)	62.5	315
Beam repetition rate (Hz)	25	25
Protons per pulse (10^{13})	1.56	7.8

The main design considerations of the MWPM are the beam induced thermal effects and the wire material selection. The carbon, tungsten and SiC are the main material types for the beam profile measurements based on the secondary-electron emission mechanism of wires [1-6]. Tungsten is selected as the wire material both in the target MWPM designs of CSNS-I&II because of its high melting point, high tensile strength and low cost. Figure 1 illustrates the temperature increase at the center and edge of the tungsten wire with a diameter of 100 μm, assuming the beam parameters listed in Table 1. The wire length is assumed to be 10 cm in this calculation, and the beam spot dimension is assumed to be 20 mm×20 mm taking sufficient safety redundancy into consideration (the actual size of the beam spot is significantly larger). At the center, the peak temperature is about 1700 K, while it is ~650 K at the edge. Compared to the melting point of tungsten, which is approximately 3683 K, the maximum temperature falls within a relatively safe range and remains below the threshold where the thermionic emission effect becomes significant (~1800 K) [5]. The calculated thermal stress is about 270 MPa, and a ~1-2 N pretension is sufficient to compensate the thermal deformation of wires.

Based on the experience of CSNS-I, as shown in Fig. 2, the wire interval of MWPM is limited by the size of wire holder with a spring, which is hard to decline to 4 mm.

* Work supported by the Natural Science Foundation of China (Grants No. 12105297 and U2032165).

† yangt@ipp.ac.cn, present affiliation and address: Institute of Plasma Physics, Hefei Institutes of Physical Science, Chinese Academy of Sciences, Hefei, China.

ISBN: 978-3-95450-249-3 ISSN: 2673-5350 doi: 10.18429/JACoW-IBIC2024-WEP12

A DEVELOPMENT OF WIDE DYNAMIC-RANGE HALO MONITOR FOR 8 GeV PROTON BEAMS AT FNAL*

Y. Hashimoto†, C. Omori, Y. Sato, T. Toyama, T. Mitsuhasi, M. Tejima,
T. Sasaki, M. Uota, KEK/J-PARC, Japan
R. Ainsworth, FNAL, USA
H. Sakai, Kanto Information Service, Co., Ltd., Japan

Abstract

The FNAL accelerator complex has been upgrading in increasing beam intensity and beam quality. A new beam halo diagnostic device is required in the beam transport line between booster and Recycler.

For this purpose, it was decided to introduce the wide dynamic range monitor technique that was developed in 2012 and has been in operation at the J-PARC beam transport line. The device is a two-dimensional beam profile monitor, and it has a dynamic range of approximately six digits of magnitude by using of Optical Transition Radiation and fluorescence screens. Eliminating harmful beam halos is the most important technique for high-intensity proton accelerators. Therefore, beam halo diagnosis is indispensable and becomes more and more important.

New FNAL device has been manufactured in a collaboration be-tween J-PARC and FNAL as a part of U.S.-Japan Science and Technology Cooperation Program in High Energy Physics. The equipment will be manufactured at J-PARC and will be shipped to FNAL in 2025.

We designed the device to satisfy FNAL specifications: the beam energy, intensity, and size. Currently, most of the equipment is under construction. The large-aperture optical system has been completed and its optical characteristics are being evaluated at J-PARC. We have been also investigating measurement methods corresponding to FNAL bunch trains. This paper reports on the current status of these developments.

DEVICE DESIGN

Here is described summary of the design studies [1] so far. The measurement principle is the same as that of the previous J-PARC [2, 3], which is a combination measurement of two targets (titanium foil and alumina target) (Fig. 1A).

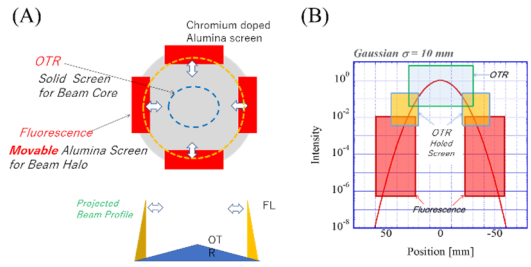

Figure 1: Device concept. (A) Combination target in front view, (B) Cover range of each target.

* Work supported by U.S.-Japan Science and Technology Cooperation Program in High Energy Physics.
† e-mail address: yoshinori.hashimoto@kek.jp

OTR from titanium foil is used to measure the beam core part, and fluorescence from an alumina target is used to measure the beam halo part. This covers a six-digit measurement range (Fig. 1B).

Table 1: Beam Intensity and Beam Size

	Beam intensity [p/bunch]	Beam size (σ) [mm]
3 GeV (J-PARC)	1×10^{13}	10
8 GeV (FNAL)	5×10^{10}	2.5

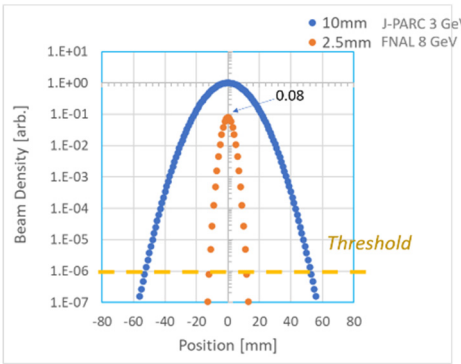

Figure 2: Beam profile in density.

A comparison of FNAL Beam and J-PARC beam is shown in Table 1 and Fig. 2. The FNAL beam is characterized by a beam density of about 8 % of J-PARC, a beam size (σ) of about 25 %, and a small beam of 2.5 mm. In addition, the optical characteristics of OTR depend on the Lorentz factor γ, and the amount of OTR light obtained per unit proton is 1.32 times that of J-PARC, and the spread angle (peak) of OTR is as narrow as 12 degrees compared to 27 degrees for J-PARC. Summarizing these, when considering the measurement of each bunch, the J-PARC measurement achieves 6-digit range, but the FNAL measurement is expected to measure about 5 digits. This is due to the low bunch intensity of FNAL. We also considered measuring a six-digit dynamic range with FNAL. By placing the diffuser screen, which is the method used for J-PARC's Unit-2 [4] as the secondary optical system for measurement, on the atmospheric side, the solid angle of the measuring instrument was increased by 12.69 times. As a result, the design can secure a dynamic range of six digits. The optical system is shown in Fig. 3.

DEVICE FABLICATION

The production of the devices is currently underway, and the status of these will be described.

ISBN: 978-3-95450-249-3 ISSN: 2673-5350 doi: 10.18429/JACoW-IBIC2024-WEP13

THE STUDY OF THE BEAM DYNAMICS AT THE VEPP-2000 COLLIDER USING A GATED CAMERA*

M. V. Timoshenko†, V. E. Boyarkina[1], V. L. Dorokhov[2], O. I. Meshkov[1], S. P. Sherstyuk[1]
Budker Institute of Nuclear Physics, Novosibirsk, Russia
[1]also at Novosibirsk State University, Novosibirsk, Russia
[2]also at SRF "SKIF", Boreskov Institute of Catalysis, Koltsovo, Russia

Abstract

The Nanogate-38 gated camera with a temporal resolution of 60 nanoseconds was used to measure the transverse beam dimensions in the BEP booster and the VEPP-2000 electron-positron collider. The camera was used in combination with a double-slit interferometer to measure the vertical beam size and with projection optics to construct a transverse beam profile in single-turn mode. Some beam characteristics were measured, such as decoherence time, radiation damping time and fast attenuation time. The purpose of these experiments was to investigate the possibility of using this camera to measure the transverse dimensions of the beam and its emittance, as well as to conduct experiments on accelerator physics at the SKIF synchrotron radiation source.

INTRODUCTION

The largest scientific project carried out by the Budker Institute of Nuclear Physics of Siberian Branch Russian Academy of Sciences (BINP) in recent years is the construction of a synchrotron radiation source of generation 4+ named Siberian Ring Photon Source (SKIF) [1]. The calculated emittance of the electron beam in SKIF is $\varepsilon_x = 75\,\text{nm} \times \text{rad}$.

One of the important tasks in beam diagnostics at a storage rings is to measure the record-low emittance. To do this it is assumed to use the traditional method of measuring the transverse horizontal beam size σ_x [2, 3] at an observation point with almost null dispersion function.

To measure the transverse beam size it is planned to use a double-slit interferometer [4, 5] which registers synchrotron radiation (SR) emitted from a dipole magnet in the ultraviolet (UV) part of the spectrum. Transverse beam oscillations at a frequency of tens of hertz which can be caused by various factors, can lead to a deterioration in the visibility of the interference pattern and overestimation of the actual beam size. This issue can become a problematic when measuring the beam emittance in SKIF, as it is common practice to compare the calculated value with the experimental with a minimum number of particles in the bunch in order to neglect collective effects. The associated proportional decrease in the number of photons emitted by the beam causes the interferogram recording time to be increased up to several seconds. While this may seem like a solution to one problem, it introduces the possibility of the another. Additionally, mechanical vibrations of optical diagnostic components can also contribute to a deterioration of visibility. Recent experiments on the KISI storage ring [6] have demonstrated that it is preferable to keep exposure time during interference pattern recording below 1 ms.

Experiments on the diagnosis of the transverse beam profile were conducted at the Budker Institute of Nuclear Physics (BINP) at the electron-positron collider VEPP-2000 [7] and its booster BEP [8]. The layout of these facilities is shown in Fig. 1.

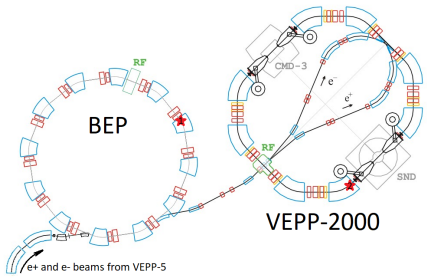

Figure 1: VEPP-2000 complex layout (red stars indicate observation points).

VEPP-2000 is a compact electron-positron collider with a circumference of 24.39 m. It has a record project luminosity ($L = 10^{32}$ cm^{-2}s^{-1}) at energy of 1 GeV per bunch. The collider operate in a 1×1 bunch mode and it is equipped with an electron-positron booster called BEP. Whole complex operates over a wide energy range of 160–1000 MeV.

The beam revolution periods for the BEP and VEPP-2000 are 74.54 ns and 81.35 ns respectively that allow obtaining single-turn bunch transverse profile by Nanogate-38 camera.

BEP operates in single-bunch mode. At a beam current of 1 mA in the BEP, the number of particles in the beam is approximately 3×10^8. The SR intensity at a BEP beam current of 25 mA is approximately equivalent to the SR intensity at the main SKIF storage ring beam current of 1 mA.

The vertical beam size in the BEP is strongly dependent on the current and is close to the calculated diffraction limit of $\sigma_y^d \approx 0.08$ mm at a wavelength of $\lambda = 550$ nm. A double-slit interferometer allows measuring beam sizes smaller than this limit.

An equally important task is to tune the beam "top up" injection into the main SKIF storage ring. In this regard, efforts have been made to investigate the possibility of de-

* This work was financially supported by the Russian Science Foundation and the Ministry of Science of the Novosibirsk Region of the Russian Federation (RSF Grant No. 22-12-20025).

† M.V.Timoshenko@inp.nsk.su

ISBN: 978-3-95450-249-3 ISSN: 2673-5350 doi: 10.18429/JACoW-IBIC2024-WEP14

BUNCH RESOLVED TRANSVERSE BEAM DIAGNOSTICS AT BESSY II*

I. Shmidt†, G.Rehm, G. Schiwietz
Helmholtz-Zentrum Berlin für Materialien und Energie, Berlin, Germany

Abstract

For diagnostics of the different bunch types at the BESSY II electron-storage ring, a streak camera and a fast-gated ICCD camera have been installed at two neighbouring beamlines, both of which are powered by visible light from the same dipole magnet. This contribution is focused on the ICCD camera and its first applications. After an improvement regarding the ICCD repetition rate, the maximum illumination rate exceeds now the BESSY II revolution frequency of 1.25 MHz. Furthermore, we have improved the optical light-transfer system and characterized the optical magnification, the spatial resolution and time resolution of the system.

Initial measurements have been restricted to direct bunch-resolved imaging of the 2-dimensional transverse shapes of different types of bunches. Specifically, the Pulse Picking by Resonant Excitation (PPRE) bunch is investigated in more detail. This bunch is horizontally broadened by a quasi-resonant incoherent perturbation and leads to pseudo single-bunch radiation within the complex multi-bunch fill-pattern at the BESSY II storage ring.

INTRODUCTION

BESSY II, like other modern synchrotron light sources, has a complex filling pattern in standard user mode. Existence of the special bunches in the ring allows to use the emitted synchrotron radiation for more purposes. Apart from the 'normal' train bunches, that have approx. 1 mA current in each of the bunches BESSY II has also one Camshaft bunch (4 mA) and two PPRE bunches (3 mA each) and seven slicing bunches (3 mA each). Especially the PPRE bunch is of interest for the bunch resolved diagnostics. This bunch makes it possible to run experiments that require pulsed synchrotron radiation with repetition rates in few MHz range in the standard user operation. To achieve that the bunch is excited in the horizontal direction which allows the user to work with the light of the PPRE bunch only just by blocking the light from the other bunches with an aperture [1]. Therefore it is important to broaden the bunch significantly without exciting large center of mass motion. An analytical model as well as numerical simulations on the excitation mechanism of PPRE bunch were already presented in [2]. To get information on the real behavior of the bunch, time consuming life time measurements or operation in the single bunch mode were required previously. However, using a fast-gated ICCD camera allows direct observation of the bunch behavior. In the following, a beamline for bunch resolved transverse diagnostics using a fast-gated ICCD camera will be described. Additionally, results of the first observations of the PPRE bunch will be presented.

BEAMLINE FOR TRANSVERSE OPTICAL DIAGNOSTICS

Both optical diagnostic beamlines - for longitudinal diagnostics with Streak camera and for transverse diagnostics with fast-gated ICCD - are located in the sector 12 of the BESSY II ring and start from the bending magnet BM2T6R [3]. For transverse diagnostics, synchrotron light is transferred from the storage ring to the diagnostic platform with two custom-made plane 70 mm×70 mm mirrors M1 and M2 with residual bending radii of > 25 km (see Fig. 1). An important part of the beamline is the X-ray blocking baffle that covers 5.31 mm in the center of the light bulk, preventing X-Rays from reaching the first mirror. Apart from the central block, the X-ray blocking baffle also defines with its outer dimensions the acceptance angle of the beamline. It has a horizontal aperture of 44 mm and vertical aperture of 31.3 mm with resulting acceptance angles of 6.10 mrad and 4.34 mrad. The vacuum part of the beamline closes with a combination of two wedged windows, that are 180° rotated relative to each other. This combination allows to avoid multiple reflections between the outlet window and mirror M2 without changing the transmitted part of the light.

At this point it is important to mention that limited acceptance of the beamline as well as the wavelength of the used light limit the spatial resolution of the beamline. According to the Rayleigh criterion, the smallest resolvable angle for the single slit of the width d illuminated with a monochrome light of the wavelength λ is $\theta = \arcsin(\frac{\lambda}{d}) \approx \frac{\lambda}{d}$. Therefore, the smallest resolvable transverse distance of the set up is: spatial resolution at the distance l from the slit, is $b = l \cdot \tan(\theta) \approx l \cdot \frac{\lambda}{d}$. Which in this case results in the smallest resolvable full width at half maximum (FWHM) of the electron beam of about 100 µm in horizontal direction and 140 µm in vertical direction for the green light.

Next, the light is guided on the optical table by three further plain 10 cm×10 cm mirrors M3 - M5 in the direction of the cameras. There are two set-ups available that focus the incoming light into both CCD and fast-gated ICCD. The overview of both optics is shown in Fig. 2. In both cases the final lens is used for additional magnification of the received image. Though for external optics just one main focusing is used. It stays on the optical table and is therefore easy to adjust and remove. In case of internal optics light is getting focused by the lens that is located inside the vacuum chamber between mirrors M1 and M2. This lens can only be moved in one direction: moved in and out of the light path. However its position can't be adjusted. Therefore one more correction

* Work supported by German Bundesministerium für Bildung und Forschung, Land Berlin, and grants of Helmholtz Association
† irma.shmidt@helmholtz-berlin.de

ISBN: 978-3-95450-249-3 ISSN: 2673-5350 doi: 10.18429/JACoW-IBIC2024-WEP15

NON-DESTRUCTIVE BEAM PROFILE MEASUREMENTS WITH AN IONISATION PROFILE MONITOR (IPM) BASED ON TIMEPIX3&4 HYBRID PIXEL DETECTORS (HPDs)

M. McLean*, W. Andreazza, G. Cabrera, C. Fleisig, J. Joul, G. Khatri, C. Pasquino, M. Teresa Ramos, J. Storey, CERN, Geneva, Switzerland

Abstract

Beam Gas Ionisation (BGI) monitors have been operating in the CERN Proton Synchrotron for 3 years now, and they were installed in the CERN Super Proton Synchrotron this year. An overview of the operating principal of the instruments is presented, followed by an update on their development. The mechanical design has been simplified and the Timepix3 devices are now mounted individually for easier assembly and maintenance. Reliability and availability have been improved with a new radiation-hard readout, using the GBTx [1] and bPOL12 [2] devices. Performance has been improved with a SoC Back-End exploiting the capabilities of both the FPGA and the Processing System. We have worked to improve the calibration of the instruments, equalization can now be performed in-situ and we have a procedure to calibrate the response between the four detectors. This paper also presents some example results from the instruments and describes our plans for future developments.

BGI OVERVIEW

A schematic cross section is shown in Figure 1 and an overview of the instrument design is shown in Figure 2 (field cage removed for clarity).

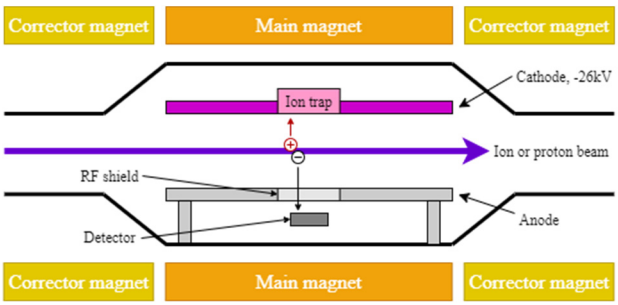

Figure 1:BGI schematic.

Rest gas ionisation electrons are accelerated by an electric drift field towards an electron imaging detector located beneath a radio-frequency shield. A magnetic field parallel to the electric field, formed by a self-compensating 0.2 T dipole magnet, helps to maintain the transverse position of the ionisation electrons during transport to the measurement plane. The electric drift field is formed by a single -26 kV cathode, without side-electrodes. The cathode includes an ion trap that prevents ion induced secondary electrons from re-entering the vacuum chamber and reaching the imaging detector [3]. The instrument is mounted on a rectangular vacuum flange with a ConFLat type seal [4].

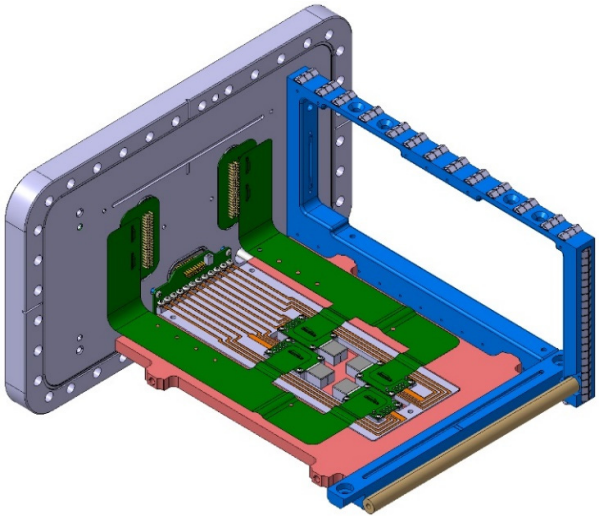

Figure 2: BGI viewed without field cage.

OPERATIONAL EXPERIENCE

During 2023/4 the PS-BGIs were compared with the wire-scanners. Data was collected from LHC-type beams at flat top with both PS-BGIs, without gas injection. An example of the good agreement with the wire-scanner is shown in Figure 3 and, as discussed in [5], the agreement in terms of normalized emittance is within 1 statistical sigma.

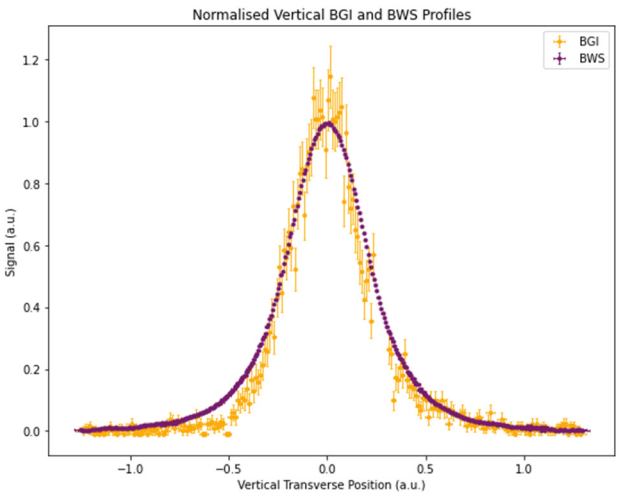

Figure 3: BGI – Wire-scanner comparison.

Despite this success, the operational adoption of the PS-BGIs has been slow, mostly because the instrument remains difficult to use. Outstanding issues include:

- Beam loss saturates the readout chain, causing subsequent profiles to be lost.

ISBN: 978-3-95450-249-3 ISSN: 2673-5350 doi: 10.18429/JACoW-IBIC2024-WEP16

UPGRADE OF THE PHASE SPACE MULTISCREEN OF FERMI LINAC

M. Veronese†, M. Bossi, G. Gaio, G. Penco, R. Sauro, M. Tudor
Elettra Sincrotrone Trieste, Basovizza, Italy

Abstract

The measurement of the longitudinal phase space at the end of FERMI linac is one of the most important characterization of the electron beam properties prior to delivery to the FEL lines. It is performed using an RF-deflecting cavity in conjunction with a dipole to spread the beam in time and energy. The beam transverse distribution is then measured with a multiscreen. The original multiscreen installed in 2009 had a large FOV with a 45deg YAG:Ce orientation and 1.5 MPx camera. An upgrade has been devised to improve resolution, frame rate and robustness to COTR contamination. The upgrade design is based on a COTR suppressing geometry, a dispersion minimizing incidence angle, a double mirror vacuum optical layout and a Scheimpflug camera geometry. The optical distortion has been characterized by using a precision checkerboard target and automatic Matlab nodes detection. This leads to a transformation matrix that is applied at the image server level to the raw image to remove the trapezoidal distortion. The detector is 8 MPx 10 Gbit/s CMOS camera fibre coupled to the image sever and capable of full frame 50 Hz acquisition.

INTRODUCTION

One of the most important measurement for the FERMI FEL and for many other similar accelerators is the phase - space measurement. This obtained by sending the electron beam through a RF-deflector and a bending magnet and detecting the transverse distribution by a screen instrumentation thus providing a two-dimensional map of the longitudinal phase space. In FERMI this particularly important in setting the desired beam peak current and in evaluating the beam phase space distortions that may potentially impact the FEL performances. With operational experience it became evident that an upgrade would be needed to overcome the intrinsic limitations of the original design that were mostly relate to insufficient resolution, depth of field and acquisition rate. The original design used a scintillator at 45 deg with respect to the electron beam with detection axis at 90 deg. As shown in [1], this is not optimal for beam resolution due to the impact of refractive index effects. Additionally, the field of view (FOV) is large compare to screens used for beam optics characterization, leading to a reduced depth of field that de facto compromise the resolving power outside the few millimetres that are in sharp focus. Moreover, the magnification is not constant along the horizontal axis thus causing unaccounted calibration errors outside the central region of the screen. The original camera was Basler ScA1400-30gm providing insufficient number of pixels per millimetre and a frame rate below the 50 Hz of FERMI operation. To overcome these limitations, we decided to implement a COTR suppressing scheme with a Scheimpflug geometry [2], upgrading both the vacuum components and the camera system.

LAYOUT

FERMI is a seeded FEL based on the high gain harmonic generation (HGHG) scheme [3]. Two FEL lines, FEL-1 and FEL-2, are presently installed at the facility. FEL-1 is a single stage seeded FEL generating coherent light in the 65-20 nm wavelength range. FEL-2 is a double stage seeded FEL based on the fresh bunch injection technique [4, 5], where the additional stage extends the spectral range to 20-4 nm. At FERMI the electron bunch is generated at 10 Hz by a photo-injector GUN with energy of 5 MeV. The electrons are accelerated by an S-band linac. The bunch length can be manipulated by means of a magnetic bunch compressor chicane (BC1). The microbunching present in the bunch can be mitigated before BC1 by a laser heater (LH) system. The final energy is up to 1.5 GeV in FEL operative conditions. After the acceleration, the electrons are injected into one of the two FEL lines (either FEL-1 or FEL-2). A layout of the FERMI FEL is shown in Fig. 1.

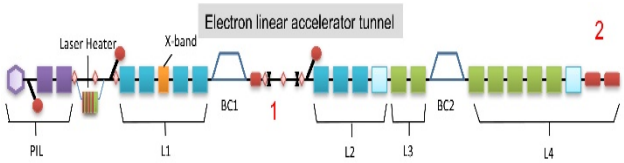

Figure 1: Layout of the FERMI linac.

At the end of the linac, the Diagnostics Beam Dump (DBD) beamline is accessible to perform the phase space measurement before delivering the electron beam to the Undulator Hall. The phase space measurement is done using the High Energy RF-Deflector (HERFD) which deflects the beam in the vertical plane [6], a bending magnet and the MSCR_DBD.01 screen diagnostics.

DESIGN

In the upgrade of this screen station, we had two constraints: maintaining the existing vacuum mechanical infrastructure with pneumatic actuation and limited available space below the beam axis. The general idea is to set the scintillator at the optimal angle and have large horizontal and vertical scintillation area while maintaining COTR suppression. The original vacuum chamber design had a limited vertical aperture. This resulted in a small vertical range usable during the RF phase scans of HERFD that are required for calibration of the device. We upgraded the

† email address: marco.veronese@elettra.eu

ISBN: 978-3-95450-249-3 ISSN: 2673-5350 doi: 10.18429/JACoW-IBIC2024-WEP17

PHYSICAL DESIGN OF AN ONLINE BEAM MONITOR FOR HEAVY-ION SINGLE EVENT EFFECTS

D. Wang†, W. Chen, Z. M. Wang, M.W. Wang, Y. H. Yan, B. C. Wang
National Key Laboratory of Intense Pulsed Radiation Simulation and Effect, Northwest Institute of Nuclear Technology, Xi'an, China

Abstract

Accurate measurement of flux rate is essential in heavy-ion single event effects tests, but it presents significant challenges for monitoring low energy (5~10 MeV/u) and low intensity (less than 1E6 /s) heavy-ion beams. In this paper, we propose a novel detector that enables real-time monitoring of flux rate by simultaneously measuring the beam intensity and profile using secondary electrons on both the front and back surfaces of thin foils. The confinement of secondary electrons through electric and magnetic fields is achieved, with CST simulation has been utilized to validate the method. This approach offers several advantages over conventional methods, including high space and time resolution, reduced mass thickness, and multi-parameter measurement capability.

INTRODUCTION

Single event effects (SEE) of integrated circuits are one of the main threats faced by spacecrafts, and heavy-ion accelerators are commonly used for SEE studies on Earth. As per the European guidelines for SEE tests [1], it is recommended that the heavy-ion flux rate be less than 1E5 /(cm^2·s), which corresponds to a maximum beam intensity of several hundred femtoamperes. Limited by the scale of general accelerators, the energy of heavy ions with higher Linear Energy Transfer (LET) values can typically only reach several MeV/u. Irradiation tests of Device Under Tests (DUTs) with heavy-ion beams are generally conducted in a vacuum environment.

In irradiation experiments, the parameters of greatest concern to users are the flux rate and its uniformity at the irradiation terminal. Therefore, real-time, direct measurement of these key parameters during the irradiation process is essential. However, online monitoring of low-energy heavy-ion beams presents considerable challenges, and commonly used detectors such as parallel ionization chambers, semiconductors, and scintillators are no longer suitable for use as non-destructive beam monitors [2].

Measuring the secondary electrons (SEs) produced by heavy ions penetration through thin foils on their surfaces is a potential solution. Due to the fact that the thickness of the thin foil is significantly smaller than the range of ions, it can serve as a non-interceptive beam monitor, named secondary emission for low-interception monitoring (SLIM). Additionally, employing Microchannel Plates (MCPs) to multiply the SEs enables measurement of low-intensity beams. Previous research on SLIM has primarily focused on utilizing single-sided SEs for profiling, beam intensity measurements, or timing analysis. This type of detector demonstrates excellent time resolution and space resolution [3-8].

PHYSICAL DESIGN

This paper introduces a novel SLIM structure that utilizes SEs emitted from front and back surfaces of the thin foil to simultaneously measure beam intensity and profile distribution, enabling online monitoring of dose rate.

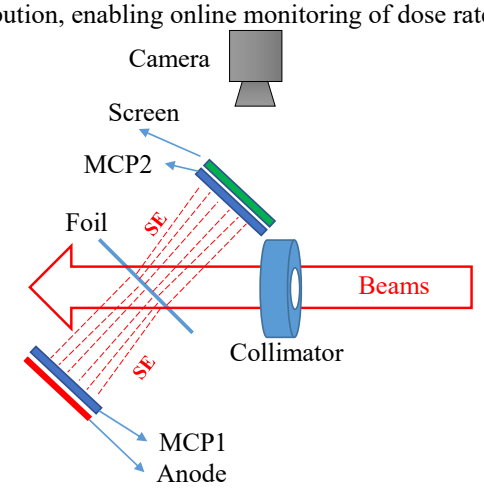

Figure 1: Conceptual illustration of the SLIM.

The thin foil is oriented at a 45° angle relative to the beam axis, with one MCP assembly positioned on each side of the foil surface (Fig. 1). The electric signal from the anode of the forward MCP1 assembly is utilized to measure the beam intensity, whereas the light signal from the fluorescent screen of the backward MCP2 assembly is employed to assess the beam profile. Concurrently, based on the beam intensity and profile distribution, the dose rate and uniformity at various positions can be acquired. H.Rothard have investigated the generation of SEs on both the front and back surfaces of thin foils [9]. The findings indicate that a greater number of SEs are produced in the forward direction compared to the backward direction. Consequently, the measurement of weak current signals should be preferentially set in the forward direction.

The confinement of SEs is a key issue due to their initial emission angle distribution. The traditional SLIM utilizes a wire mesh near the thin foil surface to create an accelerating electric field, enabling accelerated SEs to quickly reach the MCP entrance surface and reduce lateral diffusion. However, this structure has a defect in that approximately 5% to 10% of the particles will be stopped by the wire due to its comparable diameter with the range of low-

† wangdi@nint.ac.cn

ISBN: 978-3-95450-249-3 ISSN: 2673-5350 doi: 10.18429/JACoW-IBIC2024-WEP18

TROUBLESHOOTING THE IONIZATION PROFILE MONITOR (IPM) FOR CSNS 1.6 GeV RCS*

M. A. Rehman†, R. Yang‡, Z. Xu, W. Huang, X. Nie, X. Li, S. Wang
Institute of High Energy Physics, Chinese Academy of Sciences (CAS), Beijing, China
also at China Neutron Spallation Source, Dongguan, China
P. Forck, GSI Helmholtzzentrum fur Schwerionenforschung GmbH, Darmstadt, Germany
J. Sun, Paul Scherrer Institut, Villigen PSI, Switzerland

Abstract

Non-invasive and turn-by-turn beam transverse profile monitoring is essential for the tunning and operating CSNS 1.6 GeV Rapid Cyclic Synchrotron (RCS). A residual gas Ionization Profile Monitor (IPM) was designed and installed in RCS for horizontal beam profile measurement. However, several challenges related to Electromagnetic Interference (EMI), vacuum, and MCP operation in the IPM were identified. The EMI is induced by the beam itself and further accelerator components. An improved Faraday cage was implemented to counteract the EMI issues. In order to achieve the desired MCP gain, a suitable pull-down resistor was incorporated into the MCP power supply circuit. After these improvements, the IPM was commissioned successfully. This paper will describe the challenges of IPM and early beam commissioning results.

INTRODUCTION

The China Spallation Neutron Source (CSNS) [1, 2] is one of the major scientific facilities in China, constructed to deliver intense pulsed neutron beams for diverse scientific research and industrial applications. The CSNS accelerator complex comprises an injector LINAC that accelerates the H^- beam to 80 MeV. Subsequently, the H^- beam undergoes electron stripping through a foil, leaving behind a proton beam that is then injected into a Rapid Cyclic Synchrotron (RCS) to further increase beam energy to 1.6 GeV. The accelerated proton beam is delivered to a solid Tungsten target to produce neutrons. The parameters of RCS are described in Table 1.

Table 1: CSNS RCS Parameters

Parameters	Values	Units
Injection Energy	80	MeV
Ring Circumference	227.92	m
Extraction Energy	1.6	GeV
Repetition Rate	25	Hz
Number of Bunches	2	
f_{rev}	1.02 – 2.44	MHz
Beam Intensity	2.5×10^{13}	ppb

The non-invasive and turn-by-turn monitoring of the beam transverse profile plays a critical role in the tuning and operation of a high-current accelerator, such as the CSNS RCS. For this purpose, a prototype Ionization Profile Monitor (IPM) system has been developed to measure the horizontal beam profile.

The first IPM was proposed and developed in 1966 [3]. In the IPM, the charged particle beam interacts with the residual gas components in the vacuum duct, leading to the production of secondary ions/electrons. These secondary particles have the same spatial distribution as the primary beam. An external electric field is used to collect the ions/electrons products. Due to the low yield of the secondary particles, an additional detector is necessary. Typically, a Micro Channel Plate (MCP) is used as a pre-amplifier, offering a signal amplification of 10^4–10^7. A simplified illustration of the IPM principle is shown in Fig. 1 (a).

In Fig. 1 (b), the 3D model of the RCS's IPM is displayed. The field cage of the IPM comprises 14 electrodes with an aperture of 220 mm × 231 mm. The MCP [4] is a double-stage with a gain of 10^6 and consists of 32-strip anode strips, each with a width of 2.4 mm and a mutual spacing of 0.1 mm. The effective area of the MCP is 81 mm × 31 mm.

The readout cables from the MCP are first connected to the Common Mode Choke (CMC) and then connected to the 32-channel digitizer (NI, PXIe-5172). The digitizer has a bandwidth of 100 MHz and a sampling rate of 250 MSa/s. The input impedance of each channel on the digitizer is 50 Ω.

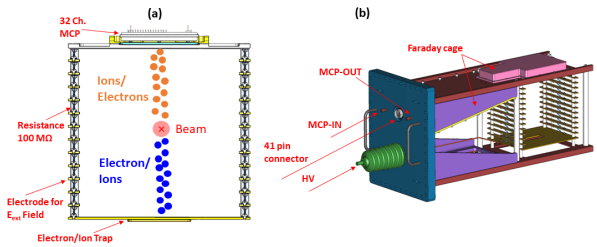

Figure 1: (a) The principle of the IPM. (b) The 3D model of the RCS IPM. The front flange consists of several feedthroughs to apply high voltage to the field cage, MCP and readout signal from the MCP. The MCP and readout cables are enclosed in the Faraday cage.

* Work supported by National Science Foundation for Young Scientists of China (12305166).

† rehman@ihep.ac.cn
‡ yangrenjun@ihep.ac.cn

ISBN: 978-3-95450-249-3 ISSN: 2673-5350 doi: 10.18429/JACoW-IBIC2024-WEP20

THE PROJECT OF OPTICAL DIAGNOSTICS OF THE BEAM DIMENSIONS OF THE SKIF STORAGE RING WITH ULTRA-LOW EMITTANCE*

V. L. Dorokhov†, [1], O. I. Meshkov[2], V.E. Boyarkina[1, 2]
Budker Institute of Nuclear Physics, SB RAS, Novosibirsk, Russian Federation
[1]also at Synchrotron Radiation Facility - Siberian Circular Photon Source "SKIF",
Boreskov Institute of Catalysis of SB RAS, Kol'tsovo, Russian Federation
[2]also at Novosibirsk State University, Novosibirsk, Russian Federation

Abstract

The Siberian Circular Photon Source (SKIF), a fourth-generation synchrotron radiation (SR) source is being constructed in Russia. This installation has an ultra-low emittance, allowing for high beam intensity in various scientific and technological fields. A crucial aspect of SKIF is its availability of diagnostic instruments that measure the beam transverse dimensions. This will allow for minimizing the emittance during operation and comparing it with a calculated value. This comparison is critical for determining whether the physical setup meets the design specifications. In addition to measuring the transverse dimensions of the beam, it is also important to observe the behaviour of the longitudinal profile and measure its parameters with good accuracy. Since the calculated emittance of 75 pm · mrad corresponds to the beam sizes of less than 8 µm at the radiation output sites, a diagnostic complex was developed as a part of the working project, including a beam size monitor based on a double-slit interferometer. Observation and measurement of the longitudinal distribution of the beam will be carried out using mutually complementary devices, such as a streak camera and electron-optical dissector.

INTRODUCTION

The emerging Synchrotron Radiation Facility - Siberian Circular Photon Source "SKIF" is a large accelerator complex. It contains a linear accelerator with an energy of 200 MeV, a booster synchrotron with a ring circumference of 158.7 m, a storage ring with a circumference of 476.14 m with 16 straight intervals and two transport channels: from linear accelerator to the booster and from booster to the storage ring (see Fig. 1).

The working energy of the SKIF main storage ring is 3 GeV. In this acceleration machine, the synchrotron radiation (SR) from bending magnets and "insertion devices" - wigglers and undulators (which will be placed in straight-line intervals) will be generated.

In the common operating mode, there 500 electron bunches with a total current of 400 mA circulate in the main storage ring. For this purpose, injection is performed by 55 bunches with a charge of about 0.3 nC in each.

Table 1: Main ring specifications

Parameter	Unit	Value
General machine parameters		
Energy	GeV	3.0
Circumference	m	476.14
Current	mA	400
Rev. freq	MHz	0.6296
Rev. time	mks	1.588
ϵ_x	pm rad	75
σ_E/E		0.001
RF freq	MHz	357
Bunch length parameters		
U_{RF}	MV	0.77
U_0	keV	536
f_s	kHz	1.13
α		$7.6 \cdot 10^{-5}$
$\sigma_t(RMS)$	ps	17.5 (5.3 mm)

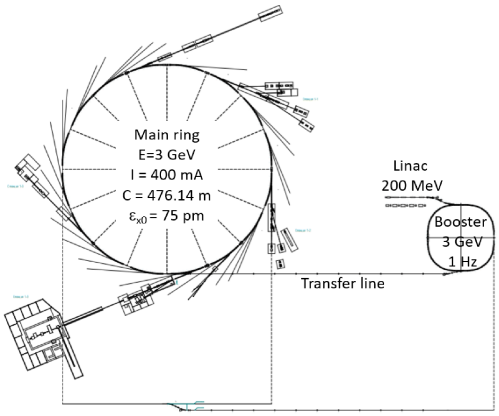

Figure 1: The common scheme of the Synchrotron Radiation Facility SKIF.

In addition, modes with one or several bunches distributed as required along the orbit are provided. That is why, control of the modulator of the injection complex gun allows obtaining one or several bunches in a train (within the envelope of 310 ns). In this case, the bunch intensity can be increased to

* work was supported by the Ministry of Science and Higher Education of the Russian Federation within the governmental order for SRF SKIF Boreskov Institute of Catalysis (project FWUR-2024-0041).
† V.L.Dorokhov@inp.nsk.su

ISBN: 978-3-95450-249-3 ISSN: 2673-5350 doi: 10.18429/JACoW-IBIC2024-WEP23

HALO MONITOR FOR HIGH-INTENSITY HADRON BEAMS BASED ON SUPERSONIC GAS CURTAIN

H. Zhang *, W. Butcher, N. Kumar, F. Mada-Parambil, M. Patel, O. Sedlacek, S. Sethi, O. Stringer, C. Welsch, University of Liverpool / Cockcroft Institute, Daresbury, Warrington, UK

Abstract

In this contribution, a supersonic gas curtain-based profile monitor is considered for beam halo measurement in high-intensity, high-power hadron accelerators. This monitor is based on the beam gas curtain (BGC), successfully used in the Large Hadron Collider. Instead of a broad curtain with uniform density, a new concept with two shorter curtain segments that can be adapted to the shape of the beam core and aimed at only the halo particles is applied. The design and operation principle of the monitor will be presented, and the anticipated integration time, signal intensity, and dynamic range will be discussed, as well as opportunities to increase the sensitivity by incorporating microchannel plates or the Timepix detector.

INTRODUCTION

Although there is no clear definition of beam halo in particle accelerators [1], it is generally regarded as particles outside of the beam core with an intensity level lower than 10^{-4} or 10^{-6} of the peaks. In high-intensity, high-power hadron accelerators, halo particles may cause emittance growth and beam loss, difficulties in beam control and collimation, increase the noise of detectors and cause activation or even damage to accelerator components.

There are many theories and simulations for the formation of halos in the accelerator due to collective effects and space charge. To test these, experimental studies are essential. Due to the presence of the beam core, halo detection requires a dynamic range at least higher than 10^4 which is very challenging and few methods can meet the required high dynamic range. In the past, there have been several efforts towards the detection of the beam halo. Allen [2] used a combination of wire scanner and scrapper for the Low Energy Demonstration Accelerator (LEDA) which showed a dynamic range of 10^4. Others used imaging techniques, such as charged injection device [3], coronagraphy [4] and adaptive masking [5] that showed a higher dynamics range of more than 10^4, but these results need further investigation and their applications to major facilities are still lacking.

In this study, a gas curtain based halo monitor is considered. The monitor will detect the signal from the interaction of the halo particles and the gas molecule. To maintain a good vacuum condition, control the gas flow in a designed way and increase the local gas density, a supersonic gas curtain will be introduced. A similar gas curtain system has been successfully installed in the LHC [6] to detect the beam profile using the fluorescence generated from the interaction between the gas molecule and the charged particle beam. To detect the beam halo, the fluorescence process no longer provides an adequate signal level and thus a higher cross-section process, such as impact ionisation will be chosen. We will discuss the principle of detection, the generation of gas curtains, the current experimental study using a laboratory electron source and a possible solution for beam halo detection for the LHC as an example.

* haozhang@liverpool.ac.uk

GAS CURTAIN GENERATION FOR HALO DETECTION

Similar to the gas curtain used for the beam profile monitor [7], the supersonic molecular beam will be generated through a nozzle-skimmer system. A test setup was shown as Fig. 1. High-pressure gas flows through a 30 µm nozzle to the low-pressure nozzle chamber to form a supersonic gas jet. Two consecutive skimmers collimate the jet to form a molecular beam while creating differential pumping stages to maintain the background pressure at a low level. The first skimmer is a conical shape with 400 µm diameter. The second skimmer is a metal plate with a round hole opening. The radius was chosen as 2 mm and can be replaced with a larger size to generate broader beams. These two skimmers separate the vacuum vessel into a nozzle chamber, skimmer I chamber and skimmer II chamber. All chambers are pumped by separate sets of pumps. The number density of the molecular beam will drop gradually after the first skimmer because of a geometric expansion. A third skimmer was used to generate the gas curtain of a specific shape for diagnostic purposes. The shape can be very flexible. For example, for the beam profile monitoring, the third skimmer will be a 45° titled slit and the curtain will be similar to a screen which allows for 2D profile measurement. As for the halo detection, the interaction of the beam core with the gas curtain is avoided by generating two segments of curtains and leaving the molecular beam blank in the centre as shown in the enlarged area in Fig. 1. A metal plate with two segments of the slits is introduced for the 3rd skimmer as shown in Fig. 2. For test purposes, the gap was set as 4 mm and each slit has a geometry of 0.4 mm × 10 mm.

To estimate the density distribution of the gas curtain generated for halo detection, simulation and experimental study were performed and the results are shown in Fig. 3. To simplify the measurement, the 3rd skimmer was installed with both slits orientated 90°. The simulation is based on the quitting surface model for the transition from the continuum flow to molecular flow. The gas jet parameters in the continuum flow can be calculated directly according to the mass and energy conservation law. The particle ray tracing can be used to simulate the molecular flow part. The ex-

ISBN: 978-3-95450-249-3 ISSN: 2673-5350 doi: 10.18429/JACoW-IBIC2024-WEP24

NEW WIRE SCANNER AT SXFEL*

F. Z. Chen†, J. Chen, J. Chen, J. Dong
Shanghai Advanced Research Institute, Chinese Academy of Sciences, Shanghai, China

Abstract

In the past year, the wire scanner at SXFEL is upgraded to a new firmware. Unlike the previous version, where a target frame is equipped with tungsten wires in three directions, the new system uses horizontal and vertical independent scanning methods. The beam loss detector adopts plastic scintillator fibre, and the PMT module is also designed with a Raspberry PI for dynamic signal conditioning. The detailed design is described in this paper.

BACKGROUD

As a kind of quasi-non-destructive beam size monitoring, wire scanners are widely used in linear accelerators all over the world [1]. The measurement principle is based on the secondary particles produced by the interaction between the wire and the beam, and the concentration of the secondary particles reaching the downstream (mainly including high-energy electrons, gamma-rays and other charged and uncharged particles and various rays) is proportional to the area of the electron beam and tungsten wire [2]. Therefore, the energy deposition of secondary particles sensed by the beam loss detector placed in the downstream of the vacuum pipe is positively correlated with the size of the fibre after being detected and amplified by the photomultiplier. Thus, the beam size measurement can be fitted by precisely controlling and measuring the moving position of the wire target and the secondary particle energy deposition induced by the corresponding beam loss detector. In addition to being used for accurate beam size measurements, one or more of these detectors can also be used for off or on-line emittance measurements and energy dispersion measurements [3].

To meet the needs of SHINE for beam size measurement with high repetition, the beam instrumentation group of Shanghai Synchrotron Radiation Facility (SSRF) conducted investigation and evaluation of major domestic and foreign accelerator devices and selected a wire scanning scheme to build a beam size measurement system. This paper mainly discussing the pick-up scheme of beam loss signal generated by the interaction of 20 μm tungsten wire. Plastic scintillation fibre is selected as the detector of beam loss signal, and PMTs with signal conditioning circuit are used to capture optical signal. At present, this set of scintillation fibre-based beam loss detection unit has been installed in the Shanghai Soft X-ray free electron laser device and the Shanghai Synchrotron Radiation Facility's storage ring. Combined with the wire scanning mechanical execution structure and the storage ring beam scrapper, there have been completed several beam experiments. The preliminary test results show that the scintillation fibre probe is sensitive to the beam loss signal of the wire scanner and can capture the beam loss signal of the whole process of wire scanning. The subsequent experiments will improve the resolution of beam loss signal amplitude extraction by optimizing the signal conditioning module.

In this paper, the hardware and software structure of the scintillation fiber-based beam loss detection module of SSRF and the beam current test results are introduced.

SYSTEM ARCHITECTURE

The hardware structure of wire scanning system is mainly composed of wire scanning mechanical actuator, beam loss detection module and data acquisition module. Among them, the output signal of the beam loss probe is directly responsive to the actual beam loss in the pipeline.

Mechanical Execution Structure

The strategy is utilizing the wire target jitter, it will introduce the system error to the beam size. Under investigation, we adopted the separating method to realize the measurement. The wire scanner has developed to a new structure of horizontal and vertical separation (see Fig. 1).

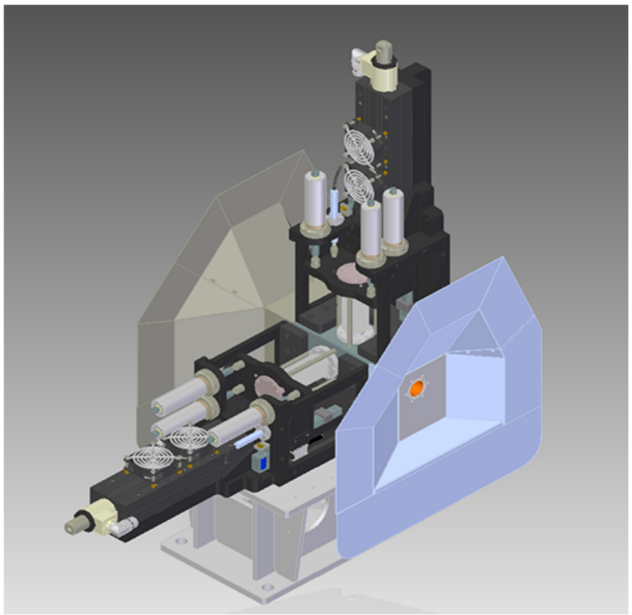

Figure 1: 3D drawing of mechanical execution structure.

- Magnetic shield: Along the beam direction, there are two trumpet type magnetic shield to avoid magnetic interference of the linear motor.
- Magnetic spring: To get more room to travel, the new structure acquires single-ended compression mode. That would be against a lot of atmospheric pressure, so the magnetic spring has been adopted to balance the atmospheric pressure.

* Work supported by NSFC(Grant No.12105346)
† email address: chenfz@sari.ac.cn

ISBN: 978-3-95450-249-3 ISSN: 2673-5350 doi: 10.18429/JACoW-IBIC2024-WEP25

ACCURATE BEAM SPOT FITTING ALGORITHM USING GENERALIZED AND SKEWED GAUSSIAN TYPE DISTRIBUTIONS*

Dongyu Wang, Mingdong Ma, Chuhan Wang, An Wang, Jinkai Lan, Ruizhe Wu, Zhengyu Wei, Xiaochao Ma, Ping Lu, Anxing Wang, Baogen Sun, Leilei Tang†
National Synchrotron Radiation Laboratory,
University of Science and Technology of China Hefei, China

Abstract

To address non-standard Gaussian beam spot profiles in injectors, this paper proposes a fitting algorithm based on Gaussian, the newly introduced Generalized Gaussian Type and Skewed Gaussian Type distributions. These distributions are specifically designed to better fit non-Gaussian and asymmetric beam spots by automatically selecting the most suitable model. Validation using beam spot images from the YAG screen after the electron gun in the Hefei Light Source II (HLS-II) injector demonstrates that the Generalized Gaussian Type is effective for fitting sharp or broad profiles, while the Skewed Gaussian Type is well-suited for handling asymmetry. Compared to traditional methods, the proposed algorithm improves fitting accuracy and adaptability, providing a practical solution for complex beam measurement challenges.

INTRODUCTION

Traditional transverse beam size measurement methods often rely on symmetric Gaussian fitting, which is adequate for many conditions. However, in practical applications, especially in linear accelerators (LINACs) based injectors, beam spots typically show non-Gaussian distributions [1], including asymmetry, skewness, or multiple peaks. These non-Gaussian features limit the effectiveness of traditional Gaussian fitting, making it insufficient for accurate transverse beam distribution measurements.

To overcome these limitations, this paper proposes an improved fitting algorithm that introduces the newly Generalized Gaussian Type and Skewed Gaussian Type distributions to more accurately fit the transverse beam spot shapes. Compared to traditional Gaussian fitting, these models can flexibly adjust symmetry, peak position, width, and skewness, offering higher fitting accuracy and better adaptability to complex beam spot shapes. The goal of this study is to determine the optimal fitting method by comparing the performance of different algorithms, thereby improving the accuracy of beam size measurements in LINACs-driven injectors of synchrotron radiation source [2].

FITTING THEORY

To accurately measure and describe the transverse beam size in synchrotron radiation sources, the fitting algorithm must be capable of flexibly handling various complex beam spot shapes. The improved algorithm proposed in this paper is based on three fitting models: the traditional Gaussian distribution, and the newly introduced Generalized Gaussian Type and Skewed Gaussian Type distributions, both of which were developed in this study. The following sections provide a detailed introduction to these three fitting models and their theoretical foundations.

Gaussian Distribution

The probability density function of the Gaussian distribution is given by:

$$f(x; a, x_0, \sigma) = a \cdot exp\left(-\frac{(x - x_0)^2}{2\sigma^2}\right), \qquad (1)$$

where a is the amplitude, representing the peak height; x_0 is the center position, indicating the peak location of the beam spot; and σ is the standard deviation, corresponding to the beam spot size. A schematic of the Gaussian distribution is shown in Fig. 1, illustrating the symmetry of the distribution and the range of the standard deviation. The standard deviation σ determines the width of the curve, reflecting the size of the transverse beam.

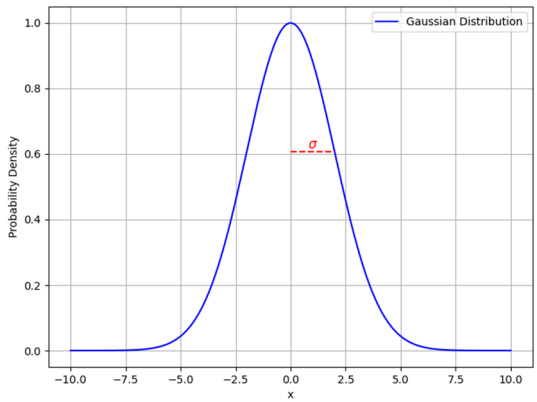

Figure 1: Schematic of the Gaussian distribution.

The Gaussian distribution assumes that the beam spot is symmetric and unimodal, which is reasonable in many cases. However, when the beam spot exhibits asymmetry, skewness, or multiple peaks, Gaussian fitting often fails to accurately represent the actual shape of the beam spot.

Generalized Gaussian Type Distribution

To better accommodate the diverse shapes of beam spots, this study introduces a distribution similar to the Generalized Gaussian, called the Generalized Gaussian

* Supported by the National Science Foundation of China (11805204, 12075236) and the Hefei Advanced Light Facility Project.
† Corresponding author (email: tanglei@ustc.edu.cn).

ISBN: 978-3-95450-249-3 ISSN: 2673-5350 doi: 10.18429/JACoW-IBIC2024-WEP28

EXPERIENCE WITH PSI'S MAIN RING CYCLOTRON LONG RADIAL PROBE

M. Sapinski*, S. Lindner, R. Martinie, M. Rohrer
Paul Scherrer Institut, Villigen, Switzerland

Abstract

A Long Radial Probe is a device used to measure the transverse beam profile in a cyclotron along its radius. The current iteration of the probe was installed in the PSI Main Ring Cyclotron in 2022. After a successful start, the probe encountered issues due to strong coupling with RF fields leaking from the cavities, which resulted in the breakage of the carbon fibers. A series of corrective measures were attempted, but the initial results were inconclusive. This paper discusses the challenges faced and presents the experiments and thermal calculations that provided insights into the RF heating issue.

INTRODUCTION

A new Long Radial Probe (RRL) was installed in PSI Main Ring Cyclotron in 2022. Its initially successful commissioning is described in [1] (see also references therein). The probe demonstrated its usefulness in measuring beam profiles across the entire beam current range, from single A up to 1.8 mA. However, after a few months of operation, several issues remained, including:

- Thermionic emission was observed and only partially suppressed, as described in [2].
- Activation hot spot has been found on the RRL structure and investigated, as described [3]. As a countermeasure the entire RRL structure has been motorized and is removed from the machine when not in used.
- A frequent generation of interlocks due to proximity of electrostatic injection septum has been observed and this issue is still under investigation.

None of the aforementioned problems have prevent the RRL from obtaining useful data on beam profiles. However, already in August 2022, the wires began to break even at low beam currents. The problem worsened during the remaining months of 2022 and persisted during the operation in 2023. The newly installed wires were damaged solely by RF fields, without the presence of a beam. We focused on investigating this critical issue and those efforts are described here.

MOVING SUPPORT DESIGN

The three wires used to measure the profile of the beam are attached to two trolleys, upper and lower one, driven by the same motor which moves two transmission belts synchronously. The two trolleys, shown in Fig. 1, can be installed and removed as a complete unit using an auxiliary device. Only the two electrical plugs, carrying the probe signals, need to be disconnected. Aluminium covers, protecting the cables from the RF fields, are not shown in Fig. 1, but can be partly seen in Fig. 2.

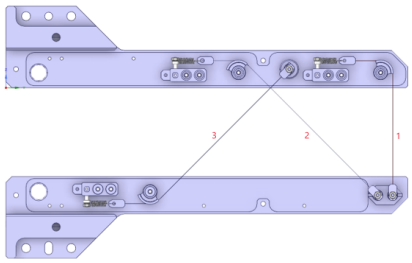

Figure 1: Layout of the RRL trolleys with covers removed.

The wires are made of 33 µm carbon fibers, which are glued to small pads made of beryllium copper (CuBe) alloy, using conductive adhesive as shown in Fig. 3. One pad is directly connected to a metallic pin that transmits the signal to the readout cable. The other pad is attached to a spring to accommodate variations in the movement of the two trolleys. In order to accommodate spring length the wires are bend 45° or 90° using deflection rollers.

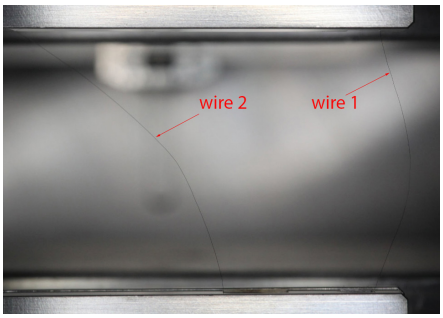

Figure 2: Typical view of damaged RRL wires obtained using Sigma 105 mm macro lens on full frame camera.

The numbering of the wires is from the right to left (see Fig. 1), i.e. the vertical wire is called *wire 1* and the two tilted wires are called *wire 2* and *wire 3*.

WIRE FAILURE

The glowing of the wire due to high temperatures induced by coupling to the RF field has been described in [1]. However, during the scans without the beam, no thermionic current was observed, indicating that the wire's temperature must have been below approximately 1700 °C - the threshold at which thermionic current should be observable with the LogIV4x4 current acquisition module, which has sensitivity

* mariusz.sapinski@psi.ch

ISBN: 978-3-95450-249-3 ISSN: 2673-5350 doi: 10.18429/JACoW-IBIC2024-WEP29

THE LARGE HADRON COLLIDER'S BEAM WIRE SCANNER CONSOLIDATION

J. Emery*, W Andreazza, D. Belohrad, N. El-Kassem, A. N. Goldblatt, A. Guerrero, M. Hamani, S. Jensen, L. Limonet, L. Littoz, C. Pasquino, M. T. Ramos Garcia, F. Roncarolo, H. Sullivan, J. Tassan-Viol, V. Varadan, R. Veness, CERN, Geneva, Switzerland

Abstract

To serve the needs of the High Luminosity Large Hadron Collider (HL-LHC) era, a consolidation of the beam wire scanner has been initiated. The instrument is a crucial tool for measuring the transverse beam profile by moving a thin carbon wire across the beam. It can only withstand a fraction of the LHC's nominal beam intensity but provides a reference to calibrate other instruments that operate non-invasively at higher beam intensities. Since the start of the LHC, the scanners have provided hundreds of thousands of measurements, but the design has technical limitations that need to be addressed to provide the required reliability and performance for the HL-LHC runs. The initial consolidation phase involved testing the injector's acquisition and control electronics in the LHC to assess its suitability for the specific beam conditions. As part of this process, we updated the mechatronic and motion controller. Beam test campaign has revealed higher performance w.r.t the existing system and a higher adaptability to varying beam conditions. Simultaneously, we are developing a novel actuator that uses a permanent magnets-based coupling replacing the standard bellows and long arm that limits the performance and induces vibrations. Before testing this new concept with beam, we have developed a calibration bench to evaluate the mechanism's precision and accuracy of the wire position determination. This contribution presents the 2023 beam and laboratory tests as well as the electromechanical developments.

LHC WIRE-SCANNERS

From the beginning of the Large Hadron Collider (LHC), eight wire scanners systems (BWS) with linear motion are in operation to characterize a fraction of the total beam intensity. These scanners provide reference measurements for machine developments and calibrate non-invasive instruments suitable at all beam intensities [1]. So far, these systems have accumulated more than 225k measurements, providing reliable data for over 15 years [2–5]. Driven by a mechanism originally designed for LEP [6, 7] visible on Fig. 1, the carbon wire is accelerated up to a velocity of 1 m/s through the beam. A scintillator followed by inter-changeable neutral density filters and a photo-multiplier evaluates the intensity of the secondary particles generated by the beam-wire interaction.

The linear motion was chosen over the rotary type due to higher precision in the carbon wire position determination and higher data points per beam sigma due to lower velocity. This velocity is safe to characterize beams with $2.7 \cdot 10^{13}$ protons at 450 GeV and $1.5 \cdot 10^{12}$ at 6.8 TeV [8]. These levels are sufficient for operational purposes and to cross-calibrate other instruments [9, 10].

After a few years of operation, early failures of some key electronic components were observed [11], leading to system unavailability until parts were replaced. These limitations were addressed with the electronics dedicated to a rotary system for the LHC injectors [12], under development at that time. The improved electronics, developed as part of the LHC injector upgrade [13], has been in operation since 2021, providing higher reliability and performance compared to previous generations [14]. More recently, the mechanism of the LHC BWS has shown reliability limitations during intensive operation, causing failures (e.g. vacuum leaks) and machine downtime.

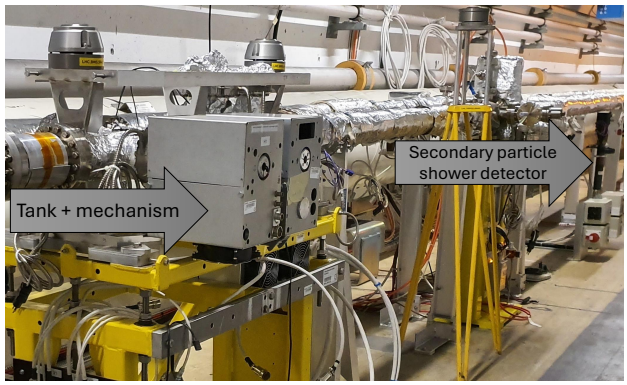

Figure 1: Beam wire-scanners on LHC Beam 1 line.

CONSOLIDATION

The consolidation aims to prepare the BWS for the HL-LHC with enhanced overall reliability and performance and to be ready for higher beam intensities and smaller beam sizes. Through this renovation, we also aim to prepare the wire scanner for future upgrades. R&D (not covered here) includes the study of low-density materials and smaller cross-sections [15]. By achieving the consolidation objectives, we will significantly reduce instrument downtime while enhancing accuracy and precision. These improvements will ensure compatibility with HL-LHC beams [16]. Table 1 summarizes key parameters of the operational system in place today (column OP), the intermediate system equipped with the consolidated electronics (column LIU), and the fully consolidated system (column HL).

* jonathan.emery@cern.ch

ISBN: 978-3-95450-249-3 ISSN: 2673-5350 doi: 10.18429/JACoW-IBIC2024-WEP30

DETAILED BENCH INVESTIGATIONS AND COMPARISON OF FOUR LOW-LIGHT CAMERAS

L. Bauer*[1], P. Forck[1], S. Udrea
GSI Helmholtzzentrum für Schwerionenforschung GmbH, Darmstadt, Germany
[1]also at Goethe-Universität, Frankfurt am Main, Germany

Abstract

We compared four low-light cameras based on different principles: an Image Intensifier equipped with a double MCP and relay-coupled to an off-the-shelf CMOS camera, an electron-multiplied CCD, and two different sCMOS cameras. LEDs generate light pulses with wavelengths in the range of 385 to 500 nm and a duration of 0.05 to 8 ms to vary the fluence at the camera sensors. Moreover, the spatial resolution is compared. Depending on the wavelength, the Image Intensifier and EMCCD have comparable sensitivity for pulse duration larger than 0.5 ms. However, the spatial resolution of the EMCCD is higher. The sCMOS cameras provide a factor of 5 to 10 lower sensitivity.

INTRODUCTION

Low-light cameras are frequently deployed in beam instrumentation for cases such as low beam current, small beam-induced photon yield or low detection probability. Examples are profile determinations by Beam Induced Fluorescence (BIF) monitors as used at GSI and CERN [1–4], scintillation screens for low beam currents or Optical Transition Radiation (OTR) for low beam velocities [5–7]. In several of the cited applications, cameras with attached Image Intensifiers (hereafter called ICCD) are used. The intensifiers comprise a photo-cathode, a Micro-Channel Plate (MCP) for photo-electron amplification and a phosphor screen. As an alternative, an electron-multiplication CCD camera (EMCCD) was tested, see, e.g. [8, 9]. The working principle of such cameras is based on a CCD sensor and the amplification of the low amount of photo-electrons by a chain of avalanche diodes.

Direct comparisons of low-light cameras for the typical parameters in beam instrumentation are rarely reported, with the exception of Ref. [10]. In the actual contribution, we compare an Image Intensifier and an EMCCD camera operational at GSI to the recently available sensitive scientific CMOS camera type from two manufacturers. Those sCMOS cameras are operated without any electron multiplication stage; instead, the analogue stages and ADC conversion are optimized for low noise. A dedicated test bench was realized to determine the photon sensitivity and any noise contributions under reproducible low-light test conditions. As a light source we used pulsed LEDs to vary the fluence independently of the background, and simulate the beam properties at pulsed ion Linacs or transfer between synchrotrons.

* l.bauer@physik.uni-frankfurt.de

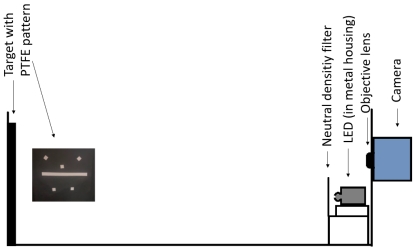

Figure 1: Schematic of the inside of the dark enclosure.

LIGHT SOURCE CHARACTERIZATION

Pulsed LEDs with nominal wavelengths in the range from 385 to 500 nm were used as light sources. Each LED was characterized by an optical spectrometer and photodiode timing measurements. It is ensured that each LED has its emission peak at a wavelength within the expected tolerances, emits in a reasonably narrow wavelength range of 4 to 13 nm (one standard deviation), and that the light pulses follow the electrical driving pulses. The individual LED characteristics are compiled in [11].

The measurements for characterizing the cameras were performed with light pulses between 0.5 and 8 ms. For the ICCD, additional measurements with a light pulse of 0.05 ms were performed. The leading edges of each light pulse was set to 0.1 µs and its trailing edge to 1 µs.

EXPERIMENTAL SET-UP AND CAMERAS

The experimental set-up for camera characterization contains in addition to the light source, a dark enclosure, a function generator (AFG 3102, Tektronix), an oscilloscope (DPO 3034, Tektronix) and a laptop to run the respective camera control software. The cameras are mounted at a wall of the dark enclosure with only the objective lens inside it. The same objective lens (FL-CC1614-2M, RICOH) with a focal length of 16 mm was used for all cameras.

Inside the dark enclosure, at a distance of 87 ± 0.5 cm to the objective lens, a target containing a pattern made of porous, sintered PTFE (PMR10, Thorlabs) is mounted. As shown in Fig. 1, the LED is installed in a dedicated housing and placed below the objective lens in front of a neutral density filter (UVFS Reflective ND Filter, Thorlabs). All non-reflective surfaces inside the dark enclosure are coated with blackened aluminium foil (BKF12, Thorlabs), with a reflectance below 5 % in the relevant wavelength range.

The ProEM:+512B (Teledyne Princeton Instruments [12]) EMCCD camera was used with different electron multiplication gains in the full frame mode. In this contribution,

ISBN: 978-3-95450-249-3 ISSN: 2673-5350 doi: 10.18429/JACoW-IBIC2024-WEP31

BEAM DIAGNOSTIC BEAMLINES AT HEPS STORAGE RING

Dechong Zhu†,1, Wan Zhang, Minxian Li, Shu Yang, Yanfeng Sui[1], Junhui Yue[1], Jianshe Cao[1]
Institute of High Energy Physics, Chinese Academy of Sciences, Beijing, China
[1]also at University of Chinese Academy of Sciences, Beijing, China

Abstract

High Energy Photon Source (HEPS) is a 6 GeV diffraction limited storage ring light source. An ultralow emittance of ~34 pm·rad is designed with a multiple-bend achromat lattice at storage ring. The transverse beam sizes at the dipoles will be less than 10 μm. In order to measure such small beam sizes in both directions, an X-ray beam diagnostic beamline is designed with bending magnet as source point. X-ray pinhole imaging and KB mirror imaging are used compatibly and comparably to capture beam image. A visible light beam diagnostic beamline is designed to measure bunch length with streak camera. During the first phase storage ring commissioning time, both diagnostic beamlines captured the first light.

INTRODUCTION

HEPS will be a 6 GeV diffraction limited storage ring [1] and have an emittance of ~34 pm·rad. Bending angle per dipole is designed small enough to achieve such small emittance. In such case, synchrotron light will travel a long distance before its vacuum pipe can reach a sufficient distance from the beam pipe, which makes beam transverse profile imaging more difficult because the installation space for the first measurement device is limited.

In this article, two beam diagnostic beamlines will be introduced to measure transverse beam sizes and longitudinal bunch length respectively. Both beamlines use the first dipoles after the straight sections as its source points, which sections located at the sectors of injection or RF to avoid taking up ID beamlines. X-ray diagnostic beamline (XBL) is dedicated to capturing beam image and measuring beam sizes using X-ray pinhole and KB mirror imaging. Streak camera (SC) is used at visible light diagnostic beamline (VBL) for bunch length measurement.

X RAY DIAGNOSTIC BEAMLINE

XBL is located at R39 where is the RF region. The source point is in the first dipole (BLG1), 1 mrad angle relative to the straight section extension line to avoid edge radiation of dipole. This small angle also allows the beamline to be led out through the reserved holes in the sawtooth wall to the hutch outside the tunnel. Table 1 lists some designed parameters of the source point. At this source point, β_y is higher about 24.3 m while β_x is 1.3 m, which makes the vertical size larger and relatively easier to measure. This point has almost no dispersion, so the contribution to the horizontal beam size comes mainly from beam emittance.

Table 1: Theoretical Parameters of the Source Point

Parameters	Value
Energy	6 GeV
Beam current	200 mA
Bending radius	41.4 m
Horizontal Emittance	34.2 pm·rad
Emittance Coupling	10%
Beta function β_x	1.3 m
Beta function β_y	24.3 m
Horizontal beam size	6.7 μm
Vertical beam size	9.1 μm

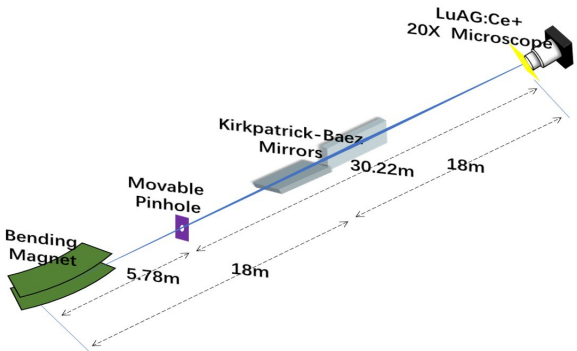

Figure 1: Schematic diagram of X ray diagnostic beamline.

As shown in Fig. 1, pinhole and KB mirrors share the same source point and also the same X-ray camera, and they are both movable by remote control. Pinhole is placed in the atmosphere at 5.78 m from the source and 30.22 m to the scintillator of X-ray camera with the magnification of ~ 5.22. There is a 1mm thick aluminum window and a copper attenuator in front of the pinhole. Pinhole assembly is made of precision machined tungsten sheets laminated together and contains slits of 20 μm, 50 μm and 400 μm both horizontally and vertically. The Pinhole assembly is mounted onto motorized stages, allowing to exchange the optical systems and to align the optics with respect to the beam axis in four degrees of freedom: two linear translations perpendicular to the beam axis, a goniometer rotation around the horizontal axis, and a rotation around the vertical axis.

It is a balance between geometric blurring and the diffraction limit. The optimum aperture that minimize the PSF can be obtained by making the two values equal. A more accurate model to calculate the PSF from the pinhole is to compute the illumination on a screen through the pinhole from a source point using the Fresnel diffraction approximation [2]. When using 20×20 μm^2 pinhole for

†zhudc@ihep.ac.cn

ISBN: 978-3-95450-249-3 ISSN: 2673-5350 doi: 10.18429/JACoW-IBIC2024-WEP32

LONG-TERM PERFORMANCE OF THE EXTENDED PULSED OPTICAL TIMING SYSTEM

F. Rossi*, P. Cinquegrana, Elettra Sincrotrone Trieste S.C.p.A., Trieste, Italy

Abstract

The optical timing system of the FERMI facility underwent a significant upgrade to accommodate requests for additional pulsed links for remote lasers or diagnostic stations. Following the successful completion of compliance tests, the long-term performance of the extended system has been evaluated through out-of-loop measurements. In the setup each of the two pulsed subsystems, synchronized to the common optical master oscillator, feeds a stabilized fiber optic link. The relative stability between the outputs has been monitored at a remote location. The results achieved and the challenges encountered during the measurements will be discussed.

INTRODUCTION

FERMI is a fourth generation light source, a seeded Free Electron Laser (FEL), operating as a user facility in Trieste, Italy. A significant milestone has been recently achieved with the successful implementation of the echo-enabled harmonic generation (EEHG) scheme in the FEL-1 line [1].

An advanced all-optical timing and synchronization system [2] is implemented as a hybrid architecture, combining pulsed and continuous wave techniques, to provide with femtosecond precision the reference for the synchronization of critical subsystems.

We implemented an upgrade [3] to the original system to fulfil the installation requests of additional pulsed clients. There are currently six stabilized links connected to the system but in the near future the number will be increased. The first link connected to the extension will feed a new Bunch Arrival Monitor station for the FEL2 line.

THE EXTENDED PULSED SYSTEM

The extension implements the same architecture of the original pulsed system – the optical signal coming from a second port of the Optical Master Oscillator (OMO) is again amplified and split. The total number of stabilized pulsed links that can be deployed for the extended system is now fourteen. One of the design constraints was to maintain mechanical and optical compatibility with the link stabilization units installed in the past.

The overall block diagram of the complete pulsed system is shown in Fig. 1. The components installed since 2009 are indicated as *master* while the devices that are part of the extension will be hereafter referred to as *slave*. In fact the slave is locked to the master to compensate for residual timing drifts among the two splitters output ports. The key element of the tracking loop is a phase detector implemented by

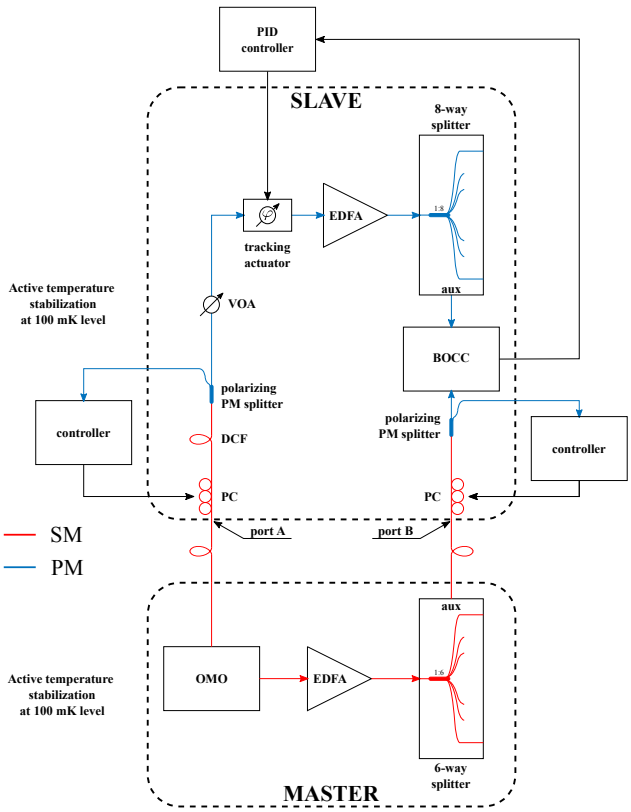

Figure 1: Simplified block diagram of the extended pulsed timing system. DCF: Dispersion Compensating Fiber, EDFA: Erbium Doped Fiber Amplifier, PC: Polarization Controller, PID: Proportional Integral Derivative, PM: Polarization Maintaining fiber, SM: Single Mode fiber, VOA: Variable Optical Attenuator.

means of a BOCC (Balanced Optical Cross-Correlator) [4]. This is commonly known as in-loop device. The error signal is used to drive an actuator – a combination of a fiber piezo stretcher and a motorized translation stage – to keep the pulses coming out from the outputs of the master and slave splitters synchronized. A manual free-space delay line is also part of the actuator block and used to align in time the pulses and set the zero-crossing of the BOCC in the dynamic range of the control loop.

The main sources of timing drifts between the master and slave subsystems are the two interconnections at ports A and B. The former is included in the controlled path of the tracking system, while the latter represents the most critical issue to be addressed from the point of view of the timing application. Indeed the length of the fiber path crossing port B cannot be very short because it includes the two optical devices used to implement the polarization control. For this reason the path must be properly temperature stabilized to

* fabio.rossi@elettra.eu

ISBN: 978-3-95450-249-3 ISSN: 2673-5350 doi: 10.18429/JACoW-IBIC2024-WEP34

DESIGN OF AN S-BAND PARALLEL-COUPLED POLARIZABLE TRANSVERSE DEFLECTING CAVITY FOR MULTI-DIMENSIONAL PHASE SPACE DIAGNOSTICS IN PHOTOINJECTORS

Qizhang Huang, Linlin Wei, Jiahang Shao*, Zongbin Li, Yong Yu
Institute of Advanced Science Facilities, Shenzhen, China
Jitao Sun, Hongli Ding, Jiayue Yang, Weiqing Zhang, Xueming Yang
Dalian Institute of Chemical Physics, Dalian, China
Hao Zha, Jiaru Shi, Huaibi Chen, Tsinghua University, Beijing, China

Abstract

Beam quality from photoinjectors is crucial for lasing in Free Electron Laser (FEL) facilities. While phase space measurement are usually limited to 2D with conventional methods, the recently-developed transverse deflecting cavities (TDCs) with variable polarization provide the capability to measure multi-dimensional phase space information. Such information could guide the improvement of beamline setup for optimal lasing performance. We therefore propose an S-band parallel-coupled TDC, in which two chains that deflect beam horizontally and vertically are independently fed by waveguides and variable polarization can be obtained by adjusting their relative amplitude and phase. This design offers several advantages, including tunability, single-frequency operation, compactness, and high shunt impedance. In this manuscript, physical and mechanical design of this TDC as well as the planned proof-of-principle experiment will be presented in detail.

INTRODUCTION

Transverse deflecting cavity imprints time-dependent transverse kick to a charged bunch, making it an essential tool for longitudinal beam diagnostics [1]. Novel TDCs with variable kick angle (polarization) can be further utilized for multi-dimensional phase space measurements as well as rapid scanning in proton therapy. Recently, several types of polarizable TDC have been developed with advanced technologies, such as fully axial-symmetric cells with E-rotator [2, 3], dual-mode dual-frequency cells [4, 5], and alternating cells with orthogonal TE_{11}°-like modes by individual feeding [6].

Based on the parallel-coupled technique applied in high gradient accelerating structures [7, 8], we have proposed a new type of polarizable TDC with two alternating but isolated chains, each containing parallel-fed cells that support horizontally or vertically polarized TM_{11}°-like mode [9]. Variable polarization is achieved by adjusting the amplitude and phase of the input power to the chains. Our design presents the following advantages: 1) the asymmetric cells can be tuned after brazing, which relaxes the machining tolerance; 2) the structure uses a single power source; 3) only two input ports are needed for the entire structure, which simplifies the waveguide network; 4) the cells operating in π-mode have high shunt impedance. This parallel-coupled polarizable TDC is intended for use at the end of the photoinjector of the planned Shenzhen Superconducting Soft X-Ray Free-Electron Laser (S^3FEL) [10].

In our recent study, we have improved our initial design so as to simplify the parallel-feeding waveguide and enhance fabrication feasibility. The physical and mechanical design of two prototype structures have been completed. The 8-cell prototype will be utilized to demonstrate the fabrication and tuning technologies, while the 16-cell prototype will undergo beam testing in the proof-of-principle experiment at Dalian Coherent Light Source (DCLS) [11].

INITIAL STRUCTURE DESIGN

In the initial design (Fig.1), the deflecting cells are racetrack-shaped to ensure large degenerate mode separation, supporting the desired polarization while minimizing coupling between neighboring cells [9]. The π-mode cells are individually fed by the parallel-coupled waveguide under critical coupling conditions. Corrugations are included in the waveguide to slow the phase speed v_p to match the speed of light c, satisfying the synchronization condition. It should be noted that the phase advance of the corrugation (denoted as θ) should be lower than π to propagate the input power and uniformly distribute it into the deflecting cells. θ is set to $2\pi/3$ in the initial design.

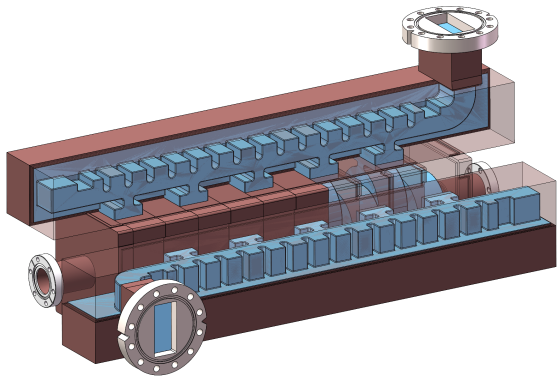

Figure 1: Schematic layout of the initial design.

In parallel-coupled accelerating structures, the cavity is usually machined as two halves to reduce fabrication costs and complexity [7, 8]. Due to the transverse surface cur-

* shaojiahang@mail.iasf.ac.cn

ISBN: 978-3-95450-249-3 ISSN: 2673-5350 doi: 10.18429/JACoW-IBIC2024-WEP35

THz RESONATOR BASED ELECTRON BEAM MANIPULATION*

Xiaoyu Liu†, Institute of High Energy Physics, Beijing, China

Abstract

In recent years, with the development of powerful THz source technologies, THz structures are widely utilized for electron beam manipulation, such as acceleration, deflection, compaction and diagnostics. Taking the bunch length measurement as an example, combining with high field strength and high resonant frequency, the THz structure based deflector could reach femtosecond or even sub-femtosecond resolution. In this paper, a 0.1 THz Fabry-Perot resonator based structure will be introduced, which could provide time-dependent deflection for short electron beam to resolve the bunch length. By adjusting the relative location of the beam pipe and the plane mirror, this structure could also work for beam acceleration.

INTRODUCTION

In the last decade, there has been increasing interest of utilizing THz structures for beam acceleration and beam manipulation, which have the potential to overcome certain limitations of conventional RF accelerators and other laser-based concepts. Generating powerful THz source has been made possible, allowing to obtain millijoule-level energy for both broadband and narrowband THz pulse [1, 2]. As a result, significant progress has been achieved to efficiently accelerate or deflect electron beam based on THz pulse.

For THz driven streaking, various setups have been proposed or even demonstrated with femtosecond or even sub-femtosecond resolution. Sub-relativistic, <100 keV kinetic energy electron beams from DC sources were characterized with roughly 10 fs resolution via THz streaking [3, 4]. For several MeV energy electron beam, a roughly 3.4 MeV electron beam was determined by a THz-driven metal slit with 1.5 fs (rms) accuracy [5]; a similar setup was used to determine the bunch duration of a 3.1 MeV (20 fs rms) electron beam with a resolution below and approaching a single femtosecond respectively [6]; a 4.5 MeV electron beam with compressed rms length less than 100 fs was measured based on a double-slit split ring structure and 10 fs resolution was reached [7]; single inverse split ring resonator or array structures are proposed with potential to reach even sub-fs resolution [8]. All previous results are applied to short electron pulse smaller than half a THz wave period, the work in Ref [9] successfully characterizing an electron pulse with a longer duration by comparing the convolution of a temporal profile of the electron pulse and electric field in a THz optoelectronic resonator with the Fourier components of a deflection time profile.

For THz based electron acceleration, acceleration with gain of >30 keV for 55 keV electron beam is obtained via a few-mJ single cycle THz pulse [4]; an energy gain of 7 keV for 60 keV electrons is observed in a 3-mm interaction length via a 10 μJ THz pulse [10]; 53 keV electrons were accelerated by approximately 1.6 keV via only ~20 nJ THz pulse due to the use of narrowband THz pulses to drive a dielectrically lined waveguide (DLW) [11]; stable and scalable beam acceleration in a multistage mini-accelerator is demonstrated, 15 keV energy gain is achieved for 3 MeV electron beam in each module with 100 nJ THz pulse [12]; a 50 keV electron beam driven by a 100 uJ, 25 cycle THz pulse experiences an energy gain of 170 keV by employing a DLW with two phase shifters [13].

The Fabry-Perot resonator based electron acceleration has already been proposed [14] with a working frequency of 42.84 GHz, the expecting accelerating gradient is roughly 1GeV/m. Therefore, we are thinking the possibility of using similar structure at 0.1 THz to reach equal of even better effect.

This paper introduces a 0.1THz Fabry-Perot resonator, the basic electromagnetic properties of which and the numerical investigation of the electron bunch inside which for acceleration and deflection are presented. This structure is not an efficient one with high acceleration gradient or high streaking speed, but as powerful THz sources are achievable and continuing to progress, and this structure has its own advantage of easily fabricated due to its suitable size, we still show the results.

Fabry Perot Resonator

Fabry Perot resonator is an optical cavity includes two reflecting mirrors with a certain distance. It is commonly utilized in various applications, including interferometers, spectrometer, and optical filters, considering its high finesse and tunability. A hemi-confocal Fabry-Perot structure is shown as in Fig.1, which includes a spherical mirror and a plane mirror, the coupling way is a waveguide WR10 embedded in center of the spherical mirror.

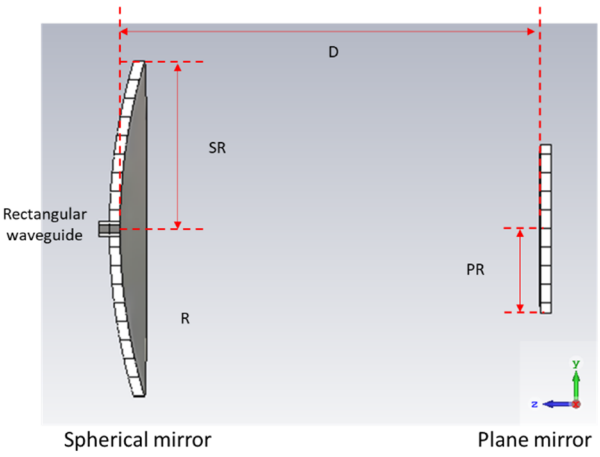

Figure 1: The cut view of a hemi-confocal Fabry-Perot resonator, the coupling is via WR10 embedded in the spherical mirror.

* Work supported by Xiejialin Scholarship (No. E25464U210)
† email address: liuxy94@ihep.ac.cn

ISBN: 978-3-95450-249-3 ISSN: 2673-5350 doi: 10.18429/JACoW-IBIC2024-WEP36

TRANSVERSE FEEDBACK TO DAMP COLLECTIVE BEAM INSTABILITIES, PAST, PRESENT AND FUTURE

T. Toyama†, Impedance-Instability-Feedback Team, KEK, Tsukuba, Japan

Abstract

Starting with my first experience of the transverse feedback damper in the KEK 12 GeV PS in 2005 - 2006, where we tested with analog system and in addition digital controller from SPring-8 team. Since then, digital systems have come to cover almost all the machines. In J-PARC MR bunch-by-bunch transverse feedback system had been introduced with a collaboration at the proton beam power around 150 kW in 2010. The weaknesses of this system quickly became apparent. It can damp only the center-of-mass motion of each bunch. It could not suppress intra-bunch betatron motion with different betatron phase in a different longitudinal bunch position. This happens in the case of a non-zero chromaticity. Then the intra-bunch feedback system was introduced in 2014 with a proton beam power of approximately 250 kW and has been operating successfully to date. But already this system cannot suppress collective beam instabilities in certain chromaticities over proton beam intensity of 2 - 3E+14 protons per pulse. The higher the sampling rate, the higher the damping efficiency. This system is currently under development.

INTRODUCTION

We encounter unwanted betatron oscillations after bunched beams are injected into synchrotrons and/or when transverse collective beam instabilities appear as beam intensity gets larger. One of the countermeasures other than Landau damping by nonlinear fields is a beam feedback system, which is essential to obtain a stable beam. Here transverse feedback systems which were studied or implemented in the proton accelerators in Japan are reviewed.

ANALOG AND DIGITAL FEEDBACK IN THE KEK 12 GeV PS

When the proton beam intensity was increased to above 6×10^{12} protons/9 bunches, transverse head-tail instability appeared, especially at the injection flat bottom and the early phase of acceleration in the 12 GeV PS in KEK [1] which stopped service operation for users in December 2005.

Horizontal instabilities were observed during the injection flat bottom and at the early phase of acceleration (Fig. 1). Typical oscillation modes were mode 1 and 2 during the injection flat bottom (Fig. 2). At the early phase of acceleration, oscillation mode 0 was mainly observed (Fig. 3). The reason why mode number changed was that the considerable sextupole fields were generated by an eddy current in the vacuum pipe inside the dipole magnets during the early phase of acceleration [1].

† takeshi.toyama@kek.jp

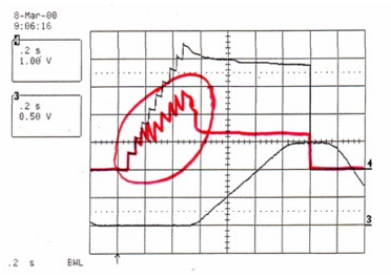

Figure 1: Beam intensities (2×10^{12} ppp/div.) measured with a feedback-CT. Red curve: beam was lost by instabilities. Black curve: stable beam.

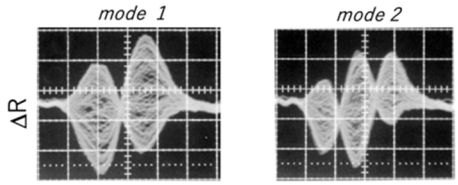

Figure 2: Horizontal position signal with instabilities during the injection flat bottom. Delta-signals are overlaid for multi-turns. Left: mode 1, Right: mode 2.

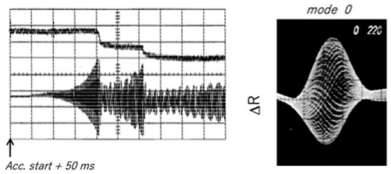

Figure 3: Beam intensity and horizontal position (delta-signal) with instabilities at the early phase of acceleration. Left: upper trace is the beam intensity; lower trace is the horizontal delta-signal. 5 k samples per division (sampling rate ~ 670 kHz). Right: delta-signal overlaid for multi-turns.

To cope with these instabilities, we tested transverse feedback system, one with analog and the other with digital system in 2005 - 2006. The whole system is depicted in Fig. 4. The analog feedback comprised a BPM, coaxial cables, low-pass filters, 180-degree hybrids, a cable delay, amplifiers and a stripline kicker, whose signal path is drawn in continuous lines in Fig. 4. The path was changed in the area indicated by the arrows for the digital feedback. With the analog feedback on, the growing horizontal delta-signal at injection flat bottom (right plot in Fig. 5) was suppressed (left plot in Fig. 5) [2]. Replacing the analog feedback with the digital feedback resulted in the stability shown in Fig. 6 [2]. Sustaining oscillation depicted in the right plot without feedback was damped with the digital

ISBN: 978-3-95450-249-3 ISSN: 2673-5350 doi: 10.18429/JACoW-IBIC2024-WEP37

PRELIMINARY DESIGN CONSIDERATION FOR CEPC FAST LUMINOSITY FEEDBACK SYSTEM

M. Li*,1,2,3, P. Bambade[3], D. Wang[1], H. Y. Shi[1], S. Bai[1]
[1]Institute of High Energy Physics, Chinese Academy of Sciences, Beijing, China
[2]University of Chinese Academy of Sciences, Beijing, China
[3]Laboratoire de Physique des 2 infinis Irène Joliot-Curie – IJCLab, Orsay, France

Abstract

Future large high-luminosity electron-positron colliders such as Circular Electron Positron Collider (CEPC) require nanometre-sized beams at interaction point (IP). The luminosity is very sensitive to the beam orbit drifts at the IP. It is essential to have a fast luminosity feedback system at the IP to maintain optimum beam collision conditions. We considered two possible methods for this purpose for CEPC. One is based on measurements of the luminosity and the other is based on measurements of the beam orbits around the IP. In this paper, we present the preliminary design consideration for a fast luminosity feedback system at the IP of CEPC.

INTRODUCTION

The CEPC is a 100 km double ring collider with two interaction points proposed to be working at four energy schemes of Z pole (45.5 GeV), WW (80 GeV), Higgs (120 GeV) and $t\bar{t}$ (180 GeV). To achieve the high luminosity of 5×10^{34} cm^{-2}s^{-1} the CEPC uses strong Final Focus System quadrupoles to focus the beams at the IP to very small sizes, typically only several tens of nanometers in the vertical direction [1]. The luminosity is very sensitive to the mechanical vibrations caused by ground motion and other effects, requiring excellent control over the two colliding beams to ensure an optimum geometrical overlap between them and thereby maintain the maximal luminosity. Therefore, fast luminosity measurements and an orbit feedback system at the IP are essential for CEPC.

ORBIT FEEDBACK METHODS AND TECHNIQUES

Beam-Beam Deflection Driven Method

The beam-beam deflection method, based on the measurement of the beam orbit with Beam Position Monitors (BPM) upstream and downstream of the IP, was first developed for the SLC project and has been successfully utilized for feedback for years at LHC, KEKB and SuperKEKB [2–4]. The small offset between the two colliding beams at IP can introduce an deflect angle due to mutual electromagnetic interaction between the beams, which will be converted into a large offset as the beams propagate forward and collide, as shown in Fig. 1. By measuring this single-pass orbit changes with BPMs upstream and downstream of the IP, we can reconstruct the offset between two beams at the IP according to Eq. (1).

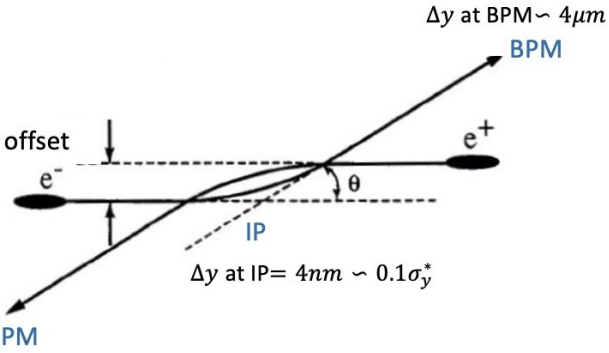

Figure 1: Schematic diagram of the beam-beam deflection driven method.

$$\Delta x_{\mathrm{BPM}} = \sqrt{\beta_x^* \beta_x^{\mathrm{BPM}}} \cdot \Delta x' = -\frac{2\pi\xi_x}{\beta_x^*}\sqrt{\beta_x^* \beta_x^{\mathrm{BPM}}}\Delta x \,,$$
$$\Delta y_{\mathrm{BPM}} = \sqrt{\beta_y^* \beta_y^{\mathrm{BPM}}} \cdot \Delta y' = -\frac{2\pi\xi_y}{\beta_y^*}\sqrt{\beta_y^* \beta_y^{\mathrm{BPM}}}\Delta y \,, \quad (1)$$

where $\beta^*_{\mathrm{x,y}}$ and $\beta^{\mathrm{BPM}}_{\mathrm{x,y}}$ are beam envelope functions at the IP and BPM, $\xi_{x,y}$ the beam-beam tune-shift parameters. With beam-beam deflection driven method, we can determine in which direction and how much we should change the orbit when the offset between the two colliding beams is detected. If the accuracy of BPM is precise enough, we can maintain the optimum collision with almost no luminosity loss. However, the accuracy of the orbit measurements and the long-term stability of the orbit measurement system may limit its application.

Luminosity Driven Method

The luminosity driven method is based on the measurement of the luminosity, which has been successfully used at PEP-II [5] and is being studied at SuperKEKB [6]. With this method we can know how much the offset between the two beams, but can not know its sign. In addition, some other effects, such as beam size and beam intensity variations, may change the luminosity at relatively low frequencies. For this reason, additional dithering system is required. One beam is dithered sinuously in the horizontal plane with an amplitude of A and frequency of f around an initial horizontal offset x_0 between the two beams, such that the luminosity varies according to

$$L(x) = L_0 \exp\left(-\frac{x^2}{2\Sigma_x^2}\right) \,, \quad (2)$$

* meng.li@ijclab.in2p3.fr

ISBN: 978-3-95450-249-3 ISSN: 2673-5350 doi: 10.18429/JACoW-IBIC2024-WEP38

ORBIT FEEDBACK SYSTEM IN SOLARIS SYNCHROTRON FINAL STEP IMPLEMENTATION AND FIRST MEASUREMENTS

R. Panaś*, A. I. Wawrzyniak, M. Piekarski, M. Mleczko, M. Żurek
NSRC SOLARIS, Kraków, Poland

Abstract

SOLARIS, a third-generation synchrotron radiation source in Kraków, Poland, is dedicated to providing high-brilliance X-ray beam for various scientific disciplines. The successful operation of a synchrotron radiation facility heavily relies on precise control of the electron beam orbit within the storage ring. Orbit deviations, even on a small scale, can adversely affect beam quality, leading to decreased performance and efficiency of experimental setups. To mitigate these effects, an Orbit Feedback System is essential, providing correction of orbit deviations. In this study, we introduce an enhanced Orbit Feedback System that integrates both fast and slow orbit correction mechanisms, along with RF drift compensation. The system utilizes advanced feedback algorithms to compute corrective actions for the actuators, which include both fast and slow correction magnets, based on real-time beam position measurements. We also present the initial measurements and tests of the system, demonstrating its effectiveness and capabilities.

HARDWARE

The SOLARIS storage ring consists of 12 double-bend achromat (DBA) cells [1]. The Slow Orbit Feedback (SOFB) system stabilizes the beam using 36 beam position monitors (BPMs) and 72 steering magnets, which operate across both the horizontal and vertical planes. The system features a ±12 A range, enabling significant corrections at a lower frequency of 1 Hz. The arrangement of the particular magnets, namely: dipoles (DIP), combined quadrupoles with sextupole content (SQFI and SQFo), defocusing sextupoles(SDO and SDI), correcting sextupoles with additional coils for slow correctors (SCi and SCo), fast correctors (FOFB), in DBA cell is illustrated in Fig.1.

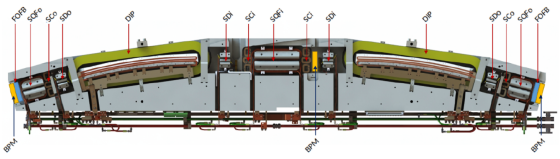

Figure 1: Placement of magnets inside DBA cell.

The newly implemented Fast Orbit Feedback (FOFB) system, which utilizes the same BPMs, employs 24 fast steering dipoles positioned at the beginning and end of each section to apply corrections. This system allows for a significantly faster response to external disturbances, operating at a repetition rate of 10 kHz. A detailed comparison of key parameters for both correction systems is provided in Table 1 below.

Table 1: Comparison of SOFB and FOFB

Correction method	FOFB	SOFB
Speed of correction [Hz]	10 000	1
Max. current on CM [A]	2	12
Number of used CMs	24	36
Number of used BPMs	36	36

FOFB DEPLOYMENT

The critical milestone was the successful launch of the Fast Orbit Feedback (FOFB) system. This deployment was built on the foundation of previously developed software and design principles [2, 3], which provided the framework for controlling the FOFB and included the capability to measure the response matrix. Following the measurement, the matrix required specific modifications to be compatible with the GDX modules in the Liberas, which are responsible for calculating and applying settings to the fast correctors. This process involved bit-cutting and matrix operations. Bit-cutting was particularly crucial, as it allowed the FPGA in the GDX module to achieve the necessary speed for executing the mathematical computations essential to the system's real-time performance.

SOFB Improvement

To ensure seamless cooperation between the SOFB and FOFB systems, the SOFB has been upgraded to respond to events triggered by the Liberas. This upgrade includes the implementation of independent correction for both axes, the integration of RF correction—previously managed by a separate script—into the system, an increase in operating frequency, and real-time updates of the golden orbit for FOFB operation.

FOFB Tuning

The subsequent objective was to fine-tune the FOFB system to ensure optimal performance. Achieving this required careful adjustment of the system's components, particularly the proportional (Kp) and integral (Ki) gains within the feedback loop's integrator. These parameters play a crucial role in dictating the system's responsiveness and stability, directly impacting the precision with which the FOFB can correct orbit deviations.

The tuning process involved systematically introducing controlled disturbances into the system and carefully monitoring its response. By analyzing how the FOFB system

* roman.panas@uj.edu.pl

ISBN: 978-3-95450-249-3 ISSN: 2673-5350 doi: 10.18429/JACoW-IBIC2024-WEP39

THE DEVELOPMENT OF BUNCH-BY-BUNCH TRANSVERSE FEEDBACK SYSTEM AT SSRF BASED ON RF DIRECT SAMPLING*

J. L. Pan, Shanghai Institute of Applied Physics, Chinese Academy of Sciences, Shanghai, China
also at University of Chinese Academy of Sciences, Beijing, China
L. W. Lai†, Y. M. Zhou, Shanghai Advanced Research Institute, Chinese Academy of Sciences, Shanghai, China

Abstract

The commonly used bunch-by-bunch transverse feedback system (TFB) is based on the scheme of analog downconversion, which down converts the $3\times f_{RF}$ beam signal to the baseband with a phase adjusted local oscillator. The system contains a large number of analog devices, which make the system complex. Today, sampling the high frequency signal directly with high performance ADC is available. A new bunch-by-bunch TFB based on RF direct sampling is under development at SSRF. The new system structure is much simpler compared to the traditional one and much powerful. The direct sampling processor has 4 input channels, which can simultaneously process horizontal, vertical, large bunch vertical feedback, and bunch charge measurement. The RF processor has 4 ADC channels (maximum sampling rate is 2.6GHz, bandwidth is 9GHz), 4 DAC channels (maximum frequency 500MHz). The processor uses Xilinx system-on-chip UltraScale+ MPSoC FPGA. Paper will introduce the system structure, the processor design and performance.

INTRODUCTION

The Shanghai Synchrotron Radiation Facility (SSRF) is a third-generation medium-energy synchrotron radiation source, which was completed in 2009. It operates with a beam energy of 3.5 GeV, a storage ring circumference of 432 meters, a harmonic number of 720, and an RF frequency of 499.654 MHz.

For a synchrotron radiation source, the quality of the beam is a key factor in evaluating its performance. The electron beam circulating in the storage ring is influenced by various complex physical factors, including higher-order modes in RF cavities, resistive wall impedance, ion instability, and multi-bunch coupling. These instabilities can collectively cause the beam to deviate from its designed trajectory, increase emittance, shorten beam lifetime, and affect the operational stability and light quality. The TFB is a critical system used for controlling beam stability in synchrotron light sources. By monitoring the beam's motion in real-time and applying feedback control, the system can effectively suppress unstable modes and maintain transverse beam stability. The main components of the TFB include the Beam Position Monitor (BPM), transverse feedback electronics, power amplifiers, and kickers. Among these, the TFB electronics, which convert the detected beam position offset signals into feedback signals, are at the core of the system.

In the early stages, due to the limitations of ADCs and processors, it was not possible to directly sample high-frequency signals, so the transverse feedback system had to perform analog downconversion before signal sampling. The first-generation transverse feedback electronics at SSRF used the sum signal from the four BPM channels as the local oscillator to downconvert the frequency band around 1.5 GHz to the baseband. Additionally, four ADCs with a sampling frequency of 125 MHz were used for delayed sampling, achieving a 500 MHz sampling rate for single-point sampling of each bunch. Starting in December 2016, as part of the Phase II upgrade project at SSRF, the beam measurement system was upgraded [1, 2], including the replacement of the transverse feedback system with Dimtel iGp12 processor paired with FBE-LT front and back ends. The principle is as follows: The BPM output signals undergo sum and difference operations and are then passed through a bandpass filter with a center frequency of 1.5 GHz and a bandwidth of 500 MHz to extract the beam signal near the 3rd harmonic of the RF frequency. The machine clock is then multiplied to 1.5 GHz and used as the local oscillator to downconvert the filtered signal to the baseband. Finally, the beam position information is obtained by single-point sampling using a 500 MHz ADC, and the processor calculates the feedback signal based on the position information.

The RF front-end structure of such schemes is complex, with numerous analog components, making it susceptible to environmental changes. Moreover, due to single-point sampling, it is prone to longitudinal oscillation effects. Additionally, in the Phase II project of SSRF, an additional feedback loop was added to handle vertical oscillations of large bunches, on top of the existing horizontal and vertical feedback loops. However, since one processor can only handle feedback for one direction, the cost is relatively high. Therefore, there is a need for new methods to address these issues.

RF DIRECT SAMPLING ELECTRONICS

In recent years, with advancements in technology, the performance of ADCs has significantly improved, making it possible to directly sample beam signals. For example, in the RF direct sampling bunch-by-bunch transverse feedback system at Spring-8, the system utilizes four ADCs with a sampling rate of 125 MHz and a bandwidth of 750

* Work supported by The National Science Foundation of China (Grant No.12175293). Youth Innovation Promotion Association, CAS (Grant No. 2019290). Outstanding member of the Youth Innovation Promotion Association, CAS. SHINE R&D and project. SSRF operation funding research project.

† Corresponding author: lailw@sari.ac.cn

ISBN: 978-3-95450-249-3 ISSN: 2673-5350 doi: 10.18429/JACoW-IBIC2024-WEP40

THE DESIGN OF SILF FAST ORBIT FEEDBACK SYSTEM

F. J. Zeng, T. Yu, H. S. Lin, Z. Z. Zhou, M. T. Kang
Institute of Advanced Science Facility, Shenzhen, Guangdong, China

Abstract

The Shenzhen Innovation Light Source Facility (SILF), as a 4th light source, is an accelerator-based multidiscipline user facility planned to be constructed in Shenzhen, Guangdong, China. It has stringent requirement for beam orbit stability: the orbit fluctuations should be below 10% of the beam RMS sizes in both horizontal and vertical directions with a bandwidth around 500Hz. The fast orbit feedback system (FOFB) is designed to correct beam orbit in the storage ring, by calculating correctors strength change to correct beam orbit error detected by the beam position monitors (BPMs). The FOFB with field programmable gate arrays (FPGA) is supposed to be achieved, to reduce feedback latency and increase bandwidth. In this paper, the structure of SILF FOFB, the structure of its electronics system and its hardware and software subsystems are designed.

INTRODUCTION

The SILF is a fourth-generation medium-energy synchrotron radiation light source that envisions a future with over 50 beamlines. Its primary focus lies in supporting the development of domestic core industries, advancing frontiers in basic science research, and addressing strategic imperatives, including integrated circuits, bio-medicine, advanced materials, and advanced manufacturing.

The accelerator complex is composed of a 200 MeV linac, a booster with ramping energy from 0.2 GeV to 3.0 GeV, and a 3.0 GeV storage ring as shown in Figure 1. Two transport lines are designed to connect the linac, booster and storage ring. The circumference of the storage ring is 696 m, which includes 28 hybrid seven-bend achromat (H7BA) lattice periodic units to achieve the emittance below 100 pm·rad. The top-up operation mode (300 mA, 928 bunches) is considered, and a brightness of about 10^{22} s^{-1} mm^{-2} $m{\cdot}rad^{-2}$ $(0.1\%\ bandwidth)^{-1}$ is expected at the photon energy of 10 keV, as illustrated in Figure 2 [1, 2].

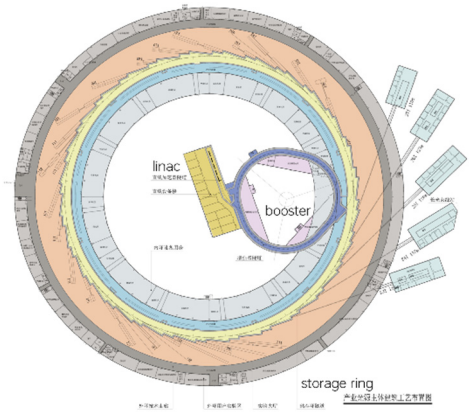

Figure 1: Schematic layout of the SILF project.

With the enhanced requirements of new synchrotron light sources and the fast development of electronic techniques, the beam orbit stability in μm level can be achieved by the FOFB with a bandwidth of several hundred Hz based on large-volume FPGAs. For SILF, there are 28 H7Bas with 12 BPMs and 12 fast correctors along the 696 m storage ring, 336 BPMs' data in both horizontal and vertical directions need to be collected and delivered to all of the FOFB sub-stations. It responds to orbital perturbations from 0.01 Hz to 500 Hz frequency range in feedback periods of tens of microseconds, which is different from slow orbit feedback system (SOFB) [3, 4].

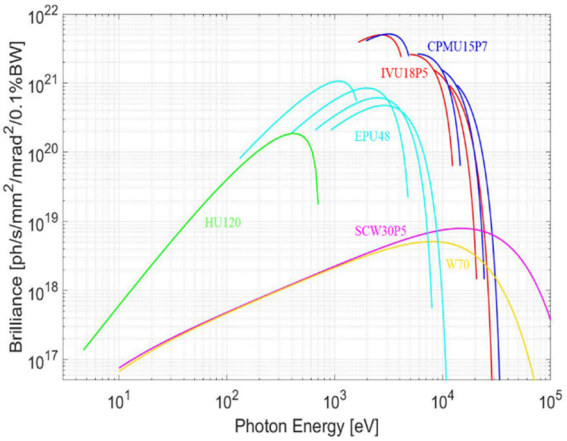

Figure 2: The available spectral brightness for SILF operated in the high brightness.

REQUIREMENT

There are many factors that affect the stability of the beam orbit, including the stability of the magnet power supply, ground vibration, temperature effects, etc.

According to ring accelerator physical design and requirements, there are BPMs to monitor the orbit and many correctors to correct the orbit in the storage ring. In order to suppress interference and keep the beam orbit stable, it is we adopt a high-intensity and high-speed orbit feedback system, a typical multiple-input and multiple-output (MIMO) system, to achieve long-term stable operation of the light source based on singular value decomposition (SVD) commonly.

The correction algorithm is based on an SVD of the orbit response matrix:

$$\Delta\overline{X} = R\,\Delta\overline{\theta} \quad and \quad R = USV^T$$

$$\Delta\overline{\theta} = VS^{(-1)}U^T\,\Delta\overline{X}, \tag{1}$$

where $\Delta\overline{X}$ is error that the current orbit is compared to the golden orbit, U and V are matrices whose columns form an

ISBN: 978-3-95450-249-3 ISSN: 2673-5350 doi: 10.18429/JACoW-IBIC2024-WEP41

OVERVIEW OF SLS 2.0 BEAM BASED FEEDBACKS AND BPM SYSTEM

B. Keil†, P. Baeta, R. Ditter, F. Marcellini, G. Marinkovic, J. Purtschert, M. Roggli
Paul Scherrer Institute, Villigen, Switzerland

Abstract

For the ongoing upgrade of the Swiss Light Source (SLS) storage ring, the previous ageing beam-based feedbacks and beam position monitor (BPM) systems are replaced by newly developed versions, where beam commissioning is scheduled for January 2025. Feedbacks include the fast orbit feedback (FOFB), transverse and longitudinal multibunch feedback (MBFB), and filling pattern feedback (FPFB). In this contribution, we give an overview of the architectures and development/production status of these feedbacks and of the BPM system, including latest pre-beam test results.

INTRODUCTION

The Paul Scherrer Institute (PSI) is presently replacing the over 20-year-old storage ring of the former Swiss Light Source ("SLS 1.0"), where the new ring ("SLS 2.0") will provide more than 40 times higher brilliance for hard X-ray experiments. During the dark time of 15 months from October 2023 to December 2024, we are also replacing most electronics, racks, cables, and significant parts of the infrastructure, while keeping the SLS 1.0 linac, booster, tunnel, and building. Table 1 contains a comparison of SLS 1.0 and 2.0 parameters.

Table 1: SLS Storage Ring Beam Parameters

Parameter	Units	SLS 1.0	SLS 2.0
Circumference	m	288	
Beam current	mA	400	
Injection charge	nC	~0.15 (1 bunch)	
Beam energy	GeV	2.4	2.7
Main RF	MHz	499.637	499.654
Harmonic no.	#	480	
Hor. emittance	pm	5030	131-158
Vert. emittance	pm	5-10	10
# Ring BPMs	#	75	136
# FOFB corr. mag.	#	73+73	115+115
Hor. betatron tune	-	20.43	39.27
Vert. betatron tune	-	8.74	15.22
FOFB corr. kick	µrad	±750	±400
Beam size at BPM	µm	> 5	> 5

FAST ORBIT FEEDBACK

Corrector Magnets

While SLS 1.0 had 73 FOFB dipole corrector magnets each for the horizontal and vertical plane, realized as additional coil windings on sextupole magnets, SLS 2.0 has 115 dedicated FOFB dipole corrector magnets per plane ("CH" and "CV") shown in Fig. 1. They are located close to BPMs, and share with them a stainless-steel beam pipe of 0.5 mm thickness to reduce eddy currents, compared to 2 mm for SLS 1.0. The iron yoke lamination thickness of the corrector magnets is 0.35 mm, also reducing eddy currents that scale with the inverse square of the lamination thickness.

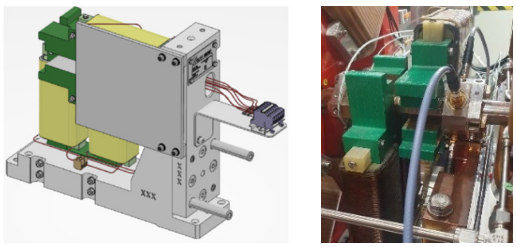

Figure 1: FOFB orbit dipole corrector magnet (left), with one magnet per plane installed next to a BPM (right).

Magnet Power Supplies

The SLS 2.0 corrector magnet power supplies (PS) were designed at PSI like for SLS 1.0, with a Xilinx/AMD Zynq UltraScale+ ("ZynqU+") MultiProcessing System-on-Chip (MPSoC) for the current regulation and external interfacing. The current regulation is presently implemented in software on an ARM CPU of the ZynqU+. While the SLS 2.0 BPMs [1] and FOFB computing engine use multi-gigabit fiber optic links for all external interfaces, the magnet PS use POF (plastic optical fiber) links as FOFB interface to stay compatible with previous PS generations, while using Ethernet for communication with the EPICS control system. The POF link transmission speed of 10 MBaud at SLS 1.0 was upgraded to 50 MBaud for SLS 2.0, using 8b/10b encoding/decoding and CRCs for safe transmission. Recent pre-beam tests of these links with long POF cables showed no transmission errors over many days.

FOFB Topology and Data Transfer

The FOFB collects data from all BPMs periodically, calculates corrective kicks to stabilize the beam, and applies these kicks by changing the currents of the corrector magnet power supplies. The nearly 25-year-old hardware of SLS had distributed the FOFB SVD algorithm on 12 DSP boards, one in each of the 12 BPM racks. The DSPs received data from 6 local BPMs via LVDS links, and from 6+6 BPMs in adjacent sectors via 160 Mbaud fiber optic point-to-point links. The SVD-inverted beam response matrix contained mainly diagonal elements, thus using only 18 of 72 BPMs per sector was sufficient for the basic orbit correction algorithm, while corrections that required the readings of all BPMs were performed by a slow high-level feedback running on a Linux server. Table 2 summarizes the differences of SLS 1.0 and SLS 2.0 FOFB.

† boris.keil@psi.ch

ISBN: 978-3-95450-249-3 ISSN: 2673-5350 doi: 10.18429/JACoW-IBIC2024-WEP42

DIRECTLY DRIVING GHz-RANGE POWER AMPLIFIERS WITH RF SYSTEMS-ON-CHIP FOR THE SLS 2.0 LONGITUDINAL MULTI-BUNCH FEEDBACK

B. Keil†, P. Baeta, G. Marinkovic, Paul Scherrer Institute, Villigen, Switzerland

Abstract

In the past, the longitudinal multibunch feedback (MBFB) at the Swiss Light Source (SLS) storage ring has used an analog upconverter to translate the output signal of a 500 MSample/s DAC to the 1.25-1.5 GHz operation frequency range of the longitudinal MBFB kicker and its power amplifier. For SLS 2.0, we have investigated the possibility of driving the power amplifier of a newly designed kicker (operating at 1.75-2 GHz) directly with the multi-GHz / multi-GSample/s DACs of an RF System-on-Chip (RFSoC). We present test results with the new SLS 2.0 kicker magnet and its power amplifier. Related methods for RFSoC-based bunch-to-bunch crosstalk compensation in the presence of transient beam loading (due to the superconducting 3rd harmonic cavity in the storage ring) and 200 ps range arrival time variations along the bunch train are also presented. Moreover, the latest status and plans for our MBFB firmware/software implementation on an RFSoC will be given.

INTRODUCTION

After the old SLS storage ring, SLS 1.0, had its last beam in September 2023, we are currently installing SLS 2.0 [1], a new diffraction-limited storage ring with up to 40 times higher brightness for hard X-rays. The first SLS 2.0 beam is scheduled for the beginning of 2025. The SLS upgrade also includes replacing aging hardware, such as the nearly 20-year-old VME-based MBFB electronics that will be replaced by a modern RFSoC-based system [2].

Like many traditional MBFB systems, our previous MBFB electronics had a single 500 MSample/s ADC and DAC each for the horizontal, vertical, and longitudinal plane, with an FPGA between ADC and DAC realizing the low-latency MBFB algorithm.

For SLS 2.0, we are replacing this hardware with an RFSoC-based solution, where the present version has eight 12-bit 4 GSample/s ADCs and eight 14-bit 6 GSample/s DACs on the same chip, plus a large FPGA for Programmable Logic ("PL"), as well as two multi-core CPUs.

Direct BPM Signal Sampling and Kicker Driver Signal Synthesis

With this new RFSoC solution, it becomes possible to eliminate the analog downconverting mixer in the RF front-end (RFFE) electronics for the MBFB BPM signals, as well as the analog upconverting mixer that was used to convert the 500 MSample/s output data of our previous DAC to the 1.25-1.5 GHz frequency range of the longitudinal kicker. Figure 1 depicts the architecture of the new system. With RFSoC technology we employ direct sampling for the sum signal, S, from the BPM electrodes, by interleaving up to 8 ADC channels at 4 GSample/s.

For direct driving, we use the I and Q signals from 2 DAC channels at 3.75 GSample/s, interleaved with 90° sample clock phase difference, to drive the power amplifier for the longitudinal kicker.

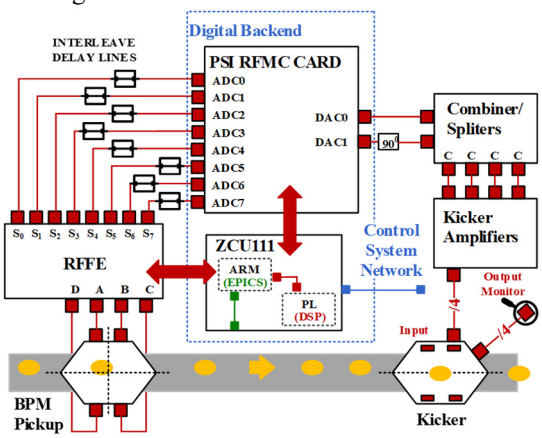

Figure 1: Hardware architecture of the SLS 2.0 Longitudinal Multi-Bunch Feedback (MBFB).

RFSOC ADC AND DAC SIGNAL PROCESSING STRATEGY

ADC Sampling and Signal Processing

For the longitudinal SLS 2.0 MBFB, four-button BPM electrode signals are combined with RF hybrids close to the beam pipe as we did for SLS 1.0. The SLS 2.0 RF front end consists of filters and a chain of amplifiers and attenuators to filter and adjust the level of the resulting broadband sum signal, S, proportional to the bunch charge. The RFFE, unlike the SLS1.0, has no mixer. The RFFE output signal is split into up to 8 ADC delay-compensated input channels of the AMD RFSoC with 1/8 sample phase delay from channel to channel, thus interleaving the ADC data. The ADCs operate at a sample rate of approximately 4 GSample/s, which is exactly 8 times the 499.654 MHz main RF reference clock that also drives the accelerating cavities of the storage ring. Alternatively, we foresee the option of using a fractional sample rate slightly below 4 GSample/s for additional interleaved oversampling of the BPM signal over several turns. The interleaving scheme by acquiring multiple turns at a fractional sampling reduces the number of ADC channels for the longitudinal MBFB, thus enabling the option of fitting longitudinal and transverse MBFB on the same RFSoC. For the SLS 2.0 startup, however, we will run transverse and longitudinal MBFB on separate RFSoC boards for maximum flexibility.

† boris.keil@psi.ch

ISBN: 978-3-95450-249-3 ISSN: 2673-5350 doi: 10.18429/JACoW-IBIC2024-WEP45

NEW FAST ORBIT FEEDBACK SYSTEM USING MicroTCA-BASED BPM ELECTRONICS FOR THE PF-RING

R. Takai*[1], T. Obina[1], M. Tadano, H. Sagehashi, M. Shiozawa
High Energy Accelerator Research Organization (KEK), Tsukuba, Ibaraki, Japan
[1]also at SOKENDAI (The Graduate University for Advanced Studies), Tsukuba, Ibaraki, Japan

Abstract

The upgrade to the fast orbit feedback (FOFB) system for the PF-ring is currently in progress. The new FOFB system features MicroTCA-based BPM electronics and a feedback control (FBC) unit. The BPM electronics are matched in number to the BPMs and synchronously transmit beam position data at a 10-kHz rate to the FBC unit via an optical data link. The FBC unit promptly calculates closed-orbit distortion from the received positional data and performs a matrix operation to correct it. The results are then converted to analog signals by fast D/A converters and applied to the power supplies of the fast-steering magnets. The immediate goal of the new FOFB system is to achieve a closed-loop bandwidth of 50 Hz, exceeding the current system performance by more than 100-fold. This paper will present the details of the new BPM electronics and the upgraded FOFB system, along with initial results obtained during beam tests.

INTRODUCTION

Beam orbit fluctuations in the storage ring can arise from various factors, including tidal forces, building deformation from sunlight, ground vibrations from traffic, electromagnet vibrations due to air conditioning and cooling water, mechanical vibrations from vacuum pumps, and magnet power supply ripple. Stabilizing the beam orbit requires a feedback system that continuously measures the current orbit, compares it to the ideal reference, and minimizes deviations. At the Photon Factory storage ring (PF-ring), a fast orbit feedback (FOFB) system stabilizes the vertical beam orbit[1]. This system includes 65 beam position monitors (BPMs), 12 analog detection circuits, a VME-standard digital signal processor (DSP), and 28 fast-steering magnets. However, the orbit feedback cycle is limited to approximately 12 ms (80 Hz), and the effective bandwidth to 0.3 Hz, due to the switching time of cascaded semiconductor switches between the BPMs and detection circuits, as well as the influence of the low-pass filters (LPFs) before the A/D converters (ADCs) to remove synchrotron oscillation components [1]. Additionally, since its introduction in 1997, hardware failures due to aging have frequently disrupted user operations.

Since FY2020, the Photon Factory (PF) has been planning an upgrade to the FOFB system. To achieve a faster feedback cycle and wider bandwidth, serial signal processing of the current system with few analog detection circuits has been replaced by parallel processing with digital circuits matching the number of BPMs. Position data from each BPM is now transmitted to a central "feedback control (FBC) unit" through an optical data link. The field-programmable gate array (FPGA) of the FBC unit performs the matrix calculation for beam orbit correction and transmits the results to fast-steering magnet power supplies through high-speed D/A converters (DACs).

This report provides an overview of new BPM electronics and the orbit feedback system utilizing them, along with test results from the actual stored beam.

NEW BPM ELECTRONICS

Electronics Configuration

The new BPM electronics utilize a digital signal processor based on the MicroTCA.4 standard, known for its high availability and high-speed data bus specifications [2]. In the MicroTCA.4 standard, multiple function expansion daughter boards, including advanced mezzanine cards (AMCs) and rear transition modules (RTMs) are installed in a common chassis, referred to as a "shelf." The four-electrode signals from the existing BPM head are first inputted into a μRTM at the back of the shelf. The μRTM is an analog front-end circuit that extracts beam-related components from raw BPM signals and adjusts their levels for compatibility with subsequent ADCs. Figure 1(a) shows a block diagram of the μRTM.

The raw signals from the BPM head are first filtered through a band-pass filter (BPF) centered at 504 MHz with a 10 MHz bandwidth, removing components outside the PF-ring's 500.1 MHz RF frequency[2]. A step attenuator and low-noise amplifiers then adjust the signal levels for the ADC. The main amplifier has a two-stage design. The first stage can be remotely enabled or disabled to achieve a wide dynamic range, from weak injection beam signals to high-intensity signals from isolated bunches during the hybrid operation. Additionally, the system includes a calibration function that outputs a tone signal at a fixed frequency, slightly offset from the beam signal frequency, via a directional coupler to the BPM head. The amplitudes of the reflected signals are periodically used to correct the gain drift in each channel.

The analog beam signals adjusted by the μRTM are converted into differential signals by a balun and sent to the frontside AMC via a high-speed "Zone 3" connector. The AMC, a digitizer and a digital signal processor, features high-speed ADCs (8 channels, 16-bit, 370 MSPS max.) and

* ryota.takai@kek.jp

[1] In contrast, the horizontal orbit is managed solely by a slow orbit feedback (SOFB) system running on a general-purpose PC CPU.

[2] The BPF is also configured for the Photon Factory Advanced Ring (PF-AR), which operates at 508.6 MHz.

ISBN: 978-3-95450-249-3 ISSN: 2673-5350 doi: 10.18429/JACoW-IBIC2024-WEP47

DEEP LEARNING FRAMEWORK FOR FAULT DETECTION IN ACCELERATORS

Michał Piekarski*, NSRC SOLARIS, Jagiellonian University, Kraków, Poland

Abstract

The main goal of NSRC SOLARIS is to provide the scientific community with high-quality synchrotron light. To achieve this, it is necessary to constantly monitor many subsystems responsible for beam stability and to analyze data about the beam itself from various diagnostic beamlines. This work presents an in-depth analysis of multi-modal, deep learning-based frameworks for fault detection within big research infrastructures, with a specific focus on accelerator facilities. The study explores diverse approaches and architectures for identifying anomalies indicating potential faults in operation. At the present stage, a binary classification is performed: stable beam operation or unstable beam operation / no beam with the accuracy of 90 %. The models and the results obtained so far are discussed, along with plans for future development.

INTRODUCTION

A key objective for any large infrastructure, whether scientific or industrial, is to achieve the highest possible reliability, reflecting strong expertise and diligent maintenance. To meet this goal, the design and maintenance procedures of all subsystems are continually refined. The integration of automation or semi-automation tools for maintenance and early fault detection is also crucial in this process. These systems typically focus on the early identification of anomalies and their root causes, allowing for prompt intervention. This approach not only enhances infrastructure availability but also minimizes the risk of major failures that could lead to unplanned shutdowns.

SOLARIS Synchrotron

SOLARIS is a third generation light source (shown in Fig. 1) operating at the Jagiellonian University in Krakow, Poland. This advanced and complex scientific infrastructure offers new highly innovative research opportunities for areas including physics, medicine and nanotechnology. Currently at SOLARIS six experimental beamlines offering various techniques, e.g.: photoemission electron microscopy, X-ray absorption spectroscopy, ultra angle-resolved photoemission spectroscopy or multi-scale X-ray and multimodal imaging, are available to the scientific community whereas another three are already at advanced level of construction or commissioning. Moreover, SOLARIS is also a National Cryo-EM Centre, with two latest generation cryo-electron microscopes enabling life science researchers to unravel life at the molecular level [1].

* michal.piekarski@uj.edu.pl

Figure 1: NSRC SOLARIS

Anomaly Detection in Accelerators

Fault and anomaly detection in accelerators is a desired process that ensures the stability, safety, and high performance of these complex systems. Accelerators, such as synchrotrons or particle colliders, rely on precise control of numerous subsystems, including magnets, power supplies, and vacuum systems, to maintain beam stability and achieve cutting-edge experimental outcomes. Anomalies in these subsystems, whether due to equipment malfunctions, environmental factors, or unforeseen interactions, can lead to beam instabilities, reduced performance, or even serious failures.

To address these risks, it is no longer enough to rely only on low-level machine protection systems. Therefore anomaly detection systems are employed, often integrating machine learning or deep learning algorithms and real-time monitoring tools. These systems continuously analyze data from various sensors within the accelerator, looking for deviations from expected patterns. Early detection of such deviations allows for prompt intervention, preventing minor issues from escalating into serious problems. By identifying potential failures before they occur, anomaly detection not only enhances the reliability and availability of the accelerator but also contributes to more efficient maintenance strategies, reducing downtime and operational costs. Moreover, as accelerators become more complex the role of automation systems is becoming increasingly vital. These systems not only improve operational safety but also enable more precise control over experimental conditions, ensuring that the high standards required for scientific research are consistently met.

The problem of anomaly detection and failure prediction in the accelerator control systems is being addressed by many

ISBN: 978-3-95450-249-3 ISSN: 2673-5350 doi: 10.18429/JACoW-IBIC2024-WEP50

RESEARCH ON VISUALIZATION AND INDEXING OF DATA BASED ON THE ELK STACK

Yukun Li[1†], Jianshe Cao[1], Qiang Ye, Yaoyao Du
Institute of High Energy Physics, Chinese Academy of Sciences, Beijing 100049, China
[1]also at University of Chinese Academy of Sciences, Beijing 100049, China

Abstract

This paper proposes a comprehensive solution for real-time collection and analysis of Beam Position Monitor (BPM) telemetry data using Kafka and the ELK stack [1]. It involves transmitting PV variables from BPM electronic devices to the Kafka messaging queue, enabling powerful and scalable data streaming. By retrieving JSON formatted data from Kafka using the ELK stack, efficient data indexing and visualization in Kibana are achieved. The paper provides detailed explanations of the architectural design, implementation details, and the advantages of using Kafka as a central hub for BPM data dissemination. This integration not only enhances the performance and reliability of the data processing pipeline but also offers a powerful tool for physicists and engineers for real-time visualization and monitoring of BPM data.

DISTRIBUTED MESSAGING SYSTEM

Kafka, in conjunction with Zookeeper, forms a distributed messaging system that ensures high reliability and consistency within the Kafka cluster. Zookeeper serves as Kafka's configuration center, storing all crucial information about Topics, Partitions, and Brokers. When Brokers in the Kafka cluster join or leave, Zookeeper dynamically adjusts the system configuration to ensure stable operation of the cluster. Moreover, Zookeeper is responsible for the fault recovery process when a Broker fails, by re-electing new leaders to maintain the continuity of the messaging system.

Kafka relies on Zookeeper to handle synchronization issues within the cluster, where the stability and reliability of Zookeeper directly impact the quality and efficiency of Kafka services. Together, they support building an efficient, scalable, and reliable real-time data processing system.

Kafka Message Queue

Apache Kafka is a distributed streaming platform capable of efficiently handling vast data streams [2]. Its core is a publish-subscribe messaging system designed for scenarios requiring high throughput and low latency data transmission.

The Architecture of Kafka is illustrated in Figure 1. The operational mechanics of Kafka include multiple Producers, Servers (Brokers), Consumers, Consumer Groups, and a Zookeeper cluster. Producers publish messages to Kafka, where messages are stably stored on Brokers' log files in chronological order. Consumers read messages from the Brokers and support message re-reads. Kafka enables message broadcasting (where each message is read by multiple consumers) and load balancing (where each message is processed by only one consumer in a consumer group) through Consumer Groups.

The operational mechanics of Kafka include multiple Producers, Servers (Brokers), Consumers, Consumer Groups, and a Zookeeper cluster. Producers publish messages to Kafka, where messages are stably stored on Brokers' log files in chronological order. Consumers read messages from the Brokers and support message re-reads. Kafka enables message broadcasting (where each message is read by multiple consumers) and load balancing (where each message is processed by only one consumer in a consumer group) through Consumer Groups.

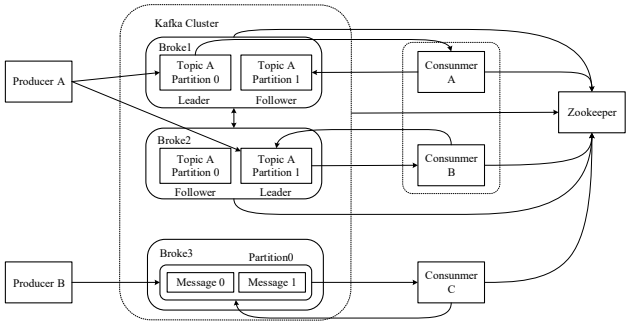

Figure 1: Kafka architecture diagram.

Zookeeper Cluster

Zookeeper is software that provides consistency services for distributed systems, maintaining configuration information, name registration, and distributed synchronization through a centralized service [3]. As a centralized coordination system for distributed applications, Zookeeper records all critical system status information, essential for the system's reliability and consistency.

In Kafka, Zookeeper manages cluster metadata and ensures synchronization among Brokers. Kafka utilizes Zookeeper for leader elections among Brokers, managing metadata of Topics, and monitoring cluster states, ensuring message availability and consistency in case of Broker failures. Each Kafka cluster includes a Zookeeper cluster to maintain consistent cluster status.

ELK STACK

The ELK technology stack, composed of Elasticsearch, Logstash, and Kibana, is a collection of three open-source tools mainly used for efficiently handling large data volumes through search, analysis, and visualization. The ELK

†Li Yukun, working on accelerator beam measurement and control.
E-mail: liyukun@ihep.ac.cn.

ISBN: 978-3-95450-249-3 ISSN: 2673-5350 doi: 10.18429/JACoW-IBIC2024-WEP51

NEW GRAPHICAL APPLICATION FOR HIGH-LEVEL SYNCHROTRON CONTROL WITH PARTICULAR EMPHASIS ON THE CORRECTION MODULE

M. Mleczko*, W. Wiatrowska, M. Floras, P. Andryszczak, E. Beyer
NSRC SOLARIS, Jagiellonian University, Krakow, Poland

Abstract

National Synchrotron Radiation Centre (NSRC) SOLARIS, as a big-science facility, is obliged to provide the best possible conditions for conducting research. Due to the complex nature of synchrotron subsystems, there is a strong need to provide the most convenient and intuitive control systems interface possible. This work aims to build graphical application in a specific architectural approach. The results of our work is a comprehensive tool which bonds crucial functionalities in high-quality-beam delivery.

INTRODUCTION

SOLARIS is a third generation light source operating at the Jagiellonian University in Krakow, Poland.

One of the primary goals of SOLARIS synchrotron is to deliver high quality beam for scientists across many different fields. SOLARIS offering various techniques, e.g., photoemission electron microscopy, X-ray absorption spectroscopy, ultra angle-resolved photoemission spectroscopy or multi-scale X-ray and multimodal imaging. What is worth to mention, SOLARIS provide two latest generation cryo-electron microscopes enabling life science researchers to unravel life at the molecular level [1].

Currently SOLARIS operate in twelve hour shift which requires two beam injections per day. To provide smooth operation we need a robust solution to successfully control all liniac and ring subsystems.

CORE CONCEPTS

Important assumptions in building a new application for operators were to implement it in modular architecture with well-known technologies.

Architecture

In order to achieve modular architecture, during the design stage, we exposed three main layers:

- *Device Server layer* which provide access to direct device control through their API,
- *Facade Device layer* where different signals from many devices are compiled by implementation of our own logic for particular widget by sharing two simple functionalities - attribute and command,
- *GUI layer* (interface) where each widget is connected to corresponding Facade Device with desirable logic.

It is a good intuition to think about those layers as a single stack functionality (shown in Figure 1) which can be connected into main structure.

This approach gives a flexibility in case of providing new functionalities in the future. What is even more important is fact that during applying any changes in application it does not interrupt other working parts. Logic we would like to add or remove is limited to single **separated** widget.

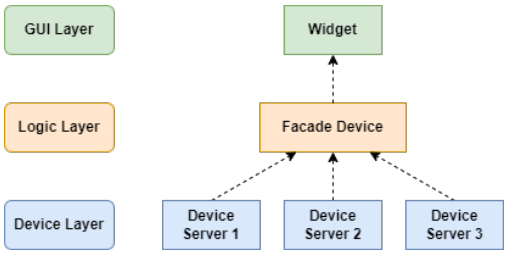

Figure 1: Example of single stack functionality.

Technologies

Main technology we use in control systems department is TANGO Controls Python Framework. Tango is an Open Source solution for SCADA and DCS [2]. It allows to create a convenient way to access and manage all physical devices in the synchrotron in one place. For this reason, it was used to create core, backend part of the application.

Frontend part was developed in PyQt graphic library.

FUNCTIONALITIES

Application covers couple of functionalities which helps in beam injection and ramping. However there is also a few of them which provides basic information about current condition of synchrotron.

General Information

One of the simplest is the widget with Machine Statuses (shown in Figure 2). It consists of information such as: *Machine State, Current, Energy, Lifetime* or *I*t* product. It also provides features to set appropriate flags like *Machine Day, Beamlines Day* or *Start Experiment*.

Another widget correlated with statuses of working synchrotron is Plena (shown in Figure 3). There are implemented features for playing messages via speakers placed in experimental hall as well as in Linac tunnel. During each stage of beam injection and ramping operators can inform users and other coworkers about current state.

* maciej.mleczko@uj.edu.pl

ISBN: 978-3-95450-249-3 ISSN: 2673-5350 doi: 10.18429/JACoW-IBIC2024-WEP52

DATA ACQUISITION AND PROCESSING PLATFORM DESIGN FOR SHINE WIRE SCANNER*

J. Dong†, J. Chen, S. S. Cao, F. Z. Chen, L. Y. Yu, R. X. Yuan, SSRF, Shanghai, China

Abstract

The Shanghai High repetition rate XFEL and Extreme light facility (SHINE) accelerates electrons to 8 GeV with a high repetition rate of up to 1 MHz. For the transverse beam profile measurement in the high energy sections wire scanner is used as an essential part of the accelerator diagnostic system, providing the tool to measure small beam size in an almost non-destructive manner. The prototype of the data acquisition and processing platform of wire scanner is designed and installed at the Shanghai soft X-ray Free Electron Laser (SXFEL) for verification. The experimental results show that the platform can be used for the SHINE.

INTRODCUTION

Motivated by the successful operation of X-ray FEL facilities worldwide and the great breakthroughs in atomic, molecular, and optical physics, condensed matter physics, matter in extreme conditions, chemistry and biology, the first hard X-ray FEL light source in China, the Shanghai HIgh repetition rate XFEL aNd Extreme light facility (SHINE) is under construction. The SHINE will utilize a photocathode electron gun combined with the superconducting to produce 8 GeV FEL quality electron beams with 1 MHz repetition rate [1].

Wire Scanner is widely used for beam profile measurements. A fork equipped with thin wires passes through the electron beam. The wire interaction with the beam produces scattered electrons and showered particles downstream the wire scanner unit which are detected by photomultipliers [2-3].

At the SHINE, each wire scanner unit consists of two motorized forks (horizontal and vertical plane) driven by a linear servo motor. This 90° configuration of motors helps to avoid vibration influences. Figure 1 shows a wire scanner motion unit installed at the SXFEL. A set of three 90° tungsten wires (20, 20 and 20 μm) is mounted on each fork. The wire position is measured with a magnetic railings ruler which has a resolution of 1.0 μm. The Beam Loss Monitors (BLMs) downstream of the wire scanner motion units are used for detection of scattered particles.

DATA ACQUISITION AND PROCESSING SYSTEM

The PMTs and preamplifiers, which convert the BLM Cherenkov light pulse and LED heartbeat light pulse into a time-shaped voltage signal, are mounted on the signal conditioning board. The BLM and Beam Position Monitor (BPM) signals are digitized and processed with the system. The magnetic railings ruler is installed next to the linear motor track to measure the position of wires. The signal outputted by the magnetic railings ruler is collected and analysed by the data acquisition board. The wire scan processing software calculates the beam parameters by merging the beam loss data, beam positions and the wires positions.

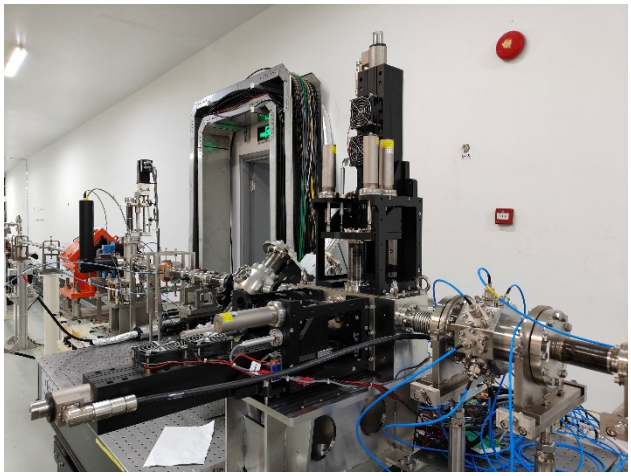

Figure 1: Wire scanner motion unit at the SXFEL.

Data Acquisition System

Figure 2 shows the structural block diagram of the data acquisition system. The analog signal acquisition module digitalizes the input signals and provides the trigger and clock interfaces. The operational amplifiers are used to convert the four input signals from single-ended to differential. The amplitude of the input signal can also be adjusted by changing the gain to maximize the ADC dynamic range. The buffers are used for external trigger signals and user-defined signals to improve their driving capabilities. The performance of operational amplifiers in the ADC front-end analog circuits directly affects the performance of the system. The fully differential amplifiers LMH5401 is selected. The LMH5401 device is a very high-performance, differential amplifier optimized for high-speed, ac or dc coupled, time-domain applications. The device is ideal for ac or dc coupled applications that require a single-ended-to-differential conversion when driving the ADC. The LMH5401 generates very low levels of second- and third-order distortion.

The quality of the sampling clock is one of the key factors determining the performance of the data acquisition system. The jitter of the sampling clock leads to the aperture error which affects the signal-to-noise ratio of the ADC and decreases the system performance. The clock of the ADC front-end analog circuits generated by the onboard crystal oscillator or external clock is used for the sampling clock, synchronization clock of ADC, and the FPGA high-speed serial transceiver. The HMC7044 is

* Work supported by the NSFC (Grant No. 12105346)
† email address: dongj@sari.ac.cn

ISBN: 978-3-95450-249-3 ISSN: 2673-5350 doi: 10.18429/JACoW-IBIC2024-WEP53

HIGH PERFORMANCE GENERIC BEAM DIAGNOSTIC SIGNAL PROCESSOR FOR SHINE*

Y. X. Han, Shanghai Institute of Applied Physics, Chinese Academy of Sciences, Shanghai, China
also at University of Chinese Academy of Sciences, Beijing, China
L. W. Lai†, Y. M. Zhou, Shanghai Advanced Research Institute, Chinese Academy of Sciences, Shanghai, China

Abstract

A generic signal processor has been developed for beam diagnostic system in SHINE. The stand-alone processor is used for the signal processing of stripline BPM, cavity BPM, cold button BPM, beam arrival measurement, bunch length measurement and other diagnostic systems. The main core is a SoC FPGA, which contains both quad-core ARM and FPGA on a chip. The ARM runs LINUX OS and EPICS IOC, and FPGA performs peripheral interfaces and high-speed real-time signal processing. An FMC carrier ADC board is mounted, which can sample 4 channels input signal with a maxi-mum sampling rate of 1 GSPS. The processor is equipped with a White Rabbit timing card, which can realize 1 MHz high repetition rate synchronous measurement. Lab test results and on-line beam tests prove that the processor has high performance. This paper will introduce the processor development and applications on SHINE.

INTRODUCTION

The Shanghai HIgh repetitioN rate XFEL and Extreme light facility (SHINE) is 30 m underground, with a total length of 3.1 km in Shanghai. The SHINE was constructed adjacent to the Shanghai Synchrotron Radiation Facility (SSRF) and the Shanghai Soft X-ray Free Electron Laser (SXFEL). It is initiated at the end of 2018, and to be completed at 2027. The facility is composed by injector, superconducting LINAC, undulators and beamlines. To meet different data acquisition requirements, we have developed a general beam diagnostics signal processor, which is used for the signal processing of stripline BPM, cold BPM, cavity BPM, BAM and BLM. SHINE needs about 500 beam diagnostics processors.

Other facilities have also developed generic electronics, such as European-XFEL [1] and SLAC LCLS-II [2]. Due to limitations in electronic device performance, a multi-FPGA system of EXFEL was developed, based on the VME64x architecture. The ADCs include a 16-bit, 160 MHz sampling rate ADC and a 12-bit, 500 MHz sampling rate ADC for different applications. The LCLS-II is based on the ATCA architecture and uses Kintex series FPGAs. The ADCs are16-bit with a sampling rate of 370 MHz to meet various application requirements.

* Work supported by The National Science Foundation of China (Grant No.12175239). Youth Innovation Promotion Association, CAS (Gant No.2019290). Outstanding member of the Youth Innovation Promotion Association, CAS. SHINE R&D and project.
† Corresponding author: lailw@sari.ac.cn

We have developed the self-developed Digital Beam Position Measurement processor (DBPM) [3], which was the first employed in the Dalian Coherent Light Source (DCLS) and the SXFEL. The DBPM is a one stand-alone processor with FPGA carrier board, an ADC board, and an ARM board. The ADC board has four input channels, the maximum sampling rate is 125 MHz, resolution is 16 bits, and bandwidth is 650 MHz. A XILINX Virtex5 FPGA is used as the core component on the carrier board.

The maximum repetition rate is 50 Hz of SXFEL. To meet the requirements for a 1 MHz high repetition rate and synchronized data acquisition and processing for SHINE, we developed the Generic Beam Diagnostic Signal Processor.

HARDWARE DESIGN

The processor is designed as a 1 U height standalone device, as Fig. 1. From the Fig. 2, we can see the core component is a Xilinx ZCU15EG FPGA, an ADC daughter board connected through FMC HPC interface, and a White Rabbit timing daughter board connected through FMC LPC interface. The external logic interfaces include 8 GB DDR4 on the PL (Programmable Logic) side and 4 GB DDR4 on the PS (Processing System) side to store raw ADC waveforms and processed data, two RJ45 connectors for Ethernet communication, 10Gbps SFP+ port, JTAG, SD slot, *et al.*. Table 1 lists the specification of processor.

Figure 1: Generic processor.

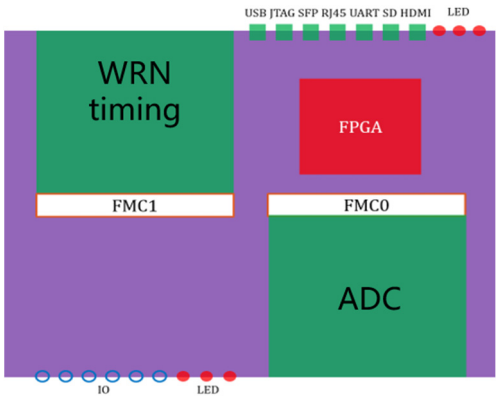

Figure 2: Processor structure.

ISBN: 978-3-95450-249-3 ISSN: 2673-5350 doi: 10.18429/JACoW-IBIC2024-WEP54

APPLICATION OF OPEN SOURCE HARDWARE IN THE BEAM LOSS MONITOR SYSTEM

Ying Zhao†, Linda Yu, Taoguang Xu, Jun He, Yanfeng Sui, Jianshe Cao
Institute of High Energy Physics, CAS, Beijing, China

Abstract

The High Energy Photon Source (HEPS) which is a fourth-generation synchrotron radiation source in China has begun commissioning since July, 2024. Beam Loss Monitor as one of the key beam instrumentation elements play an important role in the first turn and beam accumulation. An open-source hardware is applied in Beam loss Monitor system. This paper introduces SBLM electronics and the details of operating.

INTRODUCTION

High Energy Photon Source (HEPS) is a 4th generation light source which contains a 6 GeV, 1.3 km storage ring (SR), a 453 m booster injector (BS), a Linac pre-injector (LA) and three transfer lines (LTB, BTR, RTB) [1]. After successfully operating of the injector, the SR starts commissioning in July, 2024.

Beam loss monitor system is a key beam diagnostic tools for accelerators, it provides fast and sensitive signals to indicate machine status, and machine from damage.

There are two types of detector used in HEPS beam loss monitor system: scintillators and optical fibre. For SR, BS and transfer lines, scintillator (SBLM) is chosen. Optical-fibre (FBLM) is only used in BS. Most of the scintillators are equally distributed in the booster and storage ring. At least 4 detectors in each booster section and storage ring cell, extra ones are installed near the injection point and RF cavities or other. The detectors are removeable according to the demand. The distribution and quantity of HEPS BLM detectors are list in Table 1.

Table 1: Distribution of HEPS BLM Detectors

Location	Type	Detectors	Electronics
BS	SBLM	27	7
	FBLM	8	4
BTR	SBLM	20	5
RTB	SBLM	20	5
SR	SBLM	201	54

For totally 268 SBLM detectors, overall considering the costing and performance, an open source hardware is chosen for SBLM data acquisition (DAQ). In this paper, the design and prototyping test of DAQ system is described and preliminary commissioning results is also present.

ACQUISITION SYSTEM DESIGN

The purpose of the design needs to consider two aspects: as using such quantity of scintillators in BLM system is an extra plan after all budget has been fixed, therefor the design of the whole system should meet measurement requirements and be economical.

For choosing proper hardware and getting as much information as possible, types of scintillators have been tested in the Beijing Electron Positron Collider II (BEPCII) storage ring. The typical signal from detector is a negative pulse that about nanoseconds, it could be tens of nanoseconds after the transmission of a long coaxial cable which acts as a low pass filter. To ensure acquiring sufficient sampling points of the signal rising edge, the hardware must have appropriate sampling rate. Depending on the requirements, a commercial open source hardware -RedPitaya which has 14-bit ADC, 65 MHz bandwidth and 125 MHz sample rate is chosen to complete the data acquisition [2].

For making the full use of the board, 2 input RF channels are connected to the detectors which are nearby, as the cable length of the 2 detectors have equivalent length. A GPIO connector is used for trigger input for both the 2 input channels which means the delay of the 2 channels are changed simultaneously.

According to the demand of operating, the DAQ system should provides 2 modes: one is Integrate modes and another is Turn by Turn (TBT) modes. The integrate mode has been test in 2 methods: one is to add the pulse and averaging the data, second is to count the number of pulses which is over a fixed threshold. TBT mode provides the multiple turns of SBLM data as waveforms. The function of the 2 modes are completed by programs on board.

After testing in BEPCII, the counting method presents more sensitive. Figure 1 shows the result in integrate mode of SBLM acquisition electronics prototype in BEPCII decay mode. The blue and rose lines are the beam loss signal. The black and purple lines are DCCT data from the positron and electron ring. The detectors are located near the injection point, the integrate time is 1 second. The BLM signal has a high peak during the beam injection and taper off as the beam current decreasing. Green and red lines are 2 other SBLM which are in different location show less significant beam loss.

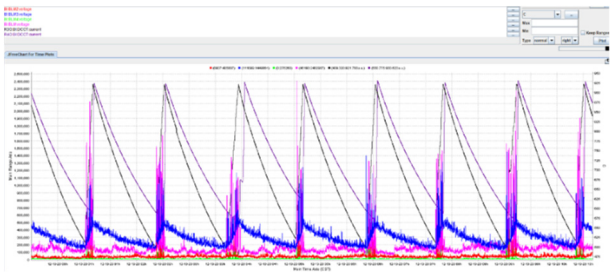

Figure 1: SBLM data and DCCT current data in BEPCII.

†zhaoying@ihep.ac.cn

ISBN: 978-3-95450-249-3 ISSN: 2673-5350 doi: 10.18429/JACoW-IBIC2024-WEP55

HIGH-SPEED ADC AND HIGH-SPEED DAC MicroTCA.4 AMC-RTM PAIR FOR A MULTIPLE OF DIAGNOSTICS AND FEEDBACK IMPLEMENTATIONS

S. Jablonski*, B. Boghrati, C. Guemues, M. Fenner, S. Pfeiffer, H. Schlarb, J. Zink
Deutsches Elektronen-Synchrotron DESY, Germany

Abstract

We present the MicroTCA.4 electronics modules, an AMC-RTM pair, for direct sampling of wideband signals with high-speed ADCs, versatile digital signal processing with the AMD RFSoC, and driving of wideband signals with high-speed DACs. The Zynq UltraScale+ RFSoC Gen 3 at the core of this system was primarily designed for telecommunication and especially software-defined radio (SDR) but also found other applications in various scientific experiments, which we will discuss in this paper. This component not only allows for the implementation of multiple diagnostics but also enables the creation of wideband feedback systems, thanks to the driving capabilities of its DACs.

This work presents a hardware architecture and shows how the modules can be set up and configured. The performance and functionalities are discussed, with particular attention paid to system noise, which is essential for high-precision scientific research.

INTRODUCTION

Modern ADC and DAC technology development allow high-frequency sampling clocks and the measurement/generation of wideband low-noise signals. Due to improved signal processing capabilities, more and more applications are simplifying their hardware by getting rid of analog down converters, shifting the measured signal bandwidth to baseband, and using the direct sampling technique. In this paper, we present two MicroTCA.4 modules, i.e. DAMC-DS5014DR and DRTM-MBFB-FE (see Fig. 1), referred to as later the AMC and the RTM. They are interconnected over Zone 3 Class RF1.1. The AMC can also be used with any other RTM (designed according to Class RF1.1) needed for special analog processing, which is not covered by any assembly version DRTM-MBFB-FE.

AMC MODULE

Zynq UltraScale+ RFSoC Gen 3

The core component for the AMC module is the RFSoC. The module offers low-noise ADCs with a high-sampling rate of 5 GS/s, with a wide input bandwidth of 6 GHz, and low-noise DACs with a high sampling rate of 10 GS/s, which are attractive components for a multiple of scientific applications. Additionally, the RFSoC includes plenty of digital resources and two different classes of ARM processors for versatile processing implementations. The detailed description of the RFSoC IC can be found in [1].

Analog Front-End and Back-End

In the AMC, various assembly options are designed to use the entire ADC/DAC bandwidth, including DC or AC coupling. The DC coupling requires an active front-end component based on a fully differential amplifier, which produces significant harmonics, especially at frequencies more than about 2.5 GHz, and other nonlinear products of input signals. If the measurement of a DC component is not needed and the input signal is >10 MHz, it is best to use the passive front-end based on an RF balun. The measured signals can be provided by the front panel or the Zone 3 connector. This is detailed further in the "Class RF1.1 Zone 3" section.

Communication Interfaces

Data can be transferred over the standardized AMC connector (see [2]) or the front panel connectors. Ports 4-15 of the AMC connector are connected to three of the FPGA's quad GTY transceivers. One quad GTY is used for PCIe 4.0 x4 (64 GT/s) that provides communication with all other AMC modules over the MCH root complex. The rest of the GTYs are connected to other AMC modules over low-latency point-to-point links (depending on the AMC backplane). Optionally, two quad GTYs can be used for PCIe 4.0 x8, but the number of point-to-point links is reduced. Ports 17-20 are MLVDS lines dedicated to timing and trigger distribution, which are critical for time-stamping data in scientific research.

The fourth quad GTY is connected to the QSFP28 optical transceiver and is accessible from the front panel. It can be used for applications such as PCIe 4.0 x4 or 100 GbE communication. USB-C connector on the front panel with USB 3.2 Gen 1 and DisplayPort.

Memory

The AMC module includes a few volatile and non-volatile memory units connected to the PL and PS banks of the RFSoC. The available non-volatile memory for fast data processing are a PS DDR4 (16 GB, 64 bit x 2400 MT/s) and two PL DDR4 (16 GB, 64 bit x 2666 MT/s each). The non-volatile memory storing the firmware, configuration data, and calibration parameters are QSPI Flash, micro SD card, and 16 GB eMMC.

* szymon.jablonski@desy.de

ISBN: 978-3-95450-249-3 ISSN: 2673-5350 doi: 10.18429/JACoW-IBIC2024-WEP56

DESIGN OF BEAM COLLIMATOR CONTROL SYSTEM FOR HEPS

Shutao Zhao, Haijing Wang, Chunhua Li, Jianshe Cao, Dapeng Jin, Nian Xie, Jia Liu, Siyu Chen
Institute of High Energy Physics, Chinese Academy of Science, Beijing, China

Abstract

The collimator for the High Energy Photon Source (HEPS) primarily intercepts lost particles caused by the Touschek effect, reducing beam losses in non-target areas, and serves as a dump station for equipment protection during emergencies. Utilizing EtherCAT industrial Ethernet technology ensures precise control, while LVDT sensors are employed for position calibration due to the intense radiation environment. The system incorporates multiple layers of safety protection, including software limits, mechanical limit switches, and emergency stop switches. Remote control is achieved through an EPICS architecture with communication between the EPICS IOC and the system via MODBUS TCP protocol. System testing indicates that the collimator achieves a repeatability precision of ±0.01 mm, validated the reliability and accuracy of the system.

INTRODUCTION

The High Energy Photon Source (HEPS) is one of the key construction projects during China's 13th Five-Year Plan, dedicated to providing high-quality synchrotron radiation to support cutting-edge scientific research. The design and implementation of the collimators are crucial for enhancing the overall performance of HEPS. HEPS is equipped with four collimators located at the R03, R15, R27, and R39 units of the storage ring. Each collimator consists of two independent stages driven by motors to achieve high-precision automatic horizontal adjustment, with a required repeatability of position ≤0.02 mm, and the capability to operate reliably in a high-radiation environment. The actual installation of the collimator in HEPS storage ring is shown in Figure 1.

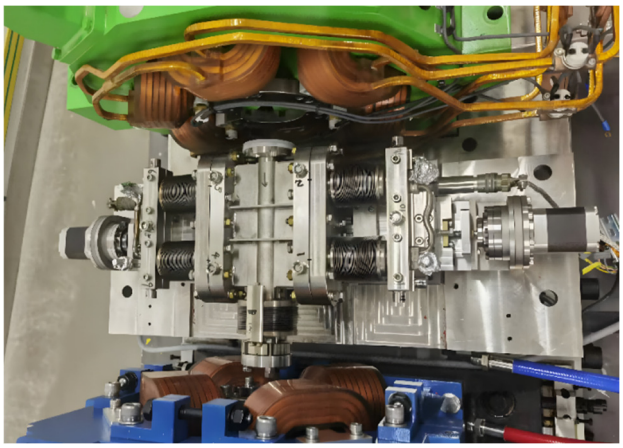

Figure 1: A collimator in HEPS storage ring.

SYSTEM DESIGN

EtherCAT Control Architecture

The EtherCAT control architecture employs a distributed system design based on EtherCAT industrial Ethernet bus technology, leveraging its capabilities for high-speed data transmission and high-precision synchronization to ensure precise control of the collimator [1]. The system consists of a master station and multiple slave stations, where the master station is responsible for issuing control commands and collecting feedback information; the slave stations include drive units for stepping motors and I/O modules for sensor signal acquisition. The schematic diagram of the EtherCAT architecture for the collimator control system is presented in Figure 2.

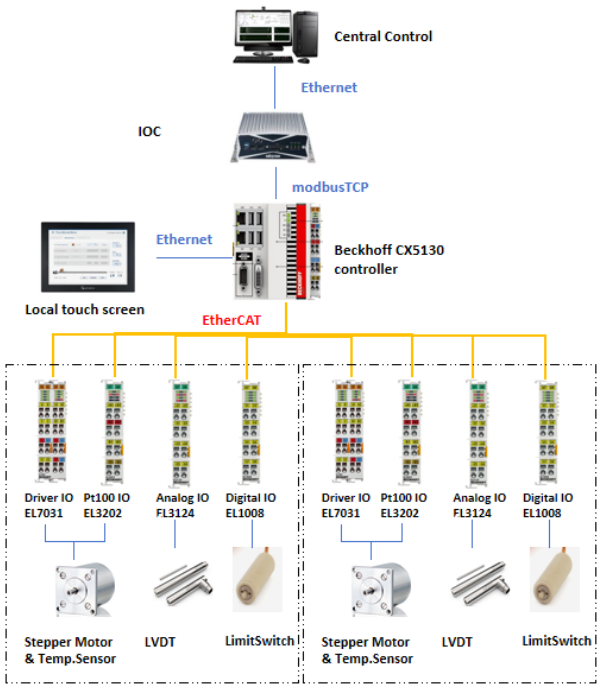

Figure 2: EtherCAT control architecture of collimator.

- Master Controller: A Beckhoff CX5130 embedded controller equipped with licensing for 10-axis drives and supporting the MODBUS/TCP protocol.
- Stepper Motor Driver: The Beckhoff EL7031 stepper motor driver, capable of driving stepper motors with high microstepping ability, achieving a resolution of 64 microsteps.
- Stepper Motor: Radiation-resistant stepper motors from AML UK, model D42.2, with a step angle of 1.8°.

The lead screw pitch of the stage is 5 mm, resulting in a calculated motion resolution of 0.08 micrometers. With this design, the system achieves high-precision motion

ISBN: 978-3-95450-249-3 ISSN: 2673-5350 doi: 10.18429/JACoW-IBIC2024-WEP58

BEAM DIAGNOSTICS CONTROL SYSTEM UPGRADE OF IPM LINAC

P. Navidpour†, S. Mohammadi Alamouti, Z. Rezaei
Iranian Light Source Facility (ILSF),
Institute for Research in Fundamental Sciences (IPM), Tehran, Iran

Abstract

A series of upgrades has now begun to industrialize the applications of the experimental IPM electron LINAC. This includes upgrading the control system of the diagnostics tools and adding new tools and equipment to the system as well.

The aim is to build an integrated control system to collect and manage all diagnostics signals. This will allow us to continuously monitor and archive all of the beam parameters for LINAC performance analysis and improvement. It is hence decided to migrate from LabVIEW to an EPICS-based control system which has many advantages in this regard. In the meantime, it is also required to employ more modern equipment with better control interfaces and add some extra diagnostics tools to the system as well. So during this upgrade, most of the job would be developing new control interfaces and high-level applications accordingly.

In this paper, after a brief summary of the current diagnostics tools and our motivation for this upgrade, the scheme of the new control system and how different parts are integrated to the EPICS framework will be described.

INTRODUCTION

The experimental IPM LINAC has been in operation for a few years. Being first-of-a-kind project in the country, it was mainly intended to provide experience in accelerator science and technologies. However, over the past years it has gone well beyond this initial goal by serving as an X-ray source in several experiments as well.

After commissioning of the LINAC with 4 MeV beam energy, the original developers introduced a plan to reach higher energies in several phases. They installed a beam profile monitor system and a faraday cup (diagnostics station) at the most downstream of the LINAC in order to measure the beam properties at each phase [1].

Since then, the Iranian Light Source Facility (ILSF) has been cooperating with IPM in controlling and maintaining various LINAC subsystems. Now that it is decided to expand the applications of this LINAC, the ILSF control team was assigned to identify the hardware and software requirements and implement the required solutions afterward. In this paper, the preliminary steps to facilitate this process, with a focus on the beam diagnostics control system will be discussed.

MOTIVATION

Although an EPICS-based control system was initially considered for the commissioning of the LINAC, the original developers ultimately opted for a LabVIEW-based system due to their team's proficiency in it. While the LINAC has been operating successfully since then, there is a significant challenge ahead with the upcoming upgrades. The original source code of the LabVIEW design is not available at hand, and this poses a problem since without the source code, making upgrades or modifications can be difficult or nearly impossible. Since the current design also lacks some sort of standardizations, it is concluded that a complete redesigning based on a popular free open-source software is a necessary course of action. With this approach, we can make sure that the implemented solutions are previously tested, cost-effective, and reliable.

THE EXISTING CONTROL SYSTEM

The layout of the existing beam diagnostics control system is depicted in Fig. 1. The so-called diagnostics station is located at the most downstream of the LINAC. Originally, it was consisted of a beam profile monitor and a faraday cup. Recently an in-house designed FCT has also been added to this setup as well. The output signals from these tools are visualized by an oscilloscope and a spectrum analyzer respectively. It is also possible to connect the spectrum analyzer to the LabVIEW control system for monitoring the RF input pulses.

The controllable components of the beam profile monitor system are the CCD camera and the screen mover system. The CCD camera is GigE Vision compliant. It is directly connected to a PC running LabVIEW NI Vision. This PC is dedicated to acquire and visualize the camera data. Similarly, the mover system is interfaced with another PC by a Moxa serial device server. This PC is running a Lab-VIEW application to control the screen position. This PC controls the whole LINAC except the camera GUI.

Unfortunately, the source codes of the applications running on these PCs are not available, and consequently, adding new tools to the GUI applications is impossible. The same issue arises with the custom designed boards of the timing system and the serial interface board (yellow parts in the Fig. 1). Self-developed codes running on these boards are not accessible either. So in order to tackle this problem, these self-developed hardware and software components will be replaced and an integrated control system based on EPICS will be built from scratch.

THE NEW CONTROL SYSTEM

Before proceeding with the upgrade, it is necessary to choose a standard based on our needs and requirements. This will help keeping consistency while designing different levels of the control system and working with different software and hardware platforms. For this reason, the first step was choosing the core software and corresponding communication protocol and network architecture.

† p.navidpour@ipm.ir

ISBN: 978-3-95450-249-3 ISSN: 2673-5350 doi: 10.18429/JACoW-IBIC2024-WEP59

BEAM PROFILE MONITORING USING INCOHERENT CHERENKOV DIFFRACTION RADIATION AND SCINTILLATING SCREENS AT ILSF

Z. Rezaei†, S. Mohammadi A., N. Khodabakhshi, P. Navidpour, S. Ahmadiannamin
Iranian Light Source Facility (ILSF),
Institute for Research in Fundamental Sciences (IPM), Tehran, Iran
Z. Pouyanrad, Amirkabir, University of Technology, Tehran, Iran
K. Noori, Iran University of Science and Technology, Tehran, Iran

Abstract

The Iranian Light Source Facility (ILSF) plays a crucial role in advancing accelerator science and applications. In this study, we explore innovative techniques for precise beam profile monitoring, focusing on two complementary methods: Incoherent Cherenkov Diffraction Radiation (ChDR) and scintillating screens. Incoherent ChDR occurs when a charged particle passes through a dielectric medium with a velocity exceeding the phase velocity of light in that medium. This phenomenon leads to the emission of electromagnetic radiation in the form of a cone. Our investigation focuses on incoherent ChDR as a powerful tool for beam position diagnostics. By analysing the angular distribution of ChDR photons, we extract valuable information about the transverse position of the electron bunch. Our simulations demonstrate the feasibility of ChDR-based diagnostics at ILSF. We discuss optimal radiator materials, and geometries.

In addition, we examine the use of YAG scintillating screens as beam profile monitors. We present detailed considerations on screen material, thickness, and the optimal orientation of the detection system to ensure high-resolution measurements.

By utilizing both ChDR and radiation from scintillating screens for comparison, we can ensure reliable and accurate beam profile measurements at ILSF.

We believe that our research significantly contributes to the development of robust and efficient beam diagnostics at the storage ring of ILSF.

INTRODUCTION

Beam diagnostics is of prime importance for the effective operation of particle accelerators. Among the various diagnostic techniques available, non-invasive ones are more advantageous as they allow continuous monitoring without disrupting the beam. Since the first observation of incoherent Cherenkov diffraction radiation (ChDR) with 5.3 GeV positrons in a 2 cm long fused silica radiator at Cornell electron-positron storage ring [1], the possibilities of ChDR as a non-destructive beam diagnostics have been extensively investigated [2, 3]. In recent years, coherent and incoherent ChDR have been employed as non-invasive beam length and position monitors in accelerator facilities worldwide [2, 4].

† Rezaei.zahra1984@gmail.com

Table 1: Beam Parameters of ILSF Storage Ring in the Middle of its Straight Sections [5]

Parameter	Value
Beam Energy	3 GeV
Beam Current	100 mA
Horizontal Beam Size (rms)	68.9 μm
Vertical Beam Size (rms)	2.96 μm

SIMULATION RESULTS

Cherenkov Diffraction Radiation [5]

The experimental chamber for this diagnostic will be located in the middle of straight sections of the ILSF storage ring, where the background synchrotron radiation from the bending magnets is reduced. The parameters of the electron beam in the storage ring are listed in Table 1.

In this chamber, the ChDR spectrum emitted from a prismatic dielectric radiator, when the electron beam moves parallel to one of its sides at a distance b, has two polarization components: vertical, which is perpendicular to beam motion, and horizontal, which is parallel to it. The spectral-angular distributions of these two polarization components are discussed in detail in Ref. [6].

The impact parameter, which is the perpendicular distance between the beam's trajectory and a reference point, influences the detected wavelengths of ChDR, as shown in Fig. 1. This wavelength dependence indicates that for a ChDR-based beam position monitor at ILSF, the optical system must account for the impact parameter. Specifically, for a working range in the millimetre region, the optical system should be optimized for optical wavelengths. Furthermore, a ChDR beam halo monitor would benefit from an optical detection system sensitive to shorter wavelengths to suppress signals from the beam's core.

In Fig. 2, the angular distribution of an electron for different wavelengths is plotted. In this figure, the impact parameter is $1mm$, and the index of refraction of the fused silica is 1.46. As it is clear in this figure, the radiation intensity decreases for shorter wavelengths. Additionally, the azimuthal distribution of horizontally polarized radiation for arbitrary θ and $\phi = 0°$ is zero, as evident in Fig. 2(b), due to symmetry of radiation.

ISBN: 978-3-95450-249-3 ISSN: 2673-5350 doi: 10.18429/JACoW-IBIC2024-WEP60

INTEGRATING InfluxDB AND GRAFANA IN A DOCKERIZED CA EPICS MONITORING SYSTEM

Z. Y. Qi, T. Q. Wang, Z. Q. Shen, L. C. Zhao, Q. M. Chen, J. L. Liu†
Harbin Institute of Technology, Harbin, China

Abstract

A data monitoring system based on CA and EPICS designed for particle accelerators is proposed, which leverages Docker containers for deployment and integrates InfluxDB for data storage and Grafana for data visualization. The Data Collection Engine built with Python gathers data through EPICS Channel Access, caches it temporarily, and stores it permanently in InfluxDB. A two-level cache design is used to optimize data access. The monitoring system also offers a web application for configuration management and a web application for online data access and visualization in real-time, which provides a powerful and user-friendly solution for data collection, storage, visualization, and management in particle accelerator experiments.

INTRODUCTION

The Space Environment Simulation and Research Infrastructure (SESRI) under construction at Harbin Institute of Technology (HIT), China, represents a significant leap forward in our ability to recreate the harsh radiation environment of space on Earth.

Tailored Particle Beams: The Power of ECR Ion Source and Linac Injector

A critical aspect of SESRI's success lies in its ability to produce a diverse range of particle beams that mimic the complex composition of space radiation,which is shown in Fig. 1.

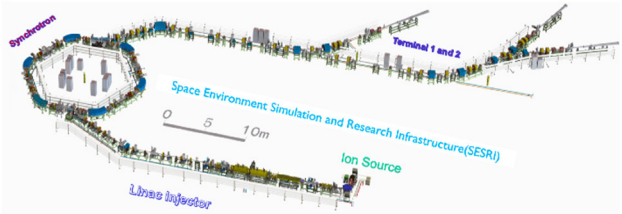

Figure 1: General scheme of the facility.

This is achieved through the synergistic operation of two key components:

ECR Ion Source: This state-of-the-art source efficiently generates a broad spectrum of stable nuclide beams, encompassing light elements like hydrogen (H_2) to heavier elements like bismuth (Bi). This versatility allows researchers to study the interaction of various space radiation types with target materials.

Linac Injector: The ECR source feeds the ions into a Linac injector, which serves as a particle booster. The Linac utilizes two specialized structures:

RFQ (Radio Frequency Quadrupole): This initial stage efficiently focuses and bunches the ion beam for further acceleration.

IH-DTL (Interdigital H-mode type Drift Tube Linac): This advanced structure significantly increases the ion beam energy, reaching 1 MeV/u for heavy ions and 5 MeV for protons.

Reaching High Energies: The Role of the Synchrotron

Following the initial boost from the Linac injector, a powerful synchrotron takes over the acceleration process. This remarkable machine propels the particles to even higher energies, critical for simulating the high-energy component of space radiation. The synchrotron can accelerate heavy ions up to a staggering 85 MeV/u and protons to a phenomenal 300 MeV.

Controlled Extraction: Achieving Experimental Flexibility

Extracting the accelerated particles in a controlled manner is essential for downstream experiments. SESRI employs two well-established techniques for this purpose:

3rd Integer Resonance: This method leverages the natural resonance behavior of particles within the synchrotron's magnetic field. By carefully controlling the magnetic field strength, researchers can achieve controlled extraction of specific particle energies.

RF-KO (RF-Knock-Out): This technique utilizes precisely timed radiofrequency pulses to nudge targeted particles out of the synchrotron's orbit, enabling controlled extraction for specific research needs.

The combination of a versatile ECR ion source, a multistage Linac injector, and a high-energy synchrotron positions SESRI's accelerator complex as a powerful tool for simulating the space radiation environment. This innovative facility holds immense potential for researchers studying the effects of space radiation on various materials, devices, biological entities, and complex space systems. The ability to control particle extraction through techniques like 3rd integer resonance and RF-KO further enhances the experimental flexibility of SESRI, paving the way for groundbreaking discoveries in space science and related fields.

DOCKER VIRTUALIZATION CLUSTER TECHNOLOGY IN PARTICLE ACCELERATORS

Particle accelerators are complex and expensive machines that are used to study the fundamental building blocks of matter and energy, becoming increasingly data-

† email address: liujianli@hit.edu.cn.

ISBN: 978-3-95450-249-3 ISSN: 2673-5350 doi: 10.18429/JACoW-IBIC2024-WEP61

TRANSVERSE PROFILE MEASUREMENT OF BEAM FOR 230MeV PROTON THERAPY BEAMLINE USING SCANNING WIRES

Tianyi Jiang, Zhiguo Yin†, Yang Wang, Yongjun Ma, Rui Xiong, Qiqi Song, Tianjue Zhang
China Institute of Atomic Energy, Beijing, China

Abstract

A superconducting cyclotron-based proton therapy system has been developed at the China Institute of Atomic Energy (CIAE). For the 230 MeV proton therapy cyclotron (CYCIAE-230), the beam profile is crucial for the adaptation of the proton therapy planning system and an important basis for the commissioning of the beam line. CIAE designed the scanning wires device for the proton therapy facility, which is for high-resolution profile measurements. A readout electronics unit with fA resolution has been included to adapt to the small signal of scanning wires. The data process unit uses ZYNQ-7035 together with 24-bit ADCs and transmits measurement results via MODBUS TCP protocol. The diagnostic electronics are placed close to the beam profile monitors (BPM) to reduce the analogue signal transmission distance. To adapt to the mode of the pulse beam during the beamline commissioning, using the RF system signal trigger sampling, to prevent the signal aliasing. Besides that, a Butterworth filter and a mean filter were used to filter measurement noise. The design of this scanning wire diagnostic system will be reviewed in this paper, together with several measurement results.

INTRODUCTION

CIAE is developing a 230 MeV superconducting cyclotron, a commercial prototype that can be used for proton therapy, which is designed to induce energy of 242 MeV and beam current over 300 nA [1,2]. During the beamline commission, CIAE used scanning wire to measure beam position and profile. Along the beamline, 7 BPM units have been included in the system. The scanning wire is designed as a double wire structure with an angle of 90°. The measuring target is a long blade of Be-Cu with a width of 5 mm and a thickness of 0.1 mm. The bias wire of Mo-Au is symmetrically installed on both sides of the measuring blade, the distance is 5 mm, and the diameter of the bias wire is 0.1 mm. Beam current limits are set at 10 uA due to heating of the blades or from beam trips caused by scattering. The motion unit is guided by a linear slide fitted with two guide blocks and welded stainless steel bellows. A stepper motor drives head movement and a linear variable differential transformer (LVDT) is used to provide head position. BPM boxes are installed at a 45° angle and have been precision manufactured to allow changing of monitor drives without realignment. Two signal blades pass through the beam at a 45° angle. Horizontal and vertical blades provide X and Y beam information (see Fig. 1).

Due to the low proton therapy beam current during beam line commissioning and the low secondary electron emissivity is low, the signal measured by scanning wires is only a few picoampere which is hard to process. A readout electronic has been designed to measure fA signal and a data process unit has been included to filter noise for high-resolution signal acquisition.

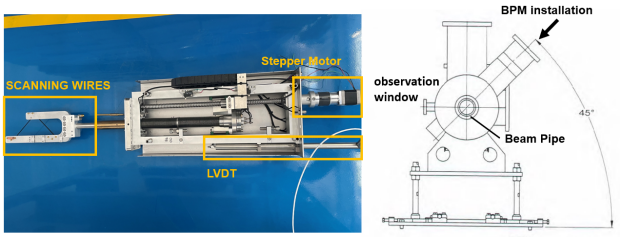

Figure 1: The scanning wires.

READOUT ELECTRONICS FOR SMALL CURRENT

The Basic Principle of Feedback Amplifier

The principle of the readout electronics is based on feedback amplifiers (see Fig. 2).

$$V_O = -I_{in} \times R \quad (1)$$

where R is a high-resistance resistor and the input impedance of the op-amp is much higher than R [3]. Feedback amplifier sensitivity increases as the value of the resistor R increases. The C is a feedback capacitance which is used to ensure the stable close-loop operation.

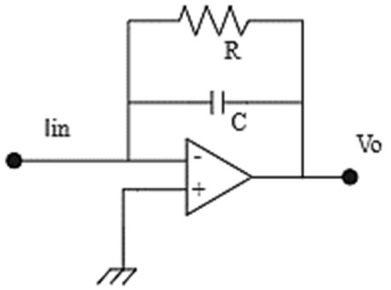

Figure 2: Basic schematic of feedback amplifier.

Design of Readout Electronics

Low input bias current (⩽20 fA) amplifier ADA4530-1 used in the readout electronics. During the beamline commission, the beam current is about 1 nA. Considering the secondary electron emissivity, it is estimated that the measured signal of the scanning wire is about 0-100 pA [4,5]. The feedback resistance is set to 10 GΩ, so the measurement sensitivity can reach 1 mV/pA. A triaxial cable is used to transmit input signals. The inner-conductor of the triaxial cable is connected to the pin2 and pin7 of ADA4530-1 to form a guard ring which is designed to reduce leakage current [6]. Besides that, two ultrahigh PSRR linear

† email address: bitbearat@hotmail.com

ISBN: 978-3-95450-249-3 ISSN: 2673-5350 doi: 10.18429/JACoW-IBIC2024-WEP63

DESIGN AND PERFORMANCE TEST OF 8 CHANNEL 125 MS/s DIGITIZER WITH 16-BIT RESOLUTION FOR BPM AND LLRF APPLICATION

Qiutong Pan, Tao Xue, Haoyan Yang, Bo Liang, Lin Jiang, Tsinghua University, Beijing, China

Abstract

In this paper, a mezzanine card is designed based on high speed ADC for particle accelerator field. FPGA firmware was built to realize high-speed A/D conversion. The performance of the ADC on the board was tested. The experimental results show that the ENOB of the ADC with a sampling rate of 125 MSPS can be as high as 12.6.

MANUSCRIPTS

In modern accelerator applications, stringent requirements are placed on the noise performance of digital converters. The noise from the digital converter will become part of the field noise seen by the beam, thus necessitating a low-noise, low-crosstalk digitizer. In response to this demand, this paper presents the design of a digital converter circuit board with 8 analog-to-digital converter (ADC) channels which has been subjected to testing. The test results indicate that the circuit board possesses low noise characteristics, rendering it suitable for reading accelerator signals.

Hardware Design

Figure 1 is the design block diagram of the mezzanine card. The circuit board has 8 SSMC RF connectors, providing 8 analog signal inputs for the ADC. The single-ended analog signal is converted into a differential signal after passing through the fully differential ADC driver. In addition, in order to facilitate the adjustment of the DC voltage component at the ADC input, the DAC output set voltage value is also required to be connected to the reverse input of the fully differential amplifier. The input clock of the ADC is 125 MHz, which is provided by the FMC connector. After the ADC collects and converts the analog signal, it is transmitted to the FMC connector in the form of an LVDS signal, and then provided to the FPGA.

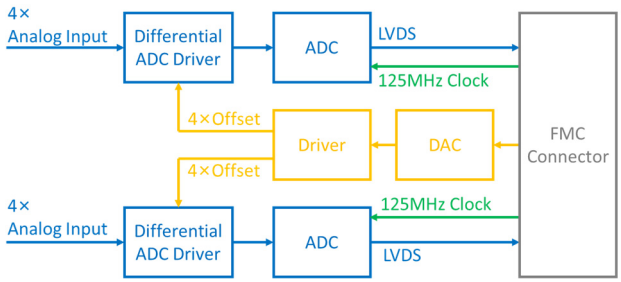

Figure 1: Block diagram of the design.

Figure 2 is the design PCB drawing of the mezzanine card, and Figure 3 is the actual picture of the PCB after welding. The PCB has a total of 8 layers, which can be divided into ground, power and signal layers. When designing, attention should be paid to impedance matching and data line length processing. In addition, during the design process, through a brief evaluation of noise, a low-noise power supply solution was selected to achieve better performance.

The ADC is ADI's AD9653, which is a 4-channel, 16-bit, 125 MSPS ADC with a conversion rate of up to 125 MSPS, excellent dynamic performance and low power consumption. The DAC is ADI's AD5686, which is a low-power, four-channel, 16-bit buffered voltage output DAC.

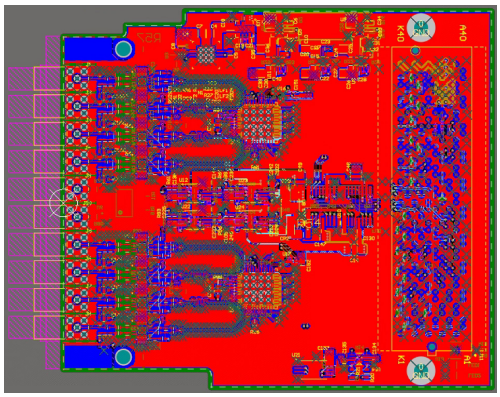

Figure 2: PCB design drawing.

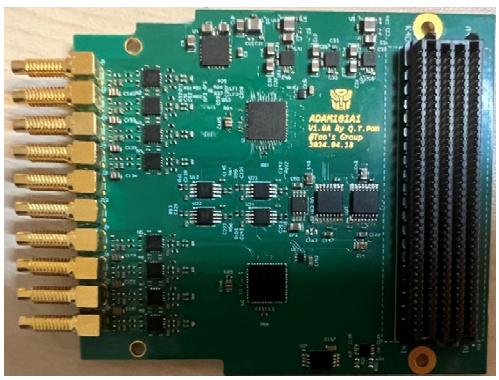

Figure 3: PCB picture.

Firmware Design and Experiment

The FPGA readout firmware is designed refer to the timing diagram in the AD9653's datasheet. The ADC readout firmware logic block diagram is shown in Figure 4. The figure shows the readout logic for only one channel; the other channels are similar.

ISBN: 978-3-95450-249-3 ISSN: 2673-5350 doi: 10.18429/JACoW-IBIC2024-WEP64

HIGH-RESOLUTION QUAD-CHANNEL PICOAMMETER: CHARACTERIZATION AND COMMISSIONING

L. Y. Tanio†, F. H. Cardoso, M.M. Donatti
Brazilian Synchrotron Light Laboratory (LNLS), Campinas, Brazil

Abstract

To address the high demand for precise low current measurements at the Sirius accelerators and its beamlines, a quad-channel high-resolution Ethernet picoammeter has been designed. The instrument can measure currents ranging from picoampere to milliampere across eight selectable ranges, featuring integrated ADCs enabling sample rates of up to 2 ksps and synchronization capabilities. This work aims to describe the design, characterization, and calibration results of the instrument. Special attention will be given to evaluating trigger latency, synchronization outcomes, as well as the device's installation and commissioning at beamlines, particularly for critical applications like on-the-fly scanning experiments. Furthermore, we will explore the interplay between trigger period, digital filter bandwidth, and front-end analog bandwidth to optimize signal-to-noise ratio in specific applications.

INTRODUCTION

This work briefly describes the hardware design, focusing on the signal path and triggered mode acquisition time analysis. There is also a discussion about the linear fit algorithm for the bandwidth and RMS current noise calculation. This paper is organized as follows: the first section discusses the hardware design, the second section presents the picoammeter operating modes, the third section performs a time analysis of triggered mode, and the fourth section presents results about the linear fitting, the trigger time analysis, and a beamline experiment. Finally, the fifth section outlines the conclusion for each section.

HARDWARE DESIGN

The quad-channel picoammeter comprises four key blocks: a current-to-voltage amplifier, an analog-to-digital converter (ADC), a microcontroller and the external interface as shown in the simplified block diagram in Figure 1. The detailed device architecture of the quad-channel picoammeter is discussed in [1].

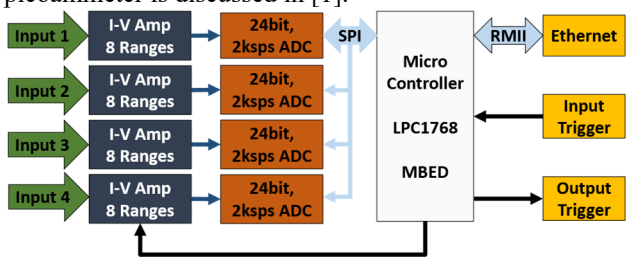

Figure 1: Quad-channel picoammeter simplified block diagram.

Analog Front-End Circuit

For each independent channel, an analog front-end circuit is composed by two fundamental blocks: the current-to-voltage amplifier, and the ADC that digitalizes the output voltage from the first block.

It is important to point out that besides the current conversion and the digitalization, both blocks also behave as low-pass filters, as shown in Figure 2.

Figure 2: Analog front-end circuit block diagram.

Current-To-Voltage Amplifier

The multi-range transimpedance amplifier was the topology selected to perform the current-to-voltage conversion due to the wide measurement range, low bandwidth applications, and noise concerns, as discussed in [1, 2].

Each current-to-voltage converter features eight selectable ranges with specific characteristics. Table 1 shows the theoretical values of the full-scale, sensitivity, and bandwidth for each selectable range.

Table 1: Transimpedance Amplifier Theoretical Characteristics: Full-Scale, Sensitivity, and Bandwidth

Scale	Full Scale	Sensitivity	Bandwidth
1	250 pA	100 pA/V	16 Hz
2	2.5 nA	1 nA/V	154 Hz
3	25 nA	10 nA/V	702 Hz
4	250 nA	100 nA/V	702 Hz
5	2.5 µA	1 µA/V	702 Hz
6	25 µA	10 µA/V	702 Hz
7	250 µA	100 µA/V	702 Hz
8	2.5 mA	1 mA/V	702 Hz

Analog-To-Digital Converter (ADC)

Considering most beamline applications: high resolution and low-speed measurements, the selected ADC features a Σ-Δ topology, 24-bit resolution, and 10 selectable sampling rates from 5 SPS to 2000 SPS. Each ADC configuration has a digital filter specification that implies different filter shapes and cutoff frequencies.

† lucas.tanio@lnls.br

ISBN: 978-3-95450-249-3 ISSN: 2673-5350 doi: 10.18429/JACoW-IBIC2024-WEP65

DESIGN OF DATA TRANSMISSION SCHEME BASED ON RDMA

Y. Q. Zhang, K. Zhou, M. Li, R. S. Mao, Institute of Modern Physics, Lanzhou, China

Abstract

With the development of precise radiotherapy, high-throughput data transmission has become a critical component of beam diagnostics. As the volume of generated measurement data rapidly increase, the data transmission mode that utilizes traditional Ethernet protocol, remote CPU and operating system to control memory read and write can not meet the transmission performance requirements. To break through these bottlenecks and achieve more real-time and efficient data transmission and processing, this paper designs a prototype data transmission system based on RDMA technology. By directly transferring memory data between hosts, the system bypasses the operating system kernel and CPU intervention, thereby minimizing transmission latency and enhancing data throughput. The system utilizes the RoCE v2 network protocol and is implemented through the libibverbs dynamic link library to establish stable RDMA sessions and develop corresponding network programs. Performance evaluations in terms of transmission latency, throughput, and CPU utilization indicate that the network transmission scheme proposed in this paper offers lower latency, higher throughput, and reduced CPU usage compared to schemes using the TCP protocol during large-scale data transfers.

INTRODUCTION

RDMA is a network protocol that enables the rapid transfer of data from one system to the memory of a remote system over various network technologies (such as InfiniBand or TCP/IP) without impacting the operating system. It eliminates context switching and data copy operations, thereby freeing up bus bandwidth and CPU cycles to enhance the performance of application systems. This paper designs a data transmission scheme based on RDMA technology by utilizing the OFED (OpenFabrics Enterprise Distribution) open-source project and the rdma-core user-space library. After a comprehensive consideration of compatibility, cost, and performance, the RoCE protocol, which offers a good balance of lower cost and satisfactory performance, was selected. Based on considerations of data integrity and transmission reliability, the Reliable Connection (RC) service type was selected.

DESIGN OF THE SYSTEM

The data transmission system is a server/client application designed to establish a duplex data channel between the communicating parties, allowing them to exchange data. As illustrated in Figure 1, the network adapters are physically connected to the transmission terminals via the PCIe interface, enabling direct read/write access to terminal memory through their DMA controllers. The network adapters between terminals are directly connected by fiber optics, serving as the physical data channel during the transmission process. Resources like the work queue pairs and completion queues created in the "registered memory" of the terminals can be abstracted as the data interface with the network adapters, forming the logical data channel for transmission.

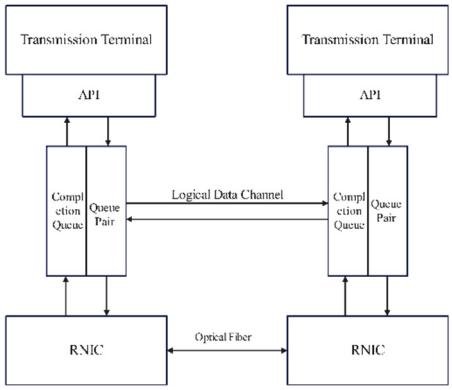

Figure 1: Transmission channel of the transmission system.

As shown in Figure 2, the client of the data transmission system is divided into five modules: resource management, communication establishment, RDMA operations, queue pair management, and resource cleanup. The server introduces a thread invocation module, which is used for concurrently handling POSIX threads from different clients for subsequent communication. Although the server and client implement different functionalities, both are integrated within the same system architecture.

The resource management module is responsible for initializing, creating, and managing all necessary system resources while controlling their lifecycle. This includes handling device context structures, protection domains (PD), completion queues (CQ), queue pairs (QP), memory regions, and data buffers, among others. The system dynamically allocates RDMA-specific memory regions (MR) within the associated PD to prevent resource leakage. At the same time, it generates unique Local Key (L_KEY) and Remote Key (R_KEY) fields for access permission verification.

In the IB (InfiniBand) specification, the QP is a core component of communication and can be abstracted as a virtual interface between software and hardware. It sequentially stores the Work Queue Elements (WQE) that the hardware needs to execute, where WQE corresponds to the Work Requests (WR) mentioned earlier from the software perspective. From a data perspective, the interface of a QP to the application layer is divided into “send (post_send)” and “receive (post_recv)” operations. This means that application layer software fills a WR into the QP, requesting the underlying hardware to perform a “send” or “receive” operation. This also helps distinguish whether the QP acts as the “sender” or “receiver” in a particular communication session. The queue pair management module triggers state

ISBN: 978-3-95450-249-3 ISSN: 2673-5350 doi: 10.18429/JACoW-IBIC2024-WEP68

RESEARCH ON NEUTRON INSTRUMENT STREAMING DATA PROCESSING AT CSNS*

P. X. Shen[1], L. Hu[1], J. J. Li[1], L. J. Liao[1], Y. X. Qiu[1], J. Y. Ren[1], Z. J. Sun[1,2], H. Y. Teng[1], X. K. Wang[1], X. Z. Wang[1], L. Xiao[1], J. Xu[1], L. Yu[1], H. Luo, J. Zhuang[1†], J. R. Zhou[1,2], K. Zhou[1], Y. B. Zhao[1]
Institute of High Energy Physics, Chinese Academy of Sciences, Beijing, China
[1] also at Spallation Neutron Source Science Center, Dongguan, China
[2] also at University of Chinese Academy of Sciences, Beijing, China

Abstract

With the construction and operation of several new neutron instruments at the China Spallation Neutron Source (CSNS), a next-generation streaming data transmission solution, based on message middleware, has been officially implemented. This paper introduces a streaming data readout and processing software designed to address the data processing requirements of neutron instrument experiments, emphasizing high throughput, extensive customization, and flexible experimental data analysis. The software has been tested and validated on various neutron instruments at CSNS and is gradually being integrated into instrument experiments.

INTRODUCTION

The China Spallation Neutron Source (CSNS) is the fourth established pulsed spallation neutron source in the world. It comprises an 80 MeV negative hydrogen ion linear accelerator, a 1.6 GeV fast cycling proton synchrotron, two beam transport lines, and a tungsten target station, with a 25 Hz frequency [1]. Twenty neutron beamlines will be established at the CSNS for different scientific researches and Three neutron spectrometers have been constructed in the first batch [2].

For the first three instruments at CSNS, their overall data readout and transmission are based on a file-based architecture [3]. The electronics front-end data acquisition modules are responsible for parsing the raw detector data into physical events and making them available for the back-end via the network. Experimental parameters or control variables, such as sample environment conditions, chopper frequencies, and other equipment data, are typically timestamped and stored in a database. The back-end data processing then combines the detector and other equipment data, saving them as standard Nexus files for further offline data reduction. However, with the increasing neutron flux, as well as the trend towards larger and more complex instruments, this method of data transmission is gradually becoming insufficient to meet the real-time and correlation data analysis demands of the new generation of high-throughput neutron instruments. In response, a streaming data platform was adopted to develop a new data acquisition and transmission system for the under construction neutron instruments at CSNS. Similar to the systems ISSI and ESS [4], the open-source Apache Kafka message queue has been utilized as the core of the streaming data architecture.

Kafka, with its high concurrency and throughput capabilities, is particularly well-suited for neutron instruments. However, for current neutron instrument experiment at CSNS, whether it involves physical data processing or equipment research tasks, the data processing framework is still based on the old data transmission approach. To integrate and align this with the new Kafka-based data transmission platform, it is necessary to design and implement appropriate low-level adaptation interfaces. To ensure that the streaming platform meets the need of data processing ad CSNS, a self-developed neutron instrument streaming data readout and processing software (NISDRP) have been designedto address the issues mentioned above. The following sections will provide a detailed introduction.

FRAMEWORK DESIGN

Overview

Figure 1 shows the data-flow of NISDRP, user initializes the main program and data processing class instances through configuration files related to data streams and data processing. This allows access to neutron event data and auxiliary experimental control data on the message middleware, thereby enabling real-time processing of experimental data. For simplicity, elegance, power, and ease of writing, Python was chosen as the development language for NISDRP.

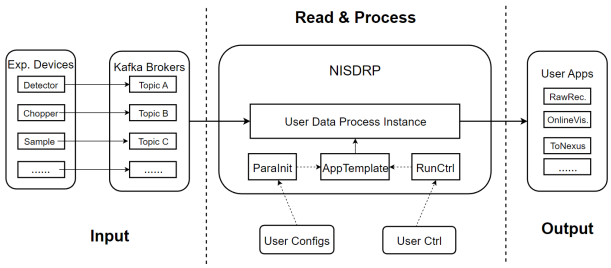

Figure 1: Overview of the NISDRP.

* Work supported by Guangdong basic and applied basic research foundation (2021A1515110984), and the National Natural Science Foundation of China (Grant No. 12405354).

† Correspoding author: zhuangj@ihep.ac.cn

ISBN: 978-3-95450-249-3 ISSN: 2673-5350 doi: 10.18429/JACoW-IBIC2024-WEP69

DESIGN AND IMPLEMENTATION OF MASS SPECTROMETER DATABASE

L. F. Liu, M. Li, R. S. Mao, Institute of Modern Physics, Lanzhou, China

Abstract

Mass spectrometer, as a type of beam instrument, is capable of measuring and analyzing the mass and charge of different molecules and ions in a sample, thus identifying the type of particles. With the continuous development of mass spectrometry technology, the management, retrieval and analysis of mass spectrometry data have become crucial in many fields such as biomedicine, environmental sciences, and crime investigation. Mass spectrometer database software is an important part of mass spectrometer, which can realize the functions of storing, managing, sharing and analyzing mass spectrometer data. Therefore, the establishment and improvement of specialized mass spectrometry databases and library retrieval techniques can facilitate the rapid identification and confirmation of compounds, providing a more efficient and accurate solution for substance detection. In this paper, a comprehensive mass spectrometry database management system is designed and implemented to simplify the user operation process from the collection, storage and management of mass spectrometry data to the querying, matching and analyzing of the data, providing a fast and accurate solution to meet the needs of scientific research on mass spectrometry data. The software uses Python for the implementation of core algorithms, builds a database based on MySQL and collects mass spectrometry data to fill in the data-base, and finally uses PyQt to design and implement a friendly and beautiful graphical user interface. While this software improves the accuracy of matches, it also optimizes processing speed. With this software, un-known compounds in the samples can be identified and their possible structures and properties can be recognized, which provides a strong support for their application fields.

INTRODUCTION

Since its introduction in the early 1970s, the mass spectrometry library search technique has occupied an important position in the field of mass spectrometry analysis by searching and analyzing mass spectrometry data by computer. The technique identifies chemical components in complex samples by converting chemicals into ions and separating, detecting, and quantitatively analyzing them. In recent years, the mass spectrometry library search technique has become a hot topic for researchers because of its high resolution, good separation and fast resolution speed. It is widely used as a fast and effective identification method in environmental monitoring, proteomics, life sciences, food testing, material analysis, petrochemical, and anti-terrorism and riot control. When analyzing unknown compounds, mass spectrometry search software provides qualitative references by comparing the mass spectra of samples with those of standards in the database and measuring the similarity by the match of mass spectra. Therefore, it is particularly important to establish an efficient and fully functional mass spectrometry data management system. Such a system not only improves the efficiency of data processing, but also enhances the ability of data integration and sharing, supports complex data analysis, and accelerates the process of scientific research and discovery.

Authoritative standard spectral libraries include the NIST Mass Spectral Library published b12/09/2024y the National Institute of Standards and Technology (NIST) [1], the NIST/EPA/NIH Library published by NIST together with the U.S. Environmental Protection Agency (EPA) and the U.S. National Institutes of Health (NIH), and the Wiley Library. In addition, there are a number of high-quality databases in China, such as the ICMSIS mass spectrometry database system of the Institute of Chemistry Chinese Academy of Sciences. The mass spectrometry database provided by the chemical specialty database system of the Shanghai Institute of Organic Chemistry [2]. There are also Sadtler databases applicable to specific fields such as criminal investigation, chemical product quality control, petroleum, plastics industry, mineral analysis, and other fields [3].

Currently, common mass spectrometry data processing systems are divided into two categories: One is the system provided by mass spectrometry instrument manufacturers, such as Agilent's Mass Hunter Chemical Workstation and Thermo Fisher Scientific's Xcalibur, which have user-friendly interfaces, high-quality technical support, and seamless connectivity to their branded mass spectrometers, but are costly and poorly customizable. The other category includes instrument-independent systems, such as NIST MS Search and AMDIS, which serve as standardized mass spectrometry databases and provide a wide range of data and tools for compound analysis and identification. However, these systems are not completely free, and many of the advanced features are hidden behind expensive licenses that increase the cost of research [4]. Given the limitations of existing systems, this study aims to develop an open source, customizable, and user-friendly mass spectrometry data management system.

DATABASE DESIGN

Database is a data storage warehouse, which refers to a collection of organized and shareable data stored in a computer over a long period of time.

Database management system is a computer system software specialized for database management, which can provide functions such as data definition, creation, query and operation for databases, and realize the control of data integrity and security. The advantages of managing mass spectrometry library data by database management system

ISBN: 978-3-95450-249-3 ISSN: 2673-5350 doi: 10.18429/JACoW-IBIC2024-WEP70

A GENERIC AND EFFICIENT AGGREGATION METHOD WITHIN NEUTRON SPECTROMETER DATA PROCESS FRAMEWORK BASED ON THE SYNCHRONOUS TRIGGER AND TAGGING SYSTEM

H. Y. Teng†, J. J. Li, J. Zhuang, Y. X. Qiu, P. X. Shen
Institute of High Energy Physics, Chinese Academy of Sciences, Beijing, China
[1]also at Neutron Source Science Center, Dongguan, China

Abstract

In the recent project of China Spallation Neutron Source (CSNS), a new designed distributed stream-processing framework is applied as the fundamental schema of data process system on user cooperative instruments. It is constructed with the open-source Apache Kafka software, which aims to aggregate the big data for manipulation sharing, and also with a synchronous trigger and tagging system, which provide synchronous ID for data correlation among different target hitting cycles. Correlated data could be identified among different measurements for aggregative analysis in a high efficient way, which greatly improve the performance of data processing. In concert with the real-time capability on stream-processing platform, WYSIWYG characteristics is achieved either. Performance and adaptability of this technique has been validated during the operation of constructed user cooperative instruments in CSNS. An increasing number of data-processing functions and experiment methods have got benefit from it.

INTRODUCTION

In the past few years, instruments on spallation neutron source have make a significant progress on beam luminance and detector technology [1-3]. Meanwhile the rise in data throughput and traditional data aggregation framework has become a new bottleneck for experiment [4-5]. Figure 1 shows a schematic view of traditional data aggregation, detector data and other measurement records are marked with a timestamp corresponding to the measuring time. Those records are saved as a file format via DAQ section, then sometime later each finished files are transported to the computing node to get analysis result. This procedure take a long chain and cost much delay on the file accumulating and transporting. Furthermore, experiments on neutron instrument usually take complementary data such as sample environment conditions, proton charge from accelerator and some meta data. Different data record associated to the identified target hitting cycle are correlated and must be synchronized correctly in aggregative analysis. For neutron experiment scientist expect to validate the physics status from data analysis in a "what you see is what you get" way. Considering the demand on WYSIWYG and low efficiency of traditional file transport framework in real-time capability, starting from the cooperative instruments of CSNS, the data process framework has been upgraded to a new designed framework "DSNI", which is constructed on the open-source streaming process platform Apache Kafka. As well as the read-time capability on streaming process platform, a synchronous trigger and tagging system is also introduced to proceed an efficient data correlation for aggregative analysis. With optimization and utilization on both hardware and software hierarchies, the DSNI framework is validated and applied to all user cooperative instruments in CSNS.

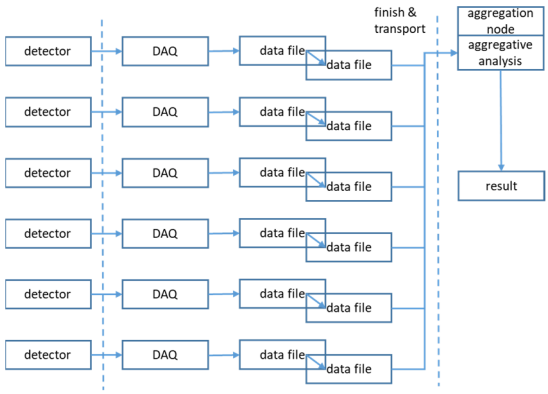

Figure 1: Traditional data aggregation framework on neutron instruments.

FRAMEWORK DESIGN

Overview

The conception of DSNI framework is to convert various measuring data into the streaming format with standard interface and then published on the distributed stream-processing platform for consumer sharing among various application. Meanwhile each streaming message are marked with a synchronous ID tag, which identify the trigger cycle number of data message corresponding to the measurement association. The distributed stream-processing platform provide many new features, e.g., scalability, fault tolerance, low latency and high performance. The most significant one is the real-time capability. On the other hand, data correlation and synchronization are simply referred to the consistent synchronous ID. With the assistance of advantages above, the later data manipulation could be setup on the unified interfaces and make aggregative analysis with efficiency.

Figure 2 shows a schematic view of DSNI framework developed on user cooperative instruments in CSNS. The synchronous and timing service consist of 2 subsystems.

* Work supported by the State Key Laboratory of Particle Detection and Electronics, SKLPDE-ZZ-202301
† tenghy@ihep.ac.cn

ISBN: 978-3-95450-249-3 ISSN: 2673-5350 doi: 10.18429/JACoW-IBIC2024-WEP71

DESIGN OF BEAM ENERGY ADJUSTMENT SYSTEM FOR HEAVY IONS TESTING OF SPACE ELECTRONICS

A. S. Bakerenkov†, P.A. Chubunov, I.V. Skorkin, G.V. Starodubtsov
Branch of JSC URSC – ISDE (ISDE), Moscow, Russia

Abstract

Electronic components in spacecrafts and satellites are subjected to impact of high energy particles and heavy ions. Radiation damage of semiconductor electronic devices depends on linear energy transfer (LET) of the particle in semiconductor material which the device is fabricated of. During radiation testing of electronic components for space applications in particle accelerators we have limited set of ions with fixed energies and LET values due to complexity of adjustment of accelerator systems. According to standard test methods it is necessary to perform tests for several LET values in range from 1 to 100 (MeV×cm^2)/mg. It is possible to enhance available LET range using special screens with different thickness (degraders) to decrease initial energy of particles and adjust LET value without reset of the accelerator for another ion type or energy. It can significantly reduce complexity and duration of test processing. In this work by numerical calculations we have designed a set of degraders, which enable us to obtain almost any LET value from 1 to 100 (MeV×cm^2)/mg in silicon devices using only four ion types with fixed energies that is acceptable for all test procedures.

INTRODUCTION

In space environment high energy heavy ions impact on semiconductor electronic components of spacecrafts and satellites. It leads to malfunctions and failures of on-board electronic devices and systems. There are several different types of effects in semiconductor electronics and integrated circuits, which are responsible for functional and parametric failures under heavy ion impact. Single Event Effect (SEE) is common name for all types of these effects.

To perform terrestrial radiation tests of electronic components for space applications it is necessary to use ions with values of linear energy transfer (LET) in range from 1 to 100 (MeV×cm^2)/mg. The value of LET is determined in material, which sensitive volume of the device under test (DUT) is made of. Usually the dependence of effective crossection of different types of SEE on LET value is obtained as the result of the test procedures. The effective crossection essentially is a ratio of number of observed SEEs to ion flux during corresponding irradiation session. The dependence of the effective crossection σ on LET Λ usually can be approximated by following expression:

$$\sigma(\Lambda) = \begin{cases} \sigma_0\left(1 - \exp\left(-\left(\frac{\Lambda-\Lambda_0}{W}\right)^S\right)\right) at\ \Lambda \geq \Lambda_0 \\ 0\ at\ \Lambda < \Lambda_0 \end{cases}, \quad (1)$$

which has four parameters; σ_0 is saturation crossection, Λ_0 is threshold LET, S and W are fitting constants. The most important for practical applications parameters are Λ_0 and σ_0. Λ_0 corresponds to low limit of LET value of an ion, which is able to produce corresponding SEE in the DUT. Any ions with LET values less than Λ_0 can't induce the SEE. σ_0 is essentially high limit of effective crossection which can be obtained in the DUT for corresponding type of SEE. The plot of the described dependence is presented in Fig. 1 with Λ_0 and σ_0 parameters. When all parameters of the dependence of σ on Λ are determined from experiments for specified DUT and SEE type we can estimate effective frequency or effective probability of corresponding SEEs for specified orbit. To perform the estimation it is necessary to use information about space particle fluxes fore this orbit and configuration of corresponding spacecraft or satellite.

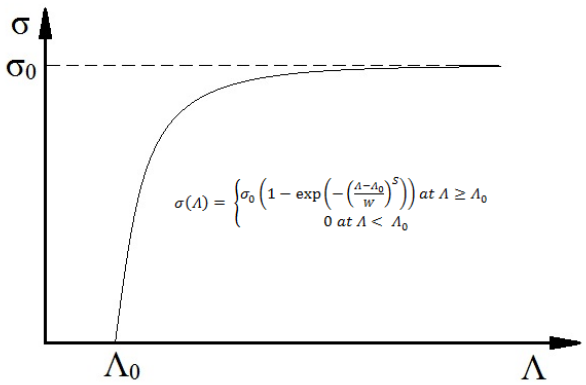

Figure 1: The dependence of SEE effective crossection on LET value.

Experiments for determination of parameters of dependences of SEE effective crossection on LET value usually are performed using ion accelerators such as Roscosmos test facility in Joint Institute of Nuclear Research in Dubna (Russia, Moscow region) [1,2]. Beam monitoring at the facility is provided by equipment and techniques described in [3-5]. Since expression (1) has four parameters we have to obtain experimentally determined effective crossection values for at least four LET values. To use least square method for extraction of the parameters from experimental data the LET values should be distributed as evenly as possible in the experimental range of LET. It is necessary to improve the accuracy of extracted parameter values. Increasing of experimental points with different LETs is also increases the accuracy of the extraction.

From the consideration performed above we can conclude, that in the radiation test processing the issue of installing of specified LET values of ions for irradiation of

† AS_Bakerenkov@list.ru (Corresponding author)

ISBN: 978-3-95450-249-3 ISSN: 2673-5350 doi: 10.18429/JACoW-IBIC2024-WEP72

COMPACT SEMICONDUCTOR SENSOR FOR MONITORING OF ENERGY DISTRIBUTION IN HEAVY ION BEAMS

A. S. Bakerenkov†, P.A. Chubunov, I.V. Skorkin, G.V. Starodubtsov
Branch of JSC URSC – ISDE (ISDE), Moscow, Russia

Abstract

During experiments in particle accelerators online monitoring of energy distribution in particle beam is useful for correction of the accelerator setting and parameters. Time of flight (ToF) technique for energy monitoring is well known and approved method, which is used widely. Nevertheless ToF technique requires long flight bases especially for high energy particles and can't be used to estimate spatial heterogeneity of the particle beam. Semiconductor energy sensors are compact and can be successfully used for these applications. Diodes with p-i-n structure are used for energy monitoring of particles with rages less than thinness of sensitive volume. High energy particles have long ranges in semiconductor materials. For online monitoring of high energy beams in this work we propose and experimentally verified a technique based on determination of linear energy transfer (LET) values of particles using diode structures with p-n junctions. Experimentally obtained LET value enables us to calculate energy if the particle type and diode semiconductor material are known. Proposed technique was successfully experimentally verified.

INTRODUCTION

Monitoring of energy of charged particles is a very actual issue in different accelerator facilities proposed for wide range of applications form fundamental nuclear physics to industrial production. For today we have number methods for measurements and determination of energy of charged particles optimized for different purposes and conditions. The most universal and widely used is Time of flight (ToF) technique. It based on essentially simple physic concept, which require to measure time interval that is necessary for particles to overfly a fixed distance. When time is determined and the distance is known it is easy to calculate the energy taking into account mass of the particle. Main complexity for implementation of this technique is sufficiently distances, which are required to reach satisfied accuracy of measurement results. Nevertheless this technique is the most popular and usually applied together with other methods.

Despite of relative simplicity of ToF technique in a number of applications it can't be used. The most obvious example is experimental installations with degraders, which are used to decrease of particle energy before it reaches a target. It is impossible to ToF technique due to usually the distance between degrader and target is to short. In this case for energy monitoring semiconductor sensors can be used successfully. Nevertheless correct applications of semiconductor sensors for energy monitoring requires understanding a number of physical mechanisms, which the operation of a particular sensor type is based on. It enables to select the most acceptable type of semiconductor sensor for specified applications.

The most popular type of semiconductor energy sensors is p-i-n diodes, which have high thicknesses of sensitive volumes that enable to determine energy of particles which ranges in the sensitive volume are less than the thickness. For correct estimation of the energy the particle mast be stopped inside the sensitive volume. It ensures that all particle energy is dissipated in the sensor and taken into account. This type of sensors is a good solution for registration of particles with medium and low ranges in the material which the sensor is fabricated of. If we are dealing with high energy light ions, which usually have extremely long ranges in many types of materials it is necessary to use another type of semiconductor sensors.

For registration of high energy particles with high ranges semiconductor sensors with thin sensitive volumes is a more acceptable solution. Theory of operation of these sensors is based on determination of linear energy transfer (LET) value of a particle in the sensitive volume. Due to the thickness of the sensitive volume is much less, than particle range we can consider LET value as constant over the particle track in the sensitive region. If we know type of the particle and LET value we can calculate energy taking into account material of the semiconductor sensor.

Before using semiconductor sensors should be calibrated for determination of dependences of output signals on LET values. It should be performed using beams of particles which type is known and energy is monitored by ToF technique.

One of main advantage of semiconductor sensors is compact dimensions that enable to assemble sensor matrixes for monitoring spatial heterogeneity of the particle beams as well as energy distributions.

In this work we will consider the issue of selection and applications of semiconductor sensors with thin sensitive volume for registration of high energy light particles with high ranges in details. The results of experimental applications of designed semiconductor sensor will be demonstrated and discussed.

SEMICONDUCTOR STRUCTURE AND PARAMETERS

Semiconductor particle sensors are essentially diodes with p-n junctions, which depletion regions act as sensitive volumes. Typical electrical circuit for operation of

† AS_Bakerenkov@list.ru (Corresponding author)

ISBN: 978-3-95450-249-3 ISSN: 2673-5350 doi: 10.18429/JACoW-IBIC2024-THAT1

LATEST ACHIEVEMENTS IN FEMTOSECOND SYNCHRONIZATION OF LARGE-SCALE FACILITIES

S. Schulz*, M. K. Czwalinna, H. Schlarb
Deutsches Elektronen-Synchrotron DESY, Hamburg, Germany

Abstract

This overview addresses the realm of electrical, hybrid and specifically optical schemes for achieving a facility-wide synchronization on the femtosecond level at free-electron lasers (FELs). After a brief introduction to the fundamental principles behind FEL operation and the significance of synchronization for full utilization of their capabilities. Subsequently, it discusses various methods employed to achieve femtosecond-precision synchronization, including low-noise timing references, different active stabilization techniques, and advanced feedback algorithms. In addition, the tutorial provides an overview of the numerous challenges encountered in femtosecond optical synchronization and solutions developed to overcome them. It discusses technological developments, such as ultra-stable optical lasers or timing diagnostics both for optical pulses and electron beams. Moreover, practical considerations for implementing such systems in FEL facilities are addressed, including stability requirements, scalability, and integration with experimental setups. Results from recent studies highlighting successful synchronization implementations at prominent FEL facilities are presented.

THE FREE-ELECTRON LASER CONCEPT

FELs can generate high-intensity radiation with narrow bandwidth and high brightness which is tuneable over a broad range of the electromagnetic spectrum, including X-rays [1].

It all begins with an electron source, where a photocathode is illuminated by a several picoseconds long optical laser pulse (often at UV wavelengths), which releases electrons via the photoelectric effect. These electrons are then accelerated to a few MeV by a radio-frequency (RF) cavity, resulting together with the focussing optics in a high-energy, low-emittance electron beam.

After this so-called injector, the electron beam enters a linear accelerator (linac, which can extend over several kilometers in total length), where the electrons are accelerated by a series of RF cavities to very high energies (up to several GeV, depending on the desired FEL radiation wavelength).

However, for efficient generation of extreme ultraviolet (XUV) or X-ray radiation, a high peak current of several kA is required, which is realized by shortening the electron bunches in time in several stages of bunch compressors. Basically, they consist of a magnetic chicane, which utilizes a particular time-energy correlation within the bunch imprinted by the acceleration process and causes the electrons at the tail of the bunch to travel a shorter path than those at the head, effectively compressing the bunch longitudinally.

After bunch compression and final acceleration, the electrons are directed into the undulator, which is a series of alternating magnetic poles. The magnetic field in the undulator forces the electrons to undergo sinusoidal motion, causing them to oscillate transversely, and emit synchrotron radiation to initiate the process of self-amplified spontaneous emission of radiation (SASE). The emitted radiation, in turn, interacts with the electron bunches, causing a microbunching effect where electrons group into smaller sub-bunches separated by the radiation wavelength. In high-gain FELs, this microbunching enhances the coherent emission of radiation exponentially leading to a high brightness, monochromatic and spatially coherent pulse of light, which is typically shorter than the electron bunch it was generated from.

The unique properties of FEL radiation compared to conventional lasers allow for investigating material properties on ultra-short dimensions and to observe dynamic processes happening on ultra-short time-scales. Experiments are often carried out in pump-probe geometry, involving additional radiation sources such as highly complex optical laser systems. One of the pulsed sources is used for initiating an excitation or modification in the sample of interest, and the mutually other pulse is used to probe the dynamics following this excitation. A “molecular movie” of these dynamics can be recorded by scanning the relative time delay of both pulses. The achievable resolution in this type of experiment strongly depends on widths of the pulses and on the precise knowledge of their relative time delay.

THE SYNCHRONIZATION MOTIVATION

Exploitation of the capabilities of state-of-the-art free-electron lasers (FELs) place demanding requirements on the timing reference distribution and control systems of the linear electron accelerators (linac) and to some extent the photon beam delivery systems. In the end, the requirements on the linac are driven by user experiments, for instance maintaining the photon energy and especially in terms of longitudinal stability for achieving femtosecond-level temporal resolution. Advanced FEL schemes like hard x-ray self-seeding, are even more sensitive to deviations in electron bunch properties, both transversely and longitudinally. Therefore, all large-scale FEL facilities require a synchronization system to ensure adequate time and phase stability. Additionally, pump-probe experiments involving multiple radiation sources (X-ray photons, optical lasers, THz radiation), the resolution is not only constrained by pulse duration, but in particular by the timing stability between the pump

* email: sebastian.schulz@desy.de

ISBN: 978-3-95450-249-3 ISSN: 2673-5350 doi: 10.18429/JACoW-IBIC2024-THAI2

COST-EFFECTIVE TIME-STRETCH TERAHERTZ ELECTRO-OPTIC RECORDERS, BY USING 1550 nm LASER PROBES*

C. Hanoun, S. Bielawski, C.Evain, E.Roussel†, C.Szwaj
Univ. Lille, CNRS, UMR 8523 - PhLAM - Physique des Lasers Atomes et Molécules, Lille, France
J.-B. Brubach, N. Hubert, M.Labat, J.-B. Ricaud, P. Roy, M.-A. Tordeux
Synchrotron SOLEIL, Synchrotron SOLEIL, Gif-sur-Yvette, France

Abstract

Photonic time-stretch is a powerful method for recording electro-optic signals with terahertz bandwidth and high repetition rates. The method consist of modulating a chirped laser probe with the signal of interest. Then, the laser pulse is stretched it in time up to several nanoseconds, so that it can be read using an oscilloscope or analog-to-digital converter (ADC) board. This technique has been shown to be efficient for monitoring the dynamics of Coherent Synchrotron Radiation (CSR) at SOLEIL, and to study electron bunch shape dynamics at KARA. However, the use of this technique has been strongly limited by the need of high bandwidth and costly oscilloscopes required for the readout. We present here a new design that allows a considerable reduction of the required oscilloscope bandwidth. A key point consists of using the 1550 nm wavelength for the probe. We will also present results obtained at SOLEIL, where THz pulses have been recorded, in single-shot and at MHz repetition rates, using an oscilloscope and ADC board with 1 to 3 GHz bandwidth.

INTRODUCTION: SINGLE-SHOT ELECTRO-OPTIC DETECTION

Single-shot recordings of THz electric fields are needed for electron bunch shape characterization and in THz coherent sources. Single-shot electro-optic (EO) detection is an efficient technique to measure THz electric fields with suppicosecond resolution. This technique has been applied in various accelerator facilities for monitoring electron bunch shapes by probing the near-field of the bunches [1–3], and is also used to record coherent radiation emitted by the relativistic electron bunches [4].

The principle of single-shot detection consists in modulating a chirped laser pulse with the electric field under interest in a Pockels crystal thanks to the electro-optic effect [5]. As a result, the spectrum of the probe laser is modulated and the THz signal can be retrieved by recording the optical spectrum of the laser (Fig. 1) using a grating-based optical spectrum analyzer (OSA). This method is commonly known as spectral encoding.

* Work supported by: ULTRASYNC ANR-DFG project, CPER photonics for society, LABEX CEMPI, METEOR CNRS MOMENTUM grant, EIC Pathfinder TWAC

† eleonore.roussel@univ-lille.fr

PHOTONIC-TIME STRETCH FOR HIGH-ACQUISITION RATE

Even though the spectral encoding electro-optic detection allows single-shot measurements, reaching high acquisition rate (in the MHz range or more) remains an open challenge. The optical readout at MHz speed is the critical part of the spectral encoding EO detection, as the speed of the commercially available cameras are typically limited to the hundred kHz range. To overcome this bottleneck, a new generation of fast linear cameras (KALYPSO), at the state-of-the-art, has been developed at Karlsruhe Institute of Technology (KIT) in order to reach the multi-MHz acquisition rates [6, 7]. In parallel, a second approach has been consisted in using the so-called photonic time-stretch strategy [8], that allows up to tens of MHz acquisition rate.

In photonic time-stretch EO, the laser output pulse is dispersed in a long fiber (typically with few kilometers length) 1(2b). The signal under investigation, at the picosecond level, is temporally stretched by a factor $M = 1 + L_2/L_1$ known as the (temporal) stretch factor. The EO signal appears as a slowed-down replica, and can be recorded using a photodetector and a conventional oscilloscope (or acquisition board) with few GHz bandwidth. The acquisition rate of the setup can thus be pushed, by design, to the hundreds of MHz range, given the repetition rate of the probe laser.

The photonic time-stretch process has been initially introduced by B. Jalali and co-authors in 1999 [9]. The technique has also been widely used to perform fast real-time spectroscopic measurements, so called Dispersive Fourier Transform (DFT), as the state-of-the-art photodetectors are much faster than traditional spectrometers [10]. Indeed, through the development of fast photodiodes for telecommunications, photodetectors with bandpass of several tens of GHz are commercially available.

CHOICE OF EO OPERATING WAVELENGTH

As previously mentioned, the principle of EO detection consists in a pump-probe system where the electric field is encoded onto a probe laser pulse. The THz electric field propagating through the EO crystal induces a birefringence. In the standard operation of EO, the THz-induced phase retardation is given by:

$$\Delta\Phi = \frac{2\pi d}{\lambda} n_0^3 r_{41} E_{THz} \quad (1)$$

ISBN: 978-3-95450-249-3 ISSN: 2673-5350 doi: 10.18429/JACoW-IBIC2024-THBI2

NON-DESTRUCTIVE BEAM ENERGY MEASUREMENT USING RF CAVITY BEAM ARRIVAL TIME MONITOR*

S. S. Cao†, L. W. Lai, J. Chen, J. Dong, X. Q. Liu, R. X. Yuan, SSRF, Shanghai, China
Y. B. Leng‡, USTC, Hefei, China

Abstract

Beam energy is a key parameter for free electron laser facilities (FELs). A commonly used non-destructive system uses a beam position monitor (BPM) to measure the bunch position in a magnetic bunch compressor. At the Shanghai Soft X-ray FEL facility (SXFEL), the chicane stripline beam position method is utilized for this purpose. However, this method relies on the initial bunch position before entering the chicane and has a limited linear region. A different non-destructive beam energy system, which measures the bunch flight time using two cavity-based bunch arrival time monitors, has been proposed and tested. This paper introduces the development of this system, including design details, build-up, and measurement results. Moreover, it also covers the comparison between the two different bunch energy measurement methods from several aspects: bunch position-based and bunch flight time-based.

INTRODUCTION

Free electron lasers (FELs) are working horses for X-ray science research all over the world for their ability to generate ultra-short and ultra-high brightness X-rays. In recent years, FELs have developed rapidly worldwide, as well as over China. Shanghai Soft X-ray FEL facility (SXFEL) and Shanghai high repetition rate XFEL and Extreme light facility (SHINE) both located at Shanghai Zhangjiang campus, are the two most representative FEL facilities in China [1-2]. Currently, SXFEL has been upgraded to a user facility and SHINE is still under construction. The development of FEL-related key technologies is important and necessary for these facilities. As one of the key parameters, beam energy measurement is also one of the important parts of FFL facilities. This is mainly due to the generation of free electron laser relies on the interaction of high energy electron bunch and seed laser in a periodic magnetic field. The radiation wavelength, λ_0, is determined by the bunch energy of the electrons, γmc^2, and also the parameters of the undulator. Thus high-precision knowledge of the beam energy can enable higher-precision knowledge of the radiation wavelength of the generated free-electron lasers. Furthermore, the precise control of keeping the beam energy stable is of great importance for the stability of both the radiation wavelength. Therefore, a high-performance online electron bunch energy measurement system is essential. Several detection schemes of electron bunch energy have already been proposed and applied in large scale accelerators over the world. For large-scale circle accelerator facilities, such as synchrotron radiation facilities and colliders, the Compton back-scattering technique [3] and the resonant spin depolarization technique (RD) [4] are two dominant methods. For FEL facilities, a commonly used approach is measuring the horizontal bunch position between the second and third dipole magnet in a chicane, either by beam position monitor or synchrotron radiation monitor [5-7].

At SXFEL-UF, profiles are used for bunch energy measurement, but it intercepts the bunch. Therefore, a chicane stripline BPM is utilized at the LINAC 1st bunch compressor of SXFEL used for bunch energy monitoring and feedback. Besides, it has new demands from new facilities (e.g., SHINE), the bunch energy at BC1 ranges from 200 MeV to 500 MeV (as shown in Fig. 1), and a wide-range high-precision robust beam energy measurement system is required.

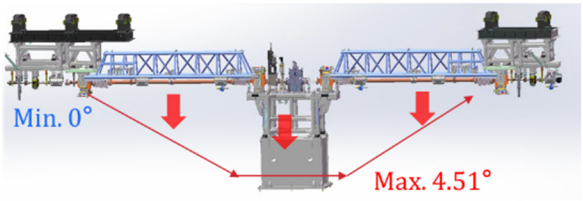

Figure 1: BC1 @ SHINE.

However, the BPM-based BEM method requires calibration of the initial position before into the chicane to obtain a more accurate beam position change, and it is limited by the SNR of the electrode signal away from the electron bunch. Instead of measuring the bunch position at Chicane, measuring the bunch flight time is another approach to knowing the energy. This has been mentioned in Ref. [5] by using EO-BAM to detect the beam flight time.

This paper is going to investigate this beam flight time-based beam energy measurement scheme, and hope to learn and compare the pros and cons of the beam flight time-based beam energy measurement method (BFT-BEM) and beam position-based beam energy measurement method (BPM-BEM).

FUNDAMENTAL PRINCIPLES

The electron bunches with different energies have different deflection angles passing through a diode magnet. As a result, it will be dispersed into different paths. As shown in Fig. 2, the electron bunches with low energy, medium energy, and high energy travel along the $S_1, S_2,$ and S_3 paths, respectively, and it results in a different horizontal bunch position (x_1, x_2, x_3) between the second and third dipole magnet (D_2, D_3). Hence the beam position monitor (BPM, purple in the figure) can be used for beam energy measurement.

* Work supported by the NSFC (Grant No. 12105346)
†email address: caoss@sari.ac.cn
‡email address: lengyb@ustc.edu.cn

ISBN: 978-3-95450-249-3 ISSN: 2673-5350 doi: 10.18429/JACoW-IBIC2024-THBC3

LASER MODULATOR FOR SSMB USED AS A DIAGNOSTIC TOOL

A. Kruschinski*, J. Feikes, Helmholtz-Zentrum Berlin (HZB), Berlin, Germany
A. Hoehl, R. Klein, Physikalisch-Technische Bundesanstalt (PTB), Berlin, Germany
X. Deng†, Tsinghua University, Beijing, China

Abstract

At the Metrology Light Source in Berlin, the concept of Steady-state microbunching (SSMB) is evaluated in a proof-of-principle (PoP) experiment. SSMB has been proposed to deliver kilowatt level average power EUV radiation from an electron storage ring. In the PoP experiment, an energy modulation is impressed onto the electron beam using an infrared laser pulse co-propagating inside an undulator. We show that the beam energy can be measured absolutely by detuning the undulator gap from optimum resonance and observing the intensity of the resulting coherent synchrotron radiation.

INTRODUCTION

Steady-state microbunching (SSMB) has been proposed [1, 2] as a new kind of storage ring based synchrotron radiation source that promises to generate high brilliance, high average power coherent radiation at wavelengths as short as the extreme ultraviolet (EUV). An SSMB storage ring would indefinitely store nanometer-length microbunches, and thus benefit from both the coherence of radiation generated from microbunches and the inherently high repetition rate of a storage ring.

Extensive theoretical studies on SSMB and related effects are ongoing [3–11], and the viability of SSMB is tested in a proof-of-principle (PoP) experiment at the Metrology Light Source (MLS) [12–17].

The MLS is an electron storage ring owned by PTB and operated by HZB in Berlin, Germany [18, 19]. It is uniquely suited as a testbed for SSMB because it has been designed and optimized for low alpha operation, and as such offers the necessary operational flexibility with dedicated sextupole and octupole magnet families to control the higher order momentum compaction. Table 1 lists the most important storage ring parameters of the MLS for standard operation and the SSMB PoP experiment.

Table 1: Machine Parameters of the MLS Storage Ring for Standard User Operation and the SSMB PoP Experiment

Parameter	Symbol	User Op.	SSMB PoP
Circumference	C_0	48 m	48 m
Beam energy	E_0	629 MeV	250 MeV
Bunch charge	q_b	400 pC	< 10 pC
Phase slippage	η_0	0.03	$< 2 \cdot 10^{-5}$

* arnold.kruschinski@helmholtz-berlin.de
† dengxiujie@mail.tsinghua.edu.cn

SETUP AND THEORETICAL ASPECTS

Experimental Setup at the MLS

In the SSMB PoP experiment as currently set up at the MLS, a simplified SSMB scheme is realized. Figure 1 shows a sketch of the setup. A single shot laser is steered to co-propagate with the electron beam through the only undulator installed at the MLS (for some important parameters see Table 2).

The whole storage ring optics are set up such that the energy modulation is transformed into physical microbunching after one revolution, this is achieved by applying quasi-isochronous optics. The same undulator used for modulation is also employed to generate coherent radiation, which is detected at the undulator beamline using a fast photodiode. Detection of coherent radiation at the first undulator harmonic is non-trivial, as the strong modulation laser pulse is also present in the detection path at the same wavelength [13, 14].

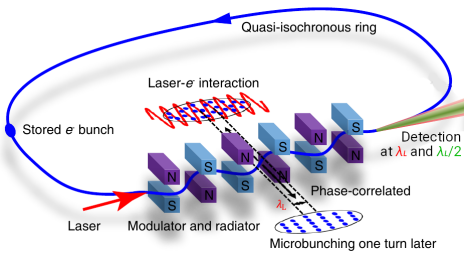

Figure 1: Schematic setup of the SSMB PoP experiment.

Table 2: Undulator and Laser Parameters for the SSMB PoP Experiment.

Parameter	Symbol	Value
Undulator period	λ_u	125 mm
Number of periods	N	30
Laser wavelength	λ_L	1064 nm
Laser repetition rate		1.25 Hz
Maximum laser pulse energy	$E_{L,max}$	400 mJ
Undulator gap at λ_L	$g(\lambda_L)$	72.1 mm

Energy Modulation in an Undulator

Undulator radiation is restricted to certain wavelengths λ_r given by the well known resonance condition

$$\lambda_r = \frac{\lambda_u}{2\gamma^2}\frac{1}{n}\left(1 + \frac{K^2}{2} + \gamma^2\theta^2\right) \quad (1)$$

that arises from interference between photons emitted in different undulator periods spaced apart by λ_u. For the

ISBN: 978-3-95450-249-3 ISSN: 2673-5350 doi: 10.18429/JACoW-IBIC2024-THBC4

OBSERVATION AND STUDY OF SPACE CHARGE EFFECT FREQUENCY SHIFTS IN HIGH-INTENSITY ACCELERATORS

Yuwen An*, Yaoshuo Yuan, Liangsheng Huang, Ming-Yang Huang,
Yong Li, Zhiping Li, Shouyan Xu, Xiaohan Lu, Yue Yuan
Institute of High Energy Physics, Chinese Academy of Sciences (CAS), Beijing, China
also at Spallation Neutron Source Science Center, Dongguan, China

Abstract

The China Spallation Neutron Source Rapid Cycling Synchrotron(CSNS-RCS) is the first high-intensity pulsed proton accelerator in China and the fourth of its kind globally. One of the key challenges in enhancing its power is the space charge effect. Measuring the frequency shift induced by this effect is crucial for understanding and mitigating its impact. In our experiments, we varied the beam current by adjusting the injection pulse length and chopping rate. By employing a combination of narrow-band filtering and Fast Fourier Transform(FFT) techniques, we successfully observed a tune shift of approximately 0.02 induced by a beam power of 140 kW. These experimental results were then compared with simulation outcomes, showing good agreement.

INTRODUCTION

The China Spallation Neutron Source (CSNS) is the first high-intensity pulsed spallation neutron source in China and the fourth of its kind globally. It primarily consists of an 80 MeV (300 MeV in CSNS-II, and the upgrades schemes of CSNS is show in Table 1) negative hydrogen ion linear accelerator and a 1.6 kW rapid cycling synchrotron (RCS) [1]. The negative hydrogen ions are first accelerated through a 3 MeV Radio Frequency Quadrupole (RFQ) and an 80 MeV Drift Tube Linac (DTL). After acceleration, the ions are stripped of electrons by a carbon foil and injected into the RCS [2]. Following approximately 20,000 cycles, the beam is extracted by a kicker and transported through the Ring to Target Beam Transport line (RTBT) to the target, where pulsed neutrons are generated for spallation neutron research.

Table 1: Upgrades Schemes of the CSNS

Parameter	CSNS I	CSNS II
Beam power	100	500
Repetition Rate [Hz]	25	25
Inj. Energy [MeV]	80	300
Ext. Energy [GeV]	1.6	1.6
Beam Intensity [$\times 10^{13}$]	1.56	7.8
Harmonic number	2	4

The RCS is a crucial component of the accelerator, and the regulation of its beam dynamics is essential for the overall performance of the accelerator. The milestones in beam tuning are as follows:

- **2017**: Beam injection into the ring and stable acceleration were achieved.
- **March 2018**: Achieved 10 kW beam power, passing national acceptance.
- **End of 2018**: Supplied 50 kW beam power.
- **End of 2019**: Supplied 80 kW beam power.
- **2020**: Achieved 100 kW beam power, reaching the CSNS I design goal and stable operation.
- **2022**: Achieved 125 kW beam power.
- **2022**: Achieved 140 kW beam power.
- **2024**: Target to achieve 160 kW beam power.

Beam tuning tasks can be broadly divided into low-intensity tuning and high-intensity tuning. In low-intensity beam tuning, the primary focus is on verifying hardware parameters, such as the accuracy of power supply timing and the calibration of beam diagnostic equipment. This stage involves orbit correction and optics correction.In high-power commissioning, techniques such as transverse painting are employed to mitigate the growth of beam emittance due to space charge effects. Additionally, the introduction of sextupoles helps to correct chromaticity and instability issues. Figure 1 illustrates the power upgrade process of the spallation neutron source.

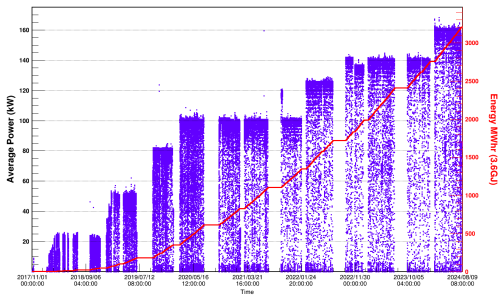

Figure 1: Power upgrade process of the spallation neutron source.

From the experience with spallation beam tuning, it is evident that low-intensity and high-intensity modes are not

* anyw@ihep.ac.cn

ISBN: 978-3-95450-249-3 ISSN: 2673-5350 doi: 10.18429/JACoW-IBIC2024-THCC2

DIRECT MEASUREMENT OF THE LONGITUDINAL EMITTANCE FOR A PROTON BEAM AT EXIT OF A RADIO FREQUENCY QUADRUPOLE*

Yong Zhang†, Ze Du, Lili Li, Jianju Su, Jia Yin, Huan jia, Yuanshuai Qin
Institute of Modern Physics, Chinese Academy of Science, Lanzhou, China

Abstract

In this contribution, we introduce a method for direct measurement of the longitudinal emittance of a proton beam at the RFQ exit, which delivers an output energy of 1.52 MeV. Initially, we developed a bunch shape monitor (BSM) inspired by Feschenko's design, achieving a resolution of 20 picoseconds. To conduct the direct measurement of longitudinal emittance, we integrate this BSM with a waist-to-waist beam transfer matrix, an energy-spread dipole, and a horizontal slit with a 0.2 mm width. The horizontal slit is positioned at the first waist at the dipole's input, while the BSM wire is situated at the second waist, at the dipole's output. This arrangement, enhanced by the waist-to-waist transfer matrix, improves the energy spread resolution to 0.03%. Through adjusting the buncher voltage and synchronous phase, we use dipole and BSM to measure different longitudinal emittances and ascertain the effects of bunching and debunching conditions on the longitudinal phase space distribution.

INTRODUCTION

The longitudinal phase space distribution refers to the distribution of particles in both phase and momentum along the direction of beam propagation. The RFQ serves as an important component in the linac, responsible for bunching and accelerating the beam. Understanding the longitudinal phase space distribution at the exit of a radio frequency quadrupole (RFQ) is crucial for precise beam tuning and minimizing beam loss in a high-power superconducting linac [1]. Here we introduce a direct measurement of longitudinal emittance by a developed bunch shape monitor (BSM), a wasit-to-waist beam transfer line, a dipole energy spread magnet and a horizontal slit in a 1.51 MeV proton MEBT. Different values of synchrotron phase with a buncher voltage of 48.4 kV will alter the distribution of longitudinal emittance at the exit of the RFQ.

DEVELOPED BSM IN IMP CAS

The developed BSM based on Feschenko's style is shown in Figure 1. It includes an RF deflector with a 325 MHz half wave resonator (HWR) and double plate-type electrodes. Tunner make sure the resonator frequency working in the differential mode of 325 MHz. The unloaded Q value is about 1923 as shown in Figure 2. The primary beam hits the target wire and produces SE. These electrons are accelerated by a negative voltage of 10 kV applied to the target wire through the first slit to the RF deflector field. The HV focusing is applied to each electrode to centre the electron envelope on the second slit through a high voltage port connected to a 1 MΩ resistance. The corrected magnet is used to control the transverse orbit of the rf-modulated SEs to pass through the energy spectrometer dipole. All SEs with the synchronous phase of the beam are collected with the secondary-electron multiplier, located at the end of the BSM. The signal is amplified through a preamplifier and sampled by a readout electronics.

Firstly, we installed the BSM in a heavy-ion linac called LEAF to test its performance. We conducted five primary measurements of the bunch shape distribution, as illustrated in Figure 3. The phase shift steps were manually adjusted during the measurements. The five measured bunch shape distributions exhibit consistency. The comparison of bunch shape distribution between the rebuncher power turning on and off are shown in Figure 4. The longitudinal distribution disappears when the re-buncher power is turned off, and when the re-buncher power is on, the full width at half maximum (FWHM) of the longitudinal distribution is 16.3° at 81.25 MHz.

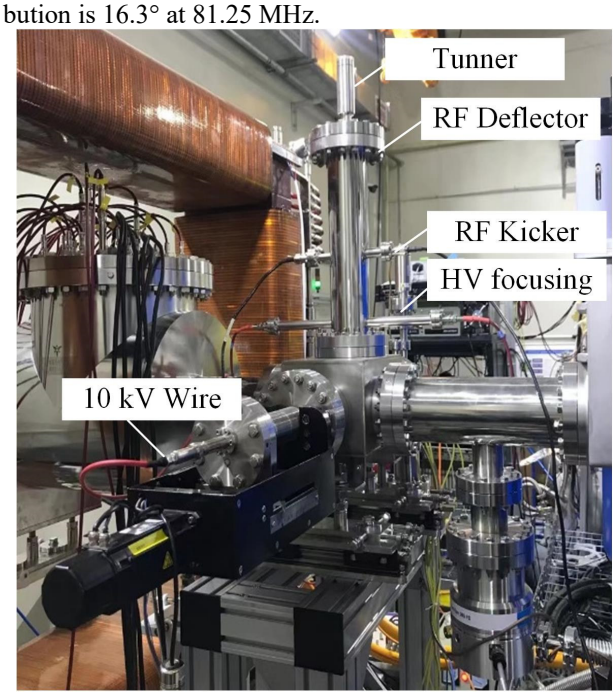

Figure 1: The developed BSM with HWR deflector.

A WASIT-TO-WAIST BEAM TRANSFER LINE AT THE EXIT OF A PROTON RFQ

The setup of longitudinal emittance measurement is shown in Figure. 5, which includes a horizontal slit (Slit2-H) at the input of dipole and the wire of BSM at the output

* Work supported by National Natural Science Foundation of China (Grant No.11675237, No. 11975291 and No. 12475169)
† email address: zhangy@impcas.ac.cn.

ISBN: 978-3-95450-249-3 ISSN: 2673-5350 doi: 10.18429/JACoW-IBIC2024-THP03

DESIGN CHOICES FOR THE CRYOGENIC CURRENT COMPARATOR FOR FAIR*

T. Sieber†, H. Braeuning, M. Schwickert, GSI, Darmstadt, Germany
L. Crescimbeni[1], F. Schmidl, Friedrich-Schiller-University Jena, Jena, Germany
R. Stolz[3], M. Schmelz[3], V. Zakosarenko[4], Leibniz IPHT, Jena, Germany
T. Stoehlker[1,2], V. Tympel[1], Helmholtz Institute Jena, Jena, Germany
J. Tan, G. Khatri, T. Koettig, CERN European Organization for Nuclear Research, Geneva, Switzerland
[1]also at GSI Helmholtz Centre for Heavy Ion Research, Darmstadt, Germany
[2]also at Institute for Optics and Quantum Electronics, Jena, Germany
[3]also at Technical University Ilmenau, Ilmenau, Germany
[4]also at supracon AG, Jena, Germany

Abstract

The Cryogenic Current Comparator (CCC) is a superconducting SQUID-based device, which measures extremely low electrical currents via their azimuthal magnetic field. Triggered by the need for nA current measurement of slow extracted beams and weak beams of exotic ions in the storage rings at FAIR and CERN, the idea of the CCC as a diagnostics instrument has been revitalized during the last ten years. The work of a collaboration of institutes specialized on the various subtopics resulted in a large variety of CCC types with respect to field-pickup, magnetic shielding, SQUID types and SQUID coupling. Many of them have been tested under laboratory and under beamline conditions, which formed a detailed picture of the application possibilities for CCCs in accelerators.

In parallel to CCC detector development the cryogenic support system has steadily been optimized, to fulfil the requirement of a standalone liquid helium cryostat, which is nonmagnetic, fit for UHV application, vibration damped, compact and accessible for maintenance and repair. We present the major development steps of the CCC for FAIR. The latest beamtime results are shown as well as recent tests with the cryogenic system. The most promising CCC type for FAIR is the so called Dual-Core CCC (DCCC), which runs two pickups in parallel with independent electronics for noise reduction. The magnetic shielding has an axial meander geometry, which provides superior attenuation of external magnetic noise.

INTRODUCTION

The CCC measures the beam intensity via the beam azimuthal magnetic field, which is for nA currents in the fT range. It consists of a superconducting shielding, which provides an attenuation of non-azimuthal external fields in the range -70 dB to -140 dB, depending on the shield geometry. The shielding guides the superconducting Meissner-Current, generated by the beam magnetic field, to an internal pickup loop. The pickup loop is a coil with only one winding around a high permeability ring core, which acts as a flux concentrator. The ring core is used in the 'classical' CCC as shown in Fig. 1 to provide an efficient coupling of the magnetic field to the SQUID circuit. The arrangement is a transformer with the particle beam as primary winding and the pickup coil as the secondary winding. The signal from the pickup coil is fed via an additional matching transformer for impedance matching to a DC SQUID (Superconducting Quantum Interference Device) magnetometer. For current calibration of the system, a second coil is added. Figure 1 shows the classical CCC arrangement, originally developed at the PTB (Physikalisch-Technische Bundesanstalt) [1] and adapted to the accelerator application at GSI [2].

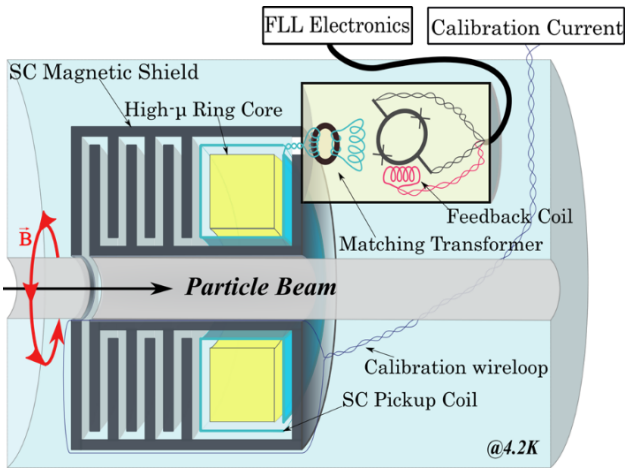

Figure 1: Classical CCC, shielding geometry with radial meanders and high permeability ring core.

The SQUID is operated in a compensation circuit, using a so called Flux Locked Loop (FLL) electronics [3, 4], which generates via a feedback system a compensation field to the beam magnetic field. If the working point of the FLL system is locked to the steepest slope of the flux/voltage curve of the SQUID, the resolution can be in the order of $\mu\Phi_0$ (Φ_0=magnetic flux quantum). Figure 2 shows a schematic of the electronics and the working point in the flux/voltage curve.

* Work supported by BMBF under contracts 05P18RDRB1 and 05P18SJRB1.

†T.Sieber@gsi.de

ISBN: 978-3-95450-249-3 ISSN: 2673-5350 doi: 10.18429/JACoW-IBIC2024-THP04

MEASUREMENT OF BEAM PHASE AND ENERGY USING BPMs AND FCTs AT THE MEBT SECTION OF CSNS H⁻ LINAC

F. Li*, M. A. Rehman, Z. Xu, W. Huang, R. Qiu, L. Zeng, R. Yang, T. Yang
Institute of High Energy Physics, Chinese Academy of Sciences (CAS), Beijing, China
also at China Neutron Spallation Source, Dongguan, China

Abstract

Accurately measuring the beam phase is critical when determining the ideal RF cavity parameters for beam acceleration. In the past, only Fast Current Transformers (FCTs) were used to measure the beam phase. However, with the upcoming upgrade of the MEBT section for the CSNS-II project, shorted strapline-type Beam Position Monitors (BPMs) will now be utilized to measure beam position, phase, and energy. LIBERA singlepass electron-ics are employed to measure the beam position and phase from the BPMs. Pairs of BPMs were used to measure beam phase shift, which can also be used to calculate beam energy. This paper compares beam phase meas-urement systematically by BPMs and FCTs.

INTRODUCTION

The China Spallation Neutron Source (CSNS) is a platform for scientific research, consisting of an RF ion source, a 3 MeV Radio Frequency Quadruple (RFQ), 80 MeV Drift Tube Linac (DTL), 1.6 GeV Rapid-Cycling Synchrotron (RCS), and several beamlines. Significant upgrades will be made to the Medium Energy Beam Transport (MEBT) for the future CSNS-II as part of a power upgrade. The MEBT section consists of 5 Fast Current Transformers (FCT) [1] and 7 Beam Position Monitors (BPM). With the upgrades planned for the second phase, the functionality of the existing FCTs will be replaced by a BPM system. Therefore, a comparative study of FCT and BPM systems for phase and energy measurements in the CSNS-II MEBT are necessary, including system calibration, consistency in phase and energy measurements, and comparison of phase stability and reliability in first and second harmonics.

The BPM system will use Libera SPH [2], an electronics device designed for beam position and phase measurement in particle accelerators and beamlines, and the FCT system has been using self-developed electronics on CSNS for about ten years. This study mainly compares two sets of closely located beam position monitors (BPM05 and BPM07) and fast current transformers (FCT03 and FCT05) in the MEBT section. Figure 1 shows the beam instruments layout of the CSNS MEBT.

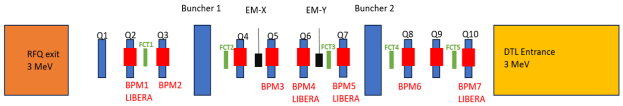

Figure 1: Layout of the CSNS MEBT.

* lifang@ihep.ac.cn

CABLE OFFSET MEASUREMENT OF BPM SYSTEM

Factors affecting the accuracy of accelerator beam phase measurement are detector performance, cable delay, electronics discrepancies, and other factors. The transmission of beam signals is influenced by cable delays, leading to measurement deviations. Therefore, accurate calibration and compensating cable delays are necessary to ensure measurement accuracy. Discrepancies between electronic modules, such as signal processing speed and response time, can result in inconsistent measurement results. Calibration and adjustment of electronic differences are required to ensure measurement consistency. Other factors affecting the accurate measurement of the accelerator beam phase include environmental conditions, such as temperature and humidity.

Considering these factors, accurate measurement of the accelerator beam phase requires a comprehensive assessment of detector performance, cable delay, electronics discrepancies, and other factors [3]. Effective control and calibration of these factors during the measurement process are essential to ensure the accuracy and reliability of measurement results.

Since all detectors have been installed on the accelerator beamline, calibration measurement was only performed on the FCTs in the past phase, with no calibration done for the BPM. Additionally, the differences between electronic channels are minimal. Therefore, calibration is only carried out on the BPM cables in this study. The cables between the probes and electronics of each system use LMR200 at both ends and LMR400 in the middle. The goal was to investigate phase consistency and synchronization using two different measurement methods.

The first method involved utilizing a Vector Network Analyzer (VNA) to perform Time Domain Reflectometry (TDR) measurements on the cables connecting the BPM05/BPM07 shown in Fig. 2. The TDR plots generated by the VNA are analyzed to determine the cable lengths and calculate the phase offset. From Table 1, it can be observed that the lengths of the electronic cables are all around 37.9 meters, with minimal differences.

Table 1: BPM Cable Length Measurement

Cable Length	A [m]	B [m]	C [m]	D [m]
BPM05	37.81	37.93	37.93	37.93
BPM07	37.87	37.83	37.88	37.87

ISBN: 978-3-95450-249-3 ISSN: 2673-5350 doi: 10.18429/JACoW-IBIC2024-THP05

DEVELOPMENT OF BUNCH-BY-BUNCH BEAM CHARGE MONITOR FOR HIGH ENERGY PHOTON SOURCE

Z. Liu†, J. S. Cao, J. H. Yue, Y. F. Sui, S. J. Wei, Q. Ye, Y. Y. Du, T. G. Xu, Y. Zhao, J. He, L. Wang
Institute of High Energy Physics, Beijing, China

Abstract

A bunch-by-bunch beam monitor electronics for High Energy Photon Source (HEPS) was designed. The hardware of electronics consists of analog signal acquisition board and digital signal processing board. The software consists of underlying firmware and application software. The sampling frequency is 500 MHz, and the bandwidth is 1 GHz. The electronics digitizes four analog signals from BPM probe, and ZYNQ chip was used to process the beam data and calculate the charge of each bunch. This system has been used in HEPS booster and HEPS storage ring.

INTRODUCTION

The High Energy Photon Source (HEPS), the first fourth-generation synchrotron light source in China, consists of a 500 MeV LINAC, a booster synchrotron to ramp the beam energy to 6 GeV, a 6 GeV storage ring, and three beam transfer lines [1]. The operators in the Central Control Room need to acquire all the bunch charge information in every bucket of the booster and ring respectively. Thus, the Bunch Charge Measurement (BCM) system is built to help the commissioning of HEPS. Table 1 lists some physical parameters and requirements for the BCM system.

Table 1: Parameter of Booster and Ring

Parameter	Booster	Ring
RF frequency/MHz	499.8	499.8
Harmonic Number	757	756
Minimum Bunch Space/ns	2	2

SYSTEM OVERVIEW

The BCM system consists of three main parts: beam position monitor (BPM), the signal processing electronic and the software that processes the BCM data, as shown in Figure 1.

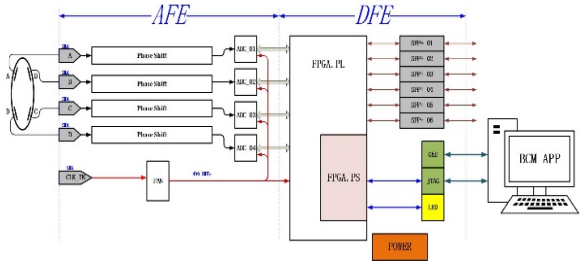

Figure 1: System diagram of BCM.

The BPM pickup generates pulse signals with a repetition frequency of 499.8 MHz, and each pulse corresponds to one beam bunch.

The front-end electronic imports the signals from the BPM, and then adjusts them. The signals are input to the signal processor and are converted to digital numbers using high-speed digital-to-analog converters (DACs).

The software converts the ADC bits to charge, displays the BCM data in the right order of bunch number, and updates the corresponding EPICS variables.

HARDWARE

The BCM electronic consists of analog signal acquisition board, which is called AFE (Analog Front End), and digital signal processing board, which is called DFE (Digital Front End), as shown in Figure 2 and Figure 3.

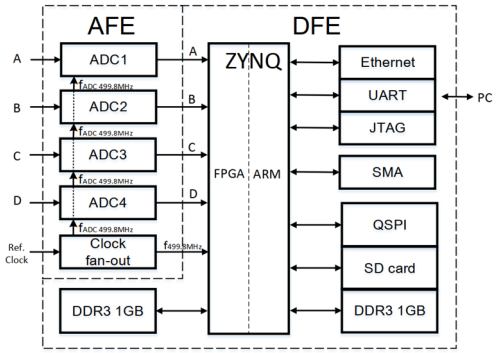

Figure 2: Hardware diagram of BCM.

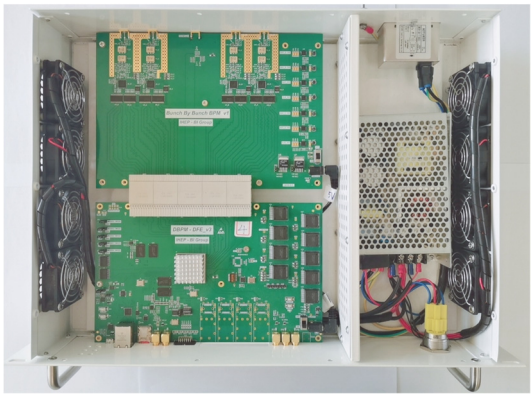

Figure 3: Picture of real BCM electronic products.

Analog Circuit Board

The AFE is used to digitize the bunch-by-bunch signal at frequency of 499.8 MHz, which synchronizes with the bunch signals from the BPM pickup. So, the main modules of AFE are detailed below.

ISBN: 978-3-95450-249-3 ISSN: 2673-5350 doi: 10.18429/JACoW-IBIC2024-THP08

USING TRANSIMPEDANCE AMPLIFIERS FOR CURRENT MEASUREMENTS OF LONG BEAM PULSES

M. Gasior, D. Alves, M. Dolenc, R. Ruffieux, CERN, Geneva, Switzerland

Abstract

CERN H^- Linac 4 (L4) and ion Linac 3 (L3) operate with millisecond beam pulses, which pose a challenge for beam current measurements based on Fast Beam Current Transformers (FBCTs). In the past the low cut-off frequencies of the FBCTs were actively lowered using a combination of transimpedance (TI) amplifiers and integrating amplifiers. Unfortunately, in many locations such amplifiers were sensitive to interference from neighbouring power systems. The situation was particularly difficult in L3, where in addition to long beam pulses, the challenge was also small beam currents. The interference problems had been addressed for years with limited success and finally it was decided that the whole FBCT front-end electronics should be renovated, with the main objective being to improve the immunity to interference. This paper describes the evolution of the FBCT front-end electronics and installations, which has finally allowed reliable beam current measurements, whose examples are provided. The key improvement was the use of small TI amplifiers directly connected to the FBCTs, which in addition simplified installations in both linacs. The TI amplifiers provide an active low impedance load to the FBCTs, extending their time constants by some two orders of magnitude, as compared to operation with a 50 Ω load. Challenges of the TI amplifier implementation are described, along with particularities of their beam commissioning.

INTRODUCTION

As illustrated in the left photograph of Fig. 1, in the past each L3 and L4 FBCT (T) was connected to its head amplifier (A) by a twisted-pair cable [1, 2][1]. Its resistance limited the smallest value of the FBCT load seen by the amplifier and therefore the lowest achievable droop of the beam signal. The cable resistance can also give rise to interference voltages induced by ground loop currents caused by nearby power equipment.

The first limitation was overcome in the past by using an integrating amplifier, which compensated the signal droop achieved by the input TI amplifier. As FBCTs even of the same type can have inductances differing by more than 100 %, each FBCT thus required a dedicated amplifier with the compensation adjusted to its inductance. With about 30 FBCTs operational in the linacs [3], this requirement heavily complicated the installations, their maintenance and spares management.

Laborious maintenance and many interference problems, which had not been properly solved for years, finally led to an upgrade programme of the linac FBCT amplifiers, along with their installations. The new scheme, shown in the right photograph of Fig. 1, is based on small amplifiers (A) installed directly on the FBCT output connectors. All three cables of the installation, namely the beam signal, the calibration signal for one-turn FBCT calibration winding and the power supply, are equipped with simple balun transformers (B) built with a few turns of cable wound on high-permeability toroids. The baluns increase the impedance of potential ground loops and therefore reduce the corresponding currents.

[1] Please note that schematics in [1] and [2] do not take into account subsequent hardware modifications to include an integrating amplifier stage present in all L3 and L4 FBCT amplifiers before the renovation described in this paper.

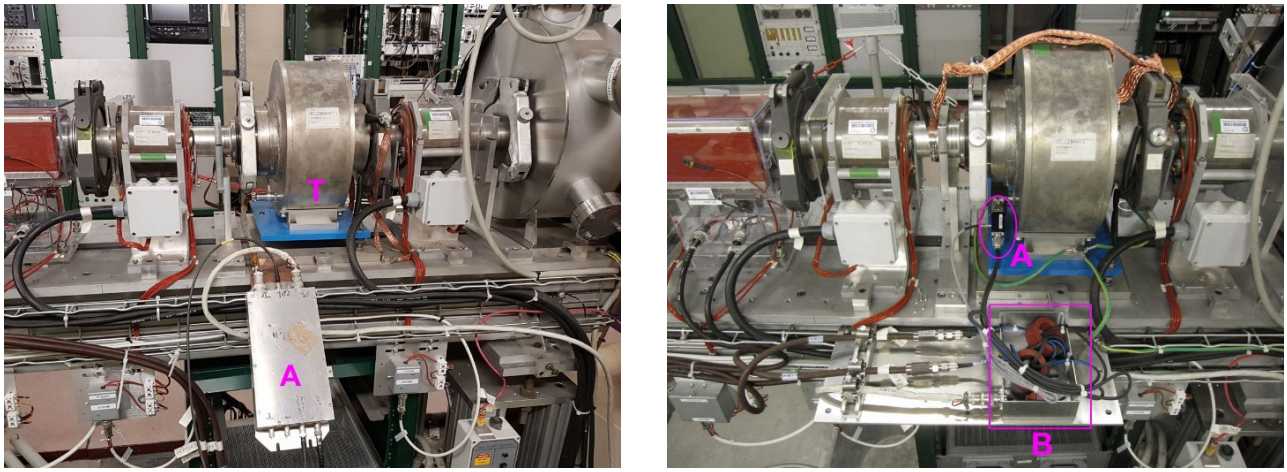

Figure 1: Photographs of the old Linac 3 FBCT installation (left) and the new (right) on the example of ITL.BCT15.

ISBN: 978-3-95450-249-3 ISSN: 2673-5350 doi: 10.18429/JACoW-IBIC2024-THP09

DEVELOPMENT OF A METAMATERIAL-BASED CAVITY BEAM CURRENT MONITOR AT HUST*

Yuexin Lu, Jiqin Li, Jian Wang, Zhengzheng Liu, Kuanjun Fan†
Huazhong University of Science and Technology, Wuhan, China
Jinfeng Yang, Osaka University, Osaka, Japan
Zhigao Fang, High Energy Accelerator Research Organization, Ibaraki, Japan
Oleg Meshkov, Budker Institute of Nuclear Physics, Novosibirsk, Russia

Abstract

The dimensions of a cavity beam diagnostic device are determined by its operating frequency, which is linked to the repetition frequency of the beam bunch. This relationship limits the effectiveness of such devices for measuring low repetition frequency bunches. In cyclotron-based proton therapy systems, where the bunch repetition frequency is relatively low, there is a need for real-time online monitoring during clinical procedures. To address this, we propose a metamaterial-loaded cavity beam diagnostic device with a fundamental mode resonant frequency that is double the bunch repetition frequency. Electromagnetic simulations demonstrate that this design significantly reduces the cavity size under low-frequency conditions and effectively mitigates the electromagnetic energy loss, resulting in improved sensitivity.

INTRODUCTION

Non-intrusive cavity diagnostic devices for beam current measurement offer significant advantages, such as high-induced signal strength and sensitivity. However, the size of a resonant cavity is inversely related to its operating frequency, leading to increased dimensions at lower frequencies, which can limit its applicability. To address the challenges in real-time monitoring of beams with low repetition rates and weak intensities, modifications to the cavity structure are needed to regulate its internal electromagnetic field distribution and reduce the operating frequency. PSI [1, 2] and HUST [3] have developed innovative cavity beam current diagnostic devices by filling the resonant cavity with dielectric materials, thereby enhancing their performance.

Metamaterials are a class of artificially engineered structures that can be designed to have negative effective permittivity and negative effective permeability [4], which can significantly alter the behavior of electromagnetic fields for various applications [5]. Previous research has shown that waveguides loaded with metamaterials can propagate quasi-TM mode waves at frequencies below the cutoff frequency of traditional metallic waveguides [6]. Building on this foundation, we designed a specially structured metamaterial and incorporated it into the resonant cavity, effectively lowering the cavity's resonant frequency and significantly reducing its size. This metal-based metamaterial overcomes the precision machining challenges associated with dielectric materials as cavity fillers while also reducing electromagnetic field losses within the cavity. The resonant frequency of this cavity-based Beam Current Monitor (BCM) is set at 146 MHz, aligning with the proton beam repetition frequency (73 MHz) of the HUST Proton Therapy Facility (HUST-PTF) at Huazhong University of Science and Technology. [7–9]

DESIGN

A cavity beam diagnostic device captures the electromagnetic field signal induced as the beam passes through the cavity, providing crucial information about the beam. In a cylindrical cavity resonator, the TM010 mode exhibits the strongest electric field at the center of the cavity. This electric field, directly proportional to the bunch charge, is concentrated almost entirely in the central region, making it highly suitable for current intensity detection.

The resonator, equipped with coupling loops, can generate a signal proportional to the beam charge q. For the TM mode, the amplitude sensitivity can be expressed as follows [10]:

$$V_{out} = \pi q f \sqrt{\frac{Z}{Q_{ext}}\left(\frac{R}{Q}\right)}. \quad (1)$$

In the equation, with given frequency f and line impedance Z, the voltage signal is related to the normalized shunt impedance R/Q and external quality factor Q_{ext}. The value of the external quality factor is determined by the antenna position.

To achieve a working frequency of around 146 MHz, a cylindrical cavity would typically require a radius of approximately 784 mm, which is impractically large for production and application. The use of metamaterials presents a viable solution to this issue. Specially designed metamaterials can exhibit negative effective permittivity or permeability depending on the frequency. Within a frequency range where the effective permittivity is negative, the TM mode can propagate. By incorporating a metamaterial unit cell, a negative refractive index passband is created, allowing the transmission of electromagnetic waves below the cutoff frequency of the resonant cavity. This feature can be utilized to significantly miniaturize the cavity.

Following the structure developed by Y. Wang et al. [11], the metamaterial unit was designed to meet the specific requirements. Metamaterial cells with a single slotted wire have smaller lateral dimensions and greater axial electric field intensity. By increasing the length of the slotted wire, the resonance frequency can be reduced. Figure 1

* Work supported by the National Key Research and Development Program of China (2022YFA1602202) and the National Natural Science Foundation of China (NSFC) (12235005)
† E-mail: kjfan@hust.edu.cn.

ISBN: 978-3-95450-249-3 ISSN: 2673-5350 doi: 10.18429/JACoW-IBIC2024-THP11

ABSOLUTE BEAM CURRENT MEASUREMENT FOR SLOW EXTRACTED BEAMS AT CERN's NORTH AREA FACILITY

J. Tan†, G. Khatri, M. McLean, T. Koettig
CERN European Organization for Nuclear Research, Geneva, Switzerland
L. Crescimbeni[1], F. Schmidl, Friedrich Schiller University Jena, Jena, Germany
T. Sieber, M. Schwickert, GSI Helmholtz Centre for Heavy Ion Research, Darmstadt, Germany
T. Stoehlker [1,2], V. Tympel[1], Helmholtz Institute Jena, Jena, Germany
[1]also at GSI Helmholtz Centre for Heavy Ion Research, Darmstadt, Germany
[2]also at Institute for Optics and Quantum Electronics, Jena, Germany

Abstract

The North Area facility (NA), built in the 1970s at CERN, hosts several secondary beam lines for a large variety of physics experiments: Neutrino Platform, Dark matter, high-energy physics, R&D, detector validation etc. 400 GeV/c primary proton beams, extracted from the SPS ring, are split along the transfer lines to fire on 4 targets and serve the users with secondary particles such as e-, e+, μ, π, hadrons, kaons... Within a typical slow extraction scheme of 4.8 s, one gets a spill intensity of about 4×10^{13} protons heading to the splitters. Available beam intensity monitors are ageing fast and are accurate up to 10 % only, which is incompatible for future high intensity physics programs and new demanding specifications for the beam instrumentation. In the wake of the NA consolidation project, it is proposed to measure the beam intensity with a Cryogenic Current Comparator (CCC). Such devices installed at FAIR (GSI) and in the Antimatter Factory (CERN) have proven to be operational and have a resolution of a few nA. This paper describes the roadmap and challenges to come for the development of the new CCC.

INTRODUCTION

The NA facilities (see Fig. 1), built in the 1970s at CERN, hosts the secondary beam lines and experimental areas of the Super Proton Synchrotron (SPS) complex. Thanks to their versatile beam lines distribution, particle type and energy reach, the demand for beam time by the physics community has been increasing from year to year. A variety of experiments spans from detector R&D and validation, fixed target experiments, Neutrino Platform and Physics Beyond Colliders [1].

During most of the physics run, about 4×10^{13} protons at 400 GeV are slowly extracted by a third-integer resonance setting for 4.8 s. The primary beam is split along the transfer line to serve the targets, for an annual integrated intensity of about 10^{19} protons on target (PoT). After 2028 the latter will steadily increase to approximately 5×10^{19} PoT with the recently approved SHiP experiment to exploit the future high intensity facility [2]. Low loss and reduced activation of the primary beam lines are of paramount importance to improve the facility's lifetime and ensure a smooth run for the coming 20–25 years.

† jocelyn.tan@cern.ch

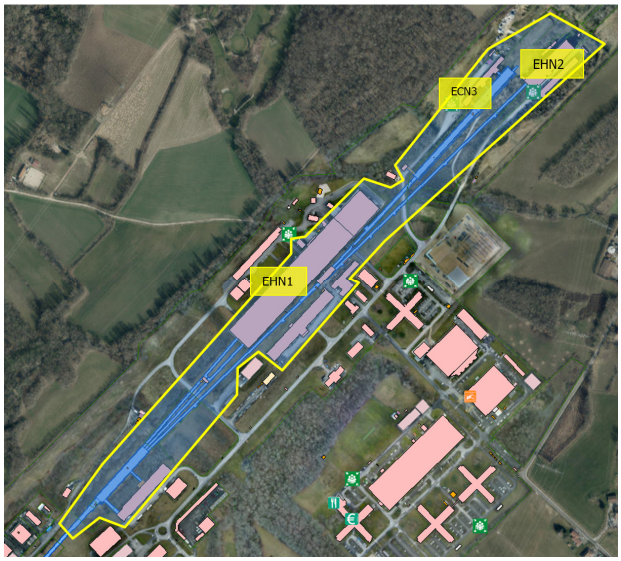

Figure 1: Aerial view of the North Area at CERN, showing the secondary beam lines (blue), two experimental halls (EHN1, EHN2) and the experimental cavern ECN3.

INTENSITY AND TRANSMISSION MEASUREMENTS

Monitoring the transmission efficiency is not trivial due to the lack of significant time structure on the extracted beam because the experiments require a continuous particle flux with a high duty-cycle, i.e. having mainly a DC time structure. Located in the primary beam lines, secondary emission chambers (SEM) are therefore used here as current monitors. Their design is robust and radiation hard. The extracted particles flux hits metal foils and generates secondary electrons which are trapped by polarised foils. In principle the signal is proportional to the spill intensity but slightly distorts the beam and doesn't provide the absolute number of particles. A joint endeavour to calibrate SEMs was difficult and time-consuming [3, 4]. It was shown that the estimated intensities could be wrong by over 20 % due to beam-induced foil damage.

Table 1 summarises the beam parameters for protons in the primary transfer lines. In addition to present operational schemes, it includes new figures compatible with the future SHiP experiment.

ISBN: 978-3-95450-249-3 ISSN: 2673-5350 doi: 10.18429/JACoW-IBIC2024-THP13

DCCT NOISE AND BEAM LIFETIME MEASUREMENT

G. Kube, K. Knaack, M. Werner
Deutsches Elektronen-Synchrotron DESY, Germany

Abstract

Beam lifetime measurements are an important tool to characterize the key storage ring and machine performance parameters. They are usually derived from dc current transformer (DCCT) data, and their accuracy depends on DCCT noise and data duration period. However, accurate dc current and fast lifetime determination are in contradiction and have to be balanced carefully. In this contribution, a model is presented which relates the relative accuracy in lifetime determination and the DCCT noise with the acquisition time. For the PETRA IV project at DESY which aims to upgrade the present PETRA III synchrotron into an ultra low-emittance source, according to this model a lifetime determination to the level of 1 % should be possible within 5 to 6 s acquisition time.

INTRODUCTION

The PETRA IV project at DESY (Hamburg, Germany) aims at the construction of a diffraction limited ultra-low emittance light source operating at 6 GeV [1,2]. The storage ring will be built in the existing PETRA III tunnel, thus inheriting the original 8-fold symmetry of the former PETRA collider. The accelerator lattice is based on a modified hybrid six-bend achromat (H6BA) cell and, taking advantage of the 2.3 km circumference, it provides electron beams with 20 pm rad emittance. The machine will be operated in two different modes, a *timing mode* with 80 bunches and 1 mA/bunch and a *brightness mode* with a homogeneous fill pattern of 1920 bunches and about 0.1 mA/bunch (baseline parameters). The expected lifetimes are 5 h (dominated by Toschek scattering) resp. 10 h in both modes.

Beam lifetime is an important measure to characterize the key storage ring and machine performance parameters, therefore their precise knowledge is of utmost importance. It is derived from the measurement of a change of the beam intensity which can be done with any intensity monitor. Usually a DCCT is used for this purpose.

In order to provide the required user stability a precise dc current measurement is mandatory, i.e. the DCCT noise should be kept to a minimum. For the PETRA IV brightness mode with 200 mA and 1920 bunches and assuming 1 % top-up level, the minimum detectable change in the beam current while filling a single bunch should amount to 1 µA. To be on the safe side, this minimum current change should be a factor of two above the noise level which results in rms(I) ≤ 0.5 µA. Reducing the noise level below this limit is usually achieved by averaging which entails a bandwidth reduction. At the other hand, from machine physical aspects a fast lifetime determination is preferable which is in contradiction to the process of long-term averaging. Therefore, accurate dc current and fast lifetime determination are in contradiction and have to be balanced carefully.

In this contribution a simple formula is derived which takes into account the dependency of lifetime accuracy and monitor noise, thus enabling to balance both quantities. The procedure is applied to the PETRA IV parameter case, indicating that it will be possible to determine the lifetime to a level of 1 % within 5 to 6 s acquisition time. Finally, the possibility is discussed to use more than one intensity monitor in order to reduce the acquisition time for lifetime determination.

MODEL DESCRIPTION

The beam current reduction caused by multipe effects (elastic and inelastic gas scattering, quantum lifetime, Touschek effect ...) as function of time in a storage ring is usually described by an exponential $I(t) = I_0 \exp(-t/\tau)$ with τ the beam lifetime. The output signal of a beam intensity resp. current monitor is recorded at a fix sampling rate, i.e. $t = n\,T_s$ with T_s the sampling time and $I_n = I(n\,T_s)$. Under normal circumstances $n\,T_s \ll \tau$ such that the exponential can be expanded, resulting in

$$\Delta I_n = I_0 - I_n = I_0 \frac{T_s}{\tau}\, n \; . \tag{1}$$

Eq. (1) represents a linear relation between a sample point n and the corresponding intensity loss ΔI_n with the lifetime information encoded in its slope. In order to derive a best guess for lifetime and lifetime uncertainty from a data set of N samples ($n = 0, \ldots, N-1$), this equation has to be analyzed which is conventionally done by means of a χ^2 minimization.

Parameter Estimation

Having N data samples (x_n, y_n) with indexing as before, for the case of a linear dependency $f(x_n) = m \cdot x_n + b$ the parameter estimation with corresponding error deviation can be performed analytically, see e.g. Ref. [3]:

$$\begin{aligned} \chi^2 &= \sum_{n=0}^{N-1} \frac{[y_n - f(x_n)]^2}{\sigma_n^2} \\ &= F - 2mE - 2bC + m^2 D + 2mbA + b^2 B \; , \end{aligned} \tag{2}$$

with the abbrevations

$$\begin{aligned} A &:= \sum_{n=0}^{N-1} \frac{x_n}{\sigma_n^2} \qquad B := \sum_{n=0}^{N-1} \frac{1}{\sigma_n^2} \qquad C := \sum_{n=0}^{N-1} \frac{y_n}{\sigma_n^2} \\ D &:= \sum_{n=0}^{N-1} \frac{x_n^2}{\sigma_n^2} \qquad E := \sum_{n=0}^{N-1} \frac{x_n y_n}{\sigma_n^2} \qquad F := \sum_{n=0}^{N-1} \frac{y_n^2}{\sigma_n^2} \; . \end{aligned} \tag{3}$$

ISBN: 978-3-95450-249-3 ISSN: 2673-5350 doi: 10.18429/JACoW-IBIC2024-THP16

STATUS AND PERFORMANCE OF LumiBelle2 IN THE 2024 BEAM OPERATION OF SuperKEKB

M. Li*, [1, 2, 3], P. Bambade[3], H. Nakayama[4], S. Uehara[4], S. Wallon[3]
[1]Institute of High Energy Physics, Chinese Academy of Sciences, Beijing, China
[2]University of Chinese Academy of Sciences, Beijing, China
[3]Laboratoire de Physique des 2 infinis Irène Joliot-Curie – IJCLab, Orsay, France
[4]KEK, Tsukuba, Japan

Abstract

LumiBelle2 is a fast luminosity monitoring system designed to do fast luminosity feedback and machine tuning for SuperKEKB. It uses sCVD diamond detectors placed in both the electron and positron rings to measure the Bhabha scattering process at vanishing photon scattering angle. The system provides Train-Integrated-Luminosity signals at 1 kHz for dithering feedback and Bunch-Integrated-Luminosity signals at 1 Hz to monitor variations along the bunch trains. After a long shutdown, in order to ensure its proper functioning during the 2024ab run, LumiBelle2 underwent testing, calibration, and upgrades. This paper describes the updated status of LumiBelle2 and presents its performance during the 2024ab run of SuperKEKB.

INTRODUCTION

SuperKEKB uses the so-called nano-beam scheme to reach a very high instantaneous luminosity of up to, nominally 8×10^{35} cm^2 s^{-1} [1]. It consists of using a large crossing angle at the interaction point (IP) to enable colliding 2500 ultralow emittance bunches with very small beam sizes (design value $\sigma_y \sim 50$ nm). The luminosity is very sensitive to beam-beam offsets, which is caused by ground motion or other external source. To maintain the optimum beam collision condition, orbit feedback systems are essential at the IP. At SuperKEKB, the beam-beam deflection method is used for vertical orbit feedback [2], while in the horizontal plane, a dithering orbit feedback system using the luminosity as input, similar to that operated in the past at PEP-II [3], has been adopted [4].

For this purpose, a fast luminosity monitor based on sCVD diamond detectors, named LumiBelle2, was developed and successfully operated in 2019-2021 [5]. By measuring the rate of Bhabha events on each side of the IP at vanishing photon scattering angle, LumiBelle2 can provide both Train-Integrated-Luminosity (TIL) signals and Bunch-Integrated-luminosity (BIL) signals simultaneously, over a large range of luminosities. The TIL signals, as input to the dithering feedback system, with relative precision better than 1 % at 1 kHz, can be used to maintain optimum overlap between the colliding beams in the horizontal plane [6, 7]. BIL signals are useful for machine tuning and beam parameters studies of the successive bunches along the trains. In addition, there is also another luminosity monitoring system named ZDLM (Zero Degree Luminosity Monitor) installed in the immediate vicinity. It uses Cherenkov and scintillator detectors, providing important complementary measurements.

From July 2022 to the end of 2023, SuperKEKB had a long shutdown for maintenance and upgrades. In order to ensure LumiBelle2 satisfactory operation during the 2024ab run, a program of checks and calibrations of the LumiBelle2 hardware and software components was implemented before the restart of the accelerator complex. In this paper, the updated status of LumiBelle2 is reported followed by a report on obtained luminosity monitoring performance, based on the new data.

CURRENT SETUP

Only five diamond detectors are currently installed in the two rings, at locations 10 and 30 meters downstream of the Interaction Point (IP) in the Low Energy Ring (LER) and High Energy Ring (HER), respectively. Detectors with both 500 and 140 µm thickness, coupled to low-noise 10 ns shaping time charge amplifiers and 2 GHz broadband current amplifiers, respectively, are used to take into important account variations in signal acceptances. In the HER, three 500 µm thick diamonds are installed, and in the LER, both 140 and 500 µm thick diamonds are used, as illustrated in Fig. 1. Both the diamond detectors and amplifiers were manufactured by CIVIDEC [8].

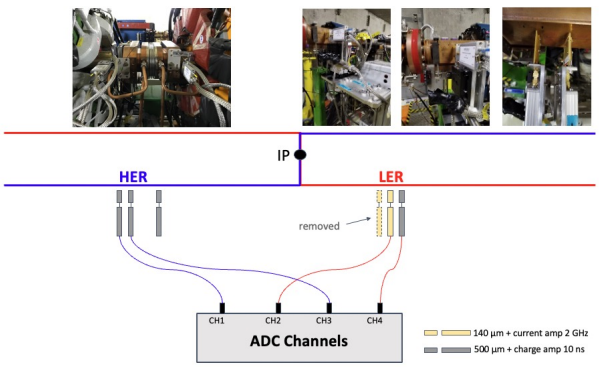

Figure 1: Current setup of diamond sensors and corresponding amplifiers of LumiBelle2 in the HER and LER.

To enhance the detection of Bhabha scattering events in the LER, a Tungsten radiator is positioned after the 45° window-shaped beam pipe. Initially, a sixth diamond detector was placed directly behind the Tungsten radiator to

* meng.li@ijclab.in2p3.fr

ISBN: 978-3-95450-249-3 ISSN: 2673-5350 doi: 10.18429/JACoW-IBIC2024-THP18

THE STATUS OF THE BEAM LOSS DIAGNOSTICS SYSTEM FOR THE SKIF SYNCHROTRON LIGHT SOURCE

O. I. Meshkov†,[1], L. B. Fomin, A. D. Khilchenko, Yu. I. Maltseva[2], Xiaochao Ma[3], E.A.Puryga, P. V. Zubarev, Budker Institute of Nuclear Physics, Novosibirsk, Russia
[1]also at Novosibirsk State University, Novosibirsk, Russia
[2]also at Novosibirsk Technical State University, Novosibirsk, Russia
[3]also at National Synchrotron Radiation Laboratory, Hefei, China

Abstract

The Siberian Ring Photon Source (SKIF) is a fourth-generation synchrotron light source that operates at a beam energy of 3 GeV. In order to ensure the reliable operation of the accelerator, a beam loss diagnostics system will be implemented. For the linear accelerator, linear accelerator-to-booster and booster-to-storage ring transfer lines, fiber-based Cherenkov beam loss sensors will be used. Multi-mode quartz fibers and photo multiplier tubes (PMTs) will provide spatial resolution for this diagnostic system at a level of about 1 meter. The storage ring will be equipped with 128 scintillation-based detectors with acquisition electronics that are placed around the circumference of the ring. These detectors will be able to measure beam losses both during beam injection and during regular SKIF operations for SR users. Since SKIF will operate in different working modes, the BLMs system will require high sensitivity, a large dynamic range, and sophisticated electronics. The paper describes the design of both types of beam line magnets (BLMs) and the choice of their positioning around the storage ring. It also discusses the final design of the acquisition electronics, the tests of the BLMs and the current status of diagnostics.

INTRODUCTION

SKIF [1] is the 4-generation synchrotron light source built by the Budker Institute of Nuclear Physics (BINP) with an energy of 3 GeV. It is expected to be completed in 2024 and begin operation in 2025. SKIF consists of an electron source [2] and a linear accelerator that provides 200 MeV electrons [3], a booster that accelerates the electrons to 3 GeV and a cyclic electron storage ring that stores 3 GeV electrons. To enhance the stability and lifetime of this system, accurate detection and tracking of beam losses are required.

In order to study the beam loss under different operating conditions, two types of beam loss detection systems will be installed at SKIF. Fiber-based Cherenkov beam loss sensors are relatively mature and have been applied in various accelerator facilities. The principle of these sensors is that charged particles produce Cherenkov radiation in optical fiber. This radiation is detected by the Photo Multiplier Tubes (PMTs) to determine the location and intensity of the beam losses. These sensors have the characteristics of suitable for narrow areas, covering a large length with ease and having fast response time. We proposed to use fiber-based Cherenkov beam loss sensors along the linear accelerator, the linac-booster transfer line and the booster-storage ring transfer line.

Scintillator based BLM detectors (SBLMs) are widely used for particle diagnostics in the various fields such as science, industry and medicine. These detectors have high sensitivity, fast response time, high efficiency and sufficient radiation hardness, as well as high reliability. The will be used around the storage ring.

BLM is an essential analysis tool for trouble-shooting and an important component in accelerator protection. There are two types of beam losses in an accelerator: irregular and regular beam loss. Irregular beam losses are usually caused by poor beam alignment or accelerator component failure, and they occur rapidly. Regular beam losses, on the other hand, are often unavoidable and relate to the beam lifetime, which occurs continuously and slowly [4].

The recording equipment of BLMs on SKIF should work in two modes. During beam injection into the storage ring, the beam loss can reach several percent in a dozen revolutions. However, during the operation of the storage ring for user experiments, the loss is significantly lower and determined by the beam lifetime, and significantly lower than first case. Therefore, BLMs need to be able to deal with both irregular and regular losses simultaneously. The dynamic range required for this is about 10^4. By combining a PMT and a scintillator, a high-sensitivity BLM system can achieve this high dynamic range through adjustable gain.

BLM signals are proportional to the number of particles lost. The ratio depends on the type of BLMs, the type of scintillator, and the type of particles interacting with the material. Electrons escaping from the beam will cause electromagnetic radiation and shower after interacting with the vacuum walls. Particles from the shower then enter the BLM scintillator which is made of a special grade of polystyrene. This is causes a flash of a light in the scintillator with a characteristic duration of about 10 nanoseconds. The photons then enter a PMT, and the signal from the PMT is recorded by an analog-to-digital converter (ADC) and transmitted to the computer. The distribution of BLMs at the SKIF facility is presented in Figure 1.

CHERENKOV FIBER-BASED BLM (CBLM)

CBLMs are applied at the straightforward sections of the accelerator's complex, such as the linac and transfer lines. Electrons lost in the accelerator collide with the vacuum wall producing high-energy secondary electrons that travel

† email address O.I.Meshkov@inp.nsk.su

ISBN: 978-3-95450-249-3 ISSN: 2673-5350 doi: 10.18429/JACoW-IBIC2024-THP19

DIAGNOSTICS OF BEAM LOSSES AT THE NOVOSIBIRSK FREE ELECTRON LASER

L. B. Fomin†, O. I. Meshkov, Y. V. Getmanov, Y. I. Maltseva, O. A. Shevchenko, A. V. Sudnik, I. A. Terentyev, A. V. Tur, Budker Institute of Nuclear Physics, Novosibirsk, Russia

Abstract

The article describes the current methods of beam losses diagnostic used at the Novosibirsk Free Electron Laser (NovoFEL). Three types of diagnostics are used: a) observation of average losses at the first track of the NovoFEL, b) observation of losses from each bunch separately, and c) observation of losses from series of bunches in so-called "macro pulses" mode of generation of radiation. Further, all three types of diagnostics are described in details.

INTRODUCTION

The Novosibirsk Free Electron Laser (NovoFEL) facility includes three free electron lasers (FEL), which are installed on the first, second and fourth tracks of a multi-turn accelerator-recuperator [1]. The wavelength of the radiation of the first FEL is adjusted in the range of 110-240 μm. The radiation of this FEL consists of a periodic sequence of short pulses following each other with a repetition frequency of 5.6 or 11.2 MHz. The average radiation power can reach a value of 0.5 kW, and the peak power is 1 MW. The second FEL operates in the wavelength range of 40-80 μm. The repetition rate of the radiation pulses is 7.5 MHz, and the values of the average and peak powers coincide with the first FEL. The wavelength range of the third FEL is 5-20 μm.

A linear accelerator-recuperator is used as an electron source for NovoFEL.

The general scheme of the facility is shown in Fig. 1, the parameters of the accelerator-recuperator in Table 1, and the radiation parameters in Table 2.

Table 1: The Accelerator-recuperator Parameters

Parameter	1st FEL	2nd FEL	3rd FEL
Maximum energy, MeV	12	22	42
Operating current, mA	10	3.2	3.2
Repetition frequency of bunches, MHz	5.6	3.75	3.75
Emittance, μm x μrad	30	30	30
Operating frequency of resonators, MHz	180.4	180.4	180.4

† email address L.B.Fomin@inp.nsk.su

Table 2: Radiation Parameters of the NovoFEL

Parameter	1st FEL	2nd FEL	3rd FEL
Wavelength, μm	110-240	40-80	5-20
Maximum average power, kW	0.5	0.5-1	10
Maximum peak power, MW	1	1	10
Pulse duration, ps	30-120	20-40	10-20

The installation can operate in one of three modes – with generation on the first track, with generation on the second track, or with generation on the fourth track (the undulator is not installed on the third track). The typical beam path in the generation mode includes up to 4 passes of accelerating resonator for energy gain, one pass of undulator and also up to 4 passes of resonator for recovery.

During the generation of radiation in the undulator, the beam is micro grouped, accompanied by an increase in its energy spread. A beam with a large energy spread, passing through optical elements with a nonzero dispersion function (e.g. bending magnets), acquires a noticeable spatial spread, which leads to significant losses of the beam on the walls of the vacuum chamber and an increase in the radiation background.

As one of the tools for adjusting the optical structure of the facility, a beam loss diagnostic system was implemented. Cherenkov sensors of this system are installed in three locations, the information from which is used by the operator to adjust the optimal beam passage.

DIAGNOSTICS OF AVERAGE LOSSES

The first sensor is installed in the final part of the first track (marked with an arrow 1 in the Fig. 1). Both accelerating and decelerating beams with a large energy spread pass through this place. As a result, a large heating of the walls of the vacuum chamber was observed in this place.

As a sensor was used a block of quartz, which is placed directly near the vacuum chamber. The beam, hitting the wall of the vacuum chamber, generates a shower of secondary particles in it, which, passing through the sensor, form

ISBN: 978-3-95450-249-3 ISSN: 2673-5350 doi: 10.18429/JACoW-IBIC2024-THP21

DEVELOPMENT OF BEAM LOSS MEASUREMENT ELECTRONICS BASED ON ZYNQ IN RCS OF CSNS-II

R. J. Yang*, Z. H. Xu†, L. Zeng, F. Li, W. L. Huang, R. Y. Qiu, M. Y. Liu, T. Yang
Institute of High Energy Physics, Chinese Academy of Sciences (CAS), Beijing, China
also at China Neutron Spallation Source, Dongguan, China

Abstract

The beam loss measurement system is an important beam measurement device in the CSNS accelerator, used to measure the beam loss signals along the entire accelerator to monitor the beam status. In CSNS, the beam loss measurement system uses NI PXIe-6358 acquisition card combined with self-developed front-end analog electronics. In the RCS of CSNS-II, a new beam loss electronics based on zynq development is planned to replace the existing electronics for beam loss signal acquisition. The CSNS-II ring beam loss measurement electronics based on zynq consists of independently developed high-voltage output modules, front-end analog boards, digital boards, as well as related driver programs, epics ioc software,etc,realizing functions such as signal acquisition, range control, data processing, epics publishing.

INTRODUCTION

The CSNS-II ring beam loss measurement electronics system is independently developed by us. The electronics consists of a custom chassis, front-end analog board, digital board developed based on zynq, and high-voltage output module. It can connect up to 6 BLM simultaneously, enabling high-voltage output, signal acquisition, MPS signal output, and data transmission through epics. At the same time, the electronics can adjust the gain according to the signal size to improve the signal measurement range and measurement accuracy [1].

SYSTEM CONSTITUTION

BLM Electronics Hardware Architecture

The BLM electronics system consists of a 3U custom chassis, AFE, High-voltage output module, and DFE. Each chassis can be configured with six AFE, two high-voltage output module, and one digital board, which can be used to connect six beam loss monitor (BLM) simultaneously. The hardware system architecture of the BLM electronics is shown in Figure 1.

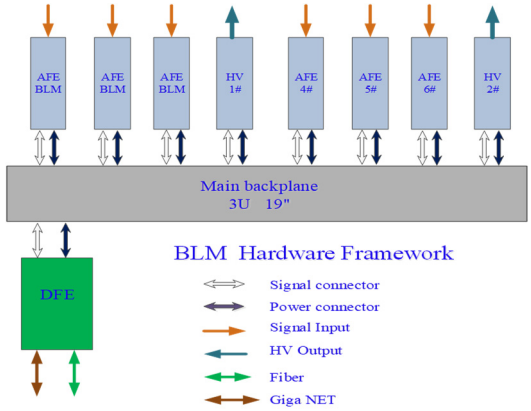

Figure 1: Electronic hardware architecture.

- AFE (front-end analog board)

In the normal operation mode of the accelerator, the BLM front-end simulation plug-in not only needs to measure the weak beam loss signal, but also needs to respond quickly to the beam loss signal exceeding the threshold, and output the MPS protection signal to the control system to achieve the alarm or beam pulling action, thus protecting the accelerator equipment [2].

According to BLM measurement requirements, the AFE front-end analog board needs to implement the following functions.schematic diagram of AFE is shown in Figure 2.

（1）I-V conversion, converting the current signal output by the BLM beam loss detector into a voltage signal within the acquisition range of the acquisition card.

（2）MPS signal output, integrate the signal, and when the signal exceeds the threshold, output the machine protection signal.

（3）Gain-adjustable signal follower for real-time observation of beam loss signal.

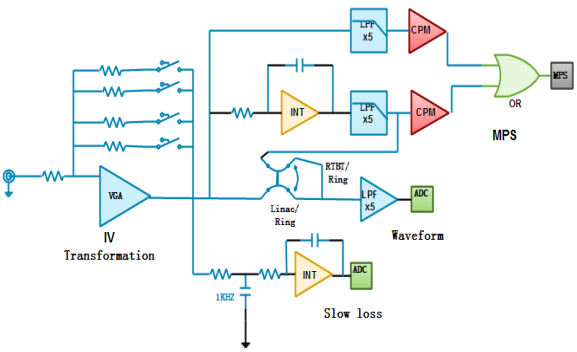

Figure 2: Schematic diagram of AFE.

*yangrenjun@ihep.ac.cn
†xuzh@ihep.ac.cn

ISBN: 978-3-95450-249-3 ISSN: 2673-5350 doi: 10.18429/JACoW-IBIC2024-THP24

DESIGN AND FIRST RESULTS OF A CRYOGENIC BEAM LOSS MONITOR INSTALLED AT THE LHC

E. Effinger*, S. Morales Vigo, B. Salvachua, J. Storey, C. Zamantzas, CERN, Geneva, Switzerland
E. Griesmayer[1], TU Wien
[1]also at CIVIDEC, Vienna, Austria

Abstract

The Large Hadron Collider (LHC) is equipped with NiTb superconducting magnets operating at the cryogenic temperature of 1.9 K. A tiny fraction of proton beam at 7 TeV impacting the beam screener has the potential to generate enough heat, to cause the loss of superconductivity in the magnet (a magnet quench). Consequently, it is imperative for machine performance to detect such beam losses before the quench event occurs. To enhance the sensitivity of magnet quench detection through the measurement of beam losses, ongoing efforts focus on the development of cryogenic beam loss monitors (CryoBLM). This contribution outlines the design improvements made to a semiconductor-based beam loss detector installed inside the magnet cryostat, positioned just outside the vacuum vessel of the superconductive LHC dispersion suppressor magnets.

Detector Locations

The location for the detectors has been chosen according to the expected losses and loss scenarios from the experience during Run 1 of the LHC. The initial installation was performed during the Long Shutdown 1 (LS1) and first measurements were done during run 2. Two different locations for the detectors were chosen. The first location is in the Insertion Point 5 (IP5) in half-cell 9L5, about 350 m from the colliding point, at the interconnect between a quadrupole MQM and a dipole MBB, which was chosen due to the measured high integrated dose in this area. This location allows to measure the luminosity losses from the physics debris of the CMS experiment.

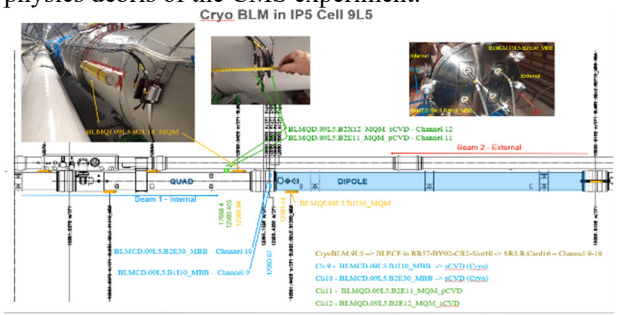

Figure 1: CryoBLM installation in IP5 half-cell 9L5.

The second location is in the Insertion Point (IP7), in half-cell 9R7, between the dipole MBA and dipole MBB interconnect. The main collimation system is located in IP7, thus, the detectors in IP7 will be able to measure the losses from the betatron halo cleaning. Additional information, concerning the detector installation during LS1 can be found in [1]. During the LHC Long Shutdown 2 (LS2), the complete design and installation of these detector types was reviewed and improved [2]. The location of the new CryoBLM remained the same. Figure 1 andFigure 2 show the installation pictures including a diagram showing the neighbouring elements. Outside the cryostat, two additional diamond detectors, one single-crystal Chemical Vapor Deposition (sCVD), one polycrystalline Chemical Vapor Deposition (pCVD) and one ionisation chamber were added to compare the signals with the CryoBLM which is based on a sCVD.

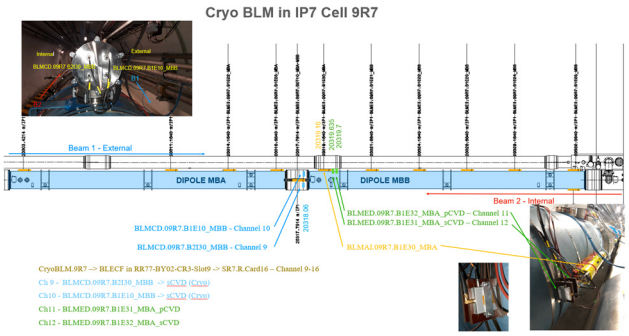

Figure 2: CryoBLM installation in IP7 half-cell 9R7.

Detector Positions

The CryoBLM detectors are located inside the cryostat and placed on the endcaps of the dipoles. In LS2, the mechanical holder was re-used from the LS1 installation, see Figure 3. The 4 rectangles in the central vertical and horizontal axis identify the possible location of the detectors.

Four holders have been welded on the endcap of the dipole, which allow fixing of the CryoBLMs on the cryostat close to the beam pipe.

Figure 3: Picture of the welded detector holder on the dipole endcap.

* Ewald.Effinger@cern.ch

ISBN: 978-3-95450-249-3 ISSN: 2673-5350 doi: 10.18429/JACoW-IBIC2024-THP25

MACHINE PROTECTION SYSTEM FOR HIAF

Y. Wei†, J. Wu, Z. Li, F. Ni, G. Zhu, J. Su, K. Gu, X. Qiu, Y. Zhang, Y. Yang
Institute of Modern Physics, Chinese Academy of Sciences, LanZhou, China

Abstract

The High Intensity Heavy-ion Accelerator Facility (HIAF), currently under construction, is a complex machine that couples a Continuous Wave (CW) superconducting ion Linear accelerator (iLinac) with a high-energy synchrotron to produce various stable and radioactive intense beams with high energies. The machine has a versatile operation mode which requires a high flexibility and reliability to the Machine Protection System (MPS). A customized and robust MPS is designed and developed to give the readiness of the machine for operation, to mitigate and analyze faults related to the relative damage potential. To get a high speed and have a high level of reliability, all interlock signal processing is processed on radiation-tolerant Field-Programmable Gate Arrays (FPGA) with triple or dual redundancy, as well as with a fail-safe design. By implementing a multiprocessing platform system-on-chip FPGA, the HIAF MPS can be tightly integrated with other systems to maximize availability pinpoint failures for operations, and give the post-mortem analysis. This paper will describe the architecture of the interlocks linking the protection systems, the strategies to manage the complexity, the detailed components, and the interlock logic of the customized HIAF MPS, as well as the test and verification of the prototype.

INTRODUCTION

The High Intensity Heavy-ion Accelerator Facility (HIAF) [1, 2] is a next-generation research facility for heavy-ion science and technology，the layout is as the Fig. 1 shown. HIAF consists of SECR (superconducting electron-cyclotron-resonance ion source), iLinac(ion Linear Accelerator), BRing(Booster Ring), HFRS(HIAF fragment separator), SRing(spectrometer ring) and several experimental terminals. The main beam parameters of HIAF are shown in Table 1.

The iLinac has three types of beam operation modes. CW mode is mainly used to supply beam between the iLinac and the T1 terminal, pulse mode is mainly used between the iLinac and the BRing, and the splitting time, in which the two ion sources supply beams and the iLinac accelerates the two types of beams in time to the T1 terminal and the BRing. The operation of the BRing is characterised by the complexity of the operation modes, the complexity of the beam structure, and the fast rate of up-conversion. The speed of BRing is fast. These pose challenges for the design of MPS.

The whole machine is split into 13 sections and the logic of the MPS is to combine different sections to meet different operation modes To have a high flexibility, the whole accelerator is partitioned by 2 master controllers master and 8 slave controllers slave. Depending on the mode of operation, different protection strategies are developed to protect the relevant beam supply areas, and interlock signals can be provided to the corresponding ion source and chopper according to the operating conditions .

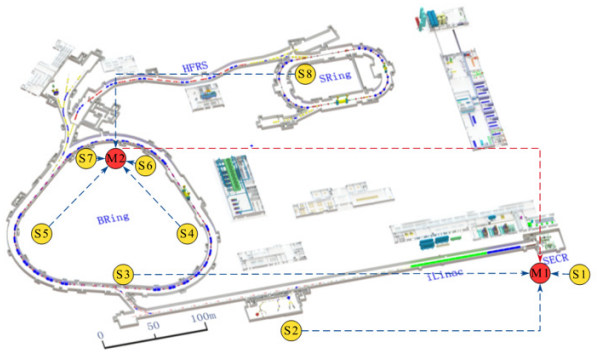

Figure 1: Layout of the HIAF.

Table 1: Overview of MPS of Several Accelerators

	SECR	iLinac	BRing	SRing
Length / circumference (m)		114	569	277
Beam energy of U (MeV/u)	0.014	17	835	800
Beam intensity of U	50 pμA	28 pμA	2×10^{11} ppp	(0.5-1) $\times10^{12}$ ppp
Operation mode	DC	CW or pulse	fast ramping (12 T/s, 3Hz)	DC, deceleration

High-energy, high intensity beams that pose a significant threat to materials and equipment. Calculations based on the beam parameters of the HIAF indicate that the power of the DC uranium beam at 1 emA, 17 MeV/u is 115.6 kJ. The thermal deposition effect of the uranium beam on the stainless steel at a beam profile of σ of 2 mm will cause the stainless steel to rise to 1398 °C at 28.8 μs, close to the melting point, as shown in Fig. 2.

To ensure a safe machine operation, especially for the CW superconducting linac, HIAF MPS needs to have a very fast response and the beam mitigation should respond within 20 μs after receiving NOK inputs. In addition, there are many operation modes at the HIAF complex, the MPS should be able to handle a large number of devices, feature configurable responses, possess signal logging for PM analysis, and must have a high level of reliability and flexibility, and so pose unique design challenges. Because of

† weiyuan@impcas.ac.cn

ISBN: 978-3-95450-249-3 ISSN: 2673-5350 doi: 10.18429/JACoW-IBIC2024-THP27

STUDY OF HIGH TRANSMITTANCE IONISATION CHAMBERS

Z. Q. Zhang*, Elekta, Beijing, China

Abstract

Ionisation chambers currently on the market have either high dose absorption or limited lifetimes. This study breaks both of these limitations and makes commercial ionisation chambers cheaper to manufacture.

After our beam test, it performed very well with various test environments as reproducibility of the dose response, proportionality of the dose response, stability of the dose response and so on.

INTRODUCTION

An ion chamber is a device used for measuring ionizing radiation. In the context of cancer X-ray treatments, it is employed to accurately measure the dose of X-rays delivered to the tumor site. This is essential for ensuring that the right amount of radiation is administered to destroy cancer cells while minimizing damage to surrounding healthy tissues.

During cancer X-ray treatment planning, ion chambers are often used in combination with other dosimetry tools to create a detailed map of the radiation dose distribution. This helps radiation oncologists optimize the treatment plan to achieve the best possible therapeutic outcome.

Moreover, ion chambers are regularly calibrated and quality-controlled to ensure their accuracy and reliability. This is particularly important in cancer treatment, where even small variations in radiation dose can have significant impacts on patient outcomes.

In summary, ion chambers are an important component of cancer X-ray treatments, providing accurate dose measurements and helping to ensure the safety and effectiveness of the treatment [1-4].

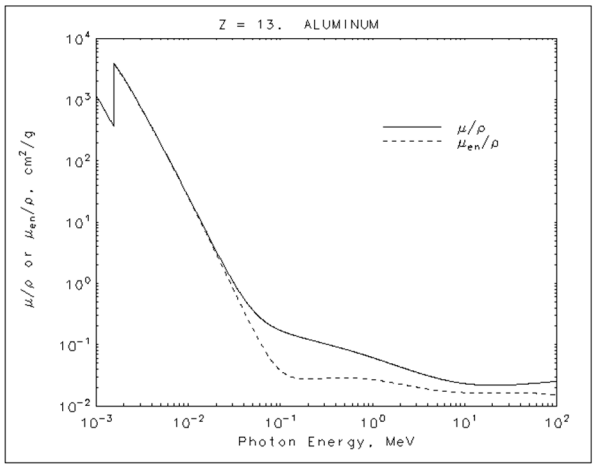

Figure 1: Al mass attenuation coefficient and mass energy-absorption coefficient.

* email address: zzq261261@gmail.com

DISIGN AND TEST RESULTS

In order to break thought the two limitations: I compared five different mental materials [5] usually used in radiation industry. They are Fe (Iron), Al (Aluminium), Cu (Copper), W (Tungsten) and Pb (Lead). Mass attenuation coefficient and mass energy-absorption coefficient of the above materials are shown as Figs. 1-5 [6].

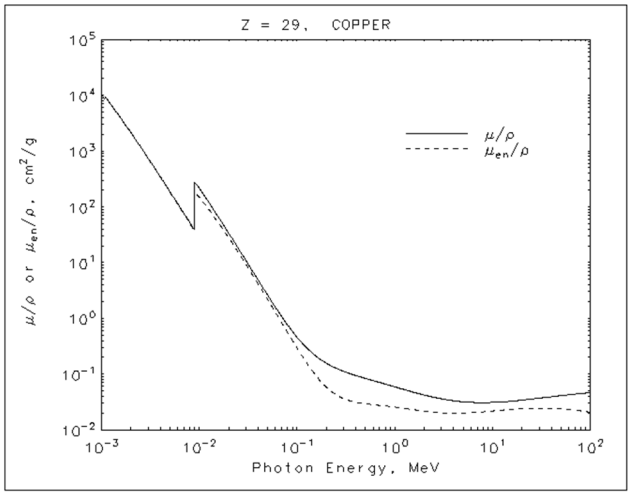

Figure 2: Cu mass attenuation coefficient and mass energy-absorption coefficient.

So I choose Al as the material to make the parts on the beam path. There is higher air pressure inside the chamber and a thin structure to reduce energy absorption. The grade of Al should meet good mechanical performance requirements, that is, have a high Young's modulus coefficient. Parts made of this kind of material will have less deformation under the same internal air pressure.

To design a long-lifecycle ion chamber, I choose a metal sealed mechanical structure to avoid components of air and water from entering. Considering the radiation environment, I designed a metal sealing structure and chose easily accessible seal materials and specifications. After comparing the hardness of Al and some other metal materials, indium wire is the best material for the sealing part. CF flanges are referenced during our new metal sealing structure design period. At last, a new metal sealing structure is invented and prototype leakage test shows that the new invention sealing structure has excellent air leakage performance. Its leakage rate is less than 1.0×10^{-10} mbar·L/s.

With the help of a physical engineer, I conducted three physical tests to verify its physical performance.

The first one is the X-ray profile in different electrons of the AL chamber. As shown in Fig. 6.

ISBN: 978-3-95450-249-3 ISSN: 2673-5350 doi: 10.18429/JACoW-IBIC2024-THP28

APPLICATION OF FIBER BEAM LOSS MONITORING SYSTEM (FBLM) AND SCINTILLATOR BEAM LOSS MONITORING SYSTEM (SBLM) AT HEPS*

L. D. Yu†, J.J. Ren, Y. Zhao, Z. Liu, T.G. Xu, L. Wang
Key Laboratory of Particle Acceleration Physics & Technology, IHEP, CAS, Beijing, China

Abstract

The High Energy Photon Source (HEPS) is a fourth-generation light source with a beam energy of 6 GeV currently under development by the Institute of High Energy Physics. The Beam Loss Monitor (BLM) system is designed for monitoring beam losses during machine commissioning. Two types of beam loss monitors have been installed in both the booster and storage ring. This paper introduces the principles and composition of these two BLMs, as well as their application in commissioning.

INTRODUCTION

The High Energy Photon Source (HEPS) constructed by the Institute of High Energy Physics (IHEP) with a beam energy of 6 GeV is doing commissioning. Beam Loss Monitor (BLM) systems are important part of the accelerators diagnostics. They are used during normal operation to identify and locate beam losses. To protect the HEPS commissioning, new Beam Loss Monitor (BLM) systems have been developed, installed and operated in HEPS. There are two types of BLMs at HEPS, including a fiber-optic beam loss monitor system (FBLM) for the booster and a scintillator beam loss monitor (SBLM) system for the storage ring. The design, installation and commissioning results are reported in this paper.

FBLMS IN THE HEPS BOOSTER

At HEPS booster, FBLMs are applicated. FBLMs are sensitive enough to record multiple large losses. There are three main components for the FBLMs, including optical fiber, Photo Multiplier Tube (PMT) and electronics.

Optical Fibers

Fiber play a role of sensor. To allow sufficient probability to detect secondary particles caused by beam losses, larger core diameter is preferred. The specification for the fibers are described in Table 1.

Table 1: Fiber Specification

Type	Core Diameter	Core/Cladding Material
HCP-M600T	600 μm	Pure Silica/ Hard Polymer

PMT and Electronics

PMT as data collector captures the light from Cherenkov radiation. The cathode spectral response for the PMT

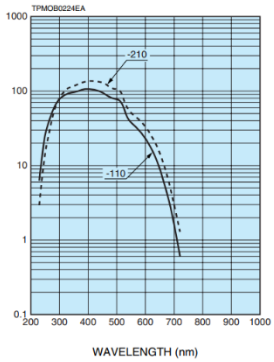

Figure 1: Cathode sensitivity for PMT.

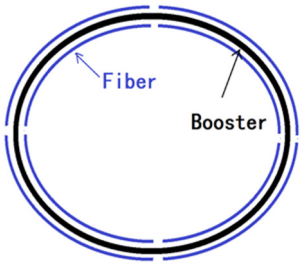

Figure 2: Schematic view of the optical fiber installation (blue line).

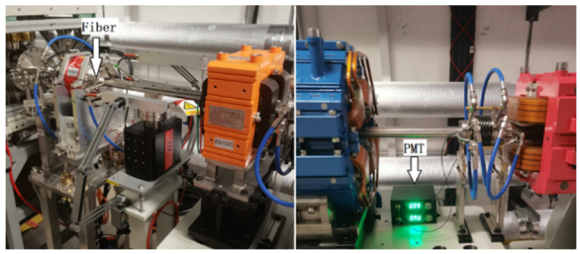

Figure 3: FBLM installed in the HEPS booster.

H10720-110 is shown in Fig. 1. The electronics is self-developed ADC with a maximum sampling rate of 500 Hz.

System Installation

The HEPS booster is 450 meters length. Figure 2 shows the schematic view of the optical fiber installation. 8 fibers are installed inside and outside the booster ring, each with a length of 110 meters, covering the entire booster. The fiber and PMT installed alongside the booster's vacuum pipe are shown in Fig. 3. For each fiber, two PMTs are connected to the fiber at both upstream side and downstream

† yuld@ihep.ac.cn

ISBN: 978-3-95450-249-3 ISSN: 2673-5350 doi: 10.18429/JACoW-IBIC2024-THP29

SIRIUS FAST BEAM ORBIT INTERLOCK SYSTEM

L.S. Perissinotto†, A.C.S. Oliveira, A.F. Giachero, D.O. Tavares, E.N. Rolim, F.H. Cardoso*,
F.H. de Sá, G.G. Saretti, G.R. Cruz, J.L.N. Brito, M.M. Donatti, T.M. d Rocha
LNLS, Campinas, Brazil
L. M. Russo, LBNL, Berkeley, CA, USA

Abstract

Insertion devices (IDs) are currently being installed at the SIRIUS storage ring to provide photon beams for upcoming high-brilliance beamlines. A fast orbit distortion detection system is imperative to safeguard critical vacuum chambers located near the straight sections of the IDs. In November 2023, an in-house Delta undulator was successfully installed, and a fast orbit interlock protection system was put in place, utilizing beam position monitors (BPMs) and the timing system infrastructure. Dedicated real time position and angle calculation is implemented in an FPGA and operates at a 6 kHz rate in the BPM processing electronics. A timing receiver board in the BPM MicroTCA.4 crate acts as a bridge between orbit distortion detection and the timing system's event generator (EVG), which sends an interlock signal to the low-level radio frequency (LLRF) controller to cut off the main RF oscillator. The main purposes of this work are to provide details about a new full-duplex timing network implementation, to discuss the main requirements of the orbit interlock, and to present measured performance results. Additionally, in pursuit of enhancing system reliability, post-mortem analysis and ongoing implementation proposals will also be presented.

INTRODUCTION

Particle accelerators have fast interlock protection systems to prevent component damage in the case of a miss-steered beam [1-3]. Insertion device (ID) safety is a concern for synchrotrons due to poorly centered beam generated radiation [4-5], which can damage storage ring (SR) and front-end (FE) devices.

SIRIUS features 3 high-brightness light sources, an operating in-house Delta undulator [6], and two new in-vacuum undulators (IVUs) that are currently being installed and are expected to be operational by November 2024. These insertion devices produce high-brightness photon beams that could potentially damage a vacuum chamber in case of an orbit distortion. Considering the worst-case scenario, with the storage ring operating at nominal current (350 mA), the Delta undulator's photon beam could pierce the vacuum chamber in approximately 20 ms. For this reason, a fast beam orbit interlock system (FBOIS) was implemented.

Reviewing the experience of other synchrotron facilities [3, 7], it was clear that upgrading the Sirius event-based timing system to support the Fast Beam Orbit Interlock System (FBOIS) would provide synchronous interlock signals, triggers for postmortem data analysis, and taking advantage of the previously installed timing infrastructure.

The FBOIS is configured through a multi-layer EPICS application for the straight sections where orbit distortion can cause damage. Its operation is automatically enabled when the storage ring current is above 10 mA, thanks to the minimum sum threshold configured in the BPMs. The BPM acquisition electronics also implements the position and angle checking, and, if a given threshold is exceeded, a physical signal is sent to a timing network device. If that happens, the event receiver (EVR) sends an interlock event upstream in the network until it reaches the event generator (EVG), which sends a beam dump event downstream tripping the LLRF signal and triggering a fast acquisition in all BPMs. The complete installed system overview is shown in Fig. 1. The straight sections orbit distortion limits for the high-brilliance IDs are summarized in Table 1.

Table 1: IDs Beam Orbit Tolerances

Dimension	Delta Undulator	IVUs
x	0.5 mm	1 mm
y	0.5 mm	1 mm
x'	0.4 mrad	0.4 mrad
y'	0.4 mrad	0.2 mrad

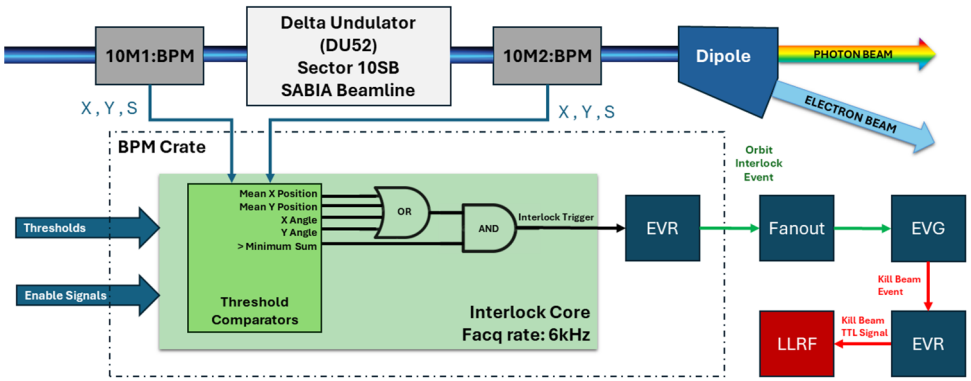

Figure 1: Fast Beam Orbit Interlock System Diagram.

† lucas.perissinotto@lnls.br
* fernando.cardoso@lnls.br

ISBN: 978-3-95450-249-3 ISSN: 2673-5350 doi: 10.18429/JACoW-IBIC2024-THP31

DESIGN AND IMPLEMENTATION OF ELECTRON CURRENT MEASUREMENT MODULE FOR SUPERCONDUCTING ACCELERATOR*

Z.Y. WANG[1], H. R. FU, W. LIU, X. W. CAI, Y. CHEN, X. D. WANG, G. J. ZHAI, Y. L. WU
SPIC Nuelectronic Company Limited, Wuxi, China
[1] also at Xi'an Jiaotong University, Xi'an, China

Abstract

The electron current measurement module is a key component of the superconducting cryomodule testing platform. Serving as a vital monitoring signal device within the coupler interlock system, this module monitors the electron cloud of high-energy power couplers and waveguide systems to ensure their effective protections. This article details the design and performance testing of the electron current measurement module, highlighting key technologies including anti-interference, weak current detection, multi-channel signal acquisition and processing, and weak current calibration. This module boasts a large dynamic range, high precision, and multi-channel weak current detection, featuring 32 detection channels with a detection range of nA~10 μA. Its detection accuracy surpasses 1 nA, and its response time is under 5ms. Additionally, the module's design took into account the impact of ionizing and electromagnetic radiation on its performance to ensure its reliability and stability.

INTRODUCTION

The metal surface of accelerating structures emits electron current when operating at radio frequency (RF) electric fields higher than 100 MV/m [1]. The capture and propagation of this field emission is known as 'dark current' and may affect different aspects of an accelerator such as diluting beam emittance for low emittance accelerators, gun dark current transported to free electron lasers (FEL) undulators may cause undulator damage, causing an increase in radiation level of the accelerator tunnel [2-4].

In this paper, we introduce a multi-channel, high precision electron current measurement module for monitoring the dark current of high-power couplers and waveguide system in superconducting accelerators, which can effectively monitor the secondary effect in the couplers and protect the safety of machine when the monitoring signal exceeds the safety threshold.

PRINCIPLE

For the measurement of weak currents, there are two most common methods in nuclear electronics [5]. One is I-F transformation, which converts weak current signals into frequency signals, such as dynamic capacitance electrostatic meters; Another type is I-V conversion, which converts weak current signals into measurable voltage signals, such as in resistive electrostatic meters. The electron current measurement module introduced in this article is based on I-V conversion.

The I-V conversion method can be further divided into high impedance method and integration method. The high impedance method is converting weak input current into voltage with a large resistor, as shown in Fig. 1. The integration method uses weak input current to charge the capacitor connected to the amplifier, thereby generating voltage at the input terminal of the amplifier. The principle is shown in Fig. 2, and the output signal expression is as follows:

$$Vo(t) = I_i R_c e^{-t/R_c C}$$

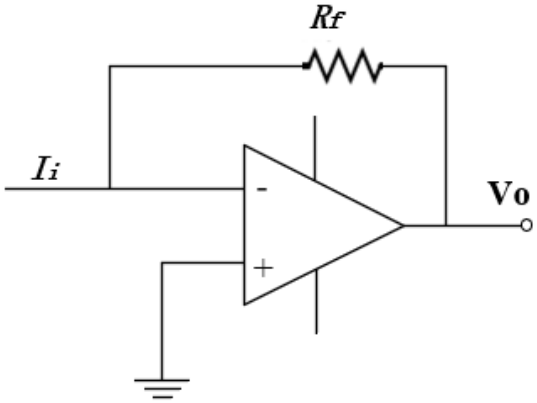

Figure 1: Schematic diagram of high impedance I-V conversion method.

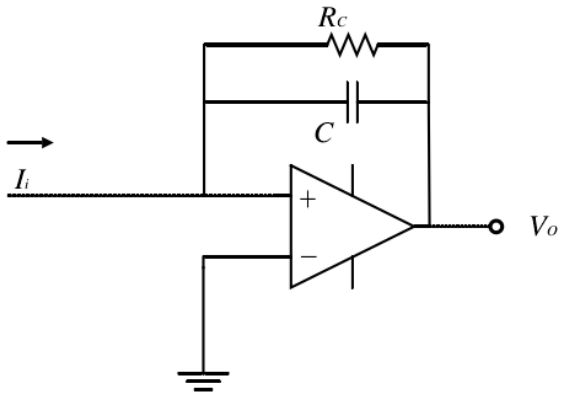

Figure 2: Schematic diagram of integral I-V conversion method.

COMPOSITION AND DESIGN

The electron current module needs to be designed in the form of 28 detection channels to meet practical accelerator demands, so it is designed in 7 groups with 4 channels per group (expandable to 32 channels).

ISBN: 978-3-95450-249-3 ISSN: 2673-5350 doi: 10.18429/JACoW-IBIC2024-THP32

NEW BEAM LOSS MONITOR IONISATION CHAMBERS ENGINEERING

G. Schneider†, Wilker Bastos, V. Griffiths, D. E. O. Tzamarias, R. Veness, W. Vigano'
CERN, Geneva, Switzerland
D. Gudkov[1], University of Liverpool
[1]Now Lawrence Berkeley National Laboratory, Berkeley, California, USA

Abstract

More than 4000 Beam Loss Monitor (BLM) systems are operating at CERN. About 93% of them are installed in the LHC machine. The Ionisation Chambers (IC) are the part of the system where the lost beam particles ionise nitrogen gas in a chamber with electrodes at high voltage. The resulting current indicates the quantity of beam lost. In the last 20 years, all BLM ICs were produced in collaboration with external institutes.

Control of all details of the materials and processes are required to ensure instrument sensitivity and precision across the large series.

CERN took back this production process in 2022 and much of the specific knowledge of design details and production technology required re-engineering.

This paper presents production specifications, design of tooling and test facilities for the first prototypes of a new series to be produced including their test at CERN facilities with beam. The future ramp-up to an industrial process to allow for a production of 1000 units in the years to come is discussed.

INTRODUCTION

The BLM ICs are the signal pick-up element of the beam loss monitoring system. The signal is measured by acquisition modules in the LHC tunnel, followed by processing and decision modules on the surface as part of the beam protection and interlock system. The BLM system latency to trigger a beam abort needs to remain below 3 beam revolutions around the LHC, corresponding to 267 µs. The beam losses in the LHC are discussed in [1]. CERN has long experience with the production of BLM ICs in collaboration with external institutions [2]. The objective of the present manufacturing campaign of 1000 BLM ICs is to prepare for the CERN High-Luminosity LHC (HL-LHC) [3] upgrade and to complete the BLM renovation in the LHC injector complex.

The design criteria is to make BLM ICs resistant to radiation in the CERN environment for to up to 30 years of operation. To achieve this objective, only metals (aluminium, copper and stainless steel) and ceramic such as Al_2O_3 can be used. Experience has shown that very strict control of all components, processes and assembly is essential in keeping the required precision.

ENGINEERING REQUIREMENTS

The standard BLM IC monitor is about 50 cm long with a diameter of 9 cm (Fig. 1). The internal volume is about 1.5 l. There are 61 parallel aluminium plates separated by 0.5 cm, filling most of the vacuum container. Between each of the plates, there is a voltage of 1.5 kV. They are equipped with a low-pass filter outside the vacuum envelope. A key element of the BLM IC is a very high impedance ceramic supporting the rods to which the parallel electrodes are fixed. The maximum current permissible across the ceramics of the assembled electrode stack is 1 pA when a voltage of 1.5 kV is applied.

Figure 1: Finished BLM (left) and electrode stack of the ionisation chamber with ceramic insulators on either side (right).

The technically admissible leak rate for the BLM ICs, with a pressure difference of 100 mbar over a 30-year span, is $1*10^{-6}$ mbar.l/s. Assuming possible leak degradation, allowing for contingencies and adhering to standard leak test practices in industry, a maximum leak rate of $1*10^{-9}$ mbar.l/s is calculated as the engineering criterion for the delivery of the ICs.

To minimise the risk of leaks, low inclusion content stainless steels of type 304L, according to CERN internal specifications [4, 5] are used for the IC chamber parts.

All welds are executed by Tungsten Inert Gas (TIG) arc welding under argon atmosphere without filler material. Alternative welding methods, such as laser or electron beam welding, may be proposed by future manufacturers but must be as cost effective as the TIG welds. The most challenging weld to perform is that of the "pinch-off" tube, an annealed copper tube welded to the end plate made of stainless steel, as shown in Fig 2. CERN has experience in performing these welds in a leak-tight and cost-effective manner using TIG welding. The welds are leak checked at the end of the BLM End Plate production.

† Gerhard.Schneider@CERN.ch

ISBN: 978-3-95450-249-3 ISSN: 2673-5350 doi: 10.18429/JACoW-IBIC2024-THP35

LONGITUDINAL PHASE SPACE RECONSTRUCTION IN AN ELECTRON STORAGE RING

Hongshuang Wang*, Shanghai Institute of Applied Physics, Shanghai, China
Yongbin Leng, National Synchrotron Radiation Laboratory, USTC, Hefei, China
Yimei Zhou, Shanghai Advanced Research Institute, Shanghai, China

Abstract

This paper proposes a novel technique for reconstructing the longitudinal phase space of freshly injected bunches in an electron storage ring to obtain initial parameters. This technique combines the development of a single-bunch injection phase space simulation software with the establishment of a bunch-by-bunch data acquisition and processing system, enabling high-precision determination of the initial parameters of the injected bunch during the injection process (including initial phase, initial bunch length, initial energy deviation, initial energy spread, and energy chirp). The experiment uses a high-speed oscilloscope to collect the beam injection signals, which are then processed by data processing scripts to extract the evolution information of the phase and bunch length of the injected bunch. A single data acquisition covers thousands of turns, achieving a phase measurement precision of 0.2 ps and a bunch length measurement precision of 1 ps. Additionally, a single-bunch simulation software based on the mbtrack2 package is developed, which can simulate the phase space evolution of the bunch after injection under different initial phase space distributions. Using a genetic algorithm and taking the Pearson coefficient and variance between experimental and simulated data as the fitness function, the optimal initial parameters of the injected bunch are obtained through iteration. This technique enables a deeper understanding of the longitudinal dynamics of particle beams. By obtaining the phase space distribution information of the particle beam, we can promptly detect and correct deviations and instabilities in the injection system, thereby improving injection efficiency and beam quality.

INTRODUCTION

In advanced synchrotron light sources, the injection process of electron storage rings is a critical factor affecting beam quality and stability. Optimizing the injection process can reduce beam loss, improve injection efficiency, and minimize interference with experiments. Therefore, in-depth research and optimization of the injection process in electron storage rings have significant theoretical and practical importance.

The arrival time and bunch length of freshly injected bunches can typically be measured directly using a streak camera. A streak camera can capture the changes in the longitudinal size of a bunch within a snapshot time[1-3]. However, it cannot simultaneously achieve high temporal resolution and a large dynamic range. Additionally, existing diagnostic tools struggle to provide direct and accurate measurements for parameters such as central energy, energy spread, and energy chirp[4]. These parameters are crucial for optimizing the injection process and enhancing the performance of light sources. However, there is still a lack of effective experimental methods for precise characterization and analysis.

This paper proposes a new technique for reconstructing the longitudinal phase space based on the current research status. A high-speed oscilloscope captures the beam signal during the injection process. It combines it with advanced data processing algorithms to achieve phase space reconstruction of the particle beam in a single injection process. The technique enables precise measurements by integrating this with a newly developed single-bunch tracking simulation software based on the mbtrack2 package[5-7]. It predicts and simulates the behavior of particle beams in storage rings, providing a powerful tool for optimizing injection.

STORAGE RING BUNCH-BY-BUNCH PHASE AND BUNCH LENGTH MEASUREMENT SYSTEM

We have developed a bunch-by-bunch diagnostic system that calculates the beam's three-dimensional position, charge, and bunch length based on raw data collected from the Beam Position Monitor (BPM). This system can cover several thousand turns in a single data acquisition, achieving a bunch-by-bunch phase measurement accuracy of 0.2 ps and a bunch length measurement accuracy of 1 ps. Below is an introduction to this system's calculation principles of phase and bunch length. For an ideal Gaussian-distributed beam, its time-domain expression is:

$$I(t) = \frac{Q}{\sqrt{2\pi}\sigma} exp\left[-\frac{(t-t_0)^2}{2\sigma^2}\right] \quad (1)$$

Where Q is the bunch charge, σ is the bunch length, and t_0 is the bunch phase. When the beam passes through a button electrode, the expression for the induced detection signal on the electrode is:

$$V_b(t) = \frac{\pi a^2}{2\pi b} \bullet \frac{1}{\beta c} \bullet Z \bullet \frac{t-t_0}{\sigma^2} I(t) \bullet F(\delta, \theta) \quad (2)$$

Where a,b are the physical dimensions of the button electrode, F(δ,θ)is the transverse position of the bunch, and Z is the transmission impedance of the button electrode. Thus, the bunch phase and length can be obtained by directly sampling the BPM signals. The entire system includes a data

* wanghongshuang@sinap.ac.cn

ISBN: 978-3-95450-249-3 ISSN: 2673-5350 doi: 10.18429/JACoW-IBIC2024-THP36

FEASIBILITY STUDY OF ELECTRON BEAM PROBE-BASED LONGITUDINAL BUNCH SHAPE MONITOR FOR HIGH-INTENSITY PROTON BEAM

H. Wang†, Tsinghua University, Beijing, China
L. Sheng, State Key Laboratory of Intense Pulsed Radiation Simulation and Effect, Xi'an, China

Abstract

The knowledge of the longitudinal bunch shape is of high interest to accelerator performance optimization and advanced beam application. Attracted by the ability to continuously monitor the beam in real time, there is always a demand for bunch-by-bunch and non-invasive diagnosis. However, such diagnosis is difficult to achieve for proton beam with high intensity and high repetition. Using the principle of electron beam deflection, electron beam probe has the potential of multi-function beam diagnosis. Here, we proposed the concept of real-time longitudinal bunch shape monitor with photocathode DC electron gun. Considering the realistic bunch distribution, we investigated the feasibility of this monitor using particle tracking simulation. The results and analysis of feasibility are reported in this paper.

INTRODUCTION

In recent years, high-current proton facilities have been developed rapidly. Many high-intensity proton LINACs based on RF acceleration have been built, and people can obtain high-quality proton beams with higher current, shorter pulse width, and smaller emittance [1]. The technology and application of laser proton accelerators have also developed rapidly. By developing high-repetition targets, it is possible to obtain short pulses of high-energy proton beams repeatedly using compact laser accelerators. In this context, advanced beam diagnosis methods are very important for accelerator beam tuning and proton beam applications.

Many methods have been developed to measure longitudinal bunch shape, such as beam position monitor, bunch shape monitor, fast Faraday cup, gas jet ionization monitor, laser bunch shape monitor, etc. [2-5]. However, these developed methods are difficult to apply to higher-intensity proton bunches due to their invasive/semi-invasive nature, in which part of the detector is directly involved in the energy deposition of the beam. The Feschenko BSM is one of the most widely used longitudinal bunch shape diagnostic devices in proton accelerators, which can work under normal operating conditions. The signal conversion process is mainly secondary electrons generated when the proton beam bombards the wire. The longitudinal distribution of secondary electron density is linear with the longitudinal distribution of proton bunch, so the shape of the proton bunch can be monitored through the diagnosis of secondary electron. However, the production and transportation of secondary electrons will be affected by the electromagnetic field of the intense bunch, and the detection results may produce irregular distortion [3]. On the other hand, due to the maturity of electron gun technology, people can obtain stable and customizable electron beams through electron guns. The active measurement of high-intensity proton beam by the electron beam is expected to realize the non-invasive, bunch-by-bunch measurement of high-intensity and high-repetition proton beam. In this work, the ability of the electron beam probe to obtain the longitudinal information of the measured bunch is studied by investigating the change of distribution shape of the electron beam under the action of the proton bunch.

PRINCIPLES

When the electron beam passes over the proton bunch, the electron beam will move laterally due to the electromagnetic field of the bunch. Assuming that the proton bunch is a slender beam, the radial electric field generated by the proton bunch is proportional to the linear charge density in the relativistic case. Thus, the longitudinal distribution of the radial electric field is proportional to the longitudinal charge distribution of the proton bunch, that is, the longitudinal shape of the proton beam.

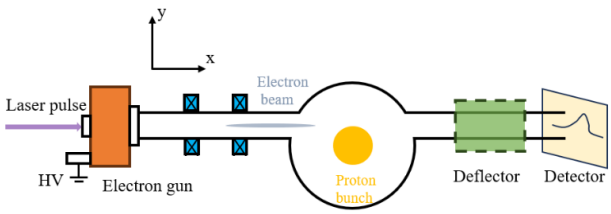

Figure 1: Schematic diagram of electron beam probe-based longitudinal bunch shape monitor.

The electron beam profiler, which has already been used in several devices, also takes advantage of the transverse electric field generated by the proton beam [6, 7]. Considering the effect of the transverse charge distribution, the deflection in the y direction of the probe electron beam is proportional to the sum of the potential components of the transverse electric field felt on the path through the x direction. That is, the change in its deflection is proportional to the charge density at the corresponding y coordinate. By scanning the electron beam position along the y-axis, the transverse bunch profile in the y-direction can be obtained.

The electron beam profiler assumes that the transverse charge distribution at different longitudinal positions of the proton beam is the same when the electron beam passes by. When we want to diagnose the longitudinal distribution with an electron beam probe, as shown in Fig. 1, we want

† wangheng21@mails.tsinghua.edu.cn

ISBN: 978-3-95450-249-3 ISSN: 2673-5350 doi: 10.18429/JACoW-IBIC2024-THP39

AUTOCORRELAION DEVICE FOR MEASURING THE DURATION OF THE NOVOFEL LASER PULSE

S. V. Reva†, V. M. Borin, O. A. Shevchenko, O. I. Meshkov, Budker Institute of Nuclear Physics SB RAS, Novosibirsk, Russia

Abstract

This paper is dedicated to the development and testing of a diagnostic system for the spectral and temporal characteristics of radiation from the third laser of the Novosibirsk Free Electron Laser (NovoFEL). The installation's scheme and its operating principle are described, along with the choice of diagnostic methods in accordance with the characteristics of the radiation being studied. Further, experiments are described to verify the accuracy of the diagnostics. Spectral characteristics of the laser radiation were measured directly on the NovoFEL's third laser, and a neodymium laser with near-infrared range radiation was used to test the feasibility of an autocorrelator.

INTRODUCTION

The Novosibirsk Free Electron Laser (NovoFEL) is a unique facility that is based on an accelerator-recuperator system. The third laser discussed in this article is located on the fourth track (see Fig. 1 and Table 1). The conditions for generating laser radiation on the fourth track require strict parameters for the electron beam and the accelerator settings. Understanding the spectral and temporal characteristics of the radiation could greatly simplify the process of tuning the accelerator and be of interest to users of the radiation. Currently, it is only possible to measure the spectral characteristics and the average power of the radiation. Measuring the pulse duration of the laser is also important, but this has not been done yet. One of the main challenges in determining the parameters of NovoFEL radiation is the lack of available measuring instruments due to the special properties of this radiation (see Table 1). The expected duration of a laser pulse is measured in tens of picoseconds. Devices used to measure ultrashort pulses, such as photocathode-based dissectors [1] and streak cameras [2], do not function in the infrared region of the spectrum [3]. Instead, autocorrelators are commonly used in this wavelength range. The aim of this study is to develop an optical setting for an autocorrelator using the available optical components.

Table 1: NovoFEL Third Laser Parameters

Parameter	Value	Unit
Wavelength range	8-11	mkm
Pulse frequency	3,76	MHz
Max average power	0,1	kW
Electron beam energy	38-42	MeV
Average electron beam current	3	mA

† st.reva@yandex.ru

AUTOCORRELATION ANALYSIS OF THE RADIATION PULSE DURATION

The autocorrelation function of a complex function *f(t)* can be defined as follows:

$$A(\tau) = \int_{-\infty}^{\infty} f(\tau) f^*(t-\tau) dt\,. \quad (1)$$

In optics, the autocorrelation function is used in relation to the strength of the electric field component of the radiation and to the intensity of radiation. They are named autocorrelation functions of the first and second order, respectively.

The first-order autocorrelation function is directly related to the spectrum through the Wiener-Khinchin theorem [4]. For a narrow Gaussian-like function, the relationship between the width of the first-order autocorrelation function σ_τ and the width of the spectrum σ_λ can be described as follows:

$$\sigma_\tau = \frac{\lambda_0^2}{2\pi c^2 \sigma_\lambda}, \quad (2)$$

where λ_0 – the wavelength of the radiation ($\sigma_\lambda \ll \lambda_0$), c– the speed of light.

The second-order autocorrelation function is directly related to the temporal distribution of the radiation intensity. Its duration τ_{ac} depends linearly on the pulse duration τ_p:

$$\tau_{ac} = k\tau_p, \quad (3)$$

where k is a coefficient depending on the shape of the pulse. The coefficient can be calculated by substituting the temporal profile of radiation into the equation:

$$A^{(2)}(\tau) = \int_{-\infty}^{\infty} I(\tau) I^*(t-\tau) dt\,. \quad (4)$$

For example, for a Gaussian distribution, $k = \sqrt{2}$, and for a pulse of the hyperbolic secant form, $k = 1.543$.

Thus, by measuring the autocorrelation functions of the first and second order, we can determine the spectral width and the duration of the radiation pulse respectively.

THE AUTOCORRELATOR SCHEME

The proposed autocorrelation method for pulse duration measurement at NovoFEL is illustrated in Fig. 2. This method is similar to a Michelson interferometer, but uses thin, flat mirrors that are separated in the transverse plane and placed in the direction of light propagation.

By moving one of the mirrors on a motorized stage, we can control the light optical path and, therefore, the time delay between the two beams. The displacement of the mirror by a distance a introduces a delay of $\Delta t = 2a/c$, where c is the speed of light. To ensure this property, the beam must fall on the mirror (3) at a right angle.

ISBN: 978-3-95450-249-3 ISSN: 2673-5350 doi: 10.18429/JACoW-IBIC2024-THP40

DEVELOPMENT OF A METHOD FOR VISUALIZING THE MAGNETIC AXIS OF MULTIPOLE MAGNETS

S. V. Reva†, O. I. Meshkov, L. E. Serdakov, V. S. Krapivin
Budker Institute of Nuclear Physics SB RAS, Novosibirsk, Russia

Abstract

This work is dedicated to the development of an alternative method for magnetic measurements based on the visualization of magnetic fields. The paper presents improvements to the basic method and provides a methodology for conducting measurements. The paper also describes experiments carried out to determine the accuracy of the technique, and an accuracy of 100 microns was achieved, which is comparable to traditional modern methods of magnetic measurement.

INTRODUCTION

The accelerator technology development requires more and more accuracy improvement of both the manufacture of magnetic elements and their positioning during the accelerator installation. To control the quality of the created magnetic elements, there are various methods of magnetic measurements [1]. Most of the actively used methods involve the use of specialized precision stands, and therefore magnetic elements are usually measured immediately after production, and then the data obtained are used at the positioning. At the same time, changes in the parameters of magnets associated with mechanical, thermal and other influences during their transportation and installation are not taken into account. This work is devoted to the study of a magnetic measurement's alternative method based on the magneto-optical effect of the light polarization plane rotation in optically active media, which makes it possible to visualize magnetic field direction distribution.

THE COTTON-MOUTON EFFECT

The magnetic measurement method is based on the Cotton-Mouton effect [2], a quadratic magneto-optic phenomenon that occurs in an external magnetic field perpendicular to the direction of wave propagation. When an electromagnetic wave enters the medium, it is divided into two plane-polarized waves with different refractive indices and polarizations, one parallel and one perpendicular to the magnetic field.

$$n_{\parallel} - n_{\perp} = C\lambda H^2, \qquad (1)$$

where $n_{\parallel}$, $n_{\perp}$ - refractive indices, C - Cotton-Mouton constant, λ – wavelength, H - magnetic field strength. As the waves pass through the substance, they gain different phases and the polarization of the total wave exiting the substance is different from the initial polarization. If the input wave has linear polarization, then the output wave's polarization will be elliptical, with a non-zero projection perpendicular to the original polarization. The absolute value of this projection depends on the difference in wave phases and, consequently, on the magnetic field strength. It also depends on the angle between the polarization vector of the input wave and the magnetic field vector, as this determines the ratio of the intensities of the waves that the input wave splits into in the medium. For example, for angles that are multiples of 90 degrees, there is no wave separation effect in the medium and the polarization of the output wave is the same as the input one. These properties form the basis of the magnetic measurement method.

OPTICAL MAGNETIC MEASUREMENTS CONCEPT

The basis of the method is described in the work [3]. The scheme is shown in Fig. 1. The idea is to place a magneto-optical active medium (4) in an external magnetic field between two crossed polarizers (3) and illuminate it with a plane-parallel beam of light. For magnets that have an inhomogeneous transverse magnetic field, the effect on the polarization is different at different positions (x and y), and this is recorded by a matrix detector (5).

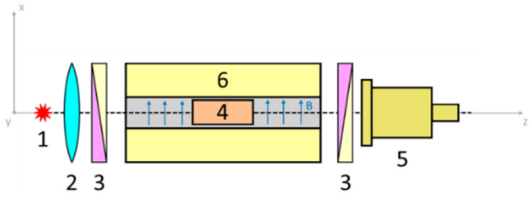

Figure 1: Optical scheme for optical magnetic measurements: 1 – radiation source; 2 –collimator; 3 crossed polarizers; 4 – magneto-optically active sample; 5 – matrix detector; 6 – magnet.

For multipole magnets, the pattern will be axisymmetric with a pronounced center. This center corresponds to the point of the magnetic axis of the multiple. Calculated patterns for the quadrupole and sextuple are shown in Fig. 2. The number of sectors is determined by the number of geometric rays on which the magnetic field's direction is either parallel or perpendicular to the polarization direction.

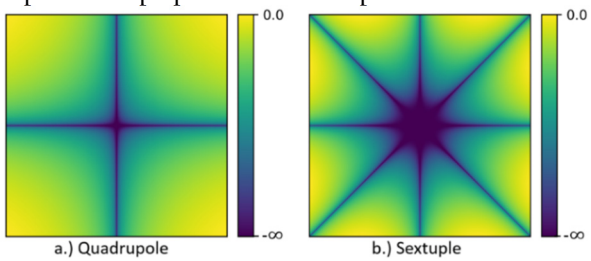

Figure 2: Calculated quadrupole and sextupole patterns.

† st.reva@yandex.ru

ISBN: 978-3-95450-249-3 ISSN: 2673-5350 doi: 10.18429/JACoW-IBIC2024-THP41

LONGITUDINAL BUNCH DIAGNOSTICS IN THE TERAHERTZ DOMAIN AT TELBE USING FAST ROOM TEMPERATURE OPERABLE ZERO-BIAS SCHOTTKY DIODES*

R. Yadav†,1, S. Preu, Terahertz Devices and Systems, TU Darmstadt, Darmstadt, Germany
A. Penirschke, High Frequency Tech., Mittelhessen Univ. of Applied Sciences, Friedberg, Germany
M. Kuntzsch, Helmholtz-Zentrum Dresden-Rossendorf, Dresden, Germany
[1]also at High Frequency Tech., Mittelhessen Univ. of Applied Sciences, Friedberg, Germany

Abstract

Modern accelerator-based light sources rely on short bunches to generate intense photon pulses. To achieve this, the electron bunches from the accelerator need to be compressed longitudinally in a magnetic chicane. A valuable tool for the measurement of the signal in the bunch compressor is the use of broadband EM-detectors covering a spectral range from few 100 GHz up to THz frequencies. With this setup, bunch length variations caused by instabilities in the acceleration process can be measured that in turn also affects the secondary photon beam. In this paper we demonstrate the pre-commissioning of broadband, room temperature Schottky THz detectors for the diagnosis of compressed short electron bunches at the ELBE facilities at the Helmholtz-Zentrum Dresden-Rossendorf, Germany. Qualitative bunch compression measurements have been carried out to diagnose the beam to optimize the machine setup and provide feedback to the beam-line scientists for optimum machine operation. These detectors are scheduled to be commissioned at free-electron facilities in near-future.

INTRODUCTION

The history of free electron lasers (FELs) can be dated way back to 1971 when Madey [1] experimentally realized the ability of using undulators for high brilliance emittance from electrons [2, 3]. The kinetic energy of electrons is converted to high brightness photon beam when electrons wiggle through the undulator. The average brightness of coherent synchronous radiation (CSR) generated by FELs is ten orders of magnitude higher than that excited by synchrotron radiation [4]. Accelerator sources can generate pulses in the range from a few fs to ps and cover a spectral bandwidth all the way from Terahertz to hard X-ray region [5]. The precise tuning of the machine parameters to adjust the properties of the electron bunches is crucial for the emission of photons with high brightness [6–9].

Third generation linear accelerator facilities are capable of producing electron bunches in sub-ps down to fs range. Diagnostic measurements require bunch compression monitors delivering ultra-fast response time. Traditionally pyroelectric detectors are employed for power measurements with response times in microsecond-scale. Faster repetition rates in range of few kHz to MHz range as for FELs demand for an ultra-fast, ultra-sensitive and broadband diagnostic tool. The III-V semiconductor based high mobility devices such as zero-bias Schottky diodes (ZBSDs) [10, 11] and high electron mobility based transistors (HEMTs) [12] are suitable detector devices. ZBSDs are the most prominent member due to their high sensitivity at sub-ns or even ps response times compared to their slower thermal counterparts such as Golay cells, Pyro-electric, Hot-electron bolometer, etc. Another solution to measure the longitudinal bunch shape would be a THz spectrometer comprising a set of narrowband array detectors, which might have lead to the limited THz bandwidth [12]. Having a compact, cost-effective, robust, broadband and ultra-fast detector would offer a suitable solution for beam diagnostics directly next to the accelerator beam-line inside the cave.

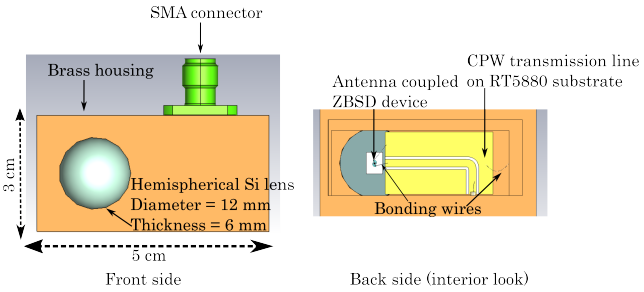

Figure 1: Schematic of developed ZBSD THz detector, left:depicts the front and right: illustrates the interior look into the detector along with Schottky diode and packaging technique.

In this paper, we present the results of pre-commissioning beam diagnostic experiments performed at TELBE by using in-house developed ZBSD based THz detectors. For this application we developed single pixel ZBSD and HEMT-based ultra-broadband and ultra-fast THz detectors that measure the electromagnetic signal emitted by the charged bunch when passing by the detector or likewise synchrotron-, diffraction- or transition radiation which all scale with its compression factor. ZBSDs operate at room-temperature and handy use of detectors eases as well as speed up the diagnostics process by applying it directly next to the beam-line in the cave.

* The work is supported by the German Federal Ministry of Education and Research (BMBF) under contract no. 05K22RO1 and 05K22RD1 for applications at Helmholz-Zentrum Dresden-Rossendorf, Accelerator Research Experiment at SINBAD (ARES) at DESY, Hamburg and Laboratory for Applications of Synchrotron Radiation (LAS) at KIT.
† rahul.yadav@iem.thm.de

ISBN: 978-3-95450-249-3 ISSN: 2673-5350 doi: 10.18429/JACoW-IBIC2024-THP42

A TEST BENCH FOR 324 MHz RF DEFLECTORS USED IN BUNCH SHAPE MONITORS FOR CSNS-II LINAC UPGRADE*

Q. R. Liu†, M. Y. Liu, University of Chinese Academy of Sciences, Beijing, China
W. L. Huang[1], X. Y. Liu, X. J. Nie, J. H. Wei, J. Liang, B. Tan, F. Li, L. Zeng, Z. H. Xu, R. Y. Qiu, M. A. Rehman, R. Yang, Institute of High Energy Physics, CAS, Beijing, China
also at China Spallation Neutron Source, Dongguan, China

Abstract

Bunch shape monitors based on the transverse modulation of low energy secondary emission electrons, will be used in the measurement of longitudinal beam density distribution in the upgrade of CSNS-II linac. A test bench for commissioning the 324 MHz RF deflectors used in BSM has been built in the laboratory, which consists of a Kimball E-gun, a vacuum chamber for electron optics, an RF stimulator, a 324 MHz RF power source, HV power supplies, a bending magnet and a set of MCP+Screen+camera+DAQ. This paper gives the design consideration, some results of the test bench and the continuing CST design of a λ/2 RF deflector.

INTRODUCTION

China Spallation Neutron Source (CSNS) is the first pulsed neutron source built in China [1]. Now its upgrade project CSNS-II has been started this year. Two Feschenko-type bunch shape monitors (BSM) are planned to be installed at the 324 MHz and 648 MHz sections of superconducting cavities [2], due to the longitudinal bunch widths at the BSM installation point will be as small as 2.77° and 1.05° separately [3]. BSM can be used to explore longitudinal beam dynamics, evaluation of longitudinal emittance, estimation of longitudinal beam halo, longitudinal beam matching etc. Using of BSM at the exit of accelerator enables to estimate a beam quality for further use [4-7].

A prototype 325 MHz RF deflector has been fabricated for the longitudinal bunch shape measurement in C-ADS. As the installation space of C-ADS is so limited, the prototype is assumed to be tested at the CSNS campus. Before the new BSM is installed in the tunnel of CSNS linac, it also needs to be tested in the lab. Therefore, a test bench was built up for both the prototype RF deflector and the new designed one.

BSM TEST BENCH SETUP

A Kimball EMG-4212/EGPS-4212 source produces a pulsed 10keV electron beam to mimic the secondary emission electrons from the tungsten wire bombarded by H- ions. The electron beam travels through a collimating slit, a 324 MHz RF deflector and a 50 cm-long vacuum chamber, then hits a YAG:Ce screen. There is a camera installed vertically right above the view port of the screen. The 3D drawing of the test bench is shown in Fig. 1. The system timing is controlled by a digital delay generator DG645, providing a TTL triggering pulse, 2~5 μs, adjustable delay, about 1~2 ms in advance of the beam. An R&S SMA-100B generates a 324 MHz reference RF signal, also acts as the stimulator of a 1 kW RF amplifier. A voltage-controlled phase shifter is used to change the RF phase for the electron transverse modulation. Two power meters (Mini-Circuit PWR-8PW-RC) are used to monitor the power fed into and out of the RF deflector.

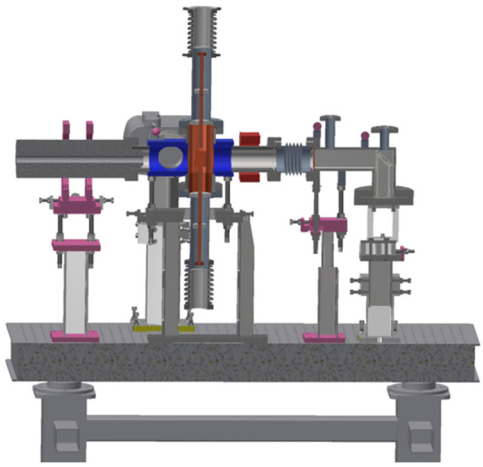

Figure 1: 3D drawing of the BSM test bench.

The test bench is built inside the D1 building at CSNS campus, with a 19" electronic rack with the depth 800 mm for BSM test bench electronics housing, as shown in Figs. 2 and 3. The camera will be shielded with a cylindrical baffle to improve SNR.

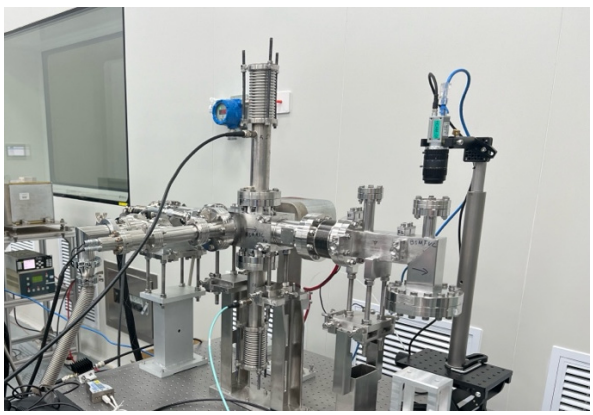

Figure 2: BSM test bench built in CSNS campus.

* Work supported by National Natural Science Foundation, 12275294 , and Mega Science Project Operation Fund of CSNS
† liuqr@ihep.ac.cn
[1] Corresponding author: huangwei@ihep.ac.cn

ISBN: 978-3-95450-249-3 ISSN: 2673-5350 doi: 10.18429/JACoW-IBIC2024-THP46

PHASE-TEMPERATURE STABILITY MEASUREMENT OF VARIOUS RF COAXIAL CABLES

X. Ma†, N. Gan, Y. Du, Y. Peng, Institute of High Energy Physics, Beijing, China

Abstract

Phase stable coaxial cables are widely used for the transmission of reference signals, monitoring signals and control signals in accelerator Low-level RF, beam measurement and control systems, especially for high requirements of time/phase stability. The change in ambient temperature will change the electrical length of the coaxial cables leading to the transmission time and signal phase drift, this effect is termed as temperature coefficient of delay (TCD). The TCD curves at room temperature (15~40°C) of various types of coaxial cables commonly used in particle accelerators and other industries are measured. Some cables are tested for the first time. The cables with lowest coefficients are CommScope LDF2-50A, Zhongtian HCAAYZ-50-12 and Trigiant HCTAYZ-50-22, for different cable diameters. According to attenuation, mechanical and TCD parameters, these three cables are chosen in the HEPS phase reference line system and Linac LLRF system respectively.

INTRODUCTION

Coaxial cables are widely used in RF, LLRF, beam instrumentation and control systems in accelerators. The phase stability is particularly important for long-distance reference signal transmission. However factors such as ambient temperature, humidity and air pressure will have an impact on the coaxial cables. These environmental changes are usually slow or the bandwidth is lower than several Hz. This will bring the drift of the key signals even the beam state which will seriously affect the performance of the facility with high stability.

Phase stable coaxial cables commonly used in accelerators have been tested in the laboratories [1-4] including Commscope, RFS, Times etc. Phase-stable coaxial cables, known as feeders in the antenna-feeder system of communication station, have perfect reliability, phase stability and EMI shielding. There are more cables manufacturers [5] such as: Trigiant, Hansheng, Datang, Zhongtian(ZTT), Kingsignal, Wutong, Hengxin etc. These coaxial cables are standard industrial products, 3/8, 1/2 and 7/8 inch outer diameters are mostly used in scientific facility and other communication industry, usually larger diameter benefits lower attenuation. The standard feeder cable has an inner conductor of copper tubes, an outer conductor of corrugated copper, and a dielectric of foam polyethylene (Foam PE). Following the communication industry standard in China [6], the 1/2" and 7/8" feeder cables' names from vendors are: HCAAYZ-50-12 and HCTAYZ-50-22.

The short cables, known as "jumpers", are mostly rigid, semi-rigid or semi-flexible PTFE cables. these PTFE cables would have a significant phase step change between 18°C-24°C [7], so it would be better set temperature of cables above 25°C to avoid phase instability.

The HEPS Linac requires four 10~50 m phase stable cables as phase reference lines, as well as about 100 10~30 m signal monitoring cables. The phase distribution system of HEPS requires hundreds of 100~1500 m long phase stable cables for the whole BI and LLRF systems. The cable vendors cannot provide detailed temperature coefficient of delay (TCD) parameter of cables in room-temperature, so measurements should be conducted in order to choose the lowest TCD cables.

MEASUREMENT PRINCIPLE

The experimental principle of temperature coefficient of delay measurement is shown in Figure 1. The temperature controlled cabinet can be heated or cooled, the temperature is programmed slowly heated from 15°C to 40°C and then slowly cooled to 15°C again. The temperature change and measurement process is about 2 hours so that the phase change could follow the temperature change. In order to monitor the uniformity of temperature changes, four PT100 temperature sensors are placed above, below, left, right of the measured cable inside the temperature controlled cabinet, another one is placed outside to measure the room temperature. The five temperature values are calibrated according to a standard PT100, the accuracy of the five temperature sensors should within ±0.1°C and the resolution is 0.01°C. The average value of the four temperature values inside the cabinet is calculated as the measured temperature. The dual-port vector network analyser (VNA) is connected with the connectors of the cable under test. The phase resolution of the VNA can be less than 0.01 degree after reasonable data smoothing settings. Since the signal frequency does not affect the TCD measurement and the higher the frequency, the better the phase/time resolution, the 2998.8MHz frequency is selected as the test signal in the experiment. The principle is similar with the method that IEC recommends but been modified for larger room temperature range [8].

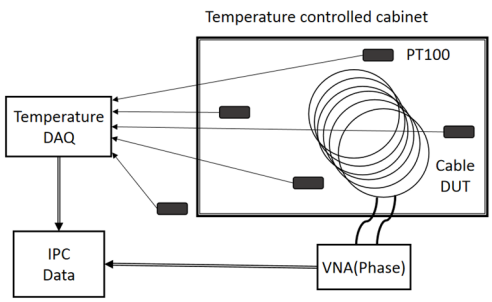

Figure 1: Experiment principle.

† maxp@ihep.ac.cn

ISBN: 978-3-95450-249-3 ISSN: 2673-5350 doi: 10.18429/JACoW-IBIC2024-THP47

THE SYNCHRONIZATION AND TIMING SYSTEM UPDATING AT CTFEL FACILITY*

Shuai Ma, Weijun Wang, Ziru Sang, Hanxun Xu, Dexin Xiao, Peng Li, Kui Zhou†, Xingfan Yang, Dai Wu, Ming Li
Institute of Applied Electronics, China Academy of Engineering Physics, Mianyang, China
Chongxian Yin, Ming Liu
Shanghai Advanced Research Institute, Chinese Academy of Sciences, Shanghai, China

Abstract

Chinese Academy of Engineering Physics terahertz free electron laser facility (CTFEL) is a superconducting linac-based user facility. It provides laser pulses with frequencies from 0.1 THz to 4.2 THz. CTFEL works in pulsed mode with a repetition of 10 Hz where up to about 54000 bunches at a bunch spacing of 18.5 ns are accelerated in one macro-pulse. To satisfy the high-precision synchronization requirement from user experiments, the synchronization system based on coaxial line is updated to a continuous laser carrier and Michelson interferometer-based system. The timing system is updated to event system.

INTRODUCTION

The user experiments performed at CTFEL facility require beam stability. Especially the pump-probe experiments need high precision synchronization at samples to obtain the low possibility interaction. In these experiments pump pulses activate the sample microparticles to high energy state and the probe pulses interact with the sample microparticles to detect the relaxation dynamic of core-excited atoms. The temporal resolution of these experiments are limited by the synchronization between the pump pulses and the probe pulses[1]. The beam arriving time jitter will transfer to pump or probe pulses jitter by the interaction between the beam and light pulse in the undulator or resonator[2]. The trigger signal from the event system to user laser will also affect temporal resolution. Several sources result in beam arriving time jitter, such as superconducting cavities' phase and amplitude jitter, magnet compressors and beam trajectory jitter. These reasons are coupled with phase reference signal distribution from master oscillator to driving laser system, RF cavity LLRF et.al. The coaxial cable based and fiber optic cable based are two main methods of phase reference signal distribution. The coaxial cable based solutions include with and without feedback control method[3, 4]. The fiber optic cable based includes the continuous laser carrier based method and the balanced optical pulse laser cross-corelated method[5–7]. A general composition of these four methods performance is shown in Table 1.

Table 1: Comparison of two methods of phase reference signal

Methods	Jitter/fs	Drift/fs
Coaxial cable based without feedback[3]	Hundreds fs @2856MHz	±500 fs @2 days,200m
Coaxial cable based with feedback[8]	54 fs @2856MHz	158 fs, p-p @14 days,30m
Fiber optic cable based CW laser carrier based[9]	< 1 fs @2856MHz	< 70 fs @2 months, 2 km
Fiber optic cable based balanced optical pulse laser cross-corelated[10]	< 1 fs @1.3GHz	0.6 fs @16 days,1.2km

Figure 1 illustrates the layout of CTFEL facility after update in 2025. At present, the acceleration part is consists of a DC injector with 320 kV and one L-band 2*4 cell superconducting cavity cryomodule. A L-band buncher is located between the DC injector and the 2*4 cell superconducting cavity cryomodule. One undulator with a period of 58 mm is in the downstream after several quadrupoles. The other undulator with a period of 38 mm and a resonator locates after a dog-leg transfer section. The new section includes two 2*9 cell superconducting cavities, two undulators with period of 35 mm and 48 mm respectively and a X-ray FLASH lab. This circular beamline is also the main part of energy recovery linac (ERL)[11] in the future. During this construction of new facility section, the synchronization and timing system is updating from the coaxial cable based without feedback to the fiber optic cable based with continues laser and Michelson intervened system. This paper presents a updating design and construction of synchronization and timing system for CTFEL. The first test results in CTFEL about the phase reference signal distribution jitter is given.

SYNCHRONIZATION AND TIMING SYSTEM DESIGN

In the new facility based on CTFEL, eight parts need synchronization signal including the driven laser, one buncher cavity LLRF, two 2*4 cell superconducting cavity LLRF and four 2*9 cell superconducting cavity LLRF. The above parts, 23 BPMs, 2 BAMs and some user facilities require trigger signal from timing system. We construct the fiber optic cable based with continues laser and Michelson intervened synchronization and event timing system, as shown in Fig. 2. The master oscillator generates 1.3 GHz reference signal in the laser room and the signal is modulated by the

* Work supported by National Key Research and Development Projects (2011YQ130018)
† zhoudakui@163.com

ISBN: 978-3-95450-249-3 ISSN: 2673-5350 doi: 10.18429/JACoW-IBIC2024-THP51

SPECIALIZED OPTICAL PULSE PICKER FOR BEAM DIAGNOSTICS IN STORAGE RING*

Mingdong Ma, Dongyu Wang, Chuhan Wang, Baogen Sun, Jigang Wang†
National Synchrotron Radiation Laboratory,
University of Science and Technology of China Hefei, China 230029

Abstract

The non-uniformity, longitudinal oscillations, and space charge effects in a multi-bunch filled electron storage ring can lead to significant deviations in the measurement of longitudinal beam parameters. Selecting a single bunch for measurement can effectively improve the measurement accuracy of longitudinal beam parameter, under normal multi-bunch operation mode. This paper introduces an optical pulse selection system based on an RTP crystal Pockels cell, which is controlled by fast electronics and high-voltage electronics, to study the complex longitudinal beam dynamics. By adjusting the driving voltage frequency and trigger delay of the high-voltage driver, precise selection of single pulses in a multi-bunch filling mode can be achieved. Offline calibration experiments have verified the potential feasibility of selecting specific bunches or bunch trains within the multi-bunch operation, which is of great significance for diagnosing longitudinal characteristics and instabilities of the beam in electron storage rings.

INTRODUCTION

The diagnosis of longitudinal beam parameters is crucial for the performance characterization of particle accelerators and the precision of experiments [1]. Longitudinal parameters mainly include the beam energy, energy spread, longitudinal emittance, bunch length, and longitudinal phase space distribution [2-4]. Accurate diagnosis of these parameters aids in understanding and optimizing beam behaviors in accelerators. Among the diagnostic tools, streak cameras have become indispensable due to its high spatio-temporal resolution and sensitivity [5-8]. However, prolonged measurement of longitudinal beam parameters can cause irretrievable damage to the photocathode, MCP, and CCD phosphor screen of the streak camera. Additionally, when performing measurements on individual bunches, stray light from other bunches may leak into the streak camera images, resulting in measurement inaccuracies [9]. Optical pulse selection technology addresses these issues by incorporating a gating structure before the entire longitudinal beam diagnostic system, that is capable of selecting specific bunches within a bunch train. Currently, common approaches include integrating a micromechanical shutter gating technique, external MCP gating, or fast electro-optic shutter gating in front of the streak camera to create the protective gating structure [10-12]. However, these methods face significant challenges in practical applications. Micromechanical shutters typically have low modulation rates and are prone to mechanical inaccuracies, while external MCP gating can introduce timing delays and operational complexity, and fast electro-optic shutters may suffer from limited response times and potential alignment issues. These limitations can lead to the reduction of accuracy and reliability in actual bunched beam measurements.

This paper develops an optical pulse selection system based on an RTP electro-optic crystal Pockels cell, utilizing high-voltage electronics and fast electronics to control the RTP crystal. By finely tuning the RF driving frequency and trigger delay of the high-voltage driver, precise selection of optical pulses is achieved. The extinction ratio of the two polarizers in the system is 5419:1, effectively reducing the optical power input to the streak camera. Additionally, the offline calibration experiment demonstrated the feasibility of the system in achieving selective light pulse extraction at a frequency of 4.533 MHz. This is of significant importance for diagnosing longitudinal characteristics and instabilities of the beam in electron storage rings.

DESCRIPTION OF THE OPTICAL PULSE PICKER

The structure and working principle description of the optical pulse selection system are illustrated in Fig. 1. The system primarily consists of two perpendicular polarizing beam splitters (PBS1 and PBS2), a Pockels cell, a high-voltage driving circuit, a delay signal generator, and a water-cooling unit. The RTP crystal (model: RTP-6-20-AR532-DMP) within the Pockels cell serves as the core optical pulse selection component in this system. It features excellent performance characteristics such as a high electro-optic modulation effect, high damage threshold, low optical loss, and a wide spectral transmission range. These properties enable the RTP crystal to operate stably at specific repetition frequencies, ensuring the precision and reliability of the optical pulse selection system.

The operating principle of the system is based on the Pockels effect, wherein the RTP crystal inside the Pockels cell alters the phase of light passing through it when high voltage is applied. The high-voltage driving circuit, designed in a dual push-pull configuration, is directly connected to the Pockels cell. This circuit applies the appropriate high voltage to the Pockels cell in response to the frequency signals output by the delay signal generator, thereby modulating the phase change of the incident light beam. Through precise adjustments of the Pockels cell, including its orientation and voltage amplitude, the system can accurately control the polarization state and phase shift of the light.

* This work was supported by the National Natural Science Foundation of China under Grant 12075236.
† Corresponding author (email: wangjg@ustc.edu.cn).

ISBN: 978-3-95450-249-3 ISSN: 2673-5350 doi: 10.18429/JACoW-IBIC2024-THP53

MEASUREMENT OF THE LONGITUDINAL BEAM SIZE AT THE NOVOSIBIRSK FEL

V. M. Borin[1, 2], N. A. Vinokurov[2], I. H. Maishanu[1], O. I. Meshkov[2], O. A, Shevchenko[2], S. V. Reva[2], V. V. Kubarev[2], Budker Institute of Nuclear Physics, Novosibirsk, Russia
[1]also at Novosibirsk State Technical University, Novosibirsk, Russia
[2]also at Novosibirsk State University, Novosibirsk, Russia

Abstract

The Novosibirsk Free Electron Laser (NovoFEL) facility consists of three free electron lasers (FELs) installed on different tracks of the Energy Recovery Linac (ERL). These FELs share a common acceleration system, which allows for the generation of high average electron currents, typically around 10 mA. This high current facilitates the production of significant average FEL powers, often exceeding 100 watts in the spectral range between THz and mid-infrared wavelengths. Precise measurement of electron beam parameters is crucial for monitoring the performance of the accelerator and fine-tuning its operating modes. The length of the electron bunch is particularly important, as it directly influences the efficiency of laser radiation generation. This study focuses on the dependence of the electron bunch length on the parameters of the radio frequency (RF) and bunching systems for the first and second FELs at NovoFEL. Measurements were conducted using a Cherenkov aerogel radiator in conjunction with a streak camera to accurately determine the electron beam properties. The measurement results, along with a plan for future experiments, are discussed in detail in this publication.

NOVOSIBIRSK FREE ELECTRON LASER

Free electron lasers (FELs) are unique radiation sources that allow obtaining and relatively quickly tuning any desired wavelength in the feasible area [1]. The electron efficiency of FELs is relatively low, and creation of lasers with high average power necessitates recovery of the electron beam energy. The Novosibirsk free electron laser (NovoFEL) facility comprises three FELs mounted on the single-, double-, and four-track energy recovery linacs (ERL) (Fig. 1). Their spectral ranges are 90–340 μm (range extension by 100 μm toward longer wavelengths is a result of a recent experiment, unpublished yet), 35–70 μm, and 5–15 μm, respectively. Electrons for all three FELs are accelerated by the common linear accelerator. Commutation of bending magnets defines the choice of the operation regime. The first two FELs in the terahertz and far-infrared wavelength ranges are sources of coherent narrowband radiation with the world's highest average power. The layout of Novosibirsk FEL is shown in Fig. 1.

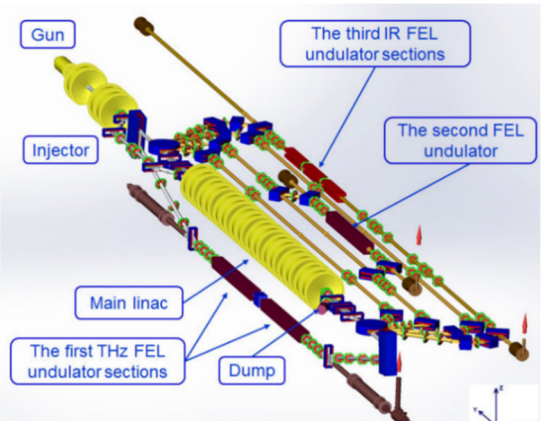

Figure 1: Layout of the Novosibirsk FEL.

OPTICAL BEAM DIAGNOSTICS

Previous Experiments

During the years of operation of the Novosibirsk FEL, there was active development of its optical diagnostic systems, which allow us to control beam parameters. More details about previous experiments on optical beam diagnostics can be found in other works [2-3]. The results of past experiments yielded interesting findings, which clearly show that the parameters of electron beam strongly depend on the accelerator's operating mode and the presence or absence of laser radiation. For example, Fig. 2 shows the radial profiles of the beam obtained by registering synchrotron radiation from the bending magnet, installed after the third laser undulator section, under different accelerator operating modes with and without laser radiation.

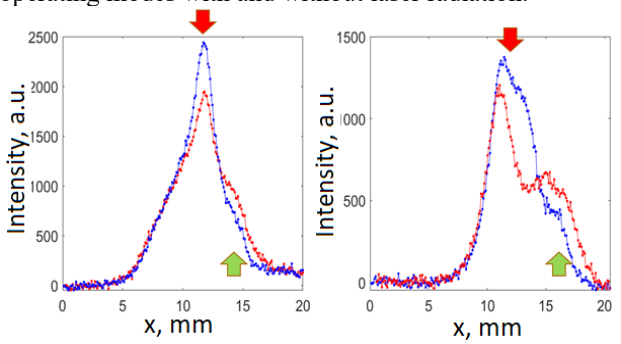

Figure 2: Radial beam profile change during lasing process for different FEL operation modes: blue – no lasing, red – lasing regime.

The observed radial profile has a complex structure. A similarity of the electron beam profile, depending on the presence or absence of lasing, is observed for different FEL operation modes. The results obtained using first beam diagnostics stations were used to enhance performance characteristics of Novosibirsk FEL, thus it is of great importance to constantly upgrade diagnostic tools available for Novosibirsk FEL.

ISBN: 978-3-95450-249-3 ISSN: 2673-5350 doi: 10.18429/JACoW-IBIC2024-THP54

RESEARCH AND DEVELOPMENT BEAMLINE FOR THE BESSY II BOOSTER

P. Ahmels*, T. Atkinson, M. Marongiu, G. Rehm, M. Ries
Helmholtz-Zentrum Berlin für Materialien und Energie (HZB), Berlin, Germany

Abstract

With the refurbishment completed, the optical beamline delivers all the required diagnostics. This paper reports on their status focusing in particular on the R&D beamline branch. The additional branch is equipped with programmable mirror and lens position controllers allowing elaborate optical optimisation. This system is used for educational purposes and for improving the source point imaging system through the study of polarisation characteristics. Test systems for an ultra-fast diode and a THz detector are equipped with CMOS cameras and polarisation filters. Furthermore the R&D branch complements the existing diagnostics to measure bunch lengths and investigate non-linear beam dynamics.

MOTIVATION

After the optimisation process of the high-end diagnostic, the main focus was on expanding the beamline further. The first addition to the R&D branch was an ultra-fast diode in combination with a CMOS camera for measuring longitudinal beam properties and photon counting. Through later including a polarisation filter, new insights regarding the non-zero divergence of the photon beam, contributed to optimise the diagnostic tool to a greater degree (Fig. 1). Furthermore, a THz detector was installed into the telescope optic to measure non-linear beam dynamics on injection [1].

Extending the beamline is essential to optimise and to increase the measurement capabilities of the diagnostic tool, to ensure tailored beams for high injection efficiency into the BESSY II storage ring.

BOOSTER BEAMLINE

The beamline consists of a motorized achromatic telescope, of 400 mm and 80 mm focal length lenses, and seven planar mirrors to transport the photons from the bending magnet to the optical table. For precise angle adjustment and fine tilt, three Mirrors are motorized. To compensate the angular dispersion entering the beamline, wedged vacuum windows are installed. On the optical table, the beamline is divided in three branches: the two main diagnostic tools on the optical table are a CCD camera with a 500 mm focusing achromatic doublet for source point analysis and a streak camera with a 300 mm focusing achromatic doublet for bunch length studies [2]. Using a mirror mounted on a linear stage, the beam is transported to one of the two branches.

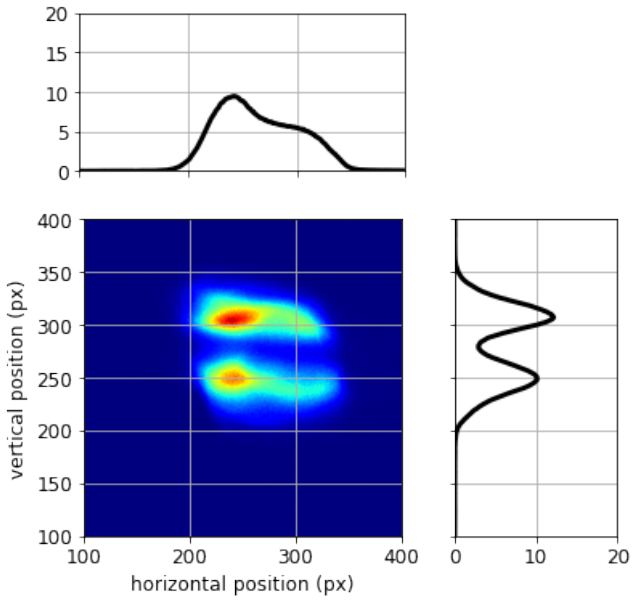

Figure 1: Image captured by CMOS camera showing circular polarisation outside of the focal point at high Booster energies with dominating vertical beam profile.

To expand the measurement possibilities, an R&D beamline is accessible via a 50/50 splitter on the optical table. The R&D beamline uses a programmable motorized mirror and 500 mm achromatic doublet to focus on one of the three different main setups shown in Fig. 2:

a) a CMOS camera from Basler [3] with a rotatable polarizer

b) an ultra-fast diode from Hamamatsu [4] connected to a 12 GHz oscilloscope and digital multimeter

c) an ultra-fast diode connected to a digital multimeter combined with a CMOS camera via a 30/70 splitter

Measurements for photon intensity, polarisation modes and bunch length are possible with these setups. Furthermore, a THz detector [5] is installed in between the telescope.

OPTIMISING PHOTON INTENSITY USING FEEDBACK

To effectively use the R&D branch the system is continually optimized. Two different approaches are used, both with the goal of maximizing the photon count on the diode. The first is a combination of the diode linked with a CMOS camera through a feedback code. The feedback code moves the motors of the mirror, changing the angle, and analyzes

* pauline.ahmels@helmholtz-berlin.de

ISBN: 978-3-95450-249-3 ISSN: 2673-5350 doi: 10.18429/JACoW-IBIC2024-THP55

TRANSVERSE AND LONGITUDINAL OPTICAL BEAM DIAGNOSTICS FOR THE BESSY II BOOSTER

M. Marongiu*, P. Ahmels, T. Atkinson, G. Rehm, M. Ries
Helmholtz-Zentrum Berlin, Berlin, Germany

Abstract

This paper describes the optical beam diagnostics available at the BESSY II booster synchrotron. For the first time, diagnostics are established to investigate the distribution of the electron beam in all three dimension. A permanent installation of a source-point imaging system aided by a telescope optic depicts the transverse properties of the electron beam. Additionally, the bunch length is measured using a streak camera with a resolution in the picosecond range. Both systems can work in parallel and are able to observe the non-equilibrium beam dynamics over the entire booster ramp.

MOTIVATION

The injector systems and diagnostics were upgraded as part of the global upgrade of the BESSY II facility. Specific for the injector were the E-gun, the bunch-by-bunch feedback, the orbit analysis, additional cavities for acceleration and the diagnostic beamline [1].

The diagnostic beamline transports visible light from a bending magnet out of the tunnel onto an optical table. This mechanical beamline consists of 8 planar mirrors (of which 3 are motorized) and a motorized telescopic lens system. Here, two lenses form an achromatic telescope and help collimate the photon beam for high transmission.

The incentive behind reducing the present bunch length is to optimise beam parameters ready for low-alpha Top-Up operation. For this special optic, the bunch length over the whole booster cycle needs to be carefully diagnosed, controlled and tailored for high injection efficiency into the BESSY II storage ring. Figure 1 shows the development of the photon intensity and with it the bunch length measurement during the injection process.

MECHANICAL BEAMLINE

The beamline uses the synchrotron radiation produced at a predetermined bending magnet. The divergence of the emitted light is corrected using refractive optics. First, the photons are transported through a wedged vacuum window to compensate the angular dispersion and protect the vacuum of the booster. Afterwards, the photons are reflected at a two-inch aluminium mirror into the tunnel system. The beam is collimated via a motorized achromatic telescope system consisting of 400 mm and 80 mm focal length lenses. This system also has a retractable THz detector installed, to study coherent radiation [2].

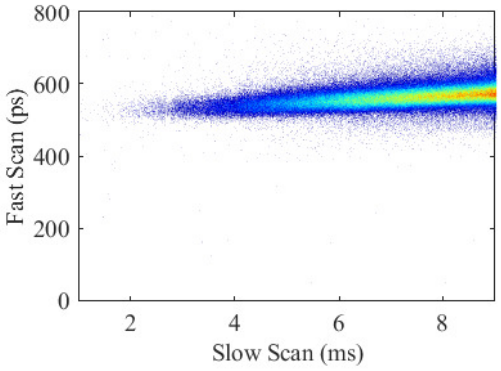

Figure 1: Image captured by the streak camera set with a blanking amplitude of 10 ms (horizontal axis) and the trigger set to observe the injection process.

After the telescope, the collimated beam is transported using the remaining six mirrors (see Fig. 2). Three mirrors are motorized for fine tilt and angle adjustments. An intermediate viewing port (IVP), consisting of a CMOS camera on a motorized linear stage was precautiously installed, to help confirm the alignment of the optical components.

The visible light reaches the optical table with an additional angle of 22° (composed of 2° outcoupled from the bending magnet and 20° due to the building constraints of the tunnel walls).

USER BEAMLINE

After exiting the labyrinth, the beam is reflected through two additional mirrors on to the optical table. The final outcome is three beamline branches: one for source point analysis of the electron beam size, the second for bunch length measurements via a streak camera and finally an R&D beamline for educational purposes [2].

The first branch is the source point analysis system. The beam is transported through a 500 mm achromatic lens mounted on a linear stage for fine-tuning the position and focused on a CCD camera. Presently installed into the set-up are three different filters: a polarized filter, a wavelength filter for 550 nm (see Fig. 3) and a ND filter for protection of the camera. The read out of the camera is shown live on a LabVIEW Interface.

On the second branch, a retractable mirror and achromatic Doublet (300 mm) are installed, focusing on a streak camera for bunch length measurements.

* marco.marongiu@helmholtz-berlin.de

ISBN: 978-3-95450-249-3 ISSN: 2673-5350 doi: 10.18429/JACoW-IBIC2024-THP56

10-fs-LEVEL SYNCHRONIZATION OF FEMTOSECOND LASER WITH RF MASTER OSCILLATOR*

J. G. Wang[1], B. W. Wu[2,3], W. Y. Zhang[1], L. Feng[1], B. Liu[1]
[1]Shanghai Advanced Research Institute, Chinese Academy of Science, Shanghai, China
[2]Shanghai Institute of Applied Physics, Chinese Academy of Sciences, Shanghai, China
[3]University of Chinese Academy of Sciences, Beijing, China

Abstract

Laser-to-RF synchronization plays a crucial role in various scientific and technological domains. It is instrumental in generating high-quality electron beams, producing high-performance FEL pulses, exploring ultrafast dynamical processes, and achieving precise measurements and transmission. Passively mode-locked femtosecond lasers are known for their exceptionally low noise characteristics, particularly in the high-offset frequency range, where jitter remains less than 5 fs from 1 kHz to 1 MHz. Meanwhile, RF master oscillators provide outstanding long-term stability in the offset frequency range. This paper demonstrates that integrating the low-noise performance of passively mode-locked femtosecond laser with the superior stability of RF master oscillator enables the achievement of 10-fs-level synchronization. By implementing an RF-based phase-locked loop (PLL) scheme, we achieved an absolute timing jitter of 17.4 fs integrated from 10 Hz to 1 MHz.

INTRODUCTION

Laser-to-RF synchronization technology has a wide range of applications in various fields, especially in areas requiring precise timing control.

Free Electron Lasers (FELs) [1-10]: In FELs, precise synchronization between laser pulses and microwave signals is essential for generating stable and controllable high-intensity light pulses used in studies of ultrafast physical and chemical processes.

Particle Accelerators [11, 12]: Laser-to-RF synchronization is used for beam control in accelerators, ensuring the proper alignment of the time distribution and phase of accelerated particles, which improves accelerator performance.

Ultrafast Electron Diffraction (UED) [13, 14]: In UED experiments, synchronization between laser pulses and microwave sources ensures temporal and spatial alignment of the electron beam and laser pulses, enabling observation of atomic-level structural changes in materials.

Ultrafast Optical Experiments [15-17]: This technology is used to generate and control ultrashort laser pulses for probing transient dynamic processes in materials, with applications in photonics, condensed matter physics, and quantum information.

Extreme Light Infrastructures [18, 19]: Precise synchronization of RF and lasers is crucial in extreme light facilities, which produce and manipulate high-intensity beams for applications in particle physics, high-energy physics, and related fields.

Precision Metrology and Time/Frequency Transfer [20, 21]: Laser-to-RF synchronization is important in metrology, including precision clocks, frequency standards, and atomic clocks, enabling high-precision time and frequency transmission.

Several methods have been developed to achieve laser-to-RF synchronization, such as photodetector direct extraction [22-24], balanced optical microwave phase detection [25-28], and femtosecond optical frequency comb synchronization [29-31], each offering distinct advantages based on the required level of precision and the specific application. Photodetector direct extraction is based on the principle of detecting periodic optical pulses and translating them into an RF domain signal. Once the electrical signal is extracted, the system utilizes feedback to match the laser's output to the reference RF signal, ensuring precise synchronization. Balanced optical microwave phase detection (BOMPD) provides a high precision by directly measuring the phase difference between the optical laser pulses and the RF signal. A balanced detector is used to suppress common-mode noise, enabling highly accurate phase synchronization. The femtosecond optical frequency comb synchronization technique generates a series of evenly spaced optical frequency "teeth", enabling frequency locking between optical and RF signals. The femtosecond frequency comb provides an extremely precise frequency reference, allowing for highly accurate synchronization between the optical and RF domains.

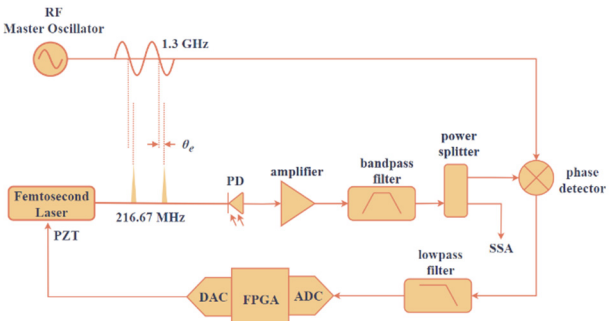

Figure 1: Simplified block diagramme of the RF-based laser-to-RF synchronization. PD: photodetector; SSA: signal source analyzer; ADC: analog-to-digital converter; DAC: digital to analog converter; FPGA: field program-mable gate array; PZT: piezoelectric.

In terms of application domains, photodetector direct extraction features a simpler structure while maintaining sufficient precision to meet the demands of most practical scenarios. Here, we demonstrate a digital phase detector designed based on the principle of photodetector direct

ISBN: 978-3-95450-249-3 ISSN: 2673-5350 doi: 10.18429/JACoW-IBIC2024-THP59

FIRST RESULTS WITH A BASE BAND TUNE (BBQ) MEASUREMENT SYSTEM AT SOLARIS

M. Gasior, CERN, Geneva, Switzerland
M. Szczepaniak, A. I. Wawrzyniak, R. Panas, Solaris NSRC, Krakow, Poland

Abstract

All CERN circular accelerators are equipped with Base Band Tune (BBQ) measurement systems, based on the direct diode detection technique, allowing to measure the tunes of hadron beams by employing their residual betatron oscillations or very small external excitation. In the framework of the Future Circular Collider (FCC) project, a study was launched to optimise such a system for operation with short electron bunches. A prototype system has been recently installed in Solaris light source. The system has immediately allowed an unprecedented detection of residual betatron oscillations, whose amplitudes, estimated to be in the 100 nm range, are more than two orders of magnitude lower than the smallest beam oscillations used for tune measurements with the Beam Position Monitoring (BPM) system. The residual oscillations allowed reliable continuous tune measurements, which have also revealed spectral content never observed before. This paper provides an overview of the installed BBQ system and describes beam measurement results obtained so far. The aim of the paper is to disseminate new results in the light source community and provide information that may help in building and installing similar systems. It is hoped that wider usage of BBQ systems will help in better understanding the observed spectra of electron beam residual oscillations.

HARDWARE

The Solaris BBQ installation, illustrated in Fig. 1 with a block diagram of one of its planes and a photograph, consists of a stripline Pick-Up (PU) with four electrodes whose output ports are connected by short coaxial cables to four Diode Detectors (DD) mounted directly on the inputs of an Analog Front-End (AFE). The coaxial cables act as low-pass filters stretching the lengths and lowering the amplitudes of the short electron beam pulses to values adequate for the detectors.

The diode detectors, illustrated in Fig. 2, are built as high impedance circuits, to minimise the power dissipated in small, high-frequency circuitry. As a result, the incoming beam pulses are reflected and ultimately dissipated in high-power RF terminators connected to the downstream ports of the stripline through short cables.

The diode detector has a simple input high-pass filter (C_{IN}, R_{IN}) blocking potential low-frequency interference. The current limiting resistor (R_{LM}) protects the following RF Schottky diodes (D, HSMS280C) during the first injections of the beam, when the detector parallel capacitors (C_{ST}, C_{FT}) have not yet been charged. With high current beams the capacitors may charge to a hundred

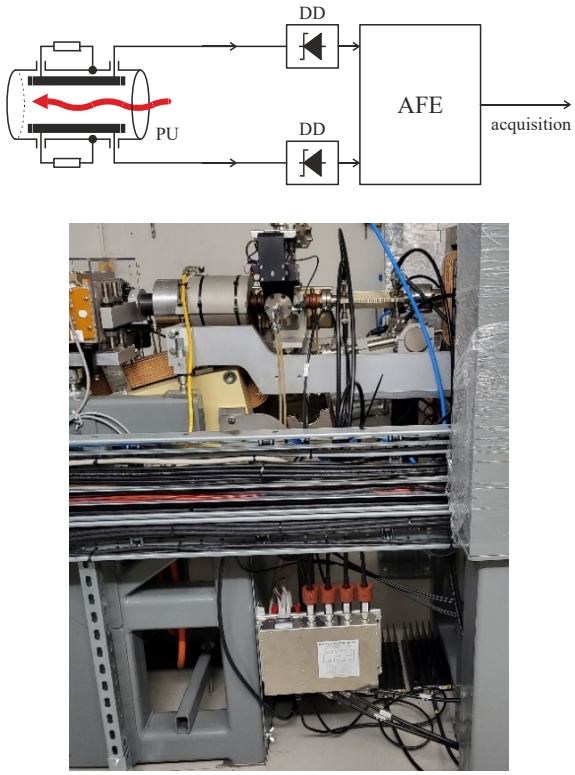

Figure 1: Diagram of one channel (top) and a photograph (bottom) of the Solaris BBQ installation.

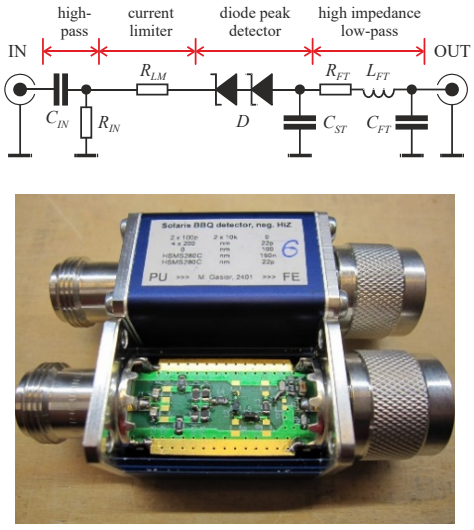

Figure 2: Block diagram (top) and a photograph (bottom) of the Solaris BBQ detector.

ISBN: 978-3-95450-249-3 ISSN: 2673-5350 doi: 10.18429/JACoW-IBIC2024-THP60

MACHINE LEARNING USED IN BPM DISPLACEMENT PREDICTION AT HLS II*

C. H. Wang, D. Y. Wang, J. K. Lan, M. D. Ma, T. Y. Zhou†, B. G. Sun
NSRL, University of Science and Technology of China, Hefei, Anhui 230029, China

Abstract

Beam orbit stability is a crucial indicator that can be used to evaluate the performance of a synchrotron radiation source. It can be improved through precise orbit measurement with beam position monitors (BPMs) and appropriate orbit feedback. The movement of BPMs directly affects the measurement of the beam orbit and indirectly affects the beam orbit through orbit feedback (OFB) system. Two sets of BPM displacement measurement system were established at Hefei Light Source II (HLS II) storage ring and some machine learning work was carried out on the system.

INTRODUCTION

Hefei Advanced Light Source (HALF), under construction by National Synchrotron Radiation Laboratory, is a fourth-generation storage ring. In order to realize the beam orbit stability of HALF, relevant studies have been performed on HLS II. In general, the beam orbit stability is required to be less than 10% of the beam size [1, 2].

The mechanical stability of BPM can be affected by both ambient environment sources and machine-inherent source [3]. The influence of BPM mechanical stability on beam position measurement is shown in Fig. 1. The BPM displacement x_d is numerically equal to the difference between the actual BPM reading x_{BPM} and real beam position x_{beam}, as shown in Eq. (1).

$$x_{beam} = x_{BPM} - x_d. \quad (1)$$

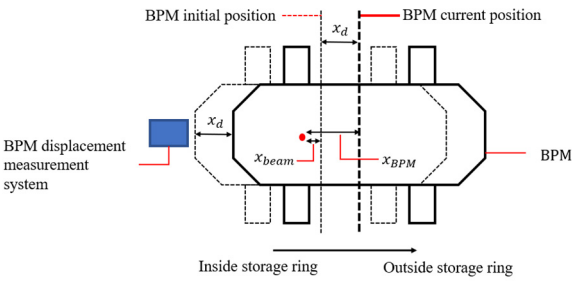

Figure 1: Model of BPM movement.

The influence of BPM displacement x_d on beam orbit can be calculated by Accelerator Toolbox (AT) in MATLAB with the linear lattice of HLS II as shown in Fig. 2. The related parameters of the HLS II storage ring are shown in Table 1. Random displacement of normal distribution $N(\mu = 0, \sigma^2 = \Delta x^2 \text{ or } \Delta y^2)$ with different Δx and Δy is added to the 32 BPMs in HLS II lattice AT file and the closed orbit distortion (COD) with orbit feedback being activate is calculated. The calculation result is shown in Fig. 3(a) and (b). After linear fitting, we have $\frac{d\ rms\ COD_x}{d\ rms\ \Delta x} = 0.907$, $\frac{d\ rms\ COD_y}{d\ rms\ \Delta y} = 0.940$, $\frac{d\ rms\ COD_x}{d\ rms\ \Delta y} = 0$, $\frac{d\ rms\ COD_y}{d\ rms\ \Delta x} = 0$.

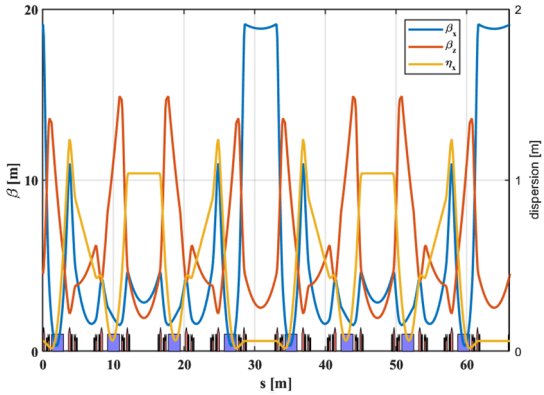

Figure 2: Schematic of the HLS II linear lattice.

Table 1: Parameters for the HLS II Storage Ring

Parameter	unit	HLS II
Circumference	m	66.131
Energy	GeV	0.8
RF frequency	MHz	204
Harmonic number	/	45
Horizontal beam size	μm	≥400
Vertical beam size	μm	≥83
Horizontal tune	/	4.445
Vertical tune	/	2.360
Lattice number	N	2

In general, the beam orbit stability is required to be less than 10% of the beam size [1, 2]. Based on the premise of considering only the influence of the BPM movement, to achieve beam orbit stability (10% beam size) for HLS II, the rms BPM displacement should be less than 44.101 μm in the horizontal plane and 8.830 μm in the vertical plane.

SYSTEM INSTALLATION

Two sets of capacitive displacement measurement systems from Micro-Epsilon [4] were installed at P1 and P2 in HLS II storage ring as shown in Fig. 4. The measurement result is shown in Fig. 5.

* Work supported by the National Natural Science Foundation of China under Grant No.12005223, 12075236 and the Hefei Advanced Light Facility Pre-research Project, and the Hefei Advanced Light Facility Project.
† tianyuzhou@ustc.edu.cn

ISBN: 978-3-95450-249-3 ISSN: 2673-5350 doi: 10.18429/JACoW-IBIC2024-THP61

LASER POLARIMETER AT VEPP-4M COLLIDER

Viacheslav V. Kaminskiy*[,1,2], Vladimir E. Blinov[1,2], Vasiliy N. Kudryavtsev[1,2], Sergei A. Nikitin[1], Ivan B. Nikolaev[1,2], Pavel A. Piminov[1], Lev I. Shekhtman[1,2]

[1]Budker Institute of Nuclear Physics, SB RAS, Novosibirsk, Russian Federation
[2]Novosibirsk State University (NSU), Novosibirsk, Russian Federation

Abstract

The VEPP-4M collider and the KEDR detector are going to measure precisely mass and leptonic width of $\Upsilon(1S)$. In this experiment the electron beam energy is measured precisely using the resonant depolarization technique at the "Laser Polarimeter" facility. The degree of electron beam polarization is measured using Compton backscattering with accuracy of 5% in 100 seconds. The beam energy is measured during KEDR data acquisition runs every 30 minutes with an accuracy of 20 keV.

INTRODUCTION

The tabulated value of the measurement uncertainty of the mass of the $\Upsilon(1S)$ meson is about 100 keV. This recent value [1] is based on reanalysis of results of the MD-1 experiments, including refined values of the electron mass, radiative corrections and interference. In a new measurement at the VEPP-4M collider and KEDR detector, it is planned to improve this result by a factor of two. This requires a beam energy measurement system at VEPP-4M with an accuracy of about 10 keV.

The essence of the method is to measure the precession frequency of the electron spin Ω_s in a guiding magnetic field of a storage ring. This frequency is related to the average energy of the electron E:

$$\Omega_s = \omega_r\Big(1 + \frac{E}{m_e}\frac{\mu'}{\mu_0}\Big) = \omega_r n \pm \omega_d, \quad n \in \mathbb{Z}, \qquad (1)$$

where ω_r is the revolution frequency ($2\pi \cdot 818$ kHz at VEPP-4M); m_e is electron rest energy; μ' and μ_0 are anomalous and normal part of electron magnetic moment. When a spin-polarized electron beam interacts with an external RF field of frequency ω_d, the polarized state of the beam is destroyed. Therefore, by measuring Ω_d, one can determinate the electron energy:

$$E = \frac{\mu_0 m_e}{\mu'}\left(n - 1 \pm \frac{\omega_d}{\omega_r}\right) = 440.648\,462\,13(14)\ [\mathrm{MeV}] \times \left(n - 1 \pm \frac{\omega_d}{\omega_0}\right). \qquad (2)$$

The high accuracy of the method is ensured by the narrow spin line width ($3 \cdot 10^{-6}$ for VEPP-4M at the beam energy of 4.7 GeV) and the fact that the electron mass and its anomalous magnetic moment are known with a relative uncertainty of $\delta m_e = 3 \cdot 10^{-10}$, $\delta\mu' = 10^{-10}$ (PDG 2023). Corrections to the formula, for instance, due to the non-commutative spin rotations under vertical orbit distortions and the connection between the average electron beam energy and the center-of-mass energy of colliding electrons and positrons, require separate study and are not considered in this work.

At low energies, i.e., in the energy region of ψ-mesons, polarization at the VEPP-4M storage ring is determined by the intensity of intra-beam scattering. However, the cross-section of this process rapidly decreases with increasing energy. So, at high energy polarization is measured using the process of Compton backscattering (or inverse Compton scattering). This method is based on measuring the asymmetry of the scattering of circularly polarized photons on a vertically polarized relativistic electron. The method of polarization measurement was proposed by Baier and Khoze in 1969 [2] and has been used in experiments on precise measurements of Υ-mesons, W- and Z-bosons masses.

Compton backscattering cross-section depends on polarizations of the initial electron and photon:

$$\frac{d\sigma(P,Q,V,\varphi,\beta)}{d\Omega} = 2\gamma^2 r_e^2\Big[\frac{1}{1+\gamma^2\theta^2+\kappa}\Big]^2 \times \Big\{\underbrace{2 + \frac{\kappa^2}{(1+\gamma^2\theta^2)(1+\gamma^2\theta^2+\kappa)} - \frac{4\gamma^2\theta^2}{(1+4\gamma^2\theta^2)^2}}_{\text{unpolarized}} \qquad (3)$$

$$+ \underbrace{\frac{4\gamma^2\theta^2 Q\,\overbrace{\cos(2[\varphi-\beta])}^{\text{quadrupole}}}{(1+4\gamma^2\theta^2)^2}}_{\text{linearly polarized}} + \underbrace{\frac{2\kappa PV\gamma\theta\,\overbrace{\sin\varphi}^{\text{dipole}}}{(1+\gamma^2\theta^2)(1+\gamma^2\theta^2+\kappa)}}_{\text{circularly polarized}}\Big\}, \qquad (4)$$

where V and Q are Stokes parameters of the photon: circular and linear polarization, respectively; β is the angle of the polarization plane; P is the electron vertical polarization; $\kappa = 4\gamma\omega_0/m_e$ is photon "hardness", or recoil parameter. When laser beam with alternating circular polarization ($V = \pm|V|$, $|V| \le 1$) hits polarized (P) electron beam, the resulting scattering asymmetry is

$$\frac{\sigma_\uparrow - \sigma_\downarrow}{\sigma_\uparrow + \sigma_\downarrow} \approx -\frac{3}{4}\frac{E\omega_0}{m_e^2}VP \approx 2\%. \qquad (5)$$

LASER POLARIMETER AT VEPP-4M

The laser polarimeter [3] is located near the experimental section of VEPP-4M (Fig. 1). TECH-527 Advanced by Laser-Export. Co. Ltd. pulsed Nd:YLF DPSS laser with acousto-optic modulator is used as a photon source. Its main parameters are listed in Table 1.

Linear laser beam polarization is transformed to circular polarization by a $\lambda/4$ phase plate. This part of the optical

* V.V.Kaminskiy@inp.nsk.su

ISBN: 978-3-95450-249-3 ISSN: 2673-5350 doi: 10.18429/JACoW-IBIC2024-THP62

THE BEAM ORBIT RECONSTRUCTION IN THE LINAC OF CSNS*

Y. Han†,1, J. Peng[1], IHEP, CAS, Beijing, 100049, China
[1]also at Spallation Neutron Source Science Center, Dongguan, China

Abstract

In the high current hadron machine, it is essential to reduce the beam loss along the machine for machine maintenance and safety reasons. The linac of Chinese Spallation Neutron Source (CSNS) delivery negative hydrogen bunches with power of 5 kW to the RCS which increase the power to 100 kW. In the following several years, the power of the linac beam will be increased from 5 kW to 100 kW, therefore it is important to deal the beam loss more carefully. In this paper, we present the reconstruction of the beam orbit along the linac using beam tracking software with the input data measured with BPMs. This kind of reconstruction is expected to provide suggestions for the future machine tuning. The requirements for the BPMs are also presented in this paper.

INTRODUCTION

The China Spallation Neutron Source (CSNS) is hadron accelerator based multidiscipline user facility located at Dongguan, Guangdong, China [1, 2]. The accelerator of CSNS consists of a 80 MeV linac and a 1.6 GeV rapid cycling synchrotron (RCS). The layout of the CSNS is illustrated in Fig.1.

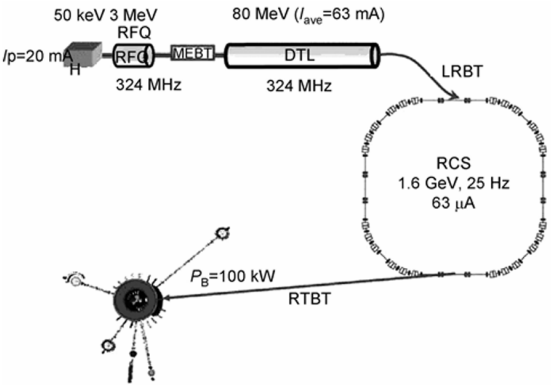

Figure 1: The layout of the CSNS.

The linac of the CSNS aims at delivering high quality negative hydrogen beam to the RCS. It includes an ion source, a RFQ, and Drift Tube Linac (DTL) and two transport lines: Medium Energy Beam Transport (MEBT) and Linac to RCS Beam Transport (LRBT). In this paper, we focus on the MEBT, DTL and LRBT.

The designed peak current for the linac at the end of RFQ is 10 mA and the beam power at the exit of RCS can reach 100 kW. Currently the peak current is around 17 mA for the 160 kW operation, which is much larger than the designed value. In the next few years, the peak current will be increased to 50 mA which may lead much higher radiation. Therefore, it is important to have good knowledge about the beam along the linac to control the beam loss.

The most important information is the beam orbit which is the base for other beam parameters. In this paper, the preliminary results for the reconstruction of the beam orbit along the MEBT and LRBT is presented.

ORBIT OF MEBT

The MEBT connects the RFQ and the DTL and match the beam parameters between them. The layout of MEBT for the CSNS is shown in Fig. 2. There are 7 BPMs and 6 correctors along the MEBT.

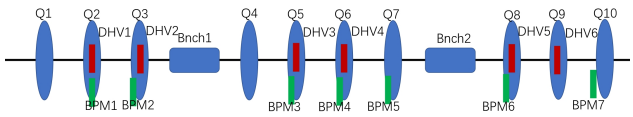

Figure 2: The layout of the MEBT.

All quadrupoles and BPMs are pre-aligned to the level of ±0.15 mm [3], which is already good enough for the transport of negative hydrogen beam. A beam-based alignment technique was applied to determine the offset between BPMs and nearby upstream quadrupoles [3]. Therefore, the orbit got from the BPMs can be considered as reliable reference for the real orbit, which lead to the successful operation of the beam through the MEBT.

Although there is no operation problem for the orbit, it is still unclear that how looks like the true beam orbit along the MEBT. The reason is that the offset of the quadrupoles are unknown. Therefore it is difficult to repeat the measured orbit using the simulation tools after considering the measured offset of BPMs. In the CSNS-II, the peak beam current will be increased to 50 mA which has the potential of higher radiation and the well knowledge of the orbit may alleviate the radiation.

Here, an optimization method is used to determine all known parameters related to the orbit, including 9 quadrupole offsets and 7 BPMs offsets. The software TRACEWIN [4] is used to perform the orbit tracking. During the tracking, the quadrupoles offsets are given and beam positions are recorded at the proper position. The BPMs offsets are added to the records of simulation and then the simulated orbit is compared with the measured orbit. For the optimization, a merit function $f = \sum (x_{\text{sim.}} - x_{\text{meas.}})^2$ is defined to determine the unknown parameters, here $x_{\text{sim.}}$ means the simulated beam position and $x_{\text{meas.}}$ means the measured position. The summation will run over BPM3 to BPM7 and the BPM1-2 will be used to give the initial orbit.

* Work supported by Open Research Foundation of Songshan Lake, DG24313511

† ylhan@ihep.ac.cn

ISBN: 978-3-95450-249-3 ISSN: 2673-5350 doi: 10.18429/JACoW-IBIC2024-THP64

RESEARCH AND DIAGNOSIS OF BEAM PARAMETERS IN THE SKIF LINEAR ACCELERATOR

O. I. Meshkov, A. E. Levichev, D. A. Nikiforov, M. V. Arsentyeva, V. L. Dorokhov, Xiaochao Ma†,1
Budker Institute of Nuclear Physics, Novosibirsk, Russia
[1]now at National Synchrotron Radiation Laboratory, Hefei, China

Abstract

The fourth-generation synchrotron light source Siberian Ring Photon Source (SKIF), located in Novosibirsk, Russia, underwent the tuning of its linear accelerator segment successfully. By deploying a designed beam diagnostic system, crucial parameters of the beam including beam transverse and longitudinal dimensions, energy spread, emittance, and current, were accurately measured. To achieve these measurements, the system was equipped with several fluorescent screens, Cherenkov radiation detectors, a dipole energy spectrometer, and a Faraday cup. This paper elaborates on the design, mode of operation, and practical applications of these diagnostic devices during the accelerator's tuning process. Further, potential areas of optimization for these diagnostic methods are explored to provide feasible directions for enhancing the performance of the linear accelerator. These precise diagnostic tools have been pivotal in the successful tuning of the SKIF linear accelerator. The results thus gathered will form a significant reference point for the development and refinement of similar accelerators in the future.

INTRODUCTION

The Siberian Ring Photon Source (SKIF) project [1] is a unique project in Russia. Its linear accelerator, part of the injection complex, has parameters that have never been achieved at any other installations operating in Russia. A specially designed diagnostic complex was used to obtain these parameters, and it allowed for successful debugging experiments on the linac at a specially designed stand (Figure. 1).

Figure 1: SKIF linear accelerator stand.

† mail address : maxiaochao@ustc.edu.cn.

LINEAR ACCELERATOR STAND

A linear accelerator with an electron energy of 200 MeV is used as the injector for the SKIF synchrotron radiation source. The accelerator consists of an RF gun, a third-harmonic grouping device, a pre-accelerator, and a system of regular accelerating structures [2]. The structure of the accelerator used in the experiments is shown in Figure 2.

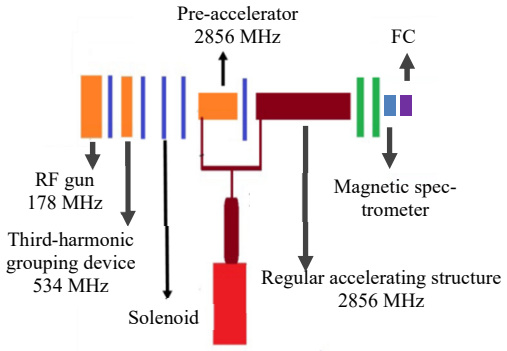

Figure 2: The layout of a linac with a single accelerating structure.

The electron source is based on an RF gun with a 178.5 MHz frequency and a thermionic cathode [3]. This produces an initial beam with an energy of 0.6 MeV. The RF gun operates at 178.5 MHz, which is half of the frequency of the resonator in the booster of SKIF, and one sixteenth of the frequency of the accelerating structure at 2856 MHz. Inside the RF gun, there is an oxide thermionic cathode installed. When the phase of the voltage in the resonator reaches 40 degrees, a trigger pulse is applied for 1 ns to the cathode-grid gap, generating an electron beam. This beam is then accelerated by the field of the resonator to an energy of 600 keV. The gun operates in a pulsed mode, with a repetition rate of 1 Hz. It is also possible to increase the repetition rate up to 20 Hz.

The pre-acceleration system is used to increase the energy of particles to 3 MeV. It includes a drift gap, a pre-accelerator structure, and a 535.5 MHz buncher that reduces the beam duration from 100 ps to 3 ps. This allows for a 1% energy spread at the output of the linear accelerator. A regular accelerating structure is designed to produce beams with energy between 20 and 50 MeV. It is based on a diaphragm waveguide with a constant impedance and an oscillation mode of $2\pi/3$. The structure is powered by a klystron that delivers 50 MW of pulse power. The full version of the linear accelerator has five accelerating structures. The maximum energy gained in the first structure is 53 MeV, and in the next stage it is 42 MeV, with a total maximum beam energy of 221 MeV.

ISBN: 978-3-95450-249-3 ISSN: 2673-5350 doi: 10.18429/JACoW-IBIC2024-THP65

BUNCH-BY-BUNCH FEEDBACK SYSTEM USED AS A DIAGNOSTIC TOOL FOR MULTI-BUNCH BEAMS IN THE DAΦNE COLLIDER

D. Quartullo*, A. D'Uffizi, T. De Nardis, A. De Santis, G. Franzini, G. Grilli,
C. Milardi, D. Pellegrini, S. Spampinati, A. Stella, M. Zobov, INFN-LNF, Frascati, Italy
O. Etisken, Kirikkale University, Kirikkale, Turkiye
S. Ozdemir, Ege University, Izmir, Turkiye, and Istanbul Nisantasi University, Istanbul, Turkiye

Abstract

DAΦNE is an electron-positron collider in operation at INFN-LNF since 2001. Bunch-by-bunch feedback systems installed in each of the two rings allow to store high-intensity and stable beams, by counteracting coupled-bunch instabilities. The feedback systems can be also used as a diagnostic tool able to measure beam parameters, which are significant for the evaluation of the instabilities. In this paper, we first describe the acquisition system used to collect the beam data provided by the feedback systems. Then we report recent transverse tune shift and grow-damp measurements with positron beams, performed using the feedback as a diagnostic tool. These measurements helped to characterize the e-cloud beam instability, which is one of the main factors currently limiting the DAΦNE performances. Finally, we describe the first measurements and feedback system setup designed to automatically record turn-by-turn bunch position displacements when a sudden loss in beam current occurs due to any faults in the collider. This tool can be very useful in identifying the causes of these events and performing beam dynamics studies and code validation.

INTRODUCTION

The DAΦNE lepton collider works at the c.m. energy of 1.02 GeV and includes two independent rings, each 97 m long. The collider has recently operated to characterize the never observed before kaonic deuterium transition [1]. DAΦNE has delivered to the SIDDHARTA-2 detector a data sample of the order of 1.5 fb^{-1}, an integrated luminosity well beyond the experiment request. In addition, most of the provided data have very high quality [1]. These remarkable results have been obtained by performing continued machine tuning, as well as dedicated machine studies.

The large luminosity provided to the experiments was the result, among other things, of the high beam currents accumulated in the rings. In 2024, the maximum stable beam currents stored in collision have been of the order of 1 A and 1.65 A, respectively for the positron and electron beams. Instabilities due to e-cloud strongly affect the positron beam dynamics, and they are one of the main factors limiting the maximum stored positron current.

To better characterize the strength of the e-cloud effects, an extensive campaign of e-cloud simulations and measurements has been performed in 2024, with the first results presented in Ref. [2]. Tune-shift and grow-damp measurements rely on the bunch-position signals, which were digitized by the signal processing unit of the bunch-by-bunch transverse feedback systems installed in the positron ring [3, 4]. These real-time systems, designed to counteract coupled-bunch instabilities, and to store high-intensities and stable beams, were therefore used as a diagnostic tool to measure beam parameters able to characterize the instabilities themselves.

The bunch-position signals acquired with the feedback system allow to study in detail the phenomenology of beam dynamics in case of fast beam losses. This approach can also provide indications about the causes of these events. The main difficulty here is to rightly trigger the acquisition, since the available buffer of recorded data is limited.

In the next section, the diagnostics acquisition system used for the measurements will be briefly described. Then, results of beam measurements using this diagnostic tool will be described, starting with tune-shift and grow-damp data, and ending with beam-death analysis.

ACQUISITION SYSTEM DESCRIPTION

The horizontal and vertical feedbacks act on the positions of the bunches centroids. The feedback corrections are provided by stripline kickers and they modify the transverse momenta of the particles. For each bunch and at a given turn, the signals from the horizontal or vertical electrodes of one BPM are subtracted from each other and sent to the signal processor (Fig. 1). These analog signals, proportional to the positions of the bunches centroids, are digitized in the ADC (12 bits, f_{sample} = 368.7 MHz, BW = 1.3 GHz) and then elaborated in FPGA to compute the correction signals, which are converted to analog in the DAC (Fig. 1). After going through RF amplifiers (Amplifier Research 250A250AM3), the corrections are sent to the horizontal or vertical kickers.

The acquisition memory in Fig. 1 has a circular buffer, i.e. data are recorded continuously, with old values being replaced by new ones. Data are recorded for each bunch turn after turn or with a user-defined down-sampling factor. Recording every turn, it is possible to obtain 34 ms of horizontal or vertical-position data for each bunch, by providing a trigger to the DIMTEL which freezes the memory buffer.

The trigger can be internal and sent by using the system interface, as was done during the tune-shift and grow-damp measurements. Otherwise, the trigger can be provided by an external system when a certain condition occurs. This second method was used during beam-death measurements, when the trigger fired as soon as the derivative of the average beam current provided by a DC current transformer went

* danilo.quartullo@lnf.infn.it

ISBN: 978-3-95450-249-3 ISSN: 2673-5350 doi: 10.18429/JACoW-IBIC2024-THP66

MEASUREMENT OF BEAM ENERGY CHARACTERISTICS AT THE LHe-FREE Nb_3Sn DEMO SRF e-LINAC*

Y. M. Chu†,1,2, Z. J. Wang‡,2, W. L. Chen[2], Z. H. Liang[1], T.L. Wang[1], Z. Q. Yang, G. Z. Jiang[3], C. Feng, D. Y. Jia[1,2], H. J. Cai, Y. Du[1], L. W. Liu[1], M. Yi[3], C. G. Su[1], T.Y. Li[1], T. Zhang[1], H. X. Li[1]
Institute of Modern Physics, Chinese Academy of Sciences, Lanzhou, China
[1] also at University of Chinese Academy of Sciences, Beijing, China
[2] also at Advanced Energy Science and Technology Guangdong Laboratory, Huizhou, China
[3] also at Lanzhou University, Lanzhou, China

Abstract

The demonstration of a 100 mA, 4.6 MeV superconducting radio frequency linear electron accelerator, based on conduction cooling and developed by the Institute of Modern Physics (IMP), aims to validate the feasibility of stable beam commissioning in a liquid helium-free 5-cell-βopt=0.82 Nb3Sn elliptical cavity, and to offer guidance for subsequent industrial applications. The beam energy characteristics, considered one of the critical parameters, need to be precisely measured. Given the high beam energy and the need for a compact, straightforward accelerator layout, we achieved high-precision measurements using only a ordinary dipole, a slit, and a Faraday Cup (FC). This paper presents the online measurement results of beam energy at different cavity voltage and provides a thorough analysis and optimization of the various errors encountered during measurement.

INTRODUCTION

To reduce the reliance on large-scale cryogenic systems and associated operational costs in superconducting accelerators, and to advance the miniaturization and industrialization of SRF accelerators, the IMP initiated a study in 2021 [1]. This research focuses on utilizing a GM cryocooler to cool Nb3Sn thin-film cavities via solid conduction, enabling operation without the use of liquid helium. A prototype Nb3Sn liquid helium-free SRF e-linac, based on solid conduction cooling, was subsequently designed and constructed. Beam commissioning were successfully conducted in 2024.

As shown in Fig. 1, the e-linac consists of a thermionic electron gun capable of producing a DC electron beam with a maximum current of 700 mA, a 650 MHz SRF cavity with an optimal β of 0.82, and two focusing solenoids. The beam parameters are listed in Table 1. As the first fully integrated prototype of a solid conduction-cooled Nb3Sn SRF e-linac in China, this system is designed to accumulate operational experience under realistic conditions. It must therefore meet compact design requirements while enabling measurements of beam current, transmission efficiency, and energy. A non-intercepting ACCT is placed upstream of the cavity to provide real-time measurement of the beam current extracted from the electron gun. At the downstream end of the straight section, a FC is installed to intercept the beam and measure the current. Given the compact layout and limited number of components in the straight section, the ratio of the beam currents measured by the FC and ACCT serves as an indicator of the cavity's transmission efficiency. Beam energy is determined through the magnetic deflection field.

Figure 1: Layout of the e-linac.

Table 1: Beam Parameters of the e-Linac.

Beam Parameters	Values	Units
Accelerated particles	electron	-
Extracted Energy	0.06	MeV
Extracted Current	200	mA
Repetition Frequency	1	Hz
Pulse Width	2	us
Energy Gain	>3	MeV
Transmission Efficiency	44	%

MEASUREMENT METHOD

Due to the requirements for a simple and compact layout in this e-linac, it is not feasible to use a complex and large high-resolution spectrometer, like those employed at LNL [2] and GANIL [3]. Additionally, the high energy of the electron beam makes the time-of-flight (TOF) method unsuitable for measuring beam energy [4].

* Work supported by the Large Research Infrastructures China initiative Accelerator Driven System Project (Grant No. 2017-000052-75-01-000590)
† chuyimeng@impcas.ac.cn
‡ Corresponding author: wangzj@impcas.ac.cn

ISBN: 978-3-95450-249-3 ISSN: 2673-5350 doi: 10.18429/JACoW-IBIC2024-THP69

MEASUREMENT OF THE H- CONTENT IN MIXED BEAM FROM ION SOURCE

B.C. Wang, W.L. Liu, M.T. Zhao, M.W. Wang, D. Wang, W. Lv,
Y.H. Yan, M.C. Wang, Y. Yang, Z.M. Wang†
National Key Laboratory of Intense Pulsed Radiation Simulation and Effect, Xi'an, China

Abstract

H- ion source produces mixed beam of H- and electrons. Usually, a bending magnet is needed to measure the contents of mixed beam. However, bending magnet is generally lacked in H- machine, because bending magnet increases the transport line length, leading to more serve decline of H-. How to measure the H- content in mixed beam without the help of bending magnet is worthy to be studied. In this paper we propose a method to measure the H- content utilizing common devices in low energy beam transport line. This method is mainly based on a solenoid. The H- and electron contents can be obtained by analyzing the change of the beam transmission when sweeping the solenoid current. The experiments were performed.

INTRODUCTION

Xi'an Proton Application Facility (XiPAF) is the first facility that is dedicated to simulations of the space radiation environment in China [1]. It can accelerate protons up to a maximum of 200 MeV, and in the future, it will have the capability to accelerate heavy ions. The H- beam is firstly accelerated to 7 MeV by linear accelerator, then stripped into protons by stripping foil, and finally injected into the synchrotron to be further accelerated to 200 MeV.

The ion source is the origin of the beam. However, negative hydrogen ion source typically outputs a beam that consists of both hydrogen ions and electrons. Accurately measuring the content of negative hydrogen in the beam extracted from the ion source is of significant value for precisely modeling the accelerator.

Typically, analyzing magnet is used to separate particles with different mass-to-charge ratios. Within a given magnetic field, particles with different mass-to-charge ratios have different deflection radius, which allows for their effective separation. However, the low energy beam transport line (LEBT) for negative hydrogen beam is less commonly equipped with analyzing magnet. Due to the influence of the ion source inlet gas, LEBT typically has higher residual gas pressure, and negative hydrogen ions suffer significant stripping losses in this environment. Analysing magnet would increase the length of the transport line, leading to a severe reduction in the number of H- ions. How to determine the content of H- ions in the beam output from the ion source without the use of analyzing magnets is worth investigating. In this paper, we propose a method for inferring the content of H- in the mixed beam by scanning the magnetic field strength of a solenoid and measuring the corresponding changes in transmission efficiency.

† wangzhongming@nint.ac.cn

ION SOURCE AND LEBT OF XIPAF

XiPAF equips an electron cyclotron resonance (ECR) negative hydrogen source. The ion source employing permanent magnets to generate the ECR magnetic field. As shown in Fig. 1, the structure of the ion source is relatively compact. Its main design parameters are shown in Table 1.

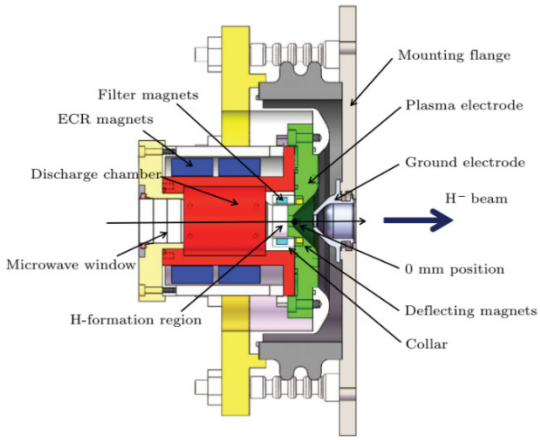

Figure 1: Schematic of the H- ion source [1].

Table 1: Main Design Parameters of the H- Ion Source

Parameter	Value	Unit
Particle	H^-	
Voltage	50	kV
Peak beam current	10	mA
Normalized RMS emittance	0.2	π · mm · mrad

The ion source is directly mounted on the first diagnostic chamber of the LEBT. Therefore, the output beam of ion source directly enters the LEBT. The ion source operates with hydrogen as the working gas, and the unconsumed hydrogen gas will pass through the extraction aperture along with the beam, entering the LEBT. Affected by the inlet hydrogen gas from the ion source, the vacuum level measured in the first diagnostic chamber is approximately at the order of 1E-3 Pa, where the stripping of negative hydrogen beams is quite serious.

As shown in Fig. 2, The XiPAF LEBT mainly consists of two solenoids, which have a large adjustment capability, allowing for a wide range of beam matching into the RFQ

ISBN: 978-3-95450-249-3 ISSN: 2673-5350 doi: 10.18429/JACoW-IBIC2024-THP71

BETATRON STOPBANDS AND COUPLING RESONANCE DRIVING TERMS CHARACTERIZATION AT VEPP-2000 COLLIDER

D. E. Chistiakov†, E. A. Perevedentsev, Y. A. Rogovsky, Budker INP SB RAS, Novosibirsk, Russia
also at Novosibirsk State University, Novosibirsk, Russia

Abstract

The final-focus solenoids of the round-beam e+e- collider VEPP-2000 can cause stopbands in the betatron tune plane. This specific stopband domain limits the available tune space in the most important region above the integer tunes. We present a study of the combined effect of coupling resonances caused by the decompensated solenoids and the integer-tune parametric resonances. The results are compared with numerical investigations of this combined effect. Presented experimental data includes scanning of the available betatron tune plane domain and evaluation of coupling RDTs using beam oscillation histories from BPMs.

INTRODUCTION

Coupled betatron oscillations caused by the decompensated final-focus solenoids of VEPP-2000 collider [1] lead to appearance of specific stopbands in the betatron tune plane. This sort of limitation along with various machine resonances limits the allowed tune plane domain. To get the working tunes in the most collider-efficient area (above the integer tunes) one needs to control and to reduce the combined effect of the solenoid stopbands and the resonances at the integers [2].

Beam oscillation histories help in finding integral and in some cases spread local characteristics of a machine.

BETATRON STOPBANDS

Matrix Approach

To describe the linear coupled transverse motion of the particles in a cyclic accelerator a matrix formalism is used. The particle's dynamical variables are given by a four-dimensional vector $X^T = (x, p_x, y, p_y)$. These terms adequately describe the combined action of the resonances and betatron stopbands.

If the uncoupled linear magnetic structure is known, a period matrix for one degree of freedom can be written:

$$M_0 = \begin{pmatrix} c_0 - w_0 w_0' \cdot s_0 & w_0^2 \cdot s_0 \\ -\left(w_0'^2 + \frac{1}{w_0^2}\right) \cdot s_0 & c_0 + w_0 w_0' \cdot s_0 \end{pmatrix}, \quad (1)$$

where $c_0 = cos\,\mu_0$, $s_0 = sin\,\mu_0$, $\mu_0 = 2\pi\nu_0$ is the betatron phase advance over the period and w_0 is the envelope function.

Close to an integer-tune parametric resonance resonance ($\nu_x = \frac{k}{2} + \Delta$), its amplitude can be found using perturbation theory [3]. After averaging over fast phase $\Psi_x = \left(\frac{k}{2} + \Delta\right)\frac{s}{R} + \chi_x(s)$ and considering Δ small, we get

$$g_k^x = \frac{1}{\Pi}\oint w_x^2(s) g^x(s) e^{-i\left(k\frac{s}{R} + 2\chi_x(s)\right)} ds. \quad (2)$$

After finding perturbed Floquet-vectors and phase advances a perturbed period matrix can be written, its elements are:

$$\begin{aligned} m_{11} &= c_r - s_r \frac{w' w(\delta + g_k \cdot c_\theta) - g_k \cdot s_\theta}{r}, \\ m_{12} &= s_r \frac{w^2(\delta + g_k \cdot c_\theta)}{r}, \\ m_{21} &= -s_r \left\{ A_m \cdot \frac{\delta}{r} + (B_m \cdot c_\theta - C_m \cdot s_\theta) \cdot \frac{g_k}{r} \right\}, \\ m_{22} &= c_r + s_r \frac{w' w(\delta + g_k \cdot c_\theta) - g_k \cdot s_\theta}{r}, \end{aligned} \quad (3)$$

where g_k is the absolute value of the resonance amplitude term [Eq. (2)], α is its complex phase, $\delta = \frac{2\Delta}{R}$,
$c_r = cos\left(\frac{1}{2} s \cdot r\right)$, $s_r = sin\left(\frac{1}{2} s \cdot r\right)$, $r = \sqrt{\delta^2 - g_k^2}$,
$c_\theta = cos(\alpha - \delta \cdot s + 2\Psi)$, $\quad s_\theta = sin(\alpha - \delta \cdot s + 2\Psi)$,
$A_m = \left(w'^2 + \frac{1}{w^2}\right)$, $B_m = \left(w'^2 - \frac{1}{w^2}\right)$, $C_m = 2\frac{w'}{w}$.

A two degree of freedom matrix with no coupling with the account of the parametric resonances is:

$$M_4 = \begin{pmatrix} M_x & 0 \\ 0 & M_y \end{pmatrix}, \quad (4)$$

where $M_{x,y}$ is constructed according to Eq. (3) with x or y betatron parameters, respectively.

The essence of betatron coupling caused by the solenoids can be described using a thin-element matrix which rotates the oscillations plane at an angle φ:

$$R = \begin{pmatrix} I \cdot cos\,\varphi & I \cdot sin\,\varphi \\ -I \cdot sin\,\varphi & I \cdot cos\,\varphi \end{pmatrix}, \quad (5)$$

where I is a 2×2 identity matrix.

So the new period matrix with coupling is a product:

$$M_{tot} = R \cdot M_4. \quad (6)$$

The betatron stopbands on the tune plane occur as a consequence of perturbation causing instability in certain tune ranges, so that not all initial tunes provide stable perturbed solutions. In general, the stable solution meets the conditions for μ as a new (perturbed) phase advance:

ISBN: 978-3-95450-249-3 ISSN: 2673-5350 doi: 10.18429/JACoW-IBIC2024-THP72

A PRELIMINARY DESIGN OF A COMPTON POLARIMETER AT BEPCII

M. Y. Su, Z. Duan*, Q. F. Han, D. H. Ji, G. Lei, Q. Li, Y. C. Li, Z. J. Liang†,
X. J. Sun, G. Y. Tang, J. L. Wang, C. H. Yu, W. Zhang, Y. L. Zhang, N. C. Zhou, D. C. Zhu,
Institute of High Energy Physics, CAS, Beijing, China
A. Martens‡, F. Zomer, Université Paris-Saclay, CNRS/IN2P3, IJCLab, Orsay, France
F. Castellanos, C. Sandoval
Departamento de Física, Universidad Nacional de Colombia, Bogotá, Colombia

Abstract

BEPCII is a double ring e+ e- collider running in the tau-charm energy region. We propose reusing the beamline of a dismantled wiggler magnet to implement a Compton polarimeter detecting scattered γ photons, to measure the self-polarization of the electron beam at BEPCII. This would enable resonant depolarization, and thus provide precision beam energy calibration for BEPCII, and serves as a testbed for future colliders like the CEPC. In this paper, the preliminary design of this Compton polarimeter is presented, and the tentative plan for the implementation and commissioning in the coming years are shown.

INTRODUCTION

Polarized lepton beams are essential for the physics program of the future colliders like the Circular Electron Positron Collider (CEPC) [1]. The preparation, manipulation and utilization of polarized beams rely on precision measurements of the beam polarization, in particular using Compton polarimeters [2] in the storage rings. As a test bed for this key technology, a Compton polarimeter has been designed for the Beijing Electron-Positron Collider (BEPCII) [3] to measure the self polarization of the electron beam, and the implementation plan has been established. This development will enable resonant depolarization [4] and other beam polarization experiments at BEPCII.

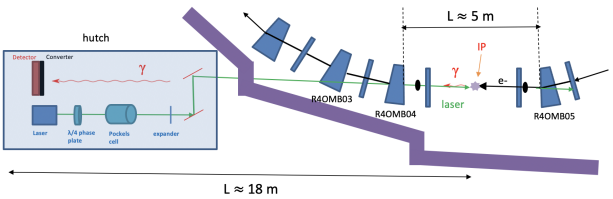

Figure 1: The layout of the Compton polarimeter at the 4W2 beamline of BEPCII.

BEPCII is a double ring e+ e- collider, with a design luminosity of $1 \times 10^{33}\mathrm{cm}^{-2}\mathrm{s}^{-1}$ at 1.89 GeV, achieved routinely in operation since 2023. Now BEPCII is under a major upgrade (BEPCII-U) to enable delivering 3 times more luminosity at 2.35 GeV and operating up to 2.8 GeV. 4W2, a wiggler-based X-ray beamline of BEPCII for high pressure studies, has retired from operation. We propose to modify the front end and the hutch of this beamline to implement a Compton polarimeter. As shown in Fig. 1, a laser system in the hutch will shoot a laser through the X-ray beamline and collide at a small vertical crossing angle with the incoming electron beam, inside the straight section where the wiggler occupied before. The backscattered γ photons will be transported back to the hutch through the same beamline, and their spatial distributions are measured by the detector system.

In this paper, we begin with the principle and design parameters of this Compton polarimeter. Next, we describe the detector system and GEANT-4 simulations. Then we discuss the planned hardware modifications, including a laser transportation experiment during this long shutdown of BEPCII. We proceed to present the design of the laser alignment targets and the proof-of-principle experiments.

DESIGN PARAMETERS

Electron beams tend to become vertically polarized in a storage ring due to the Sokolov-Ternov effect. The polarization build-up time is about 75 min at 2.35 GeV for BEPCII. This beam energy is away from first-order spin resonances and the vertical polarization level is expected to be measurable with a Compton polarimeter.

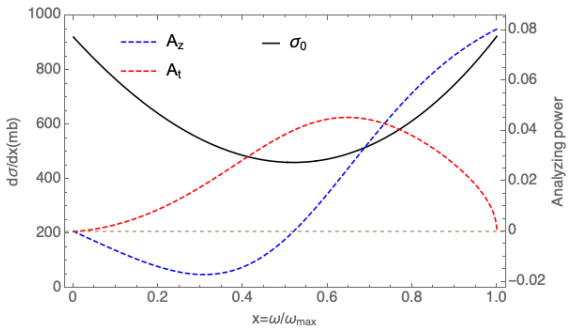

Figure 2: The differential cross section and analyzing powers as a function of the normalized scattered photon energy.

The Compton scatterings between a circularly polarized laser and a vertically polarized electron beam imprint an up-down asymmetry in the spatial distributions in both scattered γ photons and scattered electrons, the differential cross

* duanz@ihep.ac.cn
† liangzj@ihep.ac.cn
‡ aurelien.martens@ijclab.in2p3.fr

ISBN: 978-3-95450-249-3 ISSN: 2673-5350 doi: 10.18429/JACoW-IBIC2024-THP73

METHODOLOGY FOR IDENTIFYING THE CENTRE OF A SOLENOID MAGNET BASED ON THE BEAM DYNAMICS

Dong Hyuck Kim, Ji-Gwang Hwang*
Gangneung-Wonju National University, Gangneung, Republic of Korea

Abstract

The method of minimizing oscillation amplitude generated by varying the strength of a corrector magnet located upstream is commonly used for beam-based alignment of a single-pass machine. It minimises the amplitude of the centre of mass of the beams in beam diagnostics located downstream while the beam offset at the magnet is scanned by a corrector magnet upstream. The method is easily applied for a magnet capable of variable separation between horizontal and vertical planes such as a quadrupole magnet. However, in the case of a solenoid magnet, it is not suitable to apply the method since it has an azimuth magnetic component that produces mainly beam rotation. In this presentation, we propose an analytical method for identifying the centre of a solenoid magnet and present results validated by numerical simulations.

INTRODUCTION

In a practical situation, owing to the technical limits for the alignments and manufacturing imperfections, the centre of a magnet and the beam trajectory can not be aligned perfectly and the discrepancy originates a steering effect, additional focusing as well as nonlinear distribution. Therefore, during the machine operation, the offset is minimized using correctors installed in the beamline by adjusting the angle of the beam [1]. This procedure is so-called beam-based alignment (BBA). Particularly, in a linear machine, the BBA can be performed by minimizing the oscillation amplitude at a screen monitor downstream using a corrector upstream while the strength of the magnet is scanned [2]. It can be conducted based on the property of the separation of variables between two perpendicular axes in the motion of equations. However, the solenoid field, which is aligned with the beam axis introduces complexity in the beam dynamics, as the transverse motions in the x and y directions are coupled due to the solenoid field's nature. This coupling effect is the key difference from the uncoupled transverse dynamics observed in quadrupole magnets, where the x and y directions can be treated independently. This is not the case for solenoid magnets since they not only generate a strong x-y coupling but provide axisymmetric focusing properties due to the rotational symmetry of the magnetic field. The solenoids are widely used for low-energy electrons [3] and heavy ions because the focusing force is proportional to the beam radius and the structure can be easily enlarged to a large radius. In addition, providing the focus of both directions simultaneously is particularly advantageous in situations involving either the compact machine or low-energy injectors in which all elements are tightly installed in a narrow space. It was attempted to align the solenoid magnet with offline field measurement [4–6]. However, the offset between the magnet and the beam is inevitable during a machine operation driving the device. In this paper, we describe a theoretical approach to the alignment of the solenoid magnet. This presents a way to minimize the offset between the beam and the solenoid during the operation. This methodology has been proven by particle tracking simulations using the IMPACT-Z code [7].

A SOLENOID MAGNET

The understanding of the motion of charged particles in auxiliary fields, which is the core of accelerator physics, paves the way for controlling and manipulating particle beams precisely. Therefore, the basic equations for the solenoid magnet are revisited in the first part of this paper. With a hard-edge model, the solenoid field provokes a spiral motion, resulting in rotation in x-y space while propagating with a constant speed in the s-direction [8]. The magnetic field of the solenoid with steady currents can be derived by Ampère's law and can be expressed as follows

$$\oint \mathbf{B} \cdot d\mathbf{l} = \mu_0 I_{\text{enclosed}}, \tag{1}$$

where $I_{enclosed}$ represents the current enclosed by the amperian loop and μ_0 is the permeability of free space. In the case of an ideal solenoid, the magnetic field inside a solenoid is aligned along the axis of the solenoid, creating a uniform field within the central region. However, at the edges of the solenoid, the magnetic field begins to vary, forming what is known as the fringe field. Therefore, the magnetic field of the solenoid can be expressed as $\mathbf{B} = B_r(r,z)\hat{r} + B_z(r,z)\hat{z}$. This fringe field component B_r can have a significant impact on the motion of particles as they enter or exit the solenoid. In a solenoid, the magnetic field $\mathbf{B}$ can be represented by a vector potential $\mathbf{A}$ which can be calculated by

$$\oint \mathbf{A} \cdot d\mathbf{l} = \int \mathbf{B} \cdot d\mathbf{a}. \tag{2}$$

The vector potential of the solenoid is given by $\mathbf{A} = \frac{1}{2} r B_z \hat{\theta} = -\frac{B_z}{2} y\hat{x} + \frac{B_z}{2} x\hat{y}$. From the Maxwell Equation $\mathbf{B} = \nabla \times \mathbf{A}$, the radial magnetic field B_r which raises the focusing effect can be presented as

$$B_r = -\frac{\partial \mathbf{A}_\theta}{\partial z} = -\frac{1}{2} B_z' r, \tag{3}$$

In Eq. (3), there are two key points: (1) the radial magnetic field is proportional to the gradient of the axial magnetic field

* hwang@gwnu.ac.kr

ISBN: 978-3-95450-249-3 ISSN: 2673-5350 doi: 10.18429/JACoW-IBIC2024-FRAT1

SECONDARY, THERMIONIC AND DELTA ELECTRON EMISSION FROM THIN TARGETS

M. Sapinski*
Paul Scherrer Institut, Villigen, Switzerland

Abstract

Thin objects in the form of wires, foils, or strips are often used as targets in various instruments that measure beam parameters, or for other purposes. They usually cause only small beam perturbations and suffer from relatively low temperature increases. The beam induces the emission of secondary electrons, which are typically the source of the measured signal. In high-brightness beams, the targets can reach high temperatures, leading to thermionic current emission. In addition, a certain number of delta electrons are emitted, which affects the emitted current as well as beam heating. These three types of electrons have different properties and influence the measured signal and the temperature evolution of the target. This paper discusses how the signal is generated by the escaping electrons, how the bunch field affects this signal, and how the target temperature depends on electron emission.

INTRODUCTION

Thin targets, in the form of micrometer-sized wires, strips, or foils, are widely used in particle accelerators, particularly in beam instrumentation. Their small thickness reduces the disturbance to the beam and damage to the targets themselves. Electron emission from these targets is often used as a signal to probe the beam distribution. There are multiple mechanisms of electron emission from the body exposed to radiation. The properties of these various electron emission processes are important for the correct interpretation of measurements obtained using beam instruments.

In this study, we discuss three types of electron emissions that are important for proton beam profile measurements using wire scanners and SEM-grids. They contribute to the electric current flowing to the wire, which is the signal used to measure beam parameters. They interact with the bunch fields and affect the thermal behavior of the targets. The three types of electron emission are delta, low-energy secondary, and thermionic. Other types of emissions, such as photoemission or emission of Auger electrons, are not relevant for this discussion.

Motivation

This study is particularly important for beam instruments that employ thin targets and measure the current generated by the beam interacting with these targets. Typically, these devices are SEM-grids or wire scanners that rely on the readout of electric current, which is used for low-energy beams that do not produce enough of a particle shower to be efficiently measured outside of the vacuum chamber. The phenomena discussed here are especially relevant for high-brightness beams, where the power deposited on the target is so high that it reaches temperatures at which thermionic emission becomes significant and affects the measured signal.

That being said, some of the results or discussions presented here are also partly applicable to other beam conditions and types of beams.

Study Cases

The mechanisms of secondary and delta electron generation have been studied for four specific cases of proton beams at the following energies:

- 72 MeV, as in case of beam extracted from PSI's Injector 2 cyclotron.
- 590 MeV, as in case of beam extracted from PSI's Main Ring cyclotron [1].
- 3 GeV, as in case of J-PARC Main Ring synchrotron at injection [2]; while this scanner uses 7 μm carbon fiber, for ease of comparison, calculations are done for 33 μm fibers.
- 450 GeV, as in case of CERN SPS flat top [3].

Due to the high brightness of the beams under consideration, the primary target material studied is carbon fiber (CF) [1], which is considered the gold standard for handling extremely challenging beam conditions (high brightness). However, additional calculations have been performed for molybdenum, which offers a good compromise between material density and high melting temperature, as well as tungsten, which has the highest melting temperature of all metals.

THIN TARGETS

The targets are considered thin when their thickness ranges from a few micrometers to approximately 100 μm. Typically, the targets take the shape of wires with a round cross-section or foils. In this study, we focus on thin wires with a diameter of 33 μm, which is smaller than average human hair (75 μm). Even thinner targets exist, such as foils with sub-micrometer thickness (down to 25 nm). They are used in accelerators for stripping electrons out of H^- ions in charge-exchange injection or extraction processes.

In case of such ultra-thin targets, the number of particle interactions with material electrons is so low (a few), that the energy straggling function exhibits a unique shape with multiple peaks at low energy and a long high-energy tail [4]. For micrometer-size targets a Landau distribution of straggling is an accurate approximation.

* mariusz.sapinski@psi.ch

[1] The density of the carbon fibre used in the simulations is 2 g/cm^3, however the values found in the literature vary between 1.7 and 2.1 g/cm^3.

ISBN: 978-3-95450-249-3 ISSN: 2673-5350 doi: 10.18429/JACoW-IBIC2024-FRAC2

BGC MONITOR: FIRST YEAR OF OPERATION AT THE LHC

H. D. Zhang *, O. Sedlacek[1], S. Sethi, O. Stringer, C. Welsch
University of Liverpool / Cockcroft Institute, Daresbury, Warrington, UK
M. Ady, D. Butti, T. Lefevre, S. Mazzoni, C. Pasquinom, A. Rossi, M. Sameed,
G. Schneider, C. C. Sequeiro, K. Sidorowski, R. Veness, CERN, Geneva, Switzerland
P. Forck, S. Udrea, GSI, Darmstadt, Germany
[1] also at CERN, Geneva, Switzerland

Abstract

The Beam Gas Curtain (BGC) monitor was installed in the beam one of the Large Hadron Collider (LHC) during Long Shutdown 2 (LS2) and the Year-End Technical Stop (YETS) 2022. The monitor detects the fluorescence signal generated by the interaction between the charged particle beams in the LHC and the neon atoms in the supersonic gas curtain. This provides 2D images of the primary beam. In the 2023 run, it was demonstrated that transverse beam profile measurement for both, proton beam and lead ion beams in the LHC is possible across injection, energy ramp-up and top energy operation. The BGC has shown the potential to be an operational instrument and efforts to integrate the monitor into the main machine control system are being undertaken. In this contribution, we will present measurement results and discuss operational experience including observed gas loads to the LHC, observed impact on beam losses, and demonstrated resolution of the monitor. Finally, we will also discuss plans for the continued optimization of this monitor and the installation of a second monitor into beam two.

INTRODUCTION

Since the Large Hadron Collider started to operate in 2010, it has led to many discoveries, which are the frontier of high-energy physics. A stable operation of the accelerator complex will be required to achieve the integrated luminosity to reach certain statistics for these discoveries. To do that, the beam instrumentation is a key. The transverse beam profile monitor is one of many beam diagnostics in the LHC which is used for beam size measurement and emittance estimation. Widely used transverse beam profile monitors in the CERN accelerator complex include scintillating screens, wire scanners, synchrotron radiation monitors, secondary emission monitors, and ionisation profile monitors. They all have their pros and cons. A new concept of beam profile monitoring was proposed using a supersonic gas curtain and fluorescence [1]. Based on this concept, the Beam Gas Curtain monitor (BGC) was installed during long shutdown 2 (LS2) and the year-end technical stop (YETS) in 2022. During the 2023 LHC run, the monitor was successfully commissioned. The measurement of beam profiles in all stages of LHC operation including injection, energy ramping up, and the stable beam was demonstrated for both the proton beams and the lead-ion beams. Since then, efforts have been made to transfer this device to a fully operational device for daily LHC operation.

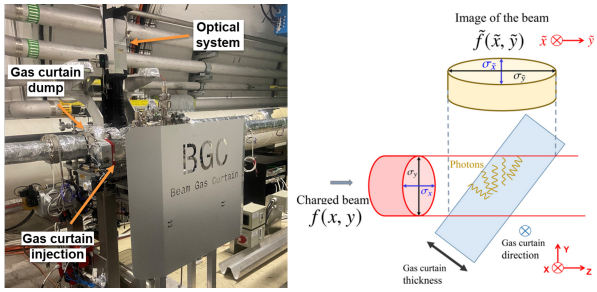

Figure 1: Picture of the BGC installed in the LHC and the detection principle.

METHOD

Using beam-induced fluorescence (BIF) to detect the beam profile was applied before. This method is minimum-invasive and the detecting system is a simple optical imaging system. In the past, because of the low cross-section of the fluorescence process and a small fraction of the signal detected due to the restrained solid angle, gas injection was always needed to reach a certain signal-to-noise ratio (SNR) and acceptable integration time. The easiest way to inject gas is to use a needle valve, but the obvious drawback is the gas load to the whole system. Using a supersonic gas curtain can avoid these issues because of the high speed and directionality of the gas molecules in the curtain. The gas expanded through a small nozzle from a high-pressure region to a low-pressure region to form a supersonic jet. Then the jet was collimated by three consecutive skimmers to form a thin curtain with an equivalent pressure of $\sim 1 \times 10^{-6}$ mbar. These skimmers are used to create differential pump stages to ensure that the pressure in the beam pipe is at a low level where the beam dump is not triggered. A fourth skimmer together with a gas dump section is used to collect the unused gas molecules from the curtain to maintain the pressure in the beam pipe. A schematic diagram of the system can be seen [2]. For the detection system, as shown in Fig. 1, the charged particle beams interact with the molecule inside the gas curtain, causing the molecule to an excited state. Then the excited molecule will emit fluorescence whose distribution is directly proportional to the previous charged particle beams. If a suitable gas, e.g. Neon, was used which has

* haozhang@liverpool.ac.uk

ISBN: 978-3-95450-249-3 ISSN: 2673-5350 doi: 10.18429/JACoW-IBIC2024-FRBI1

DEVELOPMENT OF ULTRA-FAST DIMAOND-SENSOR BASED SYSTEMS FOR ADVANCED ACCELERATOR DIAGNOSTICS*

B. A. Schumm†, F. Martinez-McKinney, T. Morris, S. Mudford, M. Nizam, R. Padilla, K.-W. Shin, M. Wilder, University of California, Santa Cruz and the Santa Cruz Institute for Particle Physics, Santa Cruz, California, USA
E. Prebys, C. Rowling, University of California, Davis and the Crocker Nuclear Laboratory, Davis, California, USA
J. Bohon, C. Grace, T. Prakash, Lawrence Berkeley National Laboratory, Berkeley, California, USA
B. Jacobson, I. Silva Torrecilla, J. Smedley, SLAC National Accelerator Laboratory, Menlo Park, California, USA
M. Gulley, D. Kim, Los Alamos National Laboratory, Los Alamos, New Mexico, USA

Abstract

The Advanced Accelerator Diagnostics collaboration has been developing diamond-sensor based high bandwidth position-sensitive diagnostics for application at next generation XFELs and other accelerator facilities. A pass-through diagnostic with 50 MHz rate capability has demonstrated pulse-by-pulse position sensitivity of 1% of delivered beam width. Progress has been made in upgrading this diagnostic approach to multi-GHz operation, involving an integrated detection system design making use of a compact signal path and proximate high-bandwidth readout ASIC. Preliminary results are presented on the performance of both the signal path and ASIC. Possible additional applications, including precision event timing and plasma ignition diagnosis, are introduced.

INTRODUCTION

The prospective diagnostic and imaging needs of future X-ray Free Electron Laser (XFEL) facilities [1,2] have driven work in the development of high-bandwidth ionizing particle detection systems that can operate at frame rates in excess of 5 GHz, an order of magnitude greater than existing prototype systems [3]. The Advanced Accelerator Diagnostics (AAD) group, a collaboration involving University of California campuses (Santa Cruz and Davis) and three National Laboratories (Los Alamos, Lawrence Berkeley and SLAC), has been exploring the use of CVD diamond sensors complemented by dedicated readout systems (including ASICs) to push the limits of readout bandwidth and dynamic range of X-ray detection systems. In this Proceedings, we report on the performance of a moderate speed (50 MHz) position-sensitive pass-through diagnostic and, more importantly, recent progress made in advancing the design of this diagnostic to allow for operation in the multi-GHz RF regime. Such a capability may prove enabling for the operation and exploitation of next-generation XFEL beams, as well as advancing diagnostic capabilities in other fields, including Fusion Energy Science [4].

In this work, the AAD collaboration makes use of monocrystalline diamond sensors, whose superior saturated drift speed of approximately 200 μm/ns [5] make them ideal for fast-signal applications. The collaboration makes use of diamond substrates purchased from industrial vendors, and fabricated by the Los Alamos National Laboratory group at its Center for Integrated Nanotechnologies.

50 MHz QUAD PASS-THROUGH DIAGNOSTIC

Motivated by the development of the cavity-based XFEL (CBXFEL) [6], the AAD collaboration has developed a quadrant pass-through diagnostic designed to provide intensity and centroid measurements of a moderate-intensity XFEL beam with 50 MHz repetition rate. This diagnostic is depicted in Fig. 1, and features a four-channel quadrant diamond sensor of total area 4x4 mm^2 and thickness 43 μm.

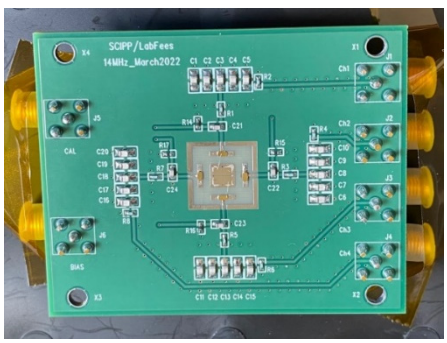

Figure 1: 50 MHz quadrant pass-through diagnostic.

* This work was supported in part by U.S. Dept. of Energy Office of Basic Energy Sciences grant numbers DE-SC0024205 (UC Santa Cruz), DE-AC02 05CH11521 (LBNL), A24-0496-S001 (UC Davis), DE-AC02-76SF00515 (SLAC) and FWP LANLE8AN (LANL), by the Office of High Energy Physics grant number and DE-SC0010107, and by the UC-National Laboratory Fees Research Program grant ID #LFR-20-653232. This work was performed, in part, at the Center for Integrated Nanotechnologies, an Office of Science User Facility operated for the U.S. Dept. of Energy (DOE) Office of Science by LANL and Sandia National Laboratories (Contract DE-NA-0003525). LANL is operated by Triad National Security, LLC, for the National Nuclear Security Administration of U.S. Dept. of Energy (Contract No. 89233218CNA000001).
† baschumm@ucsc.edu

ISBN: 978-3-95450-249-3 ISSN: 2673-5350 doi: 10.18429/JACoW-IBIC2024-FRBC2

A SYSTEMATIC INVESTIGATION OF BEAM LOSSES AND POSITION RECONSTRUCTION TECHNIQUES MEASURED WITH A NOVEL oBLM AT CLEAR

M. King*,[1], S. Benitez, E. Effinger, J. Esteban, W. Farabolini, J. M. Meyer, B. Salvachua
CERN, Geneva, Switzerland
A. Christie, P. Korysko, Oxford University, Oxford, United Kingdom
C. Welsch, University of Liverpool, Liverpool, United Kingdom
J. Wolfenden, Cockcroft Institute, Daresbury, United Kingdom
[1]also at University of Liverpool, Liverpool, United Kingdom

Abstract

Optical Beam Loss Monitors (oBLMs) allow for cost-efficient and spatially continuous measurements of beam losses at accelerator facilities. A standard oBLM consists of several tens of metres of optical fibre aligned parallel to the beamline, coupled to photosensors at either or both ends. Using the timing information from loss signals, the loss positions can be reconstructed. This contribution presents a novel oBLM system recently deployed at the CERN Linear Electron Accelerator for Research (CLEAR). Multiple methods of extracting timing and position information from measured waveforms are investigated, and the potential impact of varying beam parameters such as bunch charge or number is analysed. This work has resulted in the development of a GUI to aid operations by visualising the beam losses and their positions in real time.

INTRODUCTION

Optical beam loss monitors (oBLM) have become increasingly widespread as distributed beam loss monitoring systems since their first development in 2000 [1]. They consist of a multimode optical fibre with photosensors attached at either or both sides of the fibre. The fibre is placed parallel and as close as possible to the beamline while the photosensors are typically located somewhat shielded from radiation. Whenever beam losses occur, charged particles above a certain threshold velocity traversing the optical fibre induce Cherenkov radiation. A proportion of these photons can be captured by the optical fibre and read out by the photosensors. The signal amplitude then gives the intensity of the beam loss, while the time of arrival of the pulse indicates the loss position.

Previously, multiple studies on oBLMs have been conducted, both at CERN [2, 3], and at other accelerators around the world [4–7]. Depending on the intended use case of the respective installations, fibre thicknesses up to 710 µm and fibre lengths up to 200 m have been studied [5]. In addition, the type and placement of the photosensors vary between different institutes. Although most installations attached Silicon Photomultipliers (SiPMs) to the upstream end of the fibre, some studies chose to instead use Photomultiplier Tubes (PMTs) attached to the downstream end of the fibre [2, 5].

In the following, a novel installation at the CERN Linear Electron Accelerator for Research (CLEAR) will be introduced, and an in-depth investigation of multiple signal analysis and loss position reconstruction techniques discussed.

INSTALLATION

After promising results with a prototype setup at CLEAR [2], it was decided to install a permanent oBLM, covering the entire length of the accelerator. This new setup should help visualise beam losses along the accelerator and thereby help aid with daily beam operations.

CLEAR

CLEAR is a ~40 m long linear electron accelerator at CERN. It consists of a 20 m long accelerating section, split into three structures, followed by a 20 m long experimental beam line. A wide range of parameters can be adjusted with beam energies ranging from 60 MeV to 220 MeV. These beam settings are used to investigate, amongst others, plasma lens and THz acceleration, medical applications of electron beams and various types of beam instrumentation [8, 9].

oBLM

For this installation, it was decided to install a 200 µm thick, 130 m long 'FG200LEA' optical fibre from Thorlabs. This length was needed due to the position of the readout electronics in the gallery above the accelerator. Along the accelerator, optical posts were used to ensure a parallel installation of the fibre at a constant distance of 45 cm to the middle of the beam pipe. This was the closest distance possible due to other beam instrumentation devices along the beam line. The fibre type was chosen as it shows the lowest attenuation overall. As photosensors, S14160-3010PS SiPMs from Hamamatsu were chosen because of their relatively high photon detection efficiency of, at its peak, up to nearly 20 % over a large wavelength range from 300 nm to 900 nm and low operating voltage of 43 V.

LOSS POSITION RECONSTRUCTION

To be able to measure the accuracy of the setup, beam losses were induced at known positions along the beam line.

* m.king@cern.ch

ISBN: 978-3-95450-249-3 ISSN: 2673-5350 doi: 10.18429/JACoW-IBIC2024-FRBC3

SPS FAST SPILL MONITOR DEVELOPMENTS

S. Benítez*, E. Balci, D. Belohrad, S. Burger, A. Goldblatt, M. Martín, S. Mazzoni, F. Roncarolo
CERN, Geneva, Switzerland

Abstract

The North Area facility (NA) receives 400 GeV proton beams through a slow extraction process, so-called spill, from the CERN Super Proton Synchrotron (SPS). To improve the quality of the SPS spill, it is crucial to monitor its intensity in the range between a few nA up to a few µA, with a bandwidth extending from a few Hz up to several GHz. The most promising measurement options for this purpose are the Optical Transition Radiation-Photomultiplier (OTR-PMT) and the Cherenkov proton Flux Monitor (CpFM). This document presents recent upgrades performed on both devices based on the operational experience gathered throughout the 2023 and 2024 runs. It includes a detailed analysis and discussion of the present performance, comparing the capabilities of each instrument.

INTRODUCTION

As part of the Accelerators and Technology Sector (ATS) within the Physics Beyond Colliders (PBC) study, numerous proposals for fixed-target projects in the North Area facility (NA) were previously presented [1]. The slow extraction process takes around 2×10^5 SPS turns, that is approximately 4.8 s, providing a spill (i.e. a continuous flux of protons) towards the NA fixed target experiments. Monitoring the current fluctuations of such spillis critical for optimising extraction and successfully carrying out experiments. A list of key parameters for the development of spill monitors is shown in Table 1 [2].

As discussed in [3], currently the SPS spill time structure is monitored by one *Beam Secondary Emission intensity Monitor* (SEM) installed at the beginning of the extraction line towards the NA (TT20). This type of instrument is sensitive to de-bunched beams (for which beam current transforms cannot be used), but is limited in bandwidth to below 2 MHz and signal-to-noise ratio (SNR). *Diamond Beam Loss Monitor* (dBLM) are under study. They can reach 500 MHz but have a low frequency cut-off (e.g. 50 and 100 Hz cannot be measured) and for the moment the measured signal amplitudes are only few percent of what expected from simulated losses and detector acceptance. This contribution will focus on the development, implementation and test updates of two of other techniques considered for fast spill monitoring, the *Optical Transition Radiation - Photomultiplier Tube* (OTR-PMT) and the *Cherenkov proton Flux Monitor* (CpFM).

Table 1: Key Parameters of Interest for the SPS Spill monitors

Parameter	Value or Range	Comment
Spill Duration	4.8 s	Present operation
	1 s	Future, e.g. PBC
Spill Intensity	1 e11p to 400 e11p	
Spectrum Harmonics of Interest	50 Hz,100 Hz	Noise, PC ripples
	43.38 kHz	SPS 1^{st} and 2^{nd} Harmonics[a]
	477 kHz	PS 1^{st} Harmonic[b]
	200 MHz	RF capture
	800 MHz	RF long, blow-up
	10 GHz	Future, e.g. PBC

[a] the SPS circulating beam structure includes 2×10.5 µs injections, spaced by a 1.05 µs *abort gap* for the dump kickers rise.

[b] The slow extracted beam can still contain a time structure from the Proton Synchrotron (the SPS injector).

OPTICAL TRANSITION RADIATION-PMT MONITOR

The OTR-PMT system measures the extracted beam intensity by detecting OTR generated when the beam interacts with a titanium (Ti) foil inserted in the beam path at a 45-degree angle to the beam direction, facing upwards. The emitted radiation is captured by a fast PMT (R3377 series) with an anode pulse rise time of 0.8 ns [4], positioned vertically, approximately at 1 m from the interaction point. Next to the PMT, there is also an analogue camera (Watec WAT-902H3 ULTIMATE (CCIR)) installed to remotely visualise the centre of the screen and the presence of the OTR source. A motorised translation stage allows swapping between camera and PMT to image or integrate the OTR at the nominal measurement position. Both the PMT and the camera are protected by 15 mm thick lead shields for radiation protection. A rectangular cover surrounds the platform, ensuring that the entire setup is light-tight. In addition, an aluminium cylindrical tube is mounted on the beam pipe, featuring a door that provides easy access to its interior, where an optical lens (200 mm focal length, LA4984-ML series) system was installed to increase light collection efficiency. Finally, a ground-anchored bar supports the system, protecting the beam pipe tank from potential damage. Figure 1 shows the OTR-PMT design as described above. A new DAQ sys-

* sara.benitez.berrocal@cern.ch